S.I.S.S.A.
INTERNATIONAL SCHOOL FOR ADVANCED STUDIES

Ph.D. Course in Mathematical Analysis

Dissertation

TWO EXPLORATIONS
IN DYNAMICAL SYSTEMS
AND MECHANICS

AVOIDING CONES CONDITIONS
AND HIGHER DIMENSIONAL TWIST

↶ ❋ ↷

DIRECTIONAL FRICTION
IN BIO-INSPIRED LOCOMOTION

Candidate:
PAOLO GIDONI

Supervisor:
Prof. ALESSANDRO FONDA

Supervisor:
Prof. ANTONIO DESIMONE

ACADEMIC YEAR 2015-2016

Contents

II Directional friction in bio-inspired locomotion

Preface

All mathematics is divided into three parts: cryptography (paid for by CIA, KGB and the like), hydrodynamics (supported by manufacturers of atomic submarines) and celestial mechanics (financed by military and other institutions dealing with missiles, such as NASA).

Cryptography has generated number theory, algebraic geometry over finite fields, algebra, combinatorics and computers.

Hydrodynamics procreated complex analysis, partial differential equations, Lie groups and algebra theory, cohomology theory and scientific computing.

Celestial mechanics is the origin of dynamical systems, linear algebra, topology, variational calculus and symplectic geometry.

From *Polymathematics: Is mathematics a single science or a set of arts?*
Vladimir Igorevič Arnol'd

What is this dissertation, or more generally my PhD work, about? The simplest and most straightforward approach is dichotomy. This dissertation is divided into two parts, one more pure and one more applied. The first part investigates the notion of twist in higher dimension, generalizing some classical fixed point results. The second part analyses the role and effects on crawling locomotion of a directionality in friction. This is often the most effective way to briefly present, from scratch, my research activity, and the structure of this document reflects this view.

Yet, a dissertation should also be a time to stop, look backwards and reflect on what has been learned and accomplished in the previous years. Taking a deeper look at my activity in its entirety, I find this demarcation really blurred, obviously ruling out some visible, but quite superficial, distinguishing features. Mathematics is, in a sense, the art of recognising common patterns in different phenomena: the common thread, that crosses all my current and past research, is the investigation of processes that evolve in time*, disregarding of the techniques adopted or specific application involved. The two explorations above are just two, big clusters along this path (hopefully, others will born and develop in the future).*

Such idea is reinforced by looking to that part of my research activity that has been left out of this dissertation, for the sake of clarity — indeed, three

parts would have been too many. My PhD research activity began, a few month after arriving in Trieste, working with prof. Fonda on necessary and sufficient conditions for permanence of dynamical systems [FG15]. Only after this first paper was completed, we started to discuss about the theme of my dissertation and the idea of twist for higher dimensional generalization of the Poincaré–Birkhoff Theorem. Neither was this an isolated exception: just a few month earlier I was working again on dynamical systems, writing my Master's thesis on evolutionary game dynamics and dealing with fixed points and stability. Then, during the last four years, some quick explorations in population dynamics took place in the short, spare time between the two main projects.

As a first attempt to clarify this idea of processes dominated by time, a natural step is to explain it in the framework of differential equations. Here, this class is identified with ODEs, as opposite to PDEs, that evolve in space *(or in space and time). Yet, restricting ourself to ODEs wouldn't be too representative, since (ordinary) differential equations are, with respect to the first part of the thesis, mostly a field of application instead of the subject, whereas the second part deal prevalently with differential inclusion.*

A second attempt of explanation comes from the passage by V.I. Arnold quoted at the beginning of this preface. Without the pretence to fully grasp all the shades in Arnold's view, we can try to reformulate this partition in this way: cryptography *is discrete mathematics;* hydrodynamics *is the mathematics of systems evolving in* space *(space and time included);* celestial mechanics *is the mathematics of systems evolving in* time.[1] *With this terminology, the subject of this dissertation is definitively "celestial mechanics"; indeed dynamical systems, topology, variational calculus and symplectic geometry are all recurrent frameworks in this opus.*

Mathematics remains, anyway, a continuum, and this discussion has to be considered more as a difference in perspectives, than as a true classification. The perspective of evolution in time is what joins the parts of this dissertation, and the fascination for the study of dynamics, equilibria and their properties is what has driven me as a young researcher. I hope that the two explorations reported in this dissertation might involve the reader in this engaging view.

---

[1]The genius of Arnold cannot be contained in just a classification, and his paper is actually dedicated to the transversal relationships between these branches. Remarkably, a page later the discussion involves Poincaré's last geometric Theorem and Arnold's conjecture, from which sprouts all the framework of the first part of the dissertation.

Summary

Part I: Avoiding cones conditions and higher dimensional twist

Twist is one of the most remarkable structures in mathematics. In the planar case, it is embodied by the *Poincaré–Birkhoff fixed point Theorem* — also known as *Poincaré's last geometric Theorem* — and by the many results that stems from it. Given the success of the Poincaré–Birkhoff Theorem, it is natural to ask ourself: what would happen, when we try to extend twist to higher dimensions? In this first part of the thesis we will explore this scenario. Our purpose is to introduce a family of boundary twist conditions, called *avoiding cones conditions*, that enclose and improve some of the classical ways to identify twist in higher dimension, but at the same time maintain an intuitively identifiable and manageable definition of twist.

We begin, in Chapter 1, by reviewing the classical notion of twist, defined by the Poincaré–Birkhoff Theorem, focusing on the different situations to which it can be tailored. We will show that this framework finds a natural counterpart in Bolzano's Theorem. This puts the basis of the double edge approach carried on in the following chapters. On one hand we look at the avoiding cones conditions as a generalization of some classical fixed point results, such as the Poincaré–Miranda and Poincaré–Bohl Theorems — themselves nothing but higher dimensional counterparts of Bolzano's Theorem — thus providing a useful criterion to compute Brouwer's degree. On the other hand, we use the same idea of avoiding cones conditions to define a higher dimensional twist for a generalized Poincaré–Birkhoff Theorem.

Chapter 1 concludes with an overview of the main issues in approaching twist in higher dimension in the Poincaré–Birkhoff case, and a review of the results accomplished in literature.

In Chapter 2 we address the "Bolzano's" side of the problem. After recalling some standard results, we introduce and illustrate the main elements of our approach by proposing a first generalization of the Poincaré–Miranda Theorem. Then we construct our notion of avoiding cones condition at its full strength. We show how this condition allows to deal with functions defined on various types of convex domains, and situations where the topological

degree may be different from ± 1. An illustrative application is provided for the study of functionals having degenerate multi-saddle points.

In Chapter 3 instead we deal with the "Poincaré–Birkhoff"'s side of the situation. Following the novel approach of Fonda and Ureña [FU16b; FU16a] and keeping in mind the picture of the previous Chapter, we obtain a higher dimensional version of the Poincaré–Birkhoff Theorem for Poincaré maps of Hamiltonian systems, unifying and generalizing the twist conditions previously considered. If Chapter 2 rests on the properties of topological degree, here variational techniques are crucial; this makes imperative a different, more variational notion of the avoiding cones conditions, that will be discussed with example and comparisons throughout the chapter.

With Chapter 4 we look at the different scenarios where the twist, required by a higher dimensional Poincaré–Birkhoff Theorem, can be sought: locally, globally and at an intermediate scale. Locally, we consider the survival of periodic solution under perturbation of completely integrable systems; then, a similar picture is studied also at a larger scale. In the final part of the Chapter we consider situations where the twist is defined between zero and infinity, working in the framework of weakly coupled planar systems and adopting the pendulum equation as an inspiring example.

Part II: Directional friction in bio-inspired locomotion

The study of locomotion of biological organisms and bio-mimetic engineered replicas is receiving considerable and increasing attention in the recent literature [DT12; Men+06; ZZ07]. This approach is central in the new paradigm of *soft robotics*, with the purpose of endowing robots with new capabilities in terms of dexterity or adaptability, by exploiting large deformations typical of soft materials [KLT13]. Such features are being employed by emerging applications in medical intervention and, more generally, to situation requiring motility in an unpredictable and complex environment.

Crawling, the family of motility strategies inspired and adopted, for instance, by earthworms and snails, provides a suitable situation to address these issues, presenting a behaviour sufficiently complex, but fit to be studied with analytical tools. A feature, common in both biological and robotic crawlers, is the presence of some elements, like hair or bristles, that create an asymmetry in the friction of the crawler with the surface. The purpose of this second part of the thesis is to investigate how this directionality in friction is involved and affects crawling locomotion.

In Chapter 5 we consider a first family of continuous one-dimensional crawlers, generalizing to the case of directional friction the approach introduced in [DT12; DeS+13; NTD14]. We consider several rheologies and provide explicit formulae for the displacements attainable with reciprocal

extensions and contractions (breathing), or through the propagation of extension/contraction waves.

In the next chapters, we add to our model the elasticity of the body of the crawler. In Chapter 6 we consider, as toy model of crawler, a strip of nematic elastomer, subject to directional frictional interactions with a flat solid substrate, and cyclically actuated by a spatially uniform, time-periodic stimulus (e.g., temperature change). We consider both the case of distributed friction and that of friction only at the ends. We observe that now the shape of the crawler is no longer determined a priori, but depends also on the history of the systems.

The case with friction only at the end introduces the content of Chapter 7. Here, after developing the ideas of the previous Chapter in the abstract framework of rate-independent systems, we explore the motility of a crawler consisting of two active elastic segments, again resting on a support characterized by directional dry friction. We observe how the directionality in friction is actually pivotal in the motility of the crawler, since otherwise the motility would be dominated by inertial effects. We also show that, for a suitable range of the friction parameters, specific choices of the actuation strategy can lead to net displacements also in the direction of higher friction. Some remarks indicate how the case of a N-segment crawler is analogous. Such discrete situation is quite typical in crawlers, that often show a modular structure with contact occurring only once for each module (e.g. the rings in the earthworm).

After having considered directional friction in the previous chapters, with Chapter 8 we investigate on how this directionality is actually produced. We propose an explanation of the genesis of directional dry friction, as emergent property of the oscillations produced in a bristle-like mediating element by the interaction with microscale fluctuations on the surface. Mathematically, we extend a convergence result by Mielke, for Prandtl–Tomlinson-like systems, considering also non-homothetic scalings of a wiggly potential. This allows us to apply the result to some simple mechanical models, that exemplify the interaction of a bristle with a surface having small fluctuations. We find that the resulting friction is the product of two factors: a geometric one, depending on the bristle angle and on the fluctuation profile, and a energetic one, proportional to the normal force exchanged between the bristle-like element and the surface. This result is then applied to discuss the "with the nap/against the nap asymmetry", that aroused our interest.

Papers written during the PhD course

[DGN15]   A. DeSimone, P. Gidoni, and G. Noselli. "Liquid crystal elastomer strips as soft crawlers". *Journal of the Mechanics and Physics of Solids* 84 (2015), pp. 254–272.

[FG15]   A. Fonda and P. Gidoni. "A permanence theorem for local dynamical systems". *Nonlinear Analysis. Theory, Methods and Applications* 121 (2015), pp. 73–81.

[FG16a]   A. Fonda and P. Gidoni. "An avoiding cones condition for the Poincaré-Birkhoff Theorem," *submitted, preprint available at* `http : // www . dmi . units . it / pubblicazioni / Quaderni_ Matematici/ 647_ 2016. pdf` (2016).

[FG16b]   A. Fonda and P. Gidoni. "Generalizing the Poincaré–Miranda theorem: the avoiding cones condition". *Annali di Matematica Pura ed Applicata. Series IV* 195.4 (2016), pp. 1347–1371.

[FGG16]   A. Fonda, M. Garrione, and P. Gidoni. "Periodic perturbations of Hamiltonian systems". *Advances in Nonlinear Analysis* to appear (2016).

[GD16a]   P. Gidoni and A. DeSimone. "On the genesis of directional friction through bristle-like mediating elements". *arXiv preprint arXiv:1602.05611* (2016).

[GD16b]   P. Gidoni and A. DeSimone. "Stasis domains and slip surfaces in the locomotion of a bio-inspired two-segment crawler". *Meccanica* (2016), to appear.

[GND14]   P. Gidoni, G. Noselli, and A. DeSimone. "Crawling on directional surfaces". *International Journal of Non-Linear Mechanics* 61 (2014), pp. 65–73.

Part I

Avoiding cones conditions and higher dimensional twist

Chapter 1

On the concept of twist

Illustrated in Figure 1.1, the notion of twist on the plane, or equivalently on a cylinder, is a common and intuitive structure. Mathematically, a classical scenario where this structure is embodied is the Poincaré–Birkhoff Theorem, and the many results that stem from it. Since the purpose of this first part of the thesis will be to investigate how this concept can be extended to higher dimension, this Chapter is devoted to give a closer look at this natural idea of twist, and to construct an analogy with Bolzano's Theorem, that we will use as a guide in the following chapters. In the last part of the Chapter, we review the main issues and accomplishment in this extension to higher dimension, completing the necessary foundation of the next chapters.
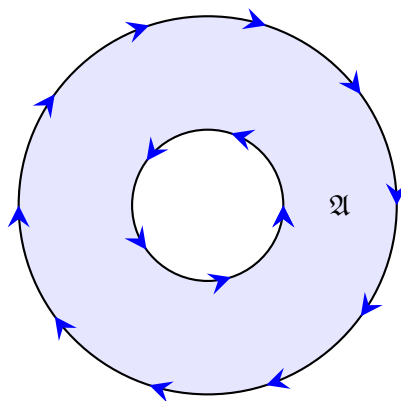
Figure 1.1: The twist condition on the planar annulus in the Poincaré–Birkhoff fixed point Theorem.
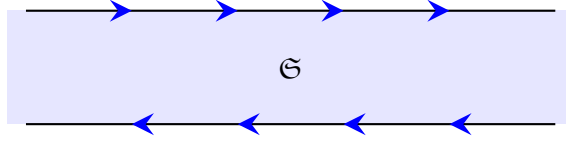
Figure 1.2: The representation of the twist condition of the Poincaré–Birkhoff fixed point Theorem, after the lift of the planar annulus to a strip.

1.1 The classical twist result: the Poincaré–Birkhoff Theorem

The Poincaré–Birkhoff Theorem states that every orientation- and area-preserving homeomorphism of the planar annulus onto itself, for which the two components of the boundary are (individually) invariant and rotated in opposite directions, has at least *two* fixed points.

This intuitive notion of twist is illustrated in Figure 1.1. A rigorous definition however relies on the lift of the annulus to the strip. Let us therefore consider the strip $\mathfrak{S} = \mathbb{R} \times [a,b]$ and an area-preserving homeomorphism $\mathcal{P} \colon \mathfrak{S} \to \mathfrak{S}$. We write the two components of $\mathcal{P}$ as $\mathcal{P}(x,y) = \big(\mathcal{P}_x(x,y), \mathcal{P}_y(x,y)\big)$ and define $\vartheta \colon \mathfrak{S} \to \mathbb{R}$ as $\vartheta(x,y) = \mathcal{P}_x(x,y) - x$, so that it describes how much a point is translated rightwards or leftwards. We also assume that the two boundary lines are invariant, that means

$$\mathcal{P}_y(\mathbb{R} \times \{a\}) = a \qquad\qquad \mathcal{P}_y(\mathbb{R} \times \{b\}) = b \qquad (1.1)$$

and that the map $\mathcal{P}$ satisfies, for every $(x,y) \in \mathfrak{S}$,

$$\mathcal{P}_x(x + 2\pi, y) = \mathcal{P}_x(x,y) + 2\pi \quad \text{and} \quad \mathcal{P}_y(x + 2\pi, y) = \mathcal{P}_y(x,y) \qquad (1.2)$$

This last assumption assures that the map $\mathcal{P}$ can be identified with the lift of a homeomorphism $\Phi \colon \mathfrak{A} \to \mathfrak{A}$, where $\mathfrak{A} = \mathbb{T} \times [a,b]$ denotes the annulus, so that, denoting with $\pi_{\mathfrak{A}}$ the canonical projection $\pi_{\mathfrak{A}} \colon \mathfrak{S} \to \mathfrak{A}$, we have for every $(x,y) \in \mathfrak{S}$

$$\Phi(\pi_{\mathfrak{A}}(x,y)) = \pi_{\mathfrak{A}}(\mathcal{P}(x,y))$$

We notice that every homeomorphism Φ satisfying the assumptions of the Poincaré–Birkhoff Theorem admits a lift $\mathcal{P}$ with all the properties above. We remark that our argument still applies if we identify the planar annulus with a subset of $\mathbb{R}^2$ of the form $\tilde{\mathfrak{A}} = \{z \in \mathbb{R}^2 : 0 < \tilde{a} \leq |z| \leq \tilde{b}\}$; indeed the lift corresponds to the choice of suitable polar coordinates, where the radial one is rescaled in order to preserve the areas. We also observe that the assumptions (1.1) and (1.2) guarantee that $\mathcal{P}$ is orientation preserving.

Regarding the twist, we notice that the natural notion of rotation is introduced by the function ϑ, which is well-defined also on the annulus since

$$\vartheta(x + 2\pi, y) = \vartheta(x,y)$$

Thus the twist condition can be defined as

$$\begin{cases} \vartheta(x,a) < 0 \\ \vartheta(x,b) > 0 \end{cases} \quad \text{or} \quad \begin{cases} \vartheta(x,a) > 0 \\ \vartheta(x,b) < 0 \end{cases} \qquad \text{for every } x \in \mathbb{R} \qquad (1.3)$$

This definition of twist is illustrated in Figure 1.2. We remark that, by continuity, all the $x \in \mathbb{R}$ will satisfy the same condition of the two alternative ones. We thus have the following "strip-formulation" of the Poincaré–Birkhoff Theorem.

Theorem 1.1. *Let $\mathcal{P}\colon \mathfrak{S} \to \mathfrak{S}$ be an area-preserving homeomorphism of annulus, satisfying* (1.1), (1.2) *and the twist condition* (1.3). *Then the map $\mathcal{P}$ has at least* two geometrically distinct *fixed points.*

We say that two points of the strip are *geometrically distinct* if their projections on the annulus are distinct. We emphasize that the fixed points found satisfy $\vartheta = 0$; this means that, when $\mathcal{P}$ is the Poincaré map generated by a given flow on the annulus, the periodic solutions associated to the fixed point recovered with the Theorem have zero winding number.

A short history of the Theorem   Despite the immediacy of its enunciate, the history of the Poincaré–Birkhoff Theorem is long and full of hardship, as often happens to clear mathematical statements. The first formulation is due to Poincaré in 1912, a few months before his death. After many month of pointless efforts, the French mathematician, concerned by his age and aware of the impact of such a result, decided with reluctance to publish it as a conjecture, checking its validity in some special cases. A first proof was proposed by Birkhoff in 1913, showing the existence of at least one fixed point. The existence of the second fixed point was only sketched with a remark based on topological degree; Birkhoff himself later admitted the inaccuracy of that passage and in 1926 published a proof of the existence of the second solution, replacing the area-preserving hypothesis with a more general topological assumption. The main idea is that any proper sub-annulus (an annulus defined by one of the circles and another closed curve rotating within the original annulus) cannot be a proper subset or superset of its image. This approach has been followed also in more modern and shorter proofs, for instance those of [LW10; Gui97]. Yet, at the beginning, this result was taken with some skepticism by the mathematicians community, until the expository paper by Brown an Neumann in 1977.

In the same paper of 1926, Birkhoff addressed also another relevant issue of the Theorem: the invariance of the boundary, that can be too restrictive and difficult to prove in applications . Birkhoff assumes the invariance only on the inner circle, requiring that the outer one is sent in a star-shaped set. Several generalizations have been proposed in this sense (e.g. [Jac76; Din83; Car82; Fra88; Reb97], cf. also the reviews [LeC11; DR02]), yet, as pointed

out in [LW10; MU07], some further steps, that commons sense suggests to hold, in removing such assumptions are actually false.

In this thesis, when dealing with higher dimensional twist, we will restrict ourself to an Hamiltonian framework. This will allow to replace this classical topological approaches to a variational one, avoiding in this way some of the criticalities and following a more consolidated path.

A Hamiltonian version To conclude this section, let us present an alternative version of the Poincaré–Birkhoff Theorem in the case of Hamiltonian systems.

Let us consider the Hamiltonian systems on the plane, with an Hamiltonian function $H = H(t, z)$ periodic in time, that is

$$\dot{z} = J\nabla H(t, z) \tag{1.4}$$

where we write $z = (x, y)$, we denote with ∇ the gradient with respect to the spatial coordinates z, and J is the matrix

$$J = \begin{pmatrix} 0 & 1 \\ -1 & 0 \end{pmatrix}$$

We assume that the Poincaré map $\mathcal{P}$ associated to time T is well defined and we express its first component in the form $\mathcal{P}_x(x, y) = x + \vartheta(x, y)$, as we did above.

Theorem 1.2. *Let $H(t, x, y) \in \mathcal{C}^2(\mathbb{R} \times \mathbb{R} \times \mathbb{R}, \mathbb{R})$ be T-periodic in t and 2π-periodic in x. Suppose that the Poincaré map $\mathcal{P}$ is well-defined and that there exists an interval $[a, b]$ such that the twist condition (1.3) is satisfied. Then the system (1.4) has at least two geometrically distinct T-periodic solutions.*

We remark that, whereas assumption (1.2) is automatically satisfied, the invariance (1.1) of the boundary of $\mathbb{R} \times [a, b]$ is no longer required, replaced by the symplectic structure of the map.

1.2 The minimal twist result: Bolzano's Theorem

The twist condition (1.3) immediately reminds of Bolzano's Theorem.

Theorem 1.3 (Bolzano)**.** *Let $\vartheta\colon [a, b] \to \mathbb{R}$ be a continuous function. If*

$$\begin{cases} \vartheta(a) < 0 \\ \vartheta(b) > 0 \end{cases} \quad or \quad \begin{cases} \vartheta(a) > 0 \\ \vartheta(b) < 0 \end{cases}$$

then ϑ has a zero in $[a, b]$. Equivalently, the map $\mathcal{P}\colon [a, b] \to \mathbb{R}$ defined as $\mathcal{P}(y) = y + \vartheta(y)$ has a fixed point.

Indeed, as we will see, Bolzano's Theorem, its corollaries and higher dimensional generalizations can provide some guidance to our exploration. More advanced issues will be considered in the next chapters; for now let us just consider the following three consequences of Bolzano's Theorem, that translate in as many classical strategies to apply the Poincaré–Birkhoff Theorem.

Theorem 1.4 (Intermediate value Theorem). *Let $\vartheta\colon [a,b] \to \mathbb{R}$ be a continuous function. If*

$$\begin{cases} \vartheta(a) < c \\ \vartheta(b) > c \end{cases} \quad or \quad \begin{cases} \vartheta(a) > c \\ \vartheta(b) < c \end{cases}$$

then there exists $\bar{y} \in [a,b]$ such that $\vartheta(\bar{y}) = c$.

The second application we consider regards the stability under perturbation of the result.

Corollary 1.5. *Let $\vartheta, g\colon [a,b] \to \mathbb{R}$ be two continuous functions, with ϑ satisfying (1.3). We define the function $\vartheta_\varepsilon(y) = \vartheta(y) + \varepsilon g(y)$. Then, for $|\varepsilon|$ sufficiently small, the function ϑ_ε has a zero in $[a,b]$.*

The third and last application introduces a local and strong notion of twist: nondegeneracy.

Corollary 1.6. *Let $\vartheta, g\colon \mathbb{R} \to \mathbb{R}$ be two continuous functions. Assume that there is a point $y_0 \in \mathbb{R}$ such that $\vartheta(y_0) = c$, ϑ is differentiable in y_0 and*

$$\vartheta(y_0) \neq 0 \tag{1.5}$$

As above, we write $\vartheta_\varepsilon(y) = \vartheta(y) + \varepsilon g(y)$. Then, for $|\varepsilon|$ sufficiently small, there exists a value y_ε, close to y_0, such that $\vartheta_\varepsilon(y_\varepsilon) = c$.

Clearly the differentiability is not necessary and condition (1.5) can be replaced with weaker notions, such as strict monotonicity or local invertibility. Nor these latter are yet necessary, for instance it suffices that ϑ assumes, in every neighbourhood of y_0, values both greater and smaller than c; an example is $\vartheta(y) = \sin(1/y)/y$ at $y_0 = 0$. Still, a nondegeneracy of the form 1.5 is what one usually proves.

From the segment to the annulus

We now discuss how the variants to Bolzano's Theorem can be translated to Poincaré–Birkhoff's setup. For simplicity we refer to the Hamiltonian version presented in Theorem 1.2, yet the same ideas apply to the general topological situation.

The intermediate value Theorem 1.4 suggests us that we can have twist not only if the two boundary circles rotate in opposite directions, but also

when one rotates faster than the other one. Clearly we no longer find fixed
points, but points that rotate at a given speed; in other terms, we no longer
find true periodic solutions but *running solutions*, in the sense that such
solutions are not periodic on the strip but, once the system is projected on
the annulus, they become periodic and rotate around the annulus.

Corollary 1.7. *Let $H(t, x, y) \in \mathcal{C}^1(\mathbb{R} \times \mathbb{R} \times \mathbb{R}, \mathbb{R})$ be T-periodic in t and
2π-periodic in x. Suppose that the Poincaré map $\mathcal{P}$ well-defined and that there
exists an interval $[a, b]$ such, for some that the twist condition*

$$\begin{cases} \vartheta(a) < c \\ \vartheta(b) > c \end{cases} \quad or \quad \begin{cases} \vartheta(a) > c \\ \vartheta(b) < c \end{cases}$$

*is satisfied for some $c = 2\pi p/q$, with $p \in \mathbb{Z}$, $q \in \mathbb{N}_0$. Then the system (1.4)
has at least two geometrically distinct solutions, that, projected on the annulus,
become qT-periodic and make in each period exactly p rotations around the
annulus. If $q > 1$, such solutions are usually called* subharmonic solutions.

The persistence of the solutions under small perturbation of Corollary 1.5
extends quite intuitively to our setup, due to the fact that twist is essentially
a topological property.

Corollary 1.8. *Let H be an Hamiltonian function satisfying all the assump-
tion of Theorem 1.2. Let $P(t, x, y) \in \mathcal{C}^1(\mathbb{R} \times \mathbb{R} \times \mathbb{R}, \mathbb{R})$ be T-periodic in t,
2π-periodic in x and such that $\|\nabla P\|_\infty < K$ for some constant $K > 0$. Then,
for $|\varepsilon|$ sufficiently small, the system*

$$\dot{z} = J\nabla(H(t, z) + \varepsilon P(t, z))$$

has at least two geometrically distinct T-periodic solutions.

Regarding nondegeneracy, it is strictly related to the concept of *monotone
twist*. Let us assume that $\mathcal{P}$ is continuously differentiable; this is true for
instance if $H \in \mathcal{C}^2$. We say that $\mathcal{P}$ is a monotone twist map if

$$\frac{\mathrm{d}\vartheta(x, y)}{\mathrm{d}y} \neq 0 \qquad \text{for every } x, y \in \mathbb{R} \times [a, b] \tag{1.6}$$

We observe that, by continuity, the derivative must assume the same sign
on all the domain. This assumption clearly represent the analogous of (1.5),
and, as expected, is mostly used when dealing with the survival of periodic
points under local perturbations.

Under the monotone twist assumption, it is possible to provide a simpler
proof of the Poincaré-Birkhoff Theorem, that holds also for the classical
formulation of Theorem 1.1. The main idea is the following. The twist
condition, combined with the monotonicity of $\vartheta(x, \cdot)$, assures us that, for every
$x \in \mathbb{R}$, there exists exactly one point $\gamma(x) \in (a, b)$ such that $\vartheta(x, \gamma(x)) = 0$.

By local invertibility we deduce that γ is continuous, besides being 2π-periodic, thus identifying a star-shaped curve when projected on the annulus. It can be shown that the map $\rho(x,y) = \mathcal{P}_y(x,y) - y$ on the curve $(x, \gamma(x))$ either is always zero, or it assumes both signs. In the classical formulation, if ρ is not null but assumes only one sign, this would mean that the smaller annulus is sent by $\mathcal{P}$ either onto a proper superset (if ρ is non-negative) or onto a proper subset (if ρ is negative) in contradiction with the area preserving assumption. In the Hamiltonian framework, our claim follows by the symplecticity of $\mathcal{P}$, that implies that ρ has zero average on the curve defined by γ. By the periodicity, it follows that ρ has at least two (geometrically distinct) zeros on the curve $(x, \gamma(x))$, that correspond with two fixed points of $\mathcal{P}$.

A usual framework where this situation is exploited are the *period annuli*, as illustrated in [FSZ12]. A period annulus is an annulus composed of concentric periodic orbits. As we will discuss later, such situation is standard in planar autonomous Hamiltonian systems. In this case the twist is represented by a change in the period of the orbits, and monotone twist correspond to a local "strong" monotonicity of the period, in the sense that the "radial" derivative of the period of the orbits is not zero. Then we can obtain the analogous of Corollary 1.6, showing that, given a T-periodic *orbit* inside a twisted period annulus, after any sufficiently small T-periodic perturbation of the systems, there are at least two T-periodic *solution* of the perturbed systems, close to the original orbit. Such situations have been studied by many authors, e.g. [Chi87; GGJ10; PZ01]. If, instead, the period of the perturbation is only commensurable with that of the orbit considered, we can look for subharmonic solutions, as done in Corollary 1.7. We will discuss the higher dimensional analogous of this situations in Chapter 4.

1.3 Twist in higher dimensions

Aiming at a generalization of the Poincaré-Birkhoff Theorem to higher dimensional systems, some crucial issues have to be addressed.

- What is the higher dimensional version of the planar annulus?

- How is it twisted?

- What properties are required on the map $\mathcal{P}$?

The kern of first question is to decide whether $\mathbb{T} = \mathcal{S}_1$ has to be considered as a torus or as a sphere; this leads to two main interpretations of the higher dimensional meaning of the annulus:

- the $2N$-dimensional annulus is the product $\mathbb{T}^N \times \mathcal{B}_N$ of a N-dimensional torus and a N-dimensional ball;

- the $2N$-dimensional annulus is the product $\mathcal{S}_{2N-1} \times \mathcal{B}$ of the $(2N-1)$-sphere and a 1-dimensional ball;

There is no right answer; indeed both views can be followed and present advantages and weeknesses. For instance, as we have seen, to define "rotation" in the plane we have exploited the canonical lift of a torus $\mathbb{T}^N$ to $\mathbb{R}^N$, whereas the rotation of the spheres is more elusive and requires more restrictive assumptions on the dynamics. On the other end, the boundary of the $\mathcal{S}_{2N-1} \times \mathcal{B}$ annulus is formed by an inner and an outer sphere, so, once the meaning of rotation is established, twist can be intuitively introduced as a difference on the rotation of the two spheres; whereas the boundary of the $\mathbb{T}^N \times \mathcal{B}_N$ annulus is connected, so in this case the difficulties concerns the meaning of twist.

In the remaining of the Chapter we discuss in more detail this two situations. As the attentive reader would have deduced by our choice of notation, in the following chapters we will focus on the $\mathbb{T}^N \times \mathcal{B}_N$ interpretation of the annulus. Obviously many other combinations can be proposed as higher dimensional annuli, however, as we will see, the two situation proposed above arise quite naturally in applications.

The equivalence $\mathbb{T} = \mathcal{S}_1$ of tori and spheres in the plane highlights once more the well known fact that dynamics on the plane present many special properties, compared to higher dimensional spaces. Indeed the various proofs of the Poincaré-Birkhoff Theorem rely all strongly on the topological structure of the plain, so we can not even expect to look for an adaptation of the demonstration techniques used for the case $N = 1$.

For this reason, it is not surprising that some additional assumptions are usually required on the map $\mathcal{P}$, in order to compensate the lost of structure in the passage to higher dimensions. The classical approach is to assume that the map $\mathcal{P}$ is the Poincaré map of a Hamiltonian system. The main advantage is that the symplectic structure allows a variational formulation of the problem. As we have seen, the topological approaches to the Poincaré-Birkhoff Theorem have proved to be hard and often tricky; a variational formulation provides a safer and beaten track. Nor it is a too restrictive assumption: Hamiltonian systems are the natural field of applications of the Theorem, since they guarantee the preservation of the area. Furthermore, the additional structure provided allows also to completely remove the assumption (1.1) on invariance of the boundary, that can be quite annoying when dealing with applications. Thus, from now on, we are interested in the Hamiltonian systems in

$$\dot{z} = \mathcal{J}\nabla H(t, z) \tag{HS}$$

where $z = (x, y) \in \mathbb{R}^N \times \mathbb{R}^N$, the matrix $\mathcal{J}$ is defined as

$$\mathcal{J} = \begin{pmatrix} 0 & \mathbb{I}_N \\ -\mathbb{I}_N & 0 \end{pmatrix}$$

and the Hamiltonian function $H(t, x, y)$ is T-periodic in the time variable t.

If $\mathbb{T} = \mathcal{S}_1$ is a torus: completely integrable systems

A classical approach to the study of the Hamiltonian system (HS) is the search for constants of motion, since they can be used for suitably transforming the system into a simpler one. The most remarkable case occurs when (HS) has N constants of motion which are independent and in involution: in this case, the system is said to be *completely integrable*, and one has a foliation of the space in N-dimensional surfaces, which are invariant for the flow.

The Liouville–Arnold theorem then assures that, when one of these surfaces is bounded and connected, it has to be an N-dimensional torus. Moreover, for any such invariant torus Γ, there exists an open neighbourhood $\tilde{\mathfrak{A}}$ of Γ and a canonical transformation $z = (x, y) \mapsto (\varphi, I)$, mapping $\tilde{\mathfrak{A}}$ onto $\mathbb{T}^N \times \mathcal{D}$, where $\mathcal{D}$ is an open subset of $\mathbb{R}^N$, so that the Hamiltonian function is reduced to the simpler form $\mathcal{H}(\varphi, I) = \mathscr{K}(I)$. The coordinates $I = (I_1, \dots, I_N) \in \mathcal{D}$ are usually known as *action variables*, whereas the coordinates $\varphi = (\varphi_1, \dots, \varphi_N) \in \mathbb{T}^N$ are called *angle variables*.

Since for every general Hamiltonian system (HS) a constant of motion is always given by the Hamiltonian function $\mathcal{H}$, we immediately deduce that every planar Hamiltonian system is completely integrable. Indeed, this is one of the reasons of the great success of the Poincaré-Birkhoff Theorem.

In higher dimensions, a classical example of completely integrable system comes from the Kepler two–body problem, or even from every central force field [LL92]. On the contrary, if more than two bodies are involved, the system is not completely integrable any more. However, assuming the masses of the "planets" to be small compared to the mass of the "Sun", the system may be seen as being decomposed in n independent two–body systems, with the addition of a small perturbative term accounting for the other interactions (cf. [Cel10; CC07] and references therein). Such problems of Celestial Mechanics have probably been the main stimulus in the development of integrability and of *Hamiltonian perturbation theory*. More recently, another family of completely integrable systems, obtained by studying the evolution of N-vortices systems, is producing a rising interest [Are07; New01; Bla08].

As a matter of fact, completely integrable Hamiltonian systems are rare, and most often the Hamiltonian function is their unique constant of motion [BGG85; Sie54]. Yet, generic Hamiltonian systems may be considered as perturbations of completely integrable systems [MM74; Rob70], usually called *nearly integrable systems*. A glance of this scenario was already grasped by Henri Poincaré [Poi92], who referred to Hamiltonian perturbation theory as the *Problème général de la Dynamique*. The efforts made by Poincaré and, among many others, by G.D. Birkhoff, led to a broad development of the theory. A detailed introduction to Hamiltonian perturbation theory can be found in [AKN06a; Ben05], while [Dum14] offers a friendly overview.

It is not surprising that, to extend the result to higher dimensional systems, a natural starting point could be provided by monotone twist, as shown by the straighforward approach illustrated in [MZ05]. A local approach to the problem, when a form of monotone twist is generated by nondegeneracy, has been proposed by Bernstein and Katok [BK87], who showed the survival under small perturbations of $N + 1$ periodic solutions, requiring a convexity assumption on the Hamiltonian function (see also [ACE87; Eke83; Wil87]), and profiting from convexity to obtain an estimate on the size of the perturbation independent from the frequency of the torus. This result has been later refined by Chen [Che92], who replaced the convexity by a classical nondegeneracy assumption. We also mention the work of Blackmore, Champanerkar and Wang [BCW05], that obtain a perturbative result.

Outside the restrictive framework of monotone twist, a first, groundbreaking result is due to Conley and Zehnder [CZ83a], that showed the existence of $N+1$ periodic solutions for systems whose Hamiltonian function is 2π-periodic in the first N variables, and asymptotically quadratic in the other N ones. These pioneering results have been generalized in several directions, in a long series of papers (cf. for instance [Szu90; Szu92]).

In our investigation, we will follow the recent approach by Fonda and Ureña [FU16b; FU16a] (cf. also the extended version [FU13; FU14]), that, starting from the results above and exploiting a prolongation technique, proved a higher dimensional generalization of the Poincaré–Birkhoff Theorem for sets of the form $\mathbb{T}^N \times \mathcal{D}$, where $\mathcal{D} \subset \mathbb{R}^N$ is a convex body, imposing a twist condition only on its boundary. Such situation recall closely that of the planar Poincaré–Birkhoff Theorem, with $\mathbb{T}^N \times \mathcal{D}$ playing the role of a N-dimensional annulus. We postpone the discussion of these results to Chapter 3, where the framework and the twist conditions will be analysed in detail.

If $\mathbb{T} = \mathcal{S}_1$ is a sphere: Maslov index

As anticipated, the main issue with the sphere-interpretation of the Poincaré–Birkhoff Theorem is to define a suitable definition of the rotation. A brilliant solutions for $2N$-dimensional linear Hamiltonian systems is given by the Maslov index, known also as Conley-Zehnder index. The theory is advanced and has been improved in several papers; since it falls outside the main purposes of this thesis, we will give just a brief overview, suggesting the books [Abb01; Lon02] for further details.

Let us consider the linear Hamiltonian system

$$\dot{z}(t) = \mathcal{J}A(t)z(t) \tag{1.7}$$

where $A(t)$ is a T-periodic symmetric matrix and the dot denotes the derivative with respect to t.

We consider the *fundamental solution* $Z(t)$ of the systems, that is the matrix that solves the associated matricial problem

$$\begin{cases} \dot{Z}(t) = \mathcal{J}A(t)Z(t) \\ Z(0) = \mathbb{I} \end{cases} \tag{1.8}$$

The matrix $Z(t)$ is sympletic for every t. The system (1.7) is said to be non degenerate if 1 is not an eigenvalue of $Z(T)$. This corresponds to say that the systems doesn't have T-periodic solution with the only exception of the trivial one $z(t) \equiv 0$. In such a case it is possible to define an integer, called T-Maslov index, associated to the path $Z(t)$ in the space of sympletic matrices $\mathrm{Sp}(2N)$. Such invariant, that we will denote with $i_T(A)$, intuitively defines how much the solutions of the system rotate around the origin.

This idea of rotation alone is sufficient to recover at least a solution, as proved by Amann and Zehnder [AZ80]. However we will use this notion to construct a form of twist. This is traditionally done considering asymptotically linear systems and assuming that the linearization at the origin has a different index i_T from the linearization at infinite.

We are thus interested in the existence of solutions for the system

$$\begin{cases} \dot{z}(t) = \mathcal{J}H'(t, z(t)) \\ z(0) = z(T) \end{cases} \tag{1.9}$$

where $H \colon \mathbb{R} \times \mathbb{R}^{2N} \to \mathbb{R}$ is an Hamiltonian function such that

(H1) $H \in \mathcal{C}^2(\mathbb{R} \times \mathbb{R}^{2N}, \mathbb{R})$ and is T-periodic in the time variable;

(H2) the Hessian matrix $H''(t, z)$ is bounded;

(H3) there exist a symmetric T-periodic matrix $A_0(t)$ such that

$$H'(t, z) = A_0(t)z + o(\|z\|) \qquad \text{for } \|z\| \to 0 \tag{1.10}$$

(H4) there exist a symmetric T-periodic matrix $A_\infty(t)$ such that

$$H'(t, z) = A_\infty(t)z + o(\|z\|) \qquad \text{for } \|z\| \to \infty \tag{1.11}$$

The prime indicates derivation in the z variable, so that H' and H'' are respectively the gradient and the Hessian matrix of H.

In 1980 Amann and Zehnder [AZ80] provided an influential Theorem in the case of autonomous A_0 and A_∞. Their result has been generalized by Conley and Zehnder [CZ84] in the following theorem.

Theorem 1.9. *Let us consider the Hamiltonian system* (1.9) *and assume that it satisfies* (H1), (H2), (H3) *and* (H4).

If the linear systems $\dot{z} = \mathcal{J}A_0(t)z$ *and* $\dot{z} = \mathcal{J}A_\infty(t)z$ *are non degenerate and* $i_T(A_0) \neq i_T(A_\infty)$, *then the system* (1.9) *admits a nontrivial solution. Furthermore, if this solution is nondegenerate, then there exists a second nontrivial solution.*

Several authors have investigated this problem, leading to many significant improvement; yet, for our purpose, we just notice that the notion of twist remains dependent of a sort of linear rotation of the systems, as that presented above, although extended to more general frameworks. The relation between this Maslov-index formulation in the planar case and the classical Poincaré–Birkhoff Theorem has been discussed in [MRZ02].

Chapter 2

From twist towards topological degree

2.1 Bolzano's Theorem in higher dimensions

The natural and general characterization in higher dimensions of the twist of Bolzano's Theorem is Brouwer's topological degree, so that condition (1.3) can be interpreted as $d_B(\vartheta, (a, b), 0) \neq 0$ and the existence of the zero of ϑ follows immediately by the properties of the degree. Indeed, topological degree embodies also the properties we discussed for Bolzano's Theorem, such as the twist of the intermediate value Theorem, given by $d_B(\vartheta, (a, b), c) \neq 0$, and the stability under perturbation.

Topological degree theory, however, does not close the investigation on the concept of twist. If, on one hand, all twist theorems (in Bolzano's sense) can be seen as corollaries of the notion of degree, on the other hand this encourages the study of twist conditions, that can be used as simple and effective tools to compute the degree, instead of a burdensome direct approach, based on a case by case construction of a suitable homotopy.

Before considering concrete results, a remark about the notation adopted is in order. Topological degree is properly defined on open sets, however for our purposes the behaviour on the boundary is pivotal and it is often convenient to work with closed sets. For this reason we denote with $\deg(\vartheta, D)$ the topological degree $d_B(\vartheta, \operatorname{int} D, 0)$, assuming that D is equal to the closure of its interior[1] and that the degree is computed with respect to the value zero.

Some classical results

Probably, the most natural higher dimensional extension of Bolzano's Theorem is the Poincaré–Miranda Theorem. To extend the notion of interval, we

---

[1] We remark that to assume that $D = \overline{\operatorname{int} D}$ is equivalent to claim that there exists an open set Ω such that $D = \overline{\Omega}$.

consider a N-dimensional rectangle

$$\mathcal{R} = [a_1, b_1] \times [a_2, b_2] \times \cdots \times [a_N, b_N]$$

and we denote its faces as

$$\mathcal{F}_k^- = \{x \in \mathcal{R} : x_k = a_k\} \quad \mathcal{F}_k^+ = \{x \in \mathcal{R} : x_k = b_k\}$$

Theorem 2.1 (Poincaré–Miranda)**.** *Let* $\vartheta = (\vartheta_1, \vartheta_2, \ldots, \vartheta_N) \colon \mathcal{R} \to \mathbb{R}^N$ *be a continuous function. If, for every* $k = 1, 2, \ldots, N$, *the component* ϑ_k *satisfies either*

$$\begin{cases} \vartheta_k(x) < 0 & \text{for every } x \in \mathcal{F}_k^- \\ \vartheta_k(x) > 0 & \text{for every } x \in \mathcal{F}_k^+ \end{cases} \tag{2.1a}$$

or

$$\begin{cases} \vartheta_k(x) > 0 & \text{for every } x \in \mathcal{F}_k^- \\ \vartheta_k(x) < 0 & \text{for every } x \in \mathcal{F}_k^+ \end{cases} \tag{2.1b}$$

then ϑ *has a zero in* $\mathcal{R}$. *More precisely, we have that* $\deg(\vartheta, \mathcal{R}) = (-1)^M$, *where* M *is the number of components* ϑ_k *that satisfy the alternative condition* (2.1b)*.*

The main improvement of the Poincaré–Miranda Theorem is to allow indefinite twist, in the sense that the field ϑ can be expansive in some direction and contractive in others; however it is quite restrictive in the shape of the set considered.

The opposite behaviour is introduced for instance by the Poincaré-Bohl Theorem, for which we can consider quite general sets, but we have more restrictions on the kind of twist.

Theorem 2.2 (Poincaré–Bohl)**.** *Assume that* Ω *is an open bounded subset of* $\mathbb{R}^N$, *with* $0 \in \Omega$, *and that* $\vartheta \colon \overline{\Omega} \to \mathbb{R}^N$ *is a continuous function such that*

$$\vartheta(x) \notin \{\alpha x : \alpha \geq 0\} \quad \text{for every } x \in \partial\Omega \tag{2.2}$$

Then, there exists $\bar{x} \in \overline{\Omega}$ *such that* $\vartheta(\bar{x}) = 0$. *Moreover,* $\mathrm{d}_B(\vartheta, \Omega, 0) = (-1)^N$.

Proof. Let us consider the homotopy $\Theta \colon \overline{\Omega} \times [0, 1] \to \mathbb{R}^N$ defined by

$$\Theta(x, \lambda) = (1 - \lambda)\vartheta(x) - \lambda x$$

We claim that $0 \notin \Theta(\partial\Omega \times [0, 1])$. By contradiction, assume that there are $x \in \partial\Omega$ and $\lambda \in [0, 1]$ such that $\Theta(x, \lambda) = 0$. Then $\lambda \neq 0$, since by the above assumption $\Theta(x) \neq 0$, and $\lambda \neq 1$, since $0 \in \Omega$. Therefore $\lambda \in (0, 1)$ and, setting $\alpha = \lambda/(1 - \lambda)$, we see that $\alpha > 0$ and $\vartheta(x) = \alpha x$, a contradiction.

Thus, we can compute the Brouwer topological degree:

$$\mathrm{d}_B(\vartheta, \Omega, 0) = \mathrm{d}_B(\Theta(\cdot, 1), \Omega, 0) = \mathrm{d}_B(\Theta(\cdot, 0), \Omega, 0) = \mathrm{d}_B(-\mathbb{I}, \Omega, 0) = (-1)^N$$

The conclusion readily follows. □

A classical trick to recover a proof of the Poincaré–Miranda is to consider the map $\tilde{\vartheta}$ obtained by changing the sign of the expansive components of ϑ, and then apply a fixed point Theorem for maps showing a given form of inwardness, such as Brouwer's fixed point Theorem, or the Poincaré–Bohl Theorem, as we now briefly illustrate.

Proof of the Poincaré–Miranda Theorem 2.1. We introduce a new function $\tilde{\vartheta} \colon \mathcal{R} \to \mathbb{R}^N$ whose components are defined as $\tilde{\vartheta}_k = -\vartheta_k$ if ϑ_k satisfies (2.1a), and $\tilde{\vartheta}_k = \vartheta_k$ if ϑ_k satisfies (2.1b), so that

$$\tilde{\vartheta}_k(x_1, \ldots, a_k, \ldots, x_N) \geq 0 \geq \tilde{\vartheta}_k(x_1, \ldots, b_k, \ldots, x_N)$$

for every $(x_1, \ldots, x_N) \in \partial\mathcal{R}$ and every $k = 1, \ldots, N$. It is easily verified that, for $\Omega = \operatorname{int}\mathcal{R}$, the assumptions of Theorem 2.2 are satisfied, and the proof is completed. $\qquad\square$

We observe that the condition required on ϑ in the proof above, is actually weaker then the one required by the Poincaré-Miranda Theorem. Yet, the fixed-point condition thus obtained would be not completely intuitive to identify, not invariant under translations (the choice of the reference point is relevant), and would loose the inward-/outward meaning.

Our approach to improve this situation is to replace the rays of the Poincaré-Bohl Theorem with normal cones. In this way the directions to be avoided dependent only on the local structure of the set, so that they are well preserved for transformations of the set. Moreover this will allow us to introduce a weak form of inward-/outwardness (cf. [FG16b]).

Let us assume that our set $D \subset \mathbb{R}^N$ is a *convex body*, that means a compact convex set in $\mathbb{R}^N$ with non-empty interior. Note that every convex body coincides with the closure of its interior.

Given a point $\bar{x} \in D$, we define the *normal cone* to D in $\bar{x}$ as

$$\mathcal{N}_D(\bar{x}) = \left\{ v \in \mathbb{R}^N : \langle v, x - \bar{x} \rangle \leq 0 \,, \text{ for every } x \in D \right\}, \qquad (2.3)$$

where, as usual, $\langle \cdot, \cdot \rangle$ denotes the Euclidean scalar product in $\mathbb{R}^N$, with associated norm $\|\cdot\|$. Trivially, $\mathcal{N}_D(x) = \{0\}$ for every $x \in \operatorname{int} D$. On the other hand, it can be shown that, if $x \in \partial D$, then its normal cone contains at least a halfline. For $x \in \partial D$, we write $\mathcal{N}_D^0(x)$ to denote the cone $\mathcal{N}_D(x)$ deprived of the origin, i.e., $\mathcal{N}_D^0(x) = \mathcal{N}_D(x) \setminus \{0\}$. Clearly, if the boundary is smooth at x, then $\mathcal{N}_D^0(x) = \{\alpha\nu(x) : \alpha > 0\}$, where $\nu : \partial D \to \mathbb{R}^N$ denotes the unit outer normal vector field.

We denote by $\pi_D : \mathbb{R}^N \to D$ the projection on the convex set D. Namely, for every $\bar{x} \in \mathbb{R}^N$, $\pi_D(\bar{x})$ is the only element of D satisfying

$$\operatorname{dist}(\bar{x}, \pi_D(\bar{x})) \leq \operatorname{dist}(\bar{x}, x), \quad \text{for every } x \in D.$$

(a) *Poincaré–Bohl condition* (2.2).   (b) *Avoiding outer cones condition* (2.4).

Figure 2.1: Comparison between condition (2.2) of the Poincaré–Bohl theorem and the avoiding outer cones condition (2.4). The red halflines and cones (intended as cones in the cotangent space) indicate the regions avoided by ϑx) for some $x \in \partial D$.

We remark that π_D is a continuous function, and

$$\pi_D(\bar{x} + v) = \bar{x} \quad \text{if and only if} \quad v \in \mathcal{N}_D(\bar{x}).$$

We observe that in dimension $N = 1$, the notion of convex body coincide with that of compact interval, and that Bolzano's condition 1.3 coincide exactly with requiring that on the boundary the map ϑ avoids the direction expressed by the normal cone. This suggests us another way to naturally generalize Bolzano's Theorem in higher dimension.

Theorem 2.3. *Assume that $D \subseteq \mathbb{R}^N$ is a convex body and that $\vartheta \colon D \to \mathbb{R}^N$ is a continuous function such that*

$$\vartheta(x) \notin \mathcal{N}_D(x) \quad \text{for every } x \in \partial D \tag{2.4}$$

Then, there is $\bar{x} \in D$ such that $\vartheta(\bar{x}) = 0$ and, more generally,

$$\deg(\vartheta, D) = (-1)^N. \tag{2.5}$$

Proof. We first notice that it is not restrictive to assume that $0 \in \operatorname{int} D$. Moreover, we may assume that $\vartheta(x) \neq 0$ for every $x \in \partial D$, since otherwise the result is trivial

Let B be an open ball, centred at the origin and such that $D \subseteq B$. We consider the homotopy $\Theta \colon \overline{B} \times [0,1] \to \mathbb{R}^N$ defined by

$$\Theta(x, \lambda) = \begin{cases} 2\lambda(\pi_D(x) - x) + (1 - 2\lambda)\vartheta(\pi_D(x)) & \text{for } 0 \leq \lambda \leq \frac{1}{2} \\ 2(1 - \lambda)\pi_D(x) - x & \text{for } \frac{1}{2} \leq \lambda \leq 1 \end{cases}$$

We check that $0 \notin \Theta(\partial B \times [0,1])$. For $\lambda \in [0, 1/2]$, we observe that, for every $x \in \partial B$, $\pi_D(x) - x \in -\mathcal{N}_D^0(\pi_D(x))$ but at the same time $\vartheta(\pi_D(x)) \notin$

$\mathcal{N}_D(\pi_D(x))$. For $\lambda \in [1/2, 1]$ we notice that, by construction, $\|x\| > \|\pi_D(x)\|$ for every $x \in \partial B$. Thus, by the properties of the topological degree,

$$(-1)^N = \mathrm{d}_B(-I, B, 0) = \mathrm{d}_B(\vartheta \circ \pi_D, B, 0) = \deg(\vartheta, D)$$

where in the last equality we used the excision property, since $\vartheta(\pi_D(x)) \neq 0$ for every $x \in \overline{B} \setminus \mathrm{int}\, D$. □

Notice that, when D is a ball centred at the origin, then $\nu(x) = x/\|x\|$ for every $x \in \partial D$, so that conditions (2.2) and (2.4) are equivalent. The differences between these two conditions in a general case are illustrated in Figure 2.1.

Clearly, the *avoiding outer cones condition* (2.4) can be replaced by an *avoiding inner cones condition*, by just changing the sign of the function ϑ. In this case, the degree in (2.5) becomes $\deg(\vartheta, D) = 1$. However, in analogy with other results in literature, in our exposition we prefer dealing with outer cones, that also allow a more intuitive visualization.

We remark that the notion of normal cone allows to extend the idea of inward and outward direction to more sophisticated situations. For generalizations of Theorem 2.3 in this sense we refer to [BK97; ĆK06; Kry05].

2.2 A first idea of avoiding cones condition

As we have seen, the two classical approaches to boundary twist condition present a sort of trade-off: the Poincaré–Miranda twist allows for indefinite twist (namely the presence of contractive and expansive regions), but requires to avoid quite large areas; on the other hand, the Poincaré–Bohl twist is minimal, but applies well only to one kind of twist (contractive vs. expansive).

In this section we construct a first step in that direction, by the use of the same trick we illustrated in the proof of Theorem 2.1. We observe that, despite being usually applied with linear transformations, the same idea works also in the more general case of homeomorphisms of the Euclidean space that fix the origin.

Theorem 2.4. *Let $f: \mathbb{R}^N \to \mathbb{R}^N$ be a homeomorphism, such that $f(0) = 0$, and assume that $D \subseteq \mathbb{R}^N$ is a convex body. Let $\vartheta: D \to \mathbb{R}^N$ be a continuous function such that*

$$\vartheta(x) \notin f(\mathcal{N}_D(x)), \quad \text{for every } x \in \partial D.$$

Then, there exists $\bar{x} \in D$ such that $\vartheta(\bar{x}) = 0$. Moreover $\deg(\vartheta, D) = (-1)^{N+\sigma_f}$, where $\sigma_f = 0$ if f is orientation preserving and $\sigma_f = 1$ if it is not.

Proof. Define $g: D \to \mathbb{R}^N$ as $g = f^{-1} \circ \vartheta$. Then $g(x) \notin \mathcal{N}_D^0(x)$, for every $x \in \partial D$, and Theorem 2.3 provides the existence of an $\bar{x} \in D$ such that

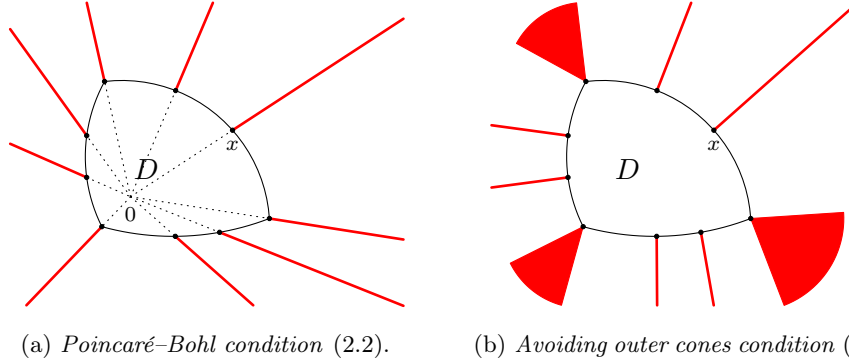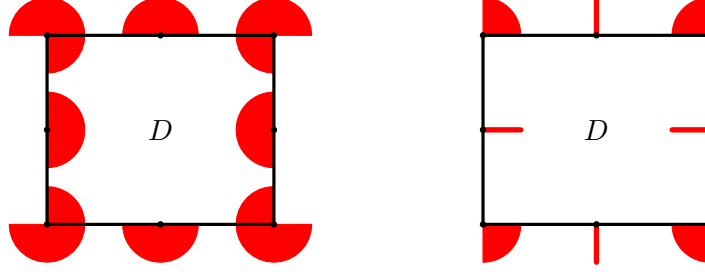(a) *Poincaré–Miranda condition.*   (b) *Avoiding cones condition.*

Figure 2.2: Comparison between condition (2.1) of the Poincaré–Miranda theorem
and the avoiding cones condition (2.6). The red halflines and cones
indicate the regions avoided by $f(x)$ for some $x \in \partial D$.

$g(\bar{x}) = 0$, and affirms that $\deg(\vartheta, D) = (-1)^N$. Being h invertible, we have
that $\vartheta(\bar{x}) = 0$, as well, while $\deg(\vartheta, D)$ can be recovered by the properties of
the degree.   □

As a simple and direct consequence of Theorem 2.4, let N_1 and N_2 be
positive integers such that $N_1 + N_2 = N$, and $K_1 \subseteq \mathbb{R}^{N_1}$, $K_2 \subseteq \mathbb{R}^{N_2}$ be two
convex bodies. We define, for every $x = (x_1, x_2) \in K_1 \times K_2$,

$$\mathcal{A}(x) = \begin{cases} \mathcal{N}_{K_1}(x_1) \times \{0\} & \text{if } x \in \partial K_1 \times \operatorname{int} K_2 \\ \{0\} \times (-\mathcal{N}_{K_2}(x_2)) & \text{if } x \in \operatorname{int} K_1 \times \partial K_2 \\ \mathcal{N}_{K_1}(x_1) \times (-\mathcal{N}_{K_2}(x_2)) & \text{if } x \in \partial K_1 \times \partial K_2 \end{cases}$$

and denote $\mathcal{A}^0(x) = \mathcal{A}(x) \setminus \{0\}$.

Corollary 2.5. *Let $\vartheta \colon K_1 \times K_2 \to \mathbb{R}^N$ be a continuous function such that*

$$\vartheta(x) \notin \mathcal{A}^0(x) \qquad \text{for every } x \in \partial(K_1 \times K_2) \tag{2.6}$$

Then, there exists $\bar{x} = (\bar{x}_1, \bar{x}_2) \in K_1 \times K_2$ such that $\vartheta(\bar{x}) = 0$, and $\deg(\vartheta, D) = (-1)^{N_1}$

Proof. The proof is a straightforward application of Theorem 2.4, with $D = K_1 \times K_2$, taking as h the linear transformation defined as the identity I_{N_1} on
$\mathbb{R}^{N_1}$ and its opposite $-I_{N_2}$ on $\mathbb{R}^{N_2}$.   □

We will refer to the condition (2.6) as the *avoiding cones condition*. To
compare it with the "classical" condition (2.1) in the Poincaré–Miranda
theorem, we consider the following example.

Example 2.6. Let us set $K_1 = [a_1, b_1]$ and $K_2 = [a_2, b_2]$, so that $D = \mathcal{R}$
is a rectangle in $\mathbb{R}^2$. We write $\vartheta(x) = (\vartheta_1(x), \vartheta_2(x))$, and, for simplicity,

we assume that that $0 \notin f(\partial D)$. Let us denote by x_1 a generic point in (a_1, b_1) and with x_2 a generic point in (a_2, b_2). The comparison between the directions prohibited by Theorem 2.1 and those by Corollary 2.5 is illustrated in Figure 2.2 and summarized in the following table:

Poincaré–Miranda	Avoiding cones condition
$f_1(a_1, x_2) < 0$	$f_1(a_1, x_2) < 0$ or $f_2(a_1, x_2) \neq 0$
$f_1(b_1, x_2) > 0$	$f_1(b_1, x_2) > 0$ or $f_2(b_1, x_2) \neq 0$
$f_2(x_1, a_2) > 0$	$f_2(x_1, a_2) > 0$ or $f_1(x_1, a_2) \neq 0$
$f_2(x_1, b_2) < 0$	$f_2(x_1, b_2) < 0$ or $f_1(x_1, b_2) \neq 0$
$f_1(a_1, a_2) < 0$ and $f_2(a_1, a_2) > 0$	$f_1(a_1, a_2) < 0$ or $f_2(a_1, a_2) > 0$
$f_1(a_1, b_2) < 0$ and $f_2(a_1, b_2) < 0$	$f_1(a_1, b_2) < 0$ or $f_2(a_1, b_2) < 0$
$f_1(b_1, a_2) > 0$ and $f_2(b_1, a_2) > 0$	$f_1(b_1, a_2) > 0$ or $f_2(b_1, a_2) > 0$
$f_1(b_1, b_2) > 0$ and $f_2(b_1, b_2) < 0$	$f_1(b_1, b_2) > 0$ or $f_2(b_1, b_2) < 0$

The same behaviour is observed also in higher dimensions. For a general point $x \in \partial \mathcal{R}$ lying on an $(N - M)$-dimensional facet of the rectangle, the Poincaré–Miranda theorem requires M inequalities, each on a different component of $\vartheta(x)$. For the same point x, our avoiding cones condition requires much less: only in the case that all the other $N - M$ components of $f(x)$ are null, then at least one of those M inequalities must be satisfied. This shows that our Corollary 2.5 also generalizes [IJ05, Theorem 3.4].

Similar considerations also apply to other variants of the Poincaré–Miranda theorem for sets D which are product of balls instead of intervals, as for instance in [Maw13, Corollary 2]. For one of these situations, namely the cylinder, the avoiding cones condition is illustrated in Figure 2.5.

There is a second way to describe the difference between the avoiding cones condition (2.6) and assumption (2.1) in the Poincaré–Miranda theorem. Whereas the avoiding cones condition requires that $\vartheta(x)$ does not lie in $\mathcal{A}(x)$, the Poincaré–Miranda theorem requires that $\vartheta(x)$ actually lies in the polar cone of $\mathcal{A}(x)$, defined as

$$\check{\mathcal{A}}(x) = \{v \in \mathbb{R}^N : \langle v, w \rangle \leq 0 \text{ for every } w \in \mathcal{A}(x)\}$$

besides possibly excluding the trivial case $\vartheta(x) = 0$.

2.3 Truncated convex bodies

The Poincaré–Miranda Theorem and many of its generalizations consider a rectangular domain, or at least the product of convex sets. We now want to replace this structural assumption by introducing a new class of sets, which will lead us to some topologically different situations.
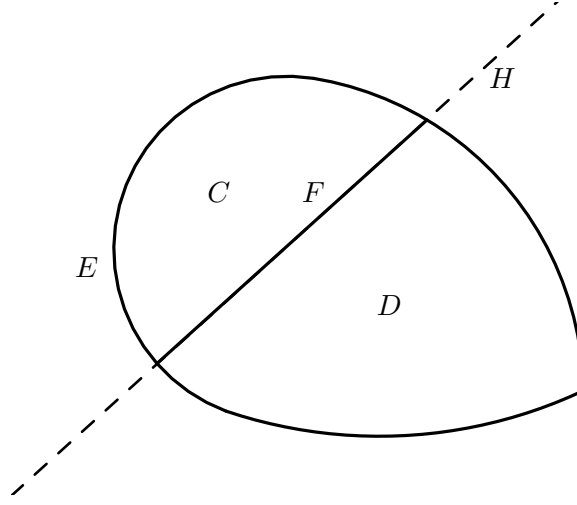
Figure 2.3: An example of truncation. The sets C and D are truncated with respect to F and E is a reconstruction for both.

Given a convex body D and a set $F \subseteq \partial D$, we say that D is *truncated* in F if there exists a convex body E and a hyperplane H with the following properties (see Figure 2.3):

- $F = D \cap H$, and H is a supporting hyperplane for the set D;

- $D = E \cap \mathcal{H}_D$, where $\mathcal{H}_D$ is the closed halfspace bounded by H that includes D;

- the set $C := \overline{E \setminus \mathcal{H}_D}$ has nonempty interior.

We call E a *reconstruction* of D with respect to F. Notice that $C = \overline{E \setminus D}$ is a convex body, which is truncated in F, as well.

As possible examples of truncated convex bodies we have rectangles, polytopes and cylinders. Balls, on the contrary, are not truncated. Neither, in general, having a $(N-1)$-dimensional face is a sufficient condition to be truncated: just consider a square with smoothed angles.

In order to investigate the properties of a face F suitable for truncation, let us denote by $\partial^{N-1} F$ the boundary of F considered as a subset of H. Moreover, along with normal cones, it is useful to consider also the set-valued analogue of the unit normal vector ν: it is the map $\boldsymbol{\nu}_D$, from ∂D to $\mathcal{S}^{N-1} = \{ y \in \mathbb{R}^N : \|y\| = 1 \}$, defined as

$$\boldsymbol{\nu}_D(x) = \left\{ \frac{y}{\|y\|} : y \in \mathcal{N}_D^0(x) \right\}$$

Denoting with cone$[A]$ the cone generated by a set A, we then have that

$$\mathcal{N}_D(x) = \operatorname{cone}\left[\boldsymbol{\nu}_D(x) \right]$$

Since the normal cone $\mathcal{N}_D$ is a map from D to the set of closed, convex subsets of $\mathbb{R}^N$, having closed graph, we can see that $\boldsymbol{\nu}_D$ is an upper semicontinuous map from ∂D to the set of compact subsets of $\mathbb{R}^N$ (for an introduction to set-valued maps, we refer to [AC84]).

We remark that our definition (2.3) of the normal cone for convex sets is equivalent to setting

$$\mathcal{N}_{\mathcal{D}}(\bar{x}) = \left\{ v \in \mathbb{R}^N : \langle v, x - \bar{x} \rangle \leq o(\|x - \bar{x}\|) , \ x \in D \right\} \qquad (2.7)$$

thus underlining the local nature of the normal cone. This definition is usually adopted to extend the notion of normal cones to non-convex sets (see, e.g., [RW98]).

Given a point $\bar{x} \in \partial D$, to every vector $v \in \mathcal{N}_D^0(\bar{x})$ we can associate the supporting hyperplane containing $\bar{x}$,

$$H_v = \{\bar{x} + w : \langle v, w \rangle = 0\}$$

and the corresponding halfspace containing D:

$$\mathcal{H}_v = \{x \in \mathbb{R}^N : \langle v, x - \bar{x} \rangle \leq 0\}$$

Being D a convex body, it coincides with the intersection of its supporting halfspaces [GH96, Prop. 2 p. 58].

Proposition 2.7. *If D is a convex body, truncated in F, then*

(i) *F is closed, convex, and $F = E \cap H$;*

(ii) *F has a non-empty interior if considered as a subset of H;*

(iii) *if $x \in \partial^{N-1} F$, then $\boldsymbol{\nu}_D(x)$ is multivalued.*

Proof. The proof of (i) is immediate, so we start with the proof of (ii). Since D and C are convex bodies, we can find two open balls $B_D = \mathcal{B}^N(p_D, \varepsilon) \subseteq D$ and $B_C = \mathcal{B}^N(p_C, \varepsilon) \subseteq C$ with the same sufficiently small radius ε. We observe that H separates B_D and B_C, and so there is a unique point p_F in $H \cap [p_D, p_C]$, denoting the intersection of H with the segment joining p_D and p_C. We have

$$B_H^{N-1}(p_F, \varepsilon) = \mathcal{B}^N(p_F, \varepsilon) \cap H \subseteq E \cap H \subseteq F$$

thus showing that F has non-empty interior as a subset of H.

Regarding (iii), it suffices to show that, if $x \in \partial^{N-1} F$, then there exist two different supporting hyperplanes for D intersecting x, which are associated with different unit outer normal vectors. Since $x \in \partial E$, there exists a supporting hyperplane $\widetilde{H}$ for E, with $x \in \widetilde{H}$, implying that $\widetilde{H}$ is also a supporting hyperplane for D. On the other hand, we know that H a supporting hyperplane for D, as well, with $x \in H$, and the set $C = \overline{E \setminus \mathcal{H}_D}$ has a nonempty interior, where $\mathcal{H}_D$ is the closed halfspace bounded by H that includes D. We obtain that $H \neq \widetilde{H}$, thus completing the proof. $\qquad \square$

An immediate consequence is that smooth convex bodies are not truncated. We can interpret (iii) as the necessity for D to have "edges" on the boundary of F.

We now consider multiple truncations. Given a convex body $D \subseteq \mathbb{R}^N$ and a family $\{F_1, \ldots, F_M\}$ of pairwise disjoint sets, we say that D is *truncated* in $\{F_1, \ldots, F_M\}$ if there exists a convex body E and some hyperplanes $H_1, \ldots, H_M$ with the following properties:

- for every i, $F_i = D \cap H_i$, and H_i is a supporting hyperplane for the set D;

- $D = E \cap \mathcal{H}_D^1 \cap \cdots \cap \mathcal{H}_D^M$, where $\mathcal{H}_D^i$ is the closed halfspace bounded by H_i that includes D;

- for every i, the set $C_i := \overline{E \setminus \mathcal{H}_D^i}$ has nonempty interior.

We call E a *reconstruction* of D with respect to $\{F_1, \ldots, F_M\}$. Notice that each C_i is a convex body, which is truncated in F_i. Moreover, the sets C_i are pairwise disjoint, and one has

$$C_1 \cup \cdots \cup C_M = \overline{E \setminus D}$$

Example 2.8 (Polygons and polyhedra)**.** In $\mathbb{R}^2$, a polygon with faces F_j is truncated in $\{F_1, \ldots, F_M\}$ if the faces $F_1, \ldots, F_M$ are not pairwise adjacent. The simplest way to construct a convex body truncated in M faces is to consider the $2M$-agon as truncated on alternate faces.

For polyhedra in $\mathbb{R}^3$ we need that the faces where truncations occur do not share any vertices. Thus, the cube can be truncated in at most two (opposite) faces, and so the octahedron, while the icosahedron can be truncated in at most four faces. One way to construct polyhedra truncated in M faces is to consider the prism with a $2M$-agonal base as truncated on alternate lateral faces.

2.4   Optimal reconstructions

Let us spend a few words about reconstructions. Clearly, for every truncated convex body D, there are infinitely many possible reconstructions; our plan is to focus on some special reconstructions which are *optimal* for our purposes. They will indeed minimize the cones $\mathcal{A}(x)$ to be avoided by the vector field, and hence provide the best choice for the application of the results to be stated in Section 2.5. Some preliminary remarks are in order.

Given $\bar{x} \in \partial D$, we can consider the intersection of all those supporting halfspaces whose boundary contains $\bar{x}$. Using the relationship with the normal cone, we can write this intersection as

$$\{x \in \mathbb{R}^N \colon \langle v, x - \bar{x} \rangle \leq 0 \,, \text{ for every } v \in \mathcal{N}_D(\bar{x})\} = \bar{x} + \check{\mathcal{N}}_D(\bar{x}) \qquad (2.8)$$

The polar $\check{\mathcal{N}}_D(\bar{x})$ of the normal cone is the so-called *tangent cone* [Cla90; RW98].

In the following, we denote by conv$[A]$ the convex hull of a given set A, that is the smallest convex set including A. The following lemma is a first step towards optimal reconstructions.

Lemma 2.9. *Let $D \subseteq \mathbb{R}^N$ be a convex body truncated in F. Then, there exists a closed convex set $E_{\max}$ such that $E_{\max} \cap \mathcal{H}_D = D$, with the property that, if E is any reconstruction of D with respect to F, then $E \subseteq E_{\max}$.*

Proof. If $x \in \partial D \setminus F$, then, in a sufficiently small neighbourhood, of x, the set D coincides with any reconstruction E with respect to F, and hence $\mathcal{N}_D(x) = \mathcal{N}_E(x)$. This means that E and D have the same supporting hyperplanes containing x and therefore, by (2.8), we have that $E \subseteq x + \check{\mathcal{N}}_D(x)$. Now, let us set

$$E_{\max} = \bigcap_{x \in \partial D \setminus F} \left[x + \check{\mathcal{N}}_D(x) \right]$$

By what we have just seen, it follows that $E \subseteq E_{\max}$ for every possible reconstruction E. Hence, $D \subseteq E_{\max} \cap \mathcal{H}_D$. Furthermore, $E_{\max}$ is a closed convex set since it is the intersection of closed convex sets.

We want to prove that $E_{\max} \cap \mathcal{H}_D = D$. First of all, we prove that $\partial D \subseteq \partial(E_{\max} \cap \mathcal{H}_D)$. Indeed, each point x of ∂D belongs to $E_{\max} \cap \mathcal{H}_D$, since $D \subseteq E_{\max} \cap \mathcal{H}_D$. If $x \in \partial D \setminus F$, then there is a supporting hyperplane of $E_{\max}$ containing x; on the other hand, if $x \in F$, then $x \in \mathcal{H}_D$. In any case, there is a supporting hyperplane of $E_{\max} \cap \mathcal{H}_D$ containing x, so $x \in \partial(E_{\max} \cap \mathcal{H}_D)$.

Suppose now by contradiction that there exists $y \in E_{\max} \cap \mathcal{H}_D$ such that $y \notin D$. Let $U = \mathcal{B}(x_0, r)$ be an open ball contained in D. By convexity, there exists a unique $\bar{x} \in \partial D \cap [x_0, y]$. It is easy to show that there exists an open neighbourhood V of $\bar{x}$ such that $V \subseteq \text{conv}[U \cup \{y\}] \subseteq E_{\max} \cap \mathcal{H}_D$. Then, $\bar{x} \notin \partial(E_{\max} \cap \mathcal{H}_D)$, contradicting the fact that $\bar{x} \in \partial D$. Thus, $E_{\max} \cap \mathcal{H}_D = D$, and the proof is completed. $\square$

An immediate consequence of the above lemma is that $E_{\max}$ is the smallest set containing every reconstruction of D with respect to F. More precisely, since the intersection of $E_{\max}$ with any arbitrarily large closed ball containing D is a reconstruction, we deduce that every point of $E_{\max}$ is contained in a reconstruction. So, $E_{\max}$ is the union of all possible reconstructions of D with respect to F.

We say that a reconstruction E is *optimal* if, for every $x \in F$,

$$\mathcal{N}_C(x) = \mathcal{N}_{C_{\max}}(x) \qquad \text{where } C_{\max} = \overline{E_{\max} \setminus D}$$
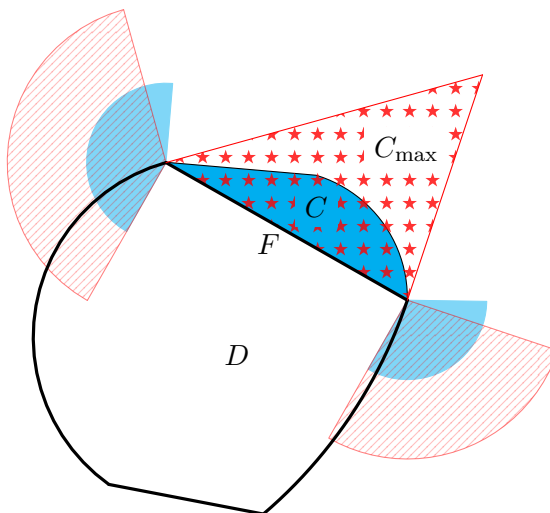
Figure 2.4: An example of non-optimal reconstruction $E = D \cup C$ (blue), compared
with the optimal reconstruction $E_{\max}$ (red, starred), with emphasis on
their respective normal cones.

Since, for every reconstruction, the inclusion $\mathcal{N}_C(x) \supseteq \mathcal{N}_{C_{\max}}(x)$ holds for
every $x \in F$, an optimal reconstruction minimizes $\mathcal{N}_C(x)$, as illustrated in
Figure 2.4.

In general, $E_{\max}$ is not bounded and therefore it is not a reconstruction;
however it is always possible to build an optimal reconstruction simply taking
$E = E_{\max} \cap K$, where K is a convex body such that $D \subseteq \operatorname{int} K$. Moreover,
one can find an optimal reconstruction E which is as close to D as desired.
Indeed, given $\varepsilon > 0$, it suffices to take $E = E_{\max} \cap \mathcal{B}[D, \varepsilon]$, where

$$\mathcal{B}[D, \varepsilon] = \{x \in \mathbb{R}^N : \operatorname{dist}(x, D) \leq \varepsilon\}$$

to have an optimal reconstruction whose distance from D is at most ε.

Example 2.10 (Cylinders/prisms)**.** Let $D = K \times [-1, 1]$, where K is a convex
body in $\mathbb{R}^{N-1}$. Then, D is truncated in any of its two bases. For instance,
we can take $H = \mathbb{R}^{N-1} \times \{1\}$, and $F = K \times \{1\}$. In this case, we see that
$E_{\max} = K \times [-1, +\infty)$, and a possible optimal reconstruction with respect to
the face F is given by $E = D \cup C$, where $C = K \times [1, 2]$. Notice that, if instead
of C we take, for instance, $C' = \{(x, y + 1) : x \in K, 0 \leq y \leq \operatorname{dist}(x, \partial K)\}$, it
is true that we have a reconstruction, but it is not optimal.

Example 2.11 (Polytopes)**.** If D is a convex polytope with faces $F_1, \ldots, F_m$,
it is truncated with respect to any of them. Let us focus on a particular one,

$F = F_j$. Correspondingly, we will have

$$E_{j,\max} = \bigcap_{\substack{i=1 \\ i \neq j}}^{m} \mathcal{H}_D^i$$

where $\mathcal{H}_D^i$ denotes the halfspace including D bounded by the supporting hyperplane H_i generated by the face F_i. If $E_{j,\max}$ is bounded, then it is an optimal reconstruction. This is the case, for instance, of the regular m-agon for $m \geq 5$ in $\mathbb{R}^2$, where the set C_j is the triangle generated by the prolongation of the adjacent edges. An example of unbounded $E_{j,\max}$ is given by regular simplices, where it is a cone.

In the case of a convex body D truncated at $\{F_1, \ldots, F_M\}$, we say that a reconstruction $E = D \cup C_1 \cup \cdots \cup C_M$ is *optimal* if, for every truncation F_i, the reconstruction $E_i = D \cup C_i$ is optimal.

2.5 Main results

Let $D \subseteq \mathbb{R}^N$ be a convex body truncated in $\{F_1, \ldots, F_M\}$, with an optimal reconstruction $E = D \cup C_1 \cup \cdots \cup C_M$. We define the map $\mathcal{A}$, from ∂D to the closed, convex cones of $\mathbb{R}^N$, as

$$\mathcal{A}(x) = \begin{cases} \mathcal{N}_{C_i}(x) & \text{if } x \in F_i \\ \mathcal{N}_D(x) & \text{if } x \in \partial D \setminus \bigcup_{i=1}^M F_i \end{cases}$$

We now state the main theorem of this paper.

Theorem 2.12. *Let $D \subseteq \mathbb{R}^N$ be a convex body truncated in $\{F_1, \ldots, F_M\}$, with $M \geq 2$, and let $\vartheta \colon D \to \mathbb{R}^N$ be a continuous function satisfying*

$$\vartheta(x) \notin \mathcal{A}(x) \quad \text{for every } x \in \partial D$$

Then, there exists $\bar{x} \in D$ such that $\vartheta(\bar{x}) = 0$, and we have

$$\deg(\vartheta, D) = (-1)^N (1 - M)$$

The proof of Theorem 2.12 will be given in Section 2.7. We now provide some examples where it can be applied.

Example 2.13 (Cylinders/prisms)**.** Let $D = K \times [-1, 1]$, where $K \subseteq \mathbb{R}^{N-1}$ is a convex body. The set D is truncated in $F_- = K \times \{-1\}$ and $F_+ = K \times \{1\}$, and we have

$$\mathcal{A}(x) = \begin{cases} \mathcal{N}_D(x) & \text{if } x \in \partial K \times \,] -1, 1[\\ -\mathcal{N}_D(x) & \text{if } x \in \text{int } K \times \{-1, 1\} \\ \mathcal{N}_K(y) \times (-\infty, 0] & \text{if } x = (y, 1), \text{ with } y \in \partial K \\ \mathcal{N}_K(y) \times [0, +\infty) & \text{if } x = (y, -1), \text{ with } y \in \partial K \end{cases}$$
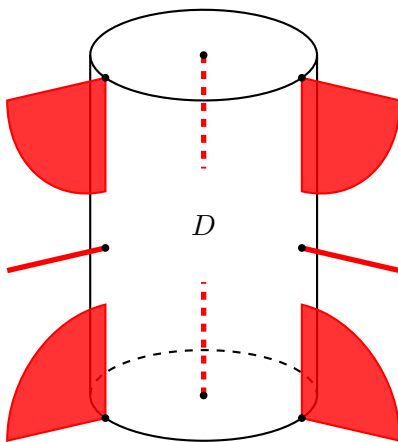
Figure 2.5: Avoiding cones in the case of the cylinder.

These cones are illustrated for the three-dimensional case in Figure 2.5, where K is a circle in $\mathbb{R}^2$. We remark that, in the case of cylinders, Theorem 2.12 coincides with Corollary 2.5.

Example 2.14 (Polytopes). Let the convex polytope D, with faces F_j, be truncated in $\{F_1, \ldots, F_M\}$. For every $x \in \partial D$, we denote by $I(x) = \{i : x \in F_i\}$ the set of indices of those faces containing x, and by ν_i the outward unit vector normal to F_i. Furthermore, we denote by $\sigma(i)$ the sign of the avoiding cones condition in F_i, namely

$$\sigma(i) = \begin{cases} -1 & \text{if } i = 1, \ldots, M \text{ (avoiding inner normal cones)} \\ +1 & \text{otherwise (avoiding outer normal cones)} \end{cases}$$

Then, $\mathcal{A}(x)$ corresponds to the convex cone generated by the set

$$\{\sigma(i)\nu_i : i \in I(x)\}$$

whose elements are the outer/inner normal cones assigned by $\mathcal{A}$ to the points in the interior of the faces containing x. We illustrate in Figure 2.6 the particular case of an hexagon truncated in three alternate faces. We observe that, being in this case $N = 2$ and $M = 3$, if ϑ satisfies the avoiding cones condition of Theorem 2.12, then

$$\deg(\vartheta, D) = (-1)^2(1 - 3) = -2$$

We finally notice that Theorem 2.3 can be interpreted as a version of Theorem 2.12, with $M = 0$. So, having Theorem 2.4 in mind, we can also write the following extension of Theorem 2.12.
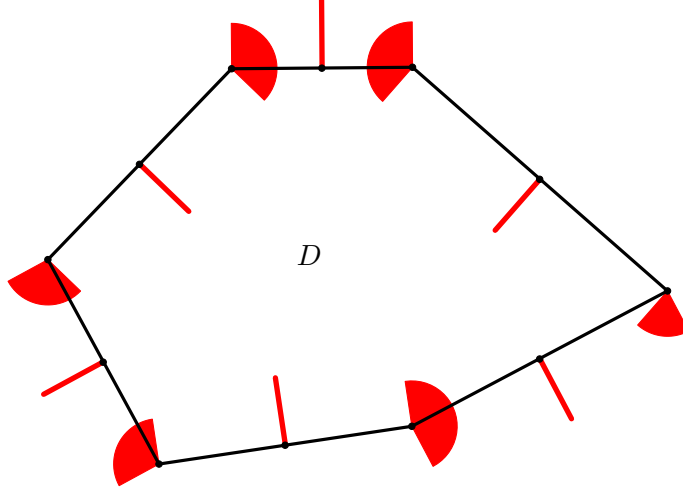
Figure 2.6: Avoiding cones in the case of a hexagon.

Theorem 2.15. *Let $f \colon \mathbb{R}^N \to \mathbb{R}^N$ be a homeomorphism, such that $f(0) = 0$, and assume that $D \subseteq \mathbb{R}^N$ is a convex body truncated in $\{F_1, \dots, F_M\}$, with $M \geq 2$. Let $\vartheta \colon D \to \mathbb{R}^N$ be a continuous function such that*

$$\vartheta(x) \notin f(\mathcal{A}(x)) \quad \text{for every } x \in \partial D$$

Then, there exists $\bar{x} \in D$ such that $\vartheta(\bar{x}) = 0$. Moreover

$$\deg(\vartheta, D) = (-1)^{N + \sigma_f}(1 - M)$$

where $\sigma_f = 0$ if f is orientation preserving and $\sigma_f = 1$ if it is not.

Until now, the domain D of our functions has been supposed to be a convex body. However, all our results can be easily extended to sets $\mathcal{D}$ which are just diffeomorphic to a convex body D. By this we mean that there are two open sets A, B in $\mathbb{R}^N$, with $D \subseteq A$, $\mathcal{D} \subseteq B$, and a diffeomorphism $\varphi \colon A \to B$, such that

$$\mathcal{D} = \varphi(D)$$

To define the normal cone to $\mathcal{D}$ at a boundary point $y \in \partial \mathcal{D}$, let us set $\psi = \varphi^{-1} \colon B \to A$, so that $\psi(y) \in \partial D$, and set

$$\mathcal{N}_{\mathcal{D}}(y) = (\psi'(y))^T \mathcal{N}_D(\psi(y))$$

We remark that this choice preserves the extended notion of normal cone recalled in (2.7).

(a) *Poincaré–Bohl condition* (2.2).   (b) *Avoiding outer cones condition* (2.9).
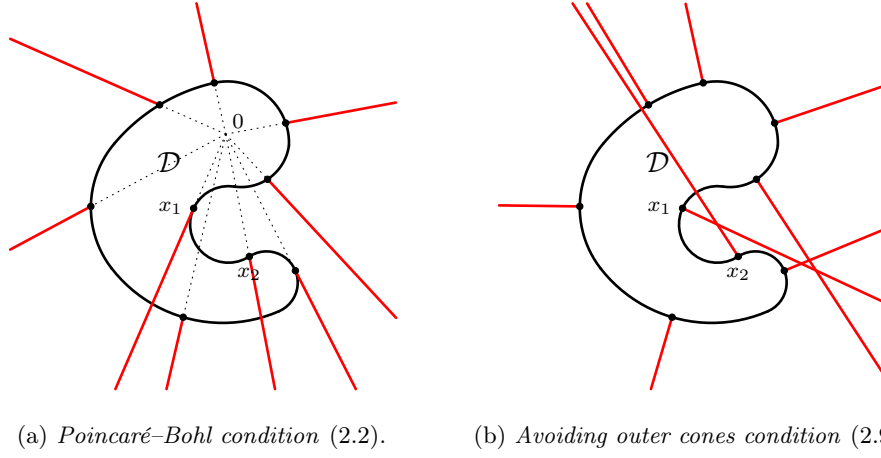
Figure 2.7: Comparison between condition (2.2) of the Poincaré–Bohl theorem and the avoiding outer cones condition (2.9). The red halflines and cones indicate the regions avoided by $f(x)$ for some $x \in \partial D$.

Let us first go back to our variant of the Poincaré–Bohl theorem. Writing, as usual, $\mathcal{N}_{\mathcal{D}}^0(y) = \mathcal{N}_{\mathcal{D}}(y) \setminus \{0\}$, we have the following extension of Theorem 2.3.

Theorem 2.16. *Assume that $\mathcal{D}$ is a subset of $\mathbb{R}^N$, diffeomorphic to a convex body. Let $\vartheta \colon \mathcal{D} \to \mathbb{R}^N$ be a continuous function such that*

$$\vartheta(y) \notin \mathcal{N}_{\mathcal{D}}^0(y) \quad \textit{for every } y \in \partial \mathcal{D} \tag{2.9}$$

Then there exists $\bar{y} \in \mathcal{D}$ such that $\vartheta(\bar{y}) = 0$. Moreover

$$\deg(\vartheta, D) = (-1)^{N + \sigma_\varphi}$$

where $\sigma_\varphi = 0$ if φ is orientation preserving and $\sigma_\varphi = 1$ if it is not.

Proof. Using the above notation, we have $D = \psi(\mathcal{D})$ and we define $\tilde{\vartheta} \colon D \to \mathbb{R}^N$ as

$$\tilde{\vartheta}(x) = (\varphi'(x))^T \vartheta(\varphi(x))$$

Then, condition (2.4) holds replacing ϑ by $\tilde{\vartheta}$, so Theorem 2.3 applies, and we easily conclude. $\qquad\square$

In Figure 2.7 we illustrate the avoiding cones condition of Theorem 2.16, in the case when $\mathcal{D}$ has a smooth boundary.

Now, in order to extend Theorem 2.12, let us consider a set $\mathcal{D}$ which is diffeomorphic to a convex body D, truncated in $\{F_1, \ldots, F_M\}$. Since $D \subseteq A$, $\mathcal{D} \subseteq B$, and both sets A an B are open, we can choose a reconstruction E

of D with respect to $\{F_1, \ldots, F_M\}$, even an optimal reconstruction, to be contained in A, as well. Setting

$$\mathcal{E} = \varphi(E), \; \mathcal{F}_1 = \varphi(F_1), \; \ldots, \; \mathcal{F}_M = \varphi(F_M)$$

we say that $\mathcal{E}$ is a *reconstruction* of $\mathcal{D}$ with respect to $\{\mathcal{F}_1, \ldots, \mathcal{F}_M\}$. We also say that $\mathcal{D}$ is *truncated* in $\{\mathcal{F}_1, \ldots, \mathcal{F}_M\}$. Then, referring to the notation introduced in Section 2.3, we have $E = D \cup C_1 \cup \cdots \cup C_M$, and setting $\mathcal{C}_1 = \varphi(C_1), \ldots, \mathcal{C}_M = \varphi(C_M)$, we can define the cones

$$\mathcal{A}(x) = \begin{cases} \mathcal{N}_{\mathcal{C}_i}(y) & \text{if } y \in \mathcal{F}_i \\ \mathcal{N}_{\mathcal{D}}(y) & \text{if } y \in \partial\mathcal{D} \setminus \bigcup_{i=1}^{M} \mathcal{F}_i \end{cases}$$

Theorem 2.17. *Let $\mathcal{D} \subseteq \mathbb{R}^N$, diffeomorphic to a convex body, be truncated in $\{\mathcal{F}_1, \ldots, \mathcal{F}_M\}$, with $M \geq 2$, and let $\vartheta \colon \mathcal{D} \to \mathbb{R}^N$ be a continuous function satisfying*

$$\vartheta(y) \notin \mathcal{A}(y) \quad \text{for every } y \in \partial\mathcal{D}$$

Then there exists $\bar{y} \in \mathcal{D}$ such that $\vartheta(\bar{y}) = 0$. Moreover

$$\deg(\vartheta, D) = (-1)^{N + \sigma_\varphi}(1 - M)$$

where $\sigma_\varphi = 0$ if φ is orientation preserving and $\sigma_\varphi = 1$ if it is not.

An example of the avoiding cones condition of Theorem 2.17 is illustrated in Figure 2.8, where the set $\mathcal{D}$ is diffeomorphic to a hexagon D (cf. Figure 2.6).

We end this section with the analogue of Theorem 2.15.

Theorem 2.18. *Let $f \colon \mathbb{R}^N \to \mathbb{R}^N$ be a homeomorphism, such that $f(0) = 0$, assume that $\mathcal{D} \subseteq \mathbb{R}^N$, diffeomorphic to a convex body, is truncated in $\{\mathcal{F}_1, \ldots, \mathcal{F}_M\}$, with $M \geq 2$, and let $\vartheta \colon \mathcal{D} \to \mathbb{R}^N$ be a continuous function satisfying*

$$\vartheta(y) \notin f(\mathcal{A}(y)) \quad \text{for every } y \in \partial\mathcal{D}$$

Then there exists $\bar{y} \in \mathcal{D}$ such that $\vartheta(\bar{y}) = 0$. Moreover

$$\deg(\vartheta, D) = (-1)^{N + \sigma_f + \sigma_\varphi}(1 - M)$$

where $\sigma_f = 0$ (resp. $\sigma_\varphi = 0$) if f (resp. φ) is orientation preserving and $\sigma_f = 1$ (resp. $\sigma_\varphi = 1$) if it is not.

2.6   An application to multiple saddles

In this section we show that our results can be applied to deal with the gradient of a potential V having degenerate multiple saddle points, where multiple expansive and contractive directions appear.
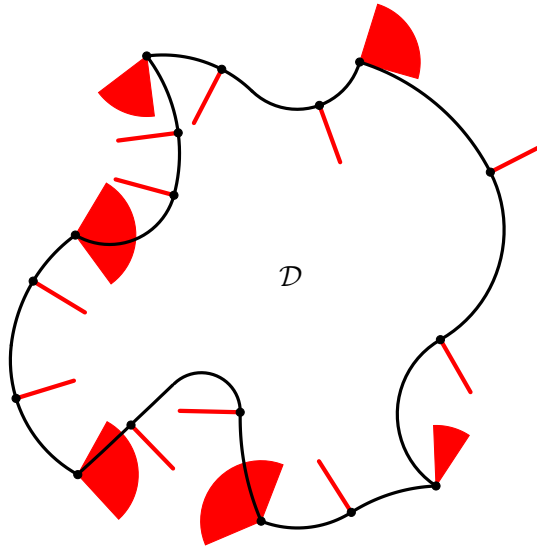
Figure 2.8: Avoiding cones in the case of a non-convex set diffeomorphic to a hexagon.

A detailed exposition for the planar case can be found in [DKV09], where the authors considered k-fold saddles formed by the alternation, around the critical point, of $k + 1$ ascending directions and $k + 1$ descending directions: the first ones identified by trajectories of the flow of ∇V escaping from the critical point, while the second ones by trajectories converging to the critical point. (For a similar situation, see also [AO98; FF05; FM06].) With this description, the standard non-degenerate saddle is an example of 1-fold saddle, whereas the monkey saddle is a 2-fold saddle (cf. Figure 2.9).

In higher dimensions, the criterion of alternation is no longer applicable
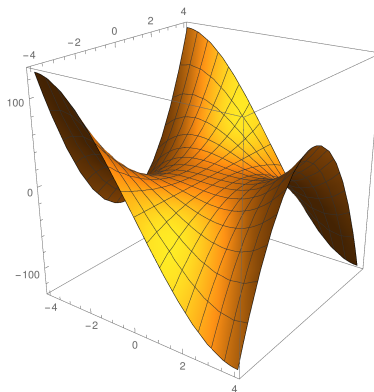
Figure 2.9: The monkey saddle $V(x_1, x_2) = x_1^3 - 3x_1 x_2^2$.

and more sophisticated situations may arise. Different approaches, mainly related to the Conley index or some of its generalizations, have been used to study the degree in the case of higher dimensional multiple saddle points (cf. [Dan84; Ryb87; Srz85]). We propose here a simpler strategy, based on our Theorem 2.12, to recover some of those results.

We consider a continuously differentiable function $V: \mathcal{B}[0, R] \to \mathbb{R}$, and assume that, near the boundary of the domain, namely for $0 < r \leq \|x\| \leq R$, it can be written in the form

$$V(x) = \rho(\|x\|)S\left(\frac{x}{\|x\|}\right) \tag{2.10}$$

where $\rho: [r, R] \to (0, +\infty)$ and $S: \mathcal{S}^{N-1} \to \mathbb{R}$ are continuously differentiable functions, and $\rho'(\xi) > 0$, for every $\xi \in [r, R]$. This factorization, in a certain sense, generalizes the idea of positive homogeneity, which corresponds to the choice $\rho(t) = t^\alpha$, for a certain $\alpha > 0$.

In this region of the domain, the field $\nabla V(x)$ can be decomposed in radial and tangential components as

$$\nabla V(x) = \rho'(\|x\|)\frac{x}{\|x\|}S\left(\frac{x}{\|x\|}\right) + \frac{\rho(\|x\|)}{\|x\|}\nabla_\mathcal{S}S\left(\frac{x}{\|x\|}\right) \tag{2.11}$$

where $\nabla_\mathcal{S}S(x)$ denotes the tangential gradient of $S(x)$; namely, for every $y \in \mathcal{S}^{N-1}$:

$$\nabla_\mathcal{S}S(x) = \nabla S(y) - \langle y, \nabla S(y) \rangle y$$

We see that $\nabla_\mathcal{S}S$ corresponds to the surface gradient on the unit sphere of the function $x \mapsto S(x/\|x\|)$, defined on $\mathbb{R}^N \setminus \{0\}$.

Since in (2.11) the two terms in the sum are orthogonal, their sum vanishes if and only if they are both zero. Hence, if $r \leq \|x\| \leq R$, we have that

$$\nabla V(x) = 0 \quad \Leftrightarrow \quad S\left(\frac{x}{\|x\|}\right) = 0 \text{ and } \nabla_\mathcal{S}S\left(\frac{x}{\|x\|}\right) = 0$$

In particular, if we want the degree $\deg(\nabla V, \mathcal{B}[0, R])$ to be well defined, we need to ask that $S(x)$ and $\nabla_\mathcal{S}S(x)$ do not vanish simultaneously at any $x \in \mathcal{S}^{N-1}$.

Let us state the main result of this section.

Theorem 2.19. *In the above setting, assume that*

(i) *if $x \in \mathcal{S}^{N-1}$ satisfies $\nabla_\mathcal{S}S(x) = 0$, then $S(x) \neq 0$;*

(ii) *the set $\{x \in \mathcal{S}^{N-1} : S(x) \geq 0\}$ is the union of M disjoint subsets, which are diffeomorphic to an $(N-1)$-dimensional ball.*

Then, $\deg(\nabla V, \mathcal{B}[0, R]) = (-1)^N (1 - M)$.

Proof. If $M = 0$, we have that $S(x) < 0$ for every $x \in \mathcal{S}^{N-1}$. Taking $D = \mathcal{B}[0, R]$, we have that, for every $x \in \partial D$, the cone to avoid is $\mathcal{N}_D(x) = \{\lambda x \colon \lambda \geq 0\}$. Being $V(x) < 0$, the radial component of $\nabla V(x)$ is not zero and points inward, so $\nabla V(x) \notin \mathcal{N}_D(x)$. Theorem 2.3 can then be applied to conclude.

So, from now on, we can assume $M \geq 1$. Given a vector $y \in \mathcal{S}^{N-1}$, for every $x \in \mathcal{S}^{N-1}$ such that $x \neq \pm y$, we define

$$\sigma(x; y) = \frac{y - x - \langle x, y - x \rangle\, x}{\|y - x - \langle x, y - x \rangle\, x\|}$$

It is the unit vector on the tangent space to $\mathcal{S}^{N-1}$ in x, associated to the shortest path from x to y. We say that a local maximum point $y \in \mathcal{S}^{N-1}$ for S is *regular* if there exists a neighbourhood U of y, with the property that

$$\langle \sigma(x; y), \nabla_{\mathcal{S}} S(x) \rangle > 0 \quad \text{for every } x \in U \cap \mathcal{S}^{N-1}$$

This condition is true, for instance, if y is a non-degenerate local maximum point. We first prove the theorem when (ii) is replaced by the following stronger assumption:

(ii*) if $y \in \mathcal{S}^{N-1}$ satisfies $\nabla_{\mathcal{S}} S(y) = 0$ and $S(y) \geq 0$, then y is a regular local maximum point for S, and $S(y) > 0$. Moreover, there are exactly M of such points.

Let $s_1, \ldots, s_M$ be the regular maximum points of condition (ii*). For any $\varepsilon \in (0, R - r)$, we set

$$\mathcal{H}_i = \{x \in \mathbb{R}^N \colon \langle x, s_i \rangle \leq R - \varepsilon\}$$

Let

$$D = \mathcal{B}[0, R] \cap \mathcal{H}_1 \cap \mathcal{H}_2 \cap \cdots \cap \mathcal{H}_M$$

and define $H_i = \partial \mathcal{H}_i$. If ε is sufficiently small, then D is a convex body truncated in $\{F_1, \ldots F_M\}$, with $F_i = \mathcal{B}[0, R] \cup H_i$, and $E = \mathcal{B}[0, R]$ is an optimal reconstruction. Let us verify that the avoiding cones condition holds, provided that ε is sufficiently small.

For $x \in \partial D \setminus \bigcup_{i=1}^{M} F_i$, the cone to avoid is $\mathcal{A}(x) = \mathcal{N}_D(x) = \{\lambda x \colon \lambda \geq 0\}$. If $V(x) < 0$, then the radial component of $\nabla V(x)$ is not zero and points inward, so $\nabla V(x) \notin \mathcal{A}(x)$. If $V(x) \geq 0$, since $x \neq Rs_i$ for each $i = 1, \ldots, M$, the tangential component of $\nabla V(x)$ is not zero and so $\nabla V(x) \notin \mathcal{A}(x)$.

If $x \in \operatorname{int}_{\partial D} F_i$ for some $i = 1, \ldots, M$, then $\mathcal{A}(x) = \{-\lambda s_i \colon \lambda \geq 0\}$. (Note that $\operatorname{int}_{\partial D} F_i$ is a $(N-1)$-dimensional ball of radius $\sqrt{\varepsilon(2R - \varepsilon)}$ centred in $(R - \varepsilon)s_i$.) Since $\nabla V((R - \varepsilon)s_i) = \lambda_i s_i$, for some $\lambda_i > 0$, if ε is sufficiently small, by continuity we deduce $\nabla V(x) \notin \mathcal{A}(x)$.

If $x \in \partial^{N-1} F_i$ for some $i = 1, \ldots, M$, denoting the boundary with respect to H_i then $\mathcal{A}(x)$ is the convex cone generated by $\{-s_i, x\}$. By definition, we have that $\langle \sigma(x; s_i), x \rangle = 0$ and, if $\|x - Rs_i\| \leq \sqrt{2}R$, then also $\langle \sigma(x; s_i), -s_i \rangle \leq 0$. Thus, if ε is sufficiently small, $\langle \sigma(x; s_i), v \rangle \leq 0$ for every $v \in \mathcal{A}(x)$. On the other hand, since s_i is a regular maximum point, taking ε sufficiently small we get

$$\langle \sigma(x; s_i), \nabla V(x) \rangle = \left\langle \sigma(x; s_i), \frac{1}{\|x\|} \nabla_{\mathcal{S}} S \left(\frac{x}{\|x\|} \right) \right\rangle > 0$$

so that $\nabla V(x) \notin \mathcal{A}(x)$.

So, in all cases, we have that $\nabla V(x) \notin \mathcal{A}(x)$. Then, by Theorem 2.12, $\deg(\nabla V, D) = (-1)^N (1 - M)$. Since there are no critical points of V in $\mathcal{B}[0, R] \setminus D$, the excision property of the degree leads us to the end of the proof, in the special case (ii*).

Let us now consider the general case. We write

$$\{x \in \mathcal{S}^{N-1} : S(x) \geq 0\} = \Sigma_1 \cup \cdots \cup \Sigma_M$$

and assume that, for every $i = 1, \ldots, M$, there exist an open set U_i containing Σ_i, an open set V_i containing $\mathcal{B}[0, 1]$ and a diffeomorphism $\psi_i \colon U_i \to V_i$, such that $\psi_i(\Sigma_i) = \mathcal{B}[0, 1]$; moreover, the sets U_i are assumed pairwise disjoint.

Define $P_i \colon U_i \to \mathbb{R}$ as

$$P_i(x) = 1 - \|\psi_i(x)\|^2$$

Then, for every $x \in \partial \Sigma_i$, there exists $\lambda_i(x) > 0$ such that $\nabla S(x) = \lambda_i(x) \nabla P_i(x)$. Hence, for $\delta > 0$ sufficiently small, $\mathcal{B}[0, 1 + \delta] \subseteq V_i$ and, writing $U_i^\delta = \psi_i^{-1}(\mathcal{B}[0, 1 + \delta])$, we have that $\Sigma_i \subseteq U_i^\delta \subseteq U_i$. Furthermore, for δ sufficiently small, we have also

$$\langle \nabla S(x), \nabla P_i(x) \rangle > 0 \quad \text{for every } x \in U_i^\delta \setminus \Sigma_i$$

Let $\mu \colon \mathbb{R} \to \mathbb{R}$ be an increasing continuously differentiable function such that

$$\mu(s) = \begin{cases} 0 & \text{if } s \leq 0 \\ 1 & \text{if } s \geq \delta \end{cases} \qquad \mu'(0) = \mu'(\delta) = 0$$

Define $W \colon \mathcal{S}^{N-1} \times [0, 1] \to \mathbb{R}$ as follows:

$$W(x, \lambda) = \begin{cases} \left[1 - \mu \Big(\operatorname{dist}(\psi_i(x), \mathcal{B}[0, 1]) \Big) \right] (\lambda P_i(x) + (1 - \lambda) S(x)) + \\ \quad + \mu \Big(\operatorname{dist}(\psi_i(x), \mathcal{B}[0, 1]) \Big) S(x) \quad \text{if } x \in U_i^\delta \text{ for some } i \\ S(x) \hspace{4.5cm} \text{otherwise} \end{cases}$$

This function is continuously differentiable and transforms $S(x) = W(x, 0)$ into a function $\widetilde{S}(x) = W(x, 1)$, satisfying (ii*). Moreover, the following two additional properties hold:

- the sign of $W(x, \lambda)$ does not depend on λ;

- the functions $W(\cdot, \lambda)$ have no critical points y with $W(y, \lambda) = 0$.

Such a function W induces an admissible homotopy $H \colon \mathcal{B}[0, R] \times [0, 1] \to \mathbb{R}^N$, defined as

$$H(x, \lambda) = \nabla \left[\rho(\|x\|) \, W \left(\frac{x}{\|x\|}, \lambda \right) \right]$$

which transforms $\nabla V(x) = H(x, 0)$ into $\nabla \widetilde{V}(x)$, where $\widetilde{V}(x)$ satisfies the assumptions of the theorem, and also the additional condition (ii*). Since the admissible homotopy preserves the degree, the proof is completed. □

The following symmetrical version of Theorem 2.19 holds.

Theorem 2.20. *Let the assumptions of Theorem 2.19 hold, with only* (ii) *replaced by*

(ii$^-$) *the set $\{x \in \mathcal{S}^{N-1} : S(x) \leq 0\}$ is the union of M disjoint subsets, which are diffeomorphic to an $(N-1)$-dimensional ball.*

Then, $\deg(\nabla V, \mathcal{B}[0, R]) = 1 - M$.

Proof. It is sufficient to apply Theorem 2.19 to $-V$ instead of V. □

The above result should be compared with [Srz85, Theorem 4.4], which is stated in a more general setting. We also notice that, when $M = 0$, Theorem 2.20 is related to a result by Krasnosel'skii [Kra68] (see also [Ama82]) stating that, when V is coercive, then, for R large enough, $\deg(\nabla V, \mathcal{B}[0, R]) = 1$.

In the planar case, conditions (ii) and (ii$^-$) can be simplified, as follows.

Corollary 2.21. *Let the assumptions of Theorem 2.19 hold, for $N = 2$, with only* (ii) *replaced by*

(ii$_2$) *the function S changes sign exactly $2M$ times on $\mathcal{S}^1$.*

Then, $\deg(\nabla V, \mathcal{B}[0, R]) = 1 - M$.

Proof. Since the zeros of S are simple, the set $\{x \in \mathcal{S}^1 : S(x) \geq 0\}$ is the union of M disjoint arcs, each of which is diffeomorphic to a compact interval of $\mathbb{R}$. □

We have thus recovered, in the planar case, a variant of the alternation criterion described in [DKV09]. We now give two simple examples where our results directly apply. The first one deals with a planar situation.

Example 2.22. Let us consider, for a positive integer k, the family of potentials

$$S_k(s) = \cos[(k+1)s]$$

where $s \in [0, 2\pi[$ is the angle which determines a point $x \in \mathcal{S}^1$. Taking $\rho_k(t) = t^{k+1}$ and identifying $\mathbb{R}^2$ with the complex plane, we get

$$V_k(z) = \rho_k(|z|)S_k(\arg z) = \Re(z^{k+1})$$

The saddle generated by S_k has $k+1$ ascending directions at the points of maximum for S_k, namely $s = 2j\pi/(k+1)$, with $j = 0, 1, \ldots, k$, and $k+1$ descending directions at the points of minimum for S_k, namely $s = (2j+1)\pi/(k+1)$. We thus see that this choice of S_k produces a model of k-fold saddle for every $k \geq 1$. In this case, $\deg(\nabla V_k, \mathcal{B}[0, R]) = -k$, for any $R > 0$.

As we said above, our main purpose is to study also non-planar situations. In our second example we show an illustrative application in $\mathbb{R}^3$.

Example 2.23. Let v_1, v_2, v_3, v_4 be the vertices of a tetrahedron centred in the origin, namely

$$v_1 = \left(0, 0, \frac{\sqrt{6}}{4}\right) \qquad\qquad v_2 = \left(-\frac{\sqrt{3}}{6}, -\frac{1}{2}, -\frac{\sqrt{6}}{12}\right)$$

$$v_3 = \left(-\frac{\sqrt{3}}{6}, \frac{1}{2}, -\frac{\sqrt{6}}{12}\right) \qquad\qquad v_4 = \left(\frac{\sqrt{3}}{3}, 0, -\frac{\sqrt{6}}{12}\right)$$

Let us consider the functions $V_a, V_b \colon \mathbb{R}^3 \to \mathbb{R}$, defined as

$$V_a(x) = \|x\|^2 \left[\frac{1}{5} - \min_{i=1,\ldots,4} \mathrm{dist}\left(\frac{x}{\|x\|}, v_i\right)^2\right]$$

$$V_b(x) = \prod_{i=1}^{4} \langle x, v_i \rangle - \frac{\|x\|^4}{150}$$

Both potentials admit the factorization (2.10), since they are positively homogeneous of degree two and four, respectively. The behaviour of their spherical components $S_a(x)$ and $S_b(x)$ is illustrated in Figure 2.10.

The potential S_a has four positive maximum points, placed in correspondence of the vertices of the tetrahedron, four negative minima, in correspondence of the centers of the faces of the tetrahedron, and six negative saddle points, in correspondence of the midpoints of the edges of the tetrahedron.

The potential S_b instead has six positive maximum points, placed in correspondence of the midpoints of the edges of the tetrahedron, defining in this way the vertices of an octahedron. It also has eight negative minima,

(a) *The potential $S_a(x)$.*   (b) *The potential $S_b(x)$.*
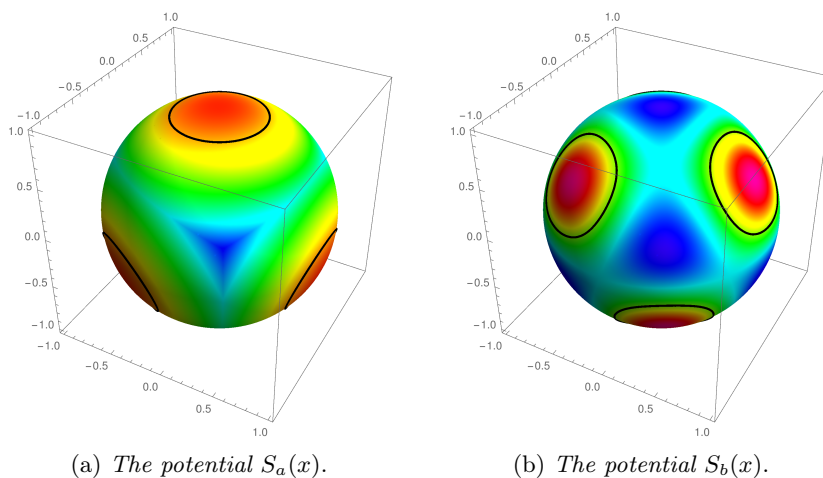
Figure 2.10: Behaviour of the functions $S_a(s)$ and $S_b(s)$ of Example 2.23 on the unit sphere. The black thick line indicates where they take value zero. The functions are positive in the red regions and negative in the blue ones.

in correspondence of both the vertices and the centers of the faces of the tetrahedron (viz. the centers of the faces of the octahedron), and twelve negative saddle points, corresponding to the midpoints of the edges of the octahedron.

Moreover, we observe that both V_a and V_b satisfy the hypotheses of Theorem 2.19, with $M_a = 4$ and $M_b = 6$, respectively, so that, for every $R > 0$, we have

$$\deg(\nabla V_a, \mathcal{B}[0, R]) = (-1)^3 (1 - M_a) = 3$$
$$\deg(\nabla V_b, \mathcal{B}[0, R]) = (-1)^3 (1 - M_b) = 5$$

2.7   Proof of Theorem 2.12

In this section, in order to provide a proof for Theorem 2.12, we will need some basic facts from the theory of set-valued maps, for which we refer to the book of Aubin and Cellina [AC84].

Let us start showing that if D is a convex body, then, for every $x \in D$,

$$v \in \mathcal{N}_D^0(x) \quad \Rightarrow \quad -v \notin \mathcal{N}_D^0(x)$$

Indeed, if on the contrary both v and $-v$ belong to $\mathcal{N}_D^0(x)$, then, for every $x \in D$, it would be

$$0 \geq \langle v, x - \bar{x} \rangle = -\langle -v, x - \bar{x} \rangle \geq 0$$

Hence, D would be included in a hyperplane orthogonal to v and so it would have empty interior, in contradiction with the assumption of being a convex body.

The following lemma will be crucial for the proof of Theorem 2.12.

Lemma 2.24. *Let $D \subseteq \mathbb{R}^N$ be a convex body truncated in F, and $E = D \cup C$ be a reconstruction of D with respect to F. If $\vartheta \colon D \to \mathbb{R}^N$ is a continuous map such that $\vartheta(x) \notin \mathcal{N}_C(x)$, for every $x \in F$, then ϑ can be extended to a continuous function $\hat{\vartheta} \colon E \to \mathbb{R}^N$, such that*

$$\hat{\vartheta}(x) \notin \mathcal{N}_C(x) \quad \text{for every } x \in \partial C$$

Proof. The core of the proof is to show the existence of a map $\widehat{\mathcal{N}}_C$ from ∂C to the closed, convex cones of $\mathbb{R}^N$, with closed graph and such that

(N1) for every $x \in \partial C$, $\mathcal{N}_C(x) \subseteq \widehat{\mathcal{N}}_C(x)$ and

$$v \in \widehat{\mathcal{N}}_C(x) \setminus \{0\} \quad \Rightarrow \quad -v \notin \widehat{\mathcal{N}}_C(x)$$

(N2) $\widehat{\mathcal{N}}_C$ admits a continuous selection $\alpha \colon \partial C \to \mathbb{R}^N$ such that

$$\alpha(x) \in \widehat{\mathcal{N}}_C \setminus \{0\} \qquad \text{for every } x \in \partial C$$

(N3) $\vartheta(x) \notin \widehat{\mathcal{N}}_C(x)$, for every $x \in F$.

Step 1. Let us define the set-valued map Φ from ∂C to $\mathbb{R}^N$ as

$$\Phi(x) = \text{conv} \left[\boldsymbol{\nu}_C(x) \right]$$

Its values are convex and compact. Let us show that Φ is upper semicontinuous. To do so, we first observe that, for a compact convex set $K \subseteq \mathbb{R}^N$, the ε-neighbourhood $\mathcal{B}(K, \varepsilon)$ is convex because of the convexity of the Euclidean distance. Now, take $x \in \partial C$ and fix $\varepsilon > 0$. Since $\boldsymbol{\nu}_C$ is upper semicontinuous and $\mathcal{B}(\Phi(x), \varepsilon)$ is a neighbourhood of $\boldsymbol{\nu}_C(x)$, there exists a neighbourhood U of x in ∂C such that $\boldsymbol{\nu}_C(U) \subseteq \mathcal{B}(\Phi(x), \varepsilon)$. From the convexity of $\mathcal{B}(\Phi(x), \varepsilon)$, it follows that $\Phi(U) \subseteq \mathcal{B}(\Phi(x), \varepsilon)$. The upper semicontinuity of Φ is thus proved.

Since $\Phi(x) \subseteq \mathcal{N}_C(x)$, we have that

$$v \in \Phi(x) \setminus \{0\} \quad \Rightarrow \quad -v \notin \Phi(x)$$

Let us now prove that $0 \notin \Phi(\partial C)$. Suppose by contradiction that $0 \in \Phi(x)$ for some $x \in \partial C$; then there exist $v_1, \dots, v_k \in \boldsymbol{\nu}_C(x)$ and $\lambda_1, \dots, \lambda_k$ in $(0,1)$, with $\lambda_1 + \cdots + \lambda_k = 1$, such that

$$0 = \sum_{i=1}^{k} \lambda_i v_i = \lambda_1 v_1 + (1 - \lambda_1)\tilde{v} \qquad \text{with } \tilde{v} = \sum_{i=2}^{k} \frac{\lambda_i v_i}{1 - \lambda_1} \in \Phi(x)$$

Let us set $\mu = \min\{\lambda_1/2, (1-\lambda_1)/2\}$; then

$$0 \neq w_1 = (\lambda_1 + \mu)v_1 + (1 - \lambda_1 - \mu)\tilde{v} \in \Phi(x)$$
$$0 \neq w_2 = (\lambda_1 - \mu)v_1 + (1 - \lambda_1 + \mu)\tilde{v} \in \Phi(x)$$

and so $w_2 = -w_1$, in contradiction with the fact that $\Phi(x)$ does not contain opposite vectors. Hence, $0 \notin \Phi(x)$ for every $x \in \partial C$.

Since Φ is upper semicontinuous and thus has a closed graph, we can set

$$\delta_0 := \operatorname{dist}(\partial C \times \{0\}, \operatorname*{graph}_{\partial C} \Phi) > 0 \tag{2.12}$$

Furthermore, we note that $\Phi(\partial C) \subseteq \mathcal{B}[0,1]$, for the convexity of the Euclidean distance, and so $\Phi(\partial C)$ is compact.

Step 2.   Since $0 \notin \vartheta(F)$, we can define $\vartheta_1 \colon F \to \mathcal{S}^{N-1} \subseteq \mathbb{R}^N$ as

$$\vartheta_1(x) = \frac{\vartheta(x)}{\|\vartheta(x)\|}$$

The function ϑ_1 is continuous and the hypothesis $\vartheta(x) \notin \mathcal{N}_C(x)$ is equivalent to $\vartheta_1(x) \notin \boldsymbol{\nu}(x)$, from which it follows that $\vartheta_1(x) \notin \Phi(x)$, for every $x \in F$. Thus we can define

$$\delta_1 := \operatorname{dist}(\operatorname*{graph}_{F} \vartheta_1, \operatorname*{graph}_{\partial C} \Phi) > 0 \tag{2.13}$$

We remark that we are considering the distance in $\mathbb{R}^N \times \mathbb{R}^N$ between two compact sets corresponding to the graphs of two functions with different domains.

By [AC84, Sect. 1.13, Theorem 1] (cf. also [Had81]), there exists a sequence of upper semicontinuous set-valued maps Φ_i, from ∂C to $\mathbb{R}^N$, satisfying

(S1) for every $i \in \mathbb{N}$, Φ_i has a continuous selection α_i;

(S2) for every $i \in \mathbb{N}$, Φ_i has closed graph and compact values;

(S3) for every $x \in \partial C$, we have

$$\Phi(x) \subseteq \cdots \subseteq \Phi_{i+1}(x) \subseteq \Phi_i(x) \subseteq \cdots \subseteq \Phi_0(x)$$

and

$$\Phi(x) = \bigcap_{i \in \mathbb{N}} \Phi_i(x)$$

Moreover, since $\Phi(\partial C)$ is compact, the maps Φ_i can be taken with convex values.

Let us introduce the set-valued maps ν_i from ∂C to $\mathbb{R}^N$ as

$$\nu_i(x) = \left\{ \frac{y}{\|y\|} : y \in \Phi_i(x) \setminus \{0\} \right\}$$

Note that the maps ν_i have compact graph. Moreover, for every $x \in \partial C$,

$$\nu_{i+1}(x) \subseteq \nu_i(x) \qquad \text{and} \qquad \bigcap_{i \in \mathbb{N}} \nu_i(x) = \nu_C(x)$$

From this and the continuity of the distance, we get that there exists an index $i' \in \mathbb{N}$ such that, for every $i \geq i'$,

$$\mathop{\mathrm{dist}}_{F}(\mathop{\mathrm{graph}} \vartheta_1, \mathop{\mathrm{graph}}_{\partial C} \nu_i) > \frac{\delta_1}{2} \tag{2.14}$$

where δ_1 has been defined in (2.13). Similarly, from (2.12) we get that there exists $\bar{\imath} \geq i'$ such that $0 \notin \Phi_i(\partial C)$, for every $i \geq \bar{\imath}$.

Step 3. We claim that, for any $j \geq \bar{\imath}$, the choice

$$\widehat{\mathcal{N}}_C(x) = \mathop{\mathrm{cone}}[\Phi_j(x)]$$

satisfies all the requirements (N1), (N2) and (N3). First of all we notice that the cone generated by a compact, convex set is always closed and convex. Similarly, since the graph of Φ_j is compact, it follows that the graph of $\widehat{\mathcal{N}}_C$ is closed. Furthermore, since $\nu_C(x) \subseteq \Phi(x) \subseteq \Phi_j(x) \subseteq \widehat{\mathcal{N}}_C(x)$, it follows that $\mathcal{N}_C(x) \subseteq \widehat{\mathcal{N}}_C(x)$.

Now let us suppose by contradiction that, for some $x \in \partial C$, there exists $v \in \widehat{\mathcal{N}}_C(x) \setminus \{0\}$ such that $-v \in \widehat{\mathcal{N}}_C(x)$. Then there exist $v_1 = a_1 v$ and $v_2 = -a_2 v$, with $a_1 > 0$, $a_2 > 0$, such that both $v_1 \in \Phi_j(x)$ and $v_2 \in \Phi_j(x)$. Since $\Phi_j(x)$ is convex, it follows that

$$0 = \frac{a_2}{a_1 + a_2} v_1 + \frac{a_1}{a_1 + a_2} v_2 \in \Phi_j(x)$$

in contradiction with $j \geq \bar{\imath}$. Hence, (N1) is satisfied.

To satisfy (N2) it is sufficient to take $\alpha = \alpha_j$, where α_j is a continuous selection of Φ_j given by (S1). Since $0 \notin \Phi_j(x)$ for every $x \in \partial C$, we have that $\alpha_j(x) \neq 0$ for every $x \in \partial C$.

Let us now define $\hat{\nu}_C(x) = \nu_j(x)$, for a fixed $j \geq \bar{\imath}$. Then, from (2.14) we have the estimate

$$\mathop{\mathrm{dist}}_{F}(\mathop{\mathrm{graph}} \vartheta_1, \mathop{\mathrm{graph}}_{\partial C} \hat{\nu}_C) > \frac{\delta_1}{2}$$

from which (N3) follows straightforwardly.

Step 4.   Now we are ready to construct the sought prolongation $\hat{\vartheta}$. Let us pick any $0 < \delta < \delta_1/2$. We define $F_\delta = \partial C \cap \mathcal{B}(F, \delta)$ and introduce the function $\vartheta_2 \colon F_\delta \to \mathcal{S}^{N-1} \subseteq \mathbb{R}^N$ as

$$\vartheta_2(x) = \vartheta_1(\pi_F(x)) = \frac{\vartheta(\pi_F(x))}{\|\vartheta(\pi_F(x))\|} \; .$$

For every $x \in F_\delta$ we have

$$\operatorname{dist}\big((x, \vartheta_2(x)), \operatorname*{graph}_F \vartheta_1\big) \leq \operatorname{dist}\big((x, \vartheta_2(x)), (\pi_F(x), \vartheta_2(x))\big) \leq \delta$$

Using the triangle inequality, this implies

$$\operatorname{dist}((x, \vartheta_2(x)), \operatorname*{graph}_{\partial C} \hat{\boldsymbol{\nu}}_C) \geq$$

$$\geq \operatorname{dist}(\operatorname*{graph}_F \vartheta_1, \operatorname*{graph}_{\partial C} \hat{\boldsymbol{\nu}}_C) - \operatorname{dist}((x, \vartheta_2(x)), \operatorname*{graph}_F \vartheta_1)$$

$$\geq \frac{\delta_1}{2} - \delta > 0$$

and so

$$\operatorname{dist}(\operatorname*{graph}_{F_\delta} \vartheta_2, \operatorname*{graph}_{\partial C} \hat{\boldsymbol{\nu}}_C) \geq \frac{\delta_1}{2} - \delta > 0$$

from which it follows that $\vartheta_2(x) \notin \hat{\boldsymbol{\nu}}(x)$, for every $x \in F_\delta$, and consequently $\vartheta(\pi_F(x)) \notin \widehat{\mathcal{N}}_C(x)$.

Writing $\lambda_x = \operatorname{dist}(x, F)/\delta$, we now set

$$\hat{\vartheta}(x) = \begin{cases} \vartheta(x) & \text{if } x \in D \\ (1 - \lambda_x)\vartheta(\pi_F(x)) - \lambda_x \alpha(x) & \text{if } x \in F_\delta \setminus F \\ -\alpha(x) & \text{if } x \in \partial C \setminus F_\delta \end{cases}$$

where $\alpha \colon \partial C \to \mathbb{R}^N$ is the continuous selection provided by (N2). We thus have a continuous function defined on $D \cup \partial C$. If we prove that $\hat{\vartheta}$ satisfies the desired property on ∂C, then the proof is completed, since we can apply Tietze's theorem to get a continuous extension $\hat{\vartheta} \colon E \to \mathbb{R}^N$. What we are actually going to show now is that

$$\hat{\vartheta}(x) \notin \widehat{\mathcal{N}}_C(x) \quad \text{for every } x \in \partial C$$

We already know by (N3) that $\hat{\vartheta}(x) \notin \widehat{\mathcal{N}}_C(x)$, for every $x \in F$. On the other hand, if $x \in \partial C \setminus F_\delta$, it is sufficient to combine (N1) and (N2). Let us now take $x \in F_\delta \setminus F$ and assume by contradiction that $\hat{\vartheta}(x) \in \widehat{\mathcal{N}}_C(x)$. Then, since $\widehat{\mathcal{N}}_C(x)$ is a convex cone and $\alpha(x) \in \widehat{\mathcal{N}}_C(x)$,

$$\vartheta(\pi_F(x)) = \frac{1}{1 - \lambda_x}\hat{\vartheta}(x) + \frac{\lambda_x}{1 - \lambda_x}\alpha(x) \in \widehat{\mathcal{N}}_C(x)$$

a contradiction with $f(\pi_F(x)) \notin \widehat{\mathcal{N}}_C(x)$. The lemma is thus proved.   □

We can now proceed to complete the proof of our theorem.

Let $E = D \cup C_1 \cup \cdots \cup C_M$ be an optimal reconstruction of the truncated convex body D. Applying iteratively Lemma 2.24 to each single partial reconstruction C_i, we obtain a continuous extension $\hat{\vartheta} \colon E \to \mathbb{R}^N$ such that

$$\hat{\vartheta}(x) \notin \mathcal{N}_{C_i}(x) \quad \text{for every } x \in \partial C_i$$

for $i = 1, \ldots, M$, and hence also

$$\hat{\vartheta}(x) \notin \mathcal{N}_E(x) \quad \text{for every } x \in \partial E$$

Thus, by Theorem 2.3, we have that

$$\deg(\hat{\vartheta}, E) = \deg(\hat{\vartheta}, C_1) = \cdots = \deg(\hat{\vartheta}, C_M) = (-1)^N .$$

By the additivity property of the topological degree, we have

$$\deg(\hat{\vartheta}, D) = \deg(\hat{\vartheta}, E) - \sum_{i=1}^{M} \deg(\hat{\vartheta}, C_i) = (-1)^N (1 - M) .$$

Since ϑ coincides with $\hat{\vartheta}$ on D, the theorem is proved.

Chapter 3

The avoiding cones condition for a higher dimensional Poincaré-Birkhoff Theorem

3.1 Twist conditions for a higher dimensional Poincaré-Birkhoff Theorem

An overview on previous results

Let us introduce in detail the framework we outlined in Chapter 1. We consider the Hamiltonian system

$$\dot{z} = \mathcal{J}\nabla H(t, z) \tag{3.1}$$

where

$$\mathcal{J} = \begin{pmatrix} 0 & \mathbb{I}_N \\ -\mathbb{I}_N & 0 \end{pmatrix}$$

denotes the standard $2N \times 2N$ symplectic matrix, and we assume the Hamiltonian function $H \colon \mathbb{R} \times \mathbb{R}^{2N} \to \mathbb{R}$ to be $\mathcal{C}^\infty$-smooth, and T-periodic in its first variable t. (Actually, such a regularity assumption can be considerably weakened, as will be discussed below.) We denote by $\nabla H(t, z)$ the gradient with respect to the variable z.

For every $\zeta \in \mathbb{R}^{2N}$, we denote by $\mathcal{Z}(\cdot, \zeta)$ the unique solution of (3.1) satisfying $\mathcal{Z}(0, \zeta) = \zeta$. We assume that these solutions can be continued to the whole time interval $[0, T]$, so that the Poincaré map $\mathcal{P} \colon \mathbb{R}^{2N} \to \mathbb{R}^{2N}$ is well defined, by setting

$$\mathcal{P}(\zeta) = \mathcal{Z}(T, \zeta)$$

and it is a diffeomorphism. The fixed points of $\mathcal{P}$ are associated with the T-periodic solutions of (3.1).

For $z \in \mathbb{R}^{2N}$, we use the notation $z = (x, y)$, with $x = (x_1, \ldots, x_N) \in \mathbb{R}^N$ and $y = (y_1, \ldots, y_N) \in \mathbb{R}^N$, and we assume that $H(t, x, y)$ is 2π-periodic in each of the variables $x_1, \ldots, x_N$. We also write

$$\mathcal{P}(x, y) = (x + \vartheta(x, y), y + \rho(x, y)) \tag{3.2}$$

Under this setting, T-periodic solutions of (3.1) appear in equivalence classes made of those solutions whose components $x_i(t)$ differ by an integer multiple of 2π. We say that two T-periodic solutions are *geometrically distinct* if they do not belong to the same equivalence class. The same will be said for two fixed points of $\mathcal{P}$.

We now recall the main twist condition proposed in literature. Since our focus is on the twist, to facilitate the comparison we enunciate all in the case of a strongly convex set $D \subseteq \mathbb{R}^N$; below we will add some remarks on each assumption.

The first twist condition, proposed in [FU13] (cf. [FU16a]), generalizes an assumption first introduced by Conley and Zehnder in [CZ83a].

(T1) There exists a regular symmetric $N \times N$ matrix $\mathbb{B}$ such that

$$\langle \vartheta(x, y), \mathbb{B}\nu_D(y) \rangle > 0 \qquad \text{for every } (x, y) \in \mathbb{R}^N \times \partial D$$

where $\nu_D(y)$ denotes the unit outward normal vector to D at y.

This condition recalls the twist (2.1) of the Poincaré–Miranda Theorem, that we discussed in the previous Chapter. As in that case, condition (T1) implies that the vector $\vartheta(x, y)$ has to avoid an entire half-space at each point of the boundary. We remark that this result holds also for every convex body D, with ν_D possibly defining a set-valued map.

The second twist condition in literature was introduced in [MZ05], restricted to the case $\mathbb{B} = I_N$ and requiring a monotone twist of the map $\vartheta(x, y)$. These two assumptions have been dropped in [FU16a].

(T2) There exist an involutory $N \times N$ matrix $\mathbb{B}$ and some point $d_0 \in \text{int } D$ with

$$\langle \vartheta(x, y), \mathbb{B}(y - d_0) \rangle > 0 \qquad \text{for every } (x, y) \in \mathbb{R}^N \times \partial D$$

As in the previous case, this condition recalls a twist condition that we discussed in the previous Chapter, namely the extension of the twist (2.2) of the Poincaré–Bohl Theorem, that we used in the proof of Theorem 2.1. Again, the map $\vartheta(x, y)$ has to avoid an entire half-space at each point of the boundary, and this result holds also for every convex body D.

The third twist condition we want to recall, named *avoiding rays condition*, was introduced in [FU14] (cf. [FU16a]), in the general case of sets D whose boundaries are diffeomorphic to a sphere.

(T3) $\qquad \vartheta(x,y) \notin \{\mu\nu_D(y) : \mu \geq 0\} \qquad$ for every $(x,y) \in \mathbb{R}^N \times \partial D$

In this case the condition recalls the twist presented in Theorem 2.3. The condition was shown to hold also in the case of sets D whose boundary is diffeomorphic to a sphere, yet the case of sets D with a non-smooth boundary had not been studied. In this case, at every point of the boundary the map ϑ has to avoid only a halfline, yet situations with indefinite twist are not included in this condition.

Under each of these twist conditions, and in the general framework presented above, it has been proved in [FU16a] that the map $\mathcal{P}$ has at least $N + 1$ geometrically distinct fixed points, all in $\mathbb{R}^N \times D$. Moreover, if all its fixed points are non degenerate, then there are at least 2^N of them.

Concerning the regularity assumptions, in [FU16a] it is shown that it is sufficient to assume that the Hamiltonian H is continuous, with a continuous gradient ∇H in the z-variables; moreover the continuity in the time variable can be further weakened, obtaining a Caratheodory-like condition. However, such a mild regularity requires a lot of technicalities, but the main line of the proof is the same. Since our focus is on the twist, we prefer here to avoid these difficulties, and present our result for $\mathcal{C}^\infty$ Hamiltonians; yet the result stated below can be extended naturally also under such weak regularity conditions.

The avoiding cones condition

As done in the previous Chapter, our plan is to introduce a general but intuitive condition, including and improving the three kind of twist presented above. Unfortunately, a different approach is needed: whereas our previous definition of *avoiding cones condition* was build for a purely topological approach, in this case we have to deal with the variational structure required in the proof of the generalize Poincaré–Birkhoff Theorem. We will therefore suggest a new definition of the set $\mathcal{A}$, with the aim to characterized the same abstract object introduced in Chapter 2. Many evidences indicate that the two definition should be the equivalent, yet the problem is still open. We also highlight that this new definition would allow also to overcome some of the restriction encountered in Chapter 2, since it an "edge" is no longer required to pass from an inward to an outward region; yet the striking intuitiveness of our previous definition would be partially sacrificed, and this suggested us the dual approach adopted in this thesis.

Let $F \colon \mathbb{R}^N \to \mathbb{R}^N$ be a $\mathcal{C}^\infty$-smooth gradient function, namely we assume that there is a function $h \colon \mathbb{R}^N \to \mathbb{R}$ such that $F = \nabla h$. We define, for every $y \in \mathbb{R}^N$, the set $\mathcal{A}_F(y)$ as follows: a vector $v \in \mathbb{R}^N$ belongs to $\mathcal{A}_F(y)$ if and only if there exist a sequence $(y_n)_n$ of points in $\mathbb{R}^N$ and a sequence $(\mu_n)_n$ of non-negative real numbers such that

$$y_n \to y, \quad \text{and} \quad \mu_n F(y_n) \to v$$

It can be easily seen that $\mathcal{A}_F(y)$ is a closed cone in $\mathbb{R}^N$.

Our main result is the following (cf. [FG16a]).

Theorem 3.1. *Let $F = \nabla h \colon \mathbb{R}^N \to \mathbb{R}^N$ be a $\mathcal{C}^\infty$-smooth function for which there are two constants $K > 0$ and $C > 0$ and a regular symmetric $N \times N$ matrix $\mathbb{S}$ such that*

$$\|F(y) - \mathbb{S}y\| \leq C \qquad \text{when } \|y\| \geq K \tag{3.3}$$

and set $D := F^{-1}(0)$. Suppose that

$$\vartheta(x,y) \notin \mathcal{A}_F(y) \quad \text{for every } (x,y) \in \mathbb{R}^N \times \partial D \tag{AC}$$

Then, $\mathcal{P}$ has at least $N + 1$ geometrically distinct fixed points, all in $\mathbb{R}^N \times D$. Moreover, if all its fixed points are non degenerate, then there are at least 2^N of them.

Assumption (AC) is our *avoiding cones condition*. In other words, for every $(x,y) \in \mathbb{R}^N \times \partial D$, one must have that $\vartheta(x,y) \neq 0$, and that there isn't any sequence $(y_n)_n$ in $\mathbb{R}^N \setminus D$ with

$$y_n \to y \quad \text{and} \quad \frac{F(y_n)}{\|F(y_n)\|} \to \frac{\vartheta(x,y)}{\|\vartheta(x,y)\|} \,.$$

The proof of Theorem 3.1 is provided in Section 3.3. The geometrical meaning of the avoiding cones condition will be discussed extensively in Section 3.2, including the study of some substantial cases.

3.2 The avoiding cones condition, concretely

We now investigate the nature of our avoiding cones condition. We first present two particular cases which already include the most relevant features. Later, we will show how these two special situations actually have a wider extent. Finally, we prove that the twist conditions (T1), (T2) and (T3) are included in (AC) and illustrate how the first two are indeed rather more restrictive.

In the following, we will start from a set $D \subseteq \mathbb{R}^N$ and construct a suitable function $F \colon \mathbb{R}^N \to \mathbb{R}^N$ satisfying the assumptions of Theorem 3.1, for which $D = F^{-1}(0)$. Before proceeding in our analysis, a couple of remarks are in order.

It is useful to introduce, in relation to the cone $\mathcal{A}_F(y)$, the set

$$\alpha_F(y) = \{v \in \mathcal{A}_F(y) \colon \|v\| = 1\}$$

so that

$$\mathcal{A}_F(y) = \{\mu v : \mu > 0\,,\ v \in \alpha_F(y)\} \cup \{0\}$$

Notice that, if $y \notin D$, we have

$$\mathcal{A}_F(y) = \{\mu F(y) : \mu \geq 0\} \qquad \alpha_F(y) = \left\{ \frac{F(y)}{\|F(y)\|} \right\}$$

on the other hand, if y belongs to $\operatorname{int} D$, then

$$\mathcal{A}_F(y) = \{0\} \qquad \alpha_F(y) = \emptyset$$

and vice versa. The case when y lies in ∂D is less trivial. We know that $\alpha_F(y) \neq \emptyset$ for every $y \in \partial D$. Indeed, if $y \in \partial D$, there exists a sequence of points $y_n \in \mathbb{R}^N \setminus D$ such that $y_n \to y$ and, consequently, a sequence of vectors $v_n \in \mathbb{R}^N$, such that $\|v_n\| = 1$ and $\alpha_F(y_n) = \{v_n\}$. By compactness, there exists a subsequence v_{n_k} such that $v_{n_k} \to v$ for some v, with $\|v\| = 1$, and therefore $v \in \alpha_F(y)$. This shows that, for $y \in \partial D$, the set $\alpha_F(y)$ is non-empty, but in general it can be multivalued, as displayed below.

In the following, we illustrate three particular situations which present the key features and provide quite natural tools for applications, minimizing at the same time the required computations. The same techniques and ideas can naturally be applied to more general situations.

In many constructions we will need to consider a $\mathcal{C}^\infty$-smooth function $\gamma \colon \mathbb{R} \to \mathbb{R}$, with

$$\gamma(s) = \begin{cases} 0 & \text{if } s \leq 0 \\ 1 & \text{if } s \geq 1 \end{cases}$$

and such that, for some $\varepsilon_\gamma > 0$,

$$\gamma'(s) > 0 \ \text{ for } s \in (0,1) \qquad \gamma''(s) > 0 \ \text{ for } s \in (0, \varepsilon_\gamma)$$

We denote by $\langle \cdot, \cdot \rangle$ the Euclidean scalar product in $\mathbb{R}^N$, with its associated norm $\|\cdot\|$. We write $\mathcal{B}^N(x_0, r)$ for the open ball in $\mathbb{R}^N$ centred at x_0 with radius $r > 0$, and $\mathcal{B}^N[x_0, r]$ for the closed ball.

The closed ball

We consider a decomposition of the form $\mathbb{R}^N = \mathbb{R}^{N_1} \times \mathbb{R}^{N_2}$, where N_1 or N_2 may possibly be zero, and we introduce the matrix

$$\mathbb{B} = \begin{pmatrix} I_{N_1} & 0 \\ 0 & -I_{N_2} \end{pmatrix} \tag{3.4}$$

Corollary 3.2. *Let $D = \mathcal{B}^N[0,1]$ and assume that, for every $(x,y) \in \mathbb{R}^N \times \partial D$,*

$$\vartheta(x,y) \notin \begin{cases} \{\mu y : \mu \geq 0\} & \text{if } \langle \mathbb{B}y, y \rangle > 0 \\ \{\mu_1 y + \mu_2 \mathbb{B}y : \mu_1 \in \mathbb{R}, \mu_2 \geq 0\} & \text{if } \langle \mathbb{B}y, y \rangle = 0 \\ \{-\mu y : \mu \geq 0\} & \text{if } \langle \mathbb{B}y, y \rangle < 0 \end{cases} \tag{3.5}$$

Then, the same conclusion of Theorem 3.1 holds.

Proof. We define the function $h \colon \mathbb{R}^N \to \mathbb{R}$ as

$$h(y) = \gamma(\|y\| - 1) \langle \mathbb{B}y, y \rangle \tag{3.6}$$

and set $F := \nabla h$, decomposed as

$$F(y) = C_1(y)y + C_2(y)\mathbb{B}y$$

with

$$C_1(y) = \frac{\gamma'(\|y\| - 1)}{\|y\|} \langle \mathbb{B}y, y \rangle \qquad C_2(y) = 2\gamma(\|y\| - 1)$$

We observe that $F^{-1}(0) = D$. Indeed, when $y \notin D$, one has $\gamma(\|y\| - 1) > 0$ and, whenever the two vectors $\langle \mathbb{B}y, y \rangle y$ and $\mathbb{B}y$ are on the same line, then they have also the same direction. We define, for every $y \notin D$, a rescaling of the coefficients $C_1(y)$ and $C_2(y)$, namely

$$c_1(y) = \frac{C_1(y)}{\sqrt{C_1(y)^2 + C_2(y)^2}} \qquad c_2(y) = \frac{C_2(y)}{\sqrt{C_1(y)^2 + C_2(y)^2}} \tag{3.7}$$

so that, for $y \notin D$, we have $\alpha_F(y) = \{c_1(y)y + c_2(y)\mathbb{B}y\}$. We will prove that, for every $y \in \partial D$,

$$\alpha_F(y) = \begin{cases} \{\operatorname{sgn}(\langle \mathbb{B}y, y \rangle)y\} & \text{if } \langle \mathbb{B}y, y \rangle \neq 0 \\ \left\{ \tau y + \sqrt{1 - \tau^2}\mathbb{B}y : \tau \in [-1, 1] \right\}, & \text{if } \langle \mathbb{B}y, y \rangle = 0 \end{cases} \tag{3.8}$$

First, let $y \in \partial D$ be such that $\langle \mathbb{B}y, y \rangle \neq 0$. We take a sequence $(Y_n)_n$ of vectors $Y_n \in \mathcal{B}^N(0, 1 + \varepsilon_\gamma) \setminus D$, with $Y_n \to y$. For $s \in (0, \varepsilon_\gamma)$, having assumed $\gamma''(s) > 0$, it follows that $\gamma(s) \leq s\gamma'(s)$, hence

$$\lim_{n \to \infty} \left| \frac{C_2(Y_n)}{C_1(Y_n)} \right| = \lim_{n \to \infty} \frac{2\|Y_n\| \gamma(\|Y_n\| - 1)}{\gamma'(\|Y_n\| - 1) |\langle \mathbb{B}Y_n, Y_n \rangle|} \leq \lim_{n \to \infty} \frac{2\|Y_n\| (\|Y_n\| - 1)}{|\langle \mathbb{B}Y_n, Y_n \rangle|} = 0$$

This implies (3.8) in the case $\langle \mathbb{B}y, y \rangle \neq 0$.

Let us now look at the case when $y \in \partial D$ and $\langle \mathbb{B}y, y \rangle = 0$. Since $C_2 \geq 0$, by the properties of the limit we deduce the $\subseteq$ inclusion in (3.8). To check the $\supseteq$ inclusion, let us take a sequence of positive real numbers $l_n \in (0, \varepsilon_\gamma)$, with $l_n \to 0$, and consider the two sequences of points

$$P_n = y + l_n y \qquad Q_n = y + l_n \mathbb{B}y$$

We observe that $P_n \to y$ and $Q_n \to y$. We have $C_1(P_n) = 0$, while

$$\lim_{n \to \infty} \left| \frac{C_2(Q_n)}{C_1(Q_n)} \right| = \lim_{n \to \infty} \left| \frac{2\|Q_n\| \gamma(\|Q_n\| - 1)}{\gamma'(\|Q_n\| - 1) \langle \mathbb{B}Q_n, Q_n \rangle} \right| \leq \lim_{n \to \infty} \frac{\sqrt{1 + l_n^2} - 1}{l_n} = 0 \,.$$

(a) $N_1 = N_2 = 1$.   (b) $N_1 = 2$ *and* $N_2 = 0$.
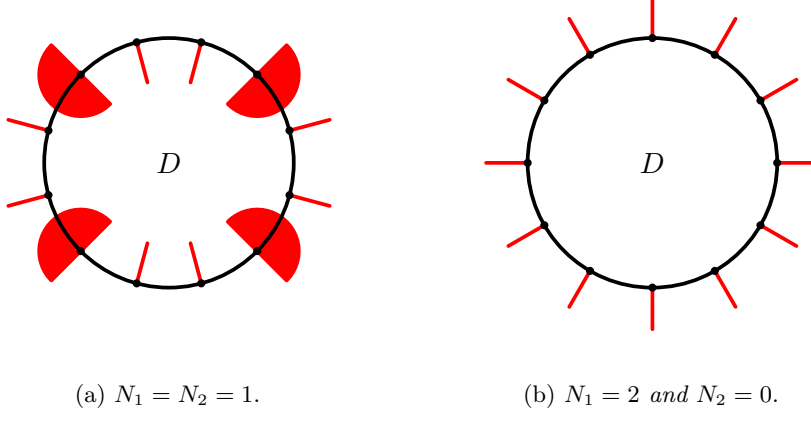
Figure 3.1: Visualization of $\mathcal{A}_F(y)$ in the framework of Corollary 3.2, for different choices of the decomposition $N = N_1 + N_2$.

Hence,

$$c_1(P_n) = 0 \qquad\qquad \lim_{n \to \infty} c_1(Q_n) = 1$$

$$c_2(P_n) = 1 \qquad\qquad \lim_{n \to \infty} c_2(Q_n) = 0$$

and so both y and $\mathbb{B}y$ belong to $\alpha_F(y)$. By continuity, for every $\tau \in (0,1)$ and every sufficiently large n, there exists $\Lambda_n \in [0,1]$ such that, setting $Y_n = \Lambda_n P_n + (1 - \Lambda_n)Q_n$,

$$c_1(Y_n) = \tau \qquad c_2(Y_n) = \sqrt{1 - \tau^2}$$

Since $Y_n \to y$, it follows that

$$\tau y + \sqrt{1 - \tau^2}\, \mathbb{B}y \in \alpha_F(y) \qquad \text{for every } \tau \in (0,1)$$

We have thus proved that

$$\alpha_F(y) \supseteq \left\{ \tau y + \sqrt{1 - \tau^2}\, \mathbb{B}y : \tau \in [0,1] \right\}$$

The remaining part of the proof, i.e. the inclusion with $\tau \in [-1,0]$, can be treated similarly, replacing in the construction above Q_n with

$$Q_n^- = y - l_n\, \mathbb{B}y$$

Hence (3.8) is established, and proof of the corollary is easily completed. □

The avoiding cones condition of Corollary 3.2 is visualized in Figure 3.1.
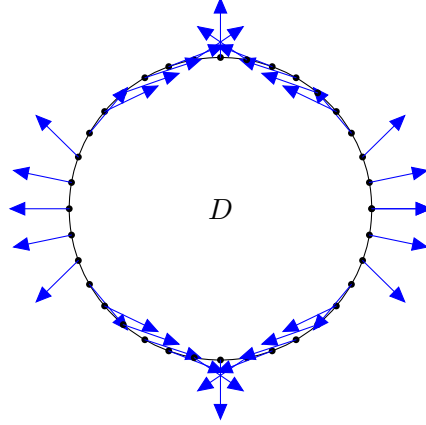
Figure 3.2: Normalized Poincaré map for the Hamiltonian system of Example 3.3.

Example 3.3. We take $D = \mathcal{B}^2[0,1]$ and define the Hamiltonian function

$$H(x_1, x_2, y_1, y_2) = y_1^2 + y_2^2 + 2\cos(\pi y_1)$$

The map $\vartheta(x,y) = (\vartheta_1(x,y), \vartheta_2(x,y))$ is given by

$$\vartheta_1(x,y) = T\frac{\partial H}{\partial y_1}(x,y) = 2T[y_1 - \pi\sin(\pi y_1)]$$

$$\vartheta_2(x,y) = T\frac{\partial H}{\partial y_2}(x,y) = 2Ty_2$$

As illustrated in Figure 3.2, the avoiding cones condition as in (3.5) is verified, for $N_1 = 0$ and $N_2 = 2$. The same property is inherited by all the sufficiently small perturbations of H, satisfying the regularity and periodicity assumptions of Theorem 3.1.

The product of two closed balls

Let us consider, as before, a decomposition of the type $\mathbb{R}^N = \mathbb{R}^{N_1} \times \mathbb{R}^{N_2}$, where N_1 or N_2 may possibly be zero. For every $y \in \mathbb{R}^{N_1} \times \mathbb{R}^{N_2}$, we write $y = \hat{y}_1 + \hat{y}_2$, with $\hat{y}_1 \in \mathbb{R}^{N_1} \times \{0\}$ and $\hat{y}_2 \in \{0\} \times \mathbb{R}^{N_2}$.

Corollary 3.4. *Let $D = D_1 \times D_2$, with $D_1 = \mathcal{B}^{N_1}[0,1]$ and $D_2 = \mathcal{B}^{N_2}[0,1]$, and assume that, for every $(x,y) \in \mathbb{R}^N \times \partial D$,*

$$\vartheta(x,y) \notin \begin{cases} \{-\mu\hat{y}_2 : \mu \geq 0\} & \text{if } y \in \text{int } D_1 \times \partial D_2 \\ \{\mu_1\hat{y}_1 - \mu_2\hat{y}_2 : \mu_1 \geq 0, \mu_2 \geq 0\} & \text{if } y \in \partial D_1 \times \partial D_2 \\ \{\mu\hat{y}_1 : \mu \geq 0\} & \text{if } y \in \partial D_1 \times \text{int } D_2 \end{cases} \quad (3.9)$$

Then, the same conclusion of Theorem 3.1 holds.

Proof. We define the function $h\colon \mathbb{R}^N \to \mathbb{R}$ as

$$h(y) = \gamma(\|\hat{y}_1\|)\,\|\hat{y}_1\|^2 - \gamma(\|\hat{y}_2\|)\,\|\hat{y}_2\|^2$$

and set $F := \nabla h$, namely

$$F(y) = C_1(y)\hat{y}_1 - C_2(y)\hat{y}_2\,,$$

with

$$C_1(y) = \gamma'(\|\hat{y}_1\|)\,\|\hat{y}_1\| + 2\gamma(\|\hat{y}_1\|) \qquad C_2(y) = \gamma'(\|\hat{y}_2\|)\,\|\hat{y}_2\| + 2\gamma(\|\hat{y}_2\|)$$

We observe that $F^{-1}(0) = D$. We will prove that, for every $y \in \partial D$,

$$\alpha_F(y) = \begin{cases} \left\{-\dfrac{\hat{y}_2}{\|\hat{y}_2\|}\right\} & \text{if } y \in \text{int}\, D_1 \times \partial D_2 \\[2mm] \left\{\tau\dfrac{\hat{y}_1}{\|\hat{y}_1\|} - \sqrt{1-\tau^2}\,\dfrac{\hat{y}_2}{\|\hat{y}_2\|},\ \tau \in [0,1]\right\} & \text{if } y \in \partial D_1 \times \partial D_2 \\[2mm] \left\{\dfrac{\hat{y}_1}{\|\hat{y}_1\|}\right\} & \text{if } y \in \partial D_1 \times \text{int}\, D_2 \end{cases} \tag{3.10}$$

First of all, we notice that, for every $y \in D_1 \times \mathbb{R}^{N_2}$, the $\mathbb{R}^{N_1}$-component of $F(y)$ is zero, since $C_1(y) = 0$; hence, if $y \in \text{int}\, D_1 \times \partial D_2$, being $D_1 \times \mathbb{R}^{N_2}$ a neighbourhood y, we deduce that (3.10) is verified in this case. The case $y \in \partial D_1 \times \text{int}\, D_2$ is analogous.

Finally, let us consider the case $y \in \partial D_1 \times \partial D_2$. The $\subseteq$ inclusion follows from the fact that the functions c_1 and c_2, defined by a rescaling of C_1 and C_2 as in (3.7), take values in $[0,1]$ and the sum of their squares is always equal to one. To check the $\supseteq$ inclusion, let us take any sequence of positive real numbers $l_n \to 0$ and consider the two sequences of points

$$P_n = (1 + l_n)\hat{y}_1 + \hat{y}_2 \qquad Q_n = \hat{y}_1 + (1 + l_n)\hat{y}_2$$

We have that $P_n \to y$, $Q_n \to y$ and

$$\begin{aligned} c_1(P_n) &= 1 & c_1(Q_n) &= 0 \\ c_2(P_n) &= 0 & c_2(Q_n) &= 1 \end{aligned}$$

By continuity, for every $\tau \in [0,1]$ and every sufficiently large n, there exists $\Lambda_n \in [0,1]$ such that

$$c_1\big(\Lambda_n P_n + (1 - \Lambda_n)Q_n\big) = \tau \qquad c_2\big(\Lambda_n P_n + (1 - \Lambda_n)Q_n\big) = \sqrt{1 - \tau^2}$$

Since $\Lambda_n P_n + (1 - \Lambda_n)Q_n \to y$, it follows that

$$\tau\frac{\hat{y}_1}{\|\hat{y}_1\|} - \sqrt{1 - \tau^2}\,\frac{\hat{y}_2}{\|\hat{y}_2\|} \in \alpha_F(y) \qquad \text{for every } \tau \in [0,1]$$

So (3.10) is verified, and the proof is easily completed. $\qquad\square$

(a) *Corollary 3.4.*   (b) *Corollary 3.6.*
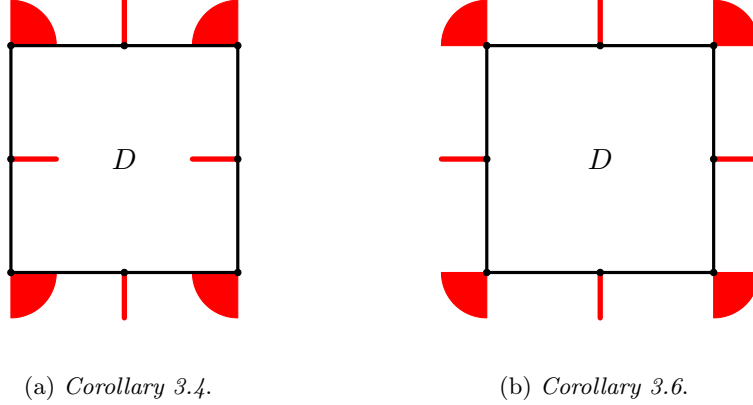
Figure 3.3: Visualization of $\mathcal{A}_F(y)$ in the framework of Corollaries 3.4 and 3.6, for $N_1 = N_2 = 1$.

The avoiding cones condition (3.9) of Corollary 3.4 is visualized in Figure 3.3(a). It can be restated as

$$\vartheta(x,y) \notin \begin{cases} \{0\} \times -\mathcal{N}_{D_2}(\hat{y}_2) & \text{if } y \in \text{int } D_1 \times \partial D_2 \\ \mathcal{N}_{D_1}(\hat{y}_1) \times -\mathcal{N}_{D_2}(\hat{y}_2) & \text{if } y \in \partial D_1 \times \partial D_2 \\ \mathcal{N}_{D_1}(\hat{y}_1) \times \{0\} & \text{if } y \in \partial D_1 \times \text{int } D_2 \end{cases}$$

Example 3.5. We take $D = [-1, 1] \times [-1, 1]$ and define the Hamiltonian function $H \colon \mathbb{R}^2 \times \mathbb{R}^2 \to \mathbb{R}$ as

$$H(x_1, x_2, y_1, y_2) = y_1^2 - y_2^2 - y_2 \sin(2\pi y_1)$$

The map $\vartheta(x, y) = (\vartheta_1(x, y), \vartheta_2(x, y))$ is such that

$$\vartheta_1(x, y) = T\frac{\partial H}{\partial y_1}(x, y) = 2T[y_1 - \pi y_2 \cos(2\pi y_1)]$$

$$\vartheta_2(x, y) = T\frac{\partial H}{\partial y_2}(x, y) = -T[2y_2 + \sin(2\pi y_1)]$$

As illustrated in Figure 3.4, we see that the avoiding cones condition (3.9) is satisfied, for $N_1 = N_2 = 1$, cf. also Figure 3.3(a). The same property is inherited by all the sufficiently small perturbations of H, satisfying the regularity and periodicity assumptions of Theorem 3.1.

With a similar approach, we can also study the following situation.

Corollary 3.6. *Let $D = D_1 \times D_2$, with $D_1 = \mathcal{B}^{N_1}[0, 1]$ and $D_2 = \mathcal{B}^{N_2}[0, 1]$, and assume that*

$$\vartheta(x, y) \notin \mathcal{N}_D(y) \qquad \text{for every } (x, y) \in \mathbb{R}^N \times \partial D \qquad (3.11)$$

Then, the same conclusion of Theorem 3.1 holds.
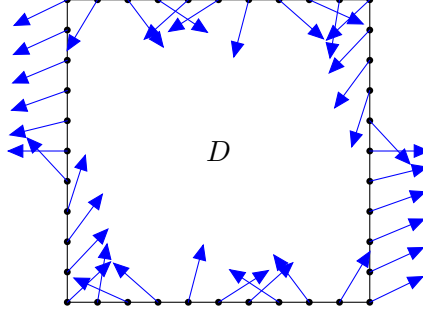
Figure 3.4: Normalized Poincaré map for the Hamiltonian system of Example 3.5.

Proof. We define the function $h \colon \mathbb{R}^N \to \mathbb{R}$ as

$$h(y) = \gamma(\|\hat{y}_1\|) \, \|\hat{y}_1\|^2 + \gamma(\|\hat{y}_2\|) \, \|\hat{y}_2\|^2$$

The same arguments used in the proof of Corollary 3.4 can be successfully applied, simply changing the sign in front of the coefficient C_2. $\qquad\square$

We notice that, in Corollary 3.6, condition (3.11) can be replaced by

$$\vartheta(x,y) \notin -\mathcal{N}_D(y) \quad \text{for every } (x,y) \in \mathbb{R}^N \times \partial D$$

by simply changing in the proof the sign of the potential h.

Combining the ideas of the previous two corollaries, let us consider the decomposition $\mathbb{R}^N = \mathbb{R}^{N^+} \times \mathbb{R}^{N^-}$, with $N^+ = N_1^+ + \cdots + N_n^+$ and $N^- = N_1^- + \cdots + N_m^-$, all summands being non-negative integers. For every $y \in \mathbb{R}^{N^+} \times \mathbb{R}^{N^-}$, we write $y = \hat{y}^+ + \hat{y}^-$, with $\hat{y}^+ \in \mathbb{R}^{N^+} \times \{0\}$ and $\hat{y}^- \in \{0\} \times \mathbb{R}^{N^-}$. We thus obtain the following more general result.

Corollary 3.7. *Let $D = D^+ \times D^-$, with*

$$D^+ = \prod_{i=1}^{n} \mathcal{B}^{N_i^+}[0,1] \qquad\qquad D^- = \prod_{i=1}^{m} \mathcal{B}^{N_i^-}[0,1]$$

Assume that, for every $(x,y) \in \mathbb{R}^N \times \partial D$,

$$\vartheta(x,y) \notin \begin{cases} \{0\} \times -\mathcal{N}_{D^-}(\hat{y}^-) & \text{if } y \in \operatorname{int} D^+ \times \partial D^- \\ \mathcal{N}_{D^+}(\hat{y}^+) \times -\mathcal{N}_{D^-}(\hat{y}^-) & \text{if } y \in \partial D^+ \times \partial D^- \\ \mathcal{N}_{D^+}(\hat{y}^+) \times \{0\} & \text{if } y \in \partial D^+ \times \operatorname{int} D^- \end{cases}$$

Then, the same conclusion of Theorem 3.1 holds.

Sets diffeomorphic to a ball

We now show how to apply our results to sets $\mathcal{D}$ which are diffeomorphic to a ball.

Let $\mathcal{D} \subset \mathbb{R}^N$ be a compact set, and let $\mathcal{D}^+$ be a relatively open subset of $\partial \mathcal{D}$. We define $\mathcal{D}^- = \partial \mathcal{D} \setminus \overline{\mathcal{D}^+}$ and $\mathcal{D}^0 = \partial \mathcal{D} \setminus (\mathcal{D}^+ \cup \mathcal{D}^-)$.

Definition 3.8. We say that the couple $(\mathcal{D}, \mathcal{D}^+)$ is *twist-generating* if there exist two regular symmetric matrices $\mathbb{B}, \mathbb{B}_\infty$, with $\mathbb{B}$ of the form (3.4), and a $\mathcal{C}^\infty$-smooth diffeomorphism $\Psi \colon \mathbb{R}^N \to \mathbb{R}^N$, such that

- $\Psi'(w) = \mathbb{B}_\infty$ for $\|w\|$ sufficiently large

- $\Psi(\mathcal{D}) = \mathcal{B}^N[0, 1]$

- $\Psi(\mathcal{D}^+) = \{y : \|y\| = 1, \langle y, \mathbb{B}y \rangle > 0\}$

Note that if $(\mathcal{D}, \mathcal{D}^+)$ is twist-generating, then $\mathcal{D}$ has smooth boundary and therefore, for every $w \in \partial \mathcal{D}$, the outer normal cone $\mathcal{N}_\mathcal{D}(w)$ is well defined, and it is the half-line generated by the outer unit normal $\nu_\mathcal{D}(w)$. Moreover, for every point $w \in \mathcal{D}^0$, we can define the vector

$$\sigma(w) = [\Psi'(w)]^T \mathbb{B} \Psi(w)$$

We see that $\sigma(w)$ is orthogonal to $\mathcal{D}^0$ and to $\nu_\mathcal{D}(w)$ (therefore tangent to $\mathcal{D}$).

Corollary 3.9. *If $(\mathcal{D}, \mathcal{D}^+)$ is twist-generating and, for every $(x, w) \in \mathbb{R}^N \times \partial \mathcal{D}$, we have*

$$\vartheta(x, w) \notin \begin{cases} \mathcal{N}_\mathcal{D}(w) & \text{if } w \in \mathcal{D}^+ \\ \{\mu_1 \nu_\mathcal{D}(w) + \mu_2 \sigma(w) : \mu_1 \in \mathbb{R}, \mu_2 \geq 0\} & \text{if } w \in \mathcal{D}^0 \\ -\mathcal{N}_\mathcal{D}(w) & \text{if } w \in \mathcal{D}^- \end{cases}$$

then the same conclusion of Theorem 3.1 holds.

Proof. We consider the function

$$h_A(y) = \gamma(\|y\| - 1) \langle \mathbb{B}y, y \rangle$$

as introduced in (3.6), and define $h \colon \mathbb{R}^N \to \mathbb{R}$ as

$$h(w) = h_A(\Psi(w))$$

All the properties required to $F = \nabla h$ are inherited from h_A, and Theorem 3.1 applies. $\qquad \square$

We observe that, in the case $\mathcal{D}^+ = \partial \mathcal{D}$, implying $\mathbb{B} = I$, we have recovered exactly the twist condition (T3).

The same line of reasoning holds if we want to generalize other situations, such as those considered in this section, by the use of a diffeomorphism. We omit the details, for briefness.

Comparison with twist conditions in literature

We now show that the twist conditions (T1), (T2) or (T3) are actually all included in the notion of avoiding cones condition (AC).

Corollary 3.10 (Fonda–Ureña)**.** *Let $D \subset \mathbb{R}^N$ be a $\mathcal{C}^\infty$-smooth strongly convex body, and assume that at least one of the twist conditions* (T1), (T2) *or* (T3) *holds. Then, the same conclusion of Theorem 3.1 holds.*

Proof. We denote by $\pi_D \colon \mathbb{R}^N \to \mathbb{R}^N$ the projection on the convex set D. Assume that (T1) holds. Let $\widetilde{\mathcal{F}}_1 \colon \mathbb{R}^N \setminus D \to \mathbb{R}^N$ be the map defined as

$$\widetilde{\mathcal{F}}_1(y) = \mathbb{B}\nu_D(\pi_D(y))$$

We define $h \colon \mathbb{R}^N \to \mathbb{R}$ by

$$h(y) = \begin{cases} 0 & \text{if } y \in D \\ \gamma(\|y - \pi_D(y)\|) \left\langle \mathbb{B}(y - \pi_D(y)), y - \pi_D(y) \right\rangle & \text{if } y \in \mathbb{R}^N \setminus D \end{cases}$$

It is clear that h is a $\mathcal{C}^\infty$-smooth function. The function $F = \nabla h$ satisfies (3.3) with $\mathbb{S} = 2\mathbb{B}$ and $F^{-1}(0) = D$, while

$$\left\langle F(y), \widetilde{\mathcal{F}}_1(y) \right\rangle > 0 \qquad \text{for every } y \in \mathbb{R}^N \setminus D$$

(For the details, see [FU16a, Sec. 3].) This implies that

$$\langle v, \mathbb{B}\nu_D(y) \rangle \geq 0 \quad \text{for every } y \in \partial D \text{ and } v \in \mathcal{A}_F(y)$$

Combining this with (T1), we have (AC).

Assume now instead that (T2) holds. Without loss of generality, we set $d_0 = 0$ and we define $\widetilde{\mathcal{F}}_2 \colon \mathbb{R}^N \setminus D \to \mathbb{R}^N$ as

$$\widetilde{\mathcal{F}}_2(y) = \mathbb{B}y$$

When $\mathbb{B}$ is orthogonal, we define $h \colon \mathbb{R}^N \to \mathbb{R}$ by

$$h(y) = \begin{cases} 0 & \text{if } y \in D \\ \gamma(\|y - \pi_D(y)\|) \left\langle \mathbb{B}y, y - \pi_D(y) \right\rangle & \text{if } y \in \mathbb{R}^N \setminus D \end{cases}$$

The function $F = \nabla h$ satisfies (3.3) and $F^{-1}(0) = D$, while

$$\left\langle F(y), \widetilde{\mathcal{F}}_2(y) \right\rangle > 0 \qquad \text{for every } y \in \mathbb{R}^N \setminus D$$

The conclusion (AC) then follows as above. In the case of a general involutory matrix $\mathbb{B}$, we can reduce to the above situation by a change of basis, since $\mathbb{B}$ is diagonalizable (see [FU13, Sec. 4]).

Finally, assume that (T3) holds. We define $h \colon \mathbb{R}^N \to \mathbb{R}$ by

$$h(y) = \gamma(\|y - \pi_D(y)\|) \|y - \pi_D(y)\|^2$$

The conclusion follows, similarly as above. $\qquad\square$

We remark that, in general, assumptions (T1) and (T2) are strictly stronger than the avoiding cones condition (AC), as shown in the following example.

Example 3.11. Let us set $D = \mathcal{B}^3[0,1]$ and $\mathbb{B} = \mathrm{diag}(1,1,-1)$. We want to compare the avoiding cones condition (AC) induced by $F = \nabla h$, with h as in (3.6), with the conditions (T1) and (T2), for $d_0 = 0$, which are equivalent, in this situation. For every $y \in \partial D$, if $\langle y, \mathbb{B}y \rangle > 0$ (resp. $\langle y, \mathbb{B}y \rangle < 0$), the avoiding cones condition (AC) requires that $\vartheta(x,y)$ is not contained in the outer (resp. inner) normal cone of D in y, a half-line, whereas (T1) requires that $\vartheta(x,y)$ avoids an entire half-space containing this half-line. If instead $\langle y, \mathbb{B}y \rangle = 0$, then the avoiding cones condition (AC) requires that $\vartheta(x,y)$ avoids the half-plane generated by $\mathbb{B}y$ and $\pm\nu_D(y)$, whereas (T1) requires that $\vartheta(x,y)$ avoids a half-space that includes that half-plane.

3.3   Proof of Theorem 3.1

The proof follows the one given in [FU16b].

Let us recall that $\mathcal{Z} \colon \mathbb{R} \times \mathbb{R}^{2N} \to \mathbb{R}^{2N}$ is the $\mathcal{C}^\infty$-map associating to each couple (t, ζ) the value at time t of the unique solution $\mathcal{Z}(\cdot, \zeta)$ of (3.1) satisfying $\mathcal{Z}(0, \zeta) = \zeta$. For $\zeta \in \mathbb{R}^{2N}$, we write $\zeta = (\xi, \eta)$, with $\xi = (\xi_1, \dots, \xi_N) \in \mathbb{R}^N$ and $\eta = (\eta_1, \dots, \eta_N) \in \mathbb{R}^N$.

Since D is a compact set and the Hamiltonian $H(t,x,y)$ is 2π-periodic in the variables x_i, the continuous image by $\mathcal{Z}$ of $[0,T] \times (\mathbb{R}^N/2\pi\mathbb{Z}^N) \times D$ is contained in $(\mathbb{R}^N/2\pi\mathbb{Z}^N) \times B_r$, for some open ball B_r. Thus, after multiplying H by a smooth cutoff function of y, there is no loss of generality in assuming that there is some $R > r$ for which

$$H(t,x,y) = 0 \qquad \text{if } \|y\| \geq R$$

Consequently, there is some constant $c > 0$ such that

$$\left\| \frac{\partial H}{\partial y}(t,x,y) \right\| < c \qquad \text{for every } (t,x,y) \in \mathbb{R} \times \mathbb{R}^N \times \mathbb{R}^N$$

As a consequence, we will have that

$$\|\vartheta(\xi, \eta)\| < cT \qquad \text{for every } \xi, \eta \in \mathbb{R}^N \tag{3.12}$$

For any t, we write $\mathcal{Z}_t := \mathcal{Z}(t, \cdot) \colon \mathbb{R}^{2N} \to \mathbb{R}^{2N}$. The following properties hold.

(i) $\mathcal{Z}_0$ *is the identity map in* $\mathbb{R}^{2N}$

(ii) $\mathcal{Z}_t(\zeta + p) = \mathcal{Z}_t(\zeta) + p, \quad$ *if* $p \in 2\pi\mathcal{Z}^N \times \{0\}$

(iii) $\mathcal{Z}(t, \xi, \eta) = (\xi, \eta), \quad$ *if* $\|\eta\| \geq R;$

(iv) *each* $\mathcal{Z}_t$ *is a symplectic* $\mathcal{C}^\infty$*-diffeomorphism of* $\mathbb{R}^{2N}$ *onto itself*

This last property is standard in Hamiltonian dynamics.

By the use of the Ascoli–Arzelà Theorem, we can find some constant $\varepsilon \in (0, 1)$ such that

$$\vartheta(\xi, \eta) \notin \{\mu F(\eta) : \mu \geq 0\} \qquad \text{if } 0 < \|F(\eta)\| < \varepsilon \qquad (3.13)$$

Recalling that $F = \nabla h$ and that (3.3) holds, we can assume without loss of generality that

$$h(y) = \frac{1}{2} \langle \mathbb{S}y, y \rangle \qquad \text{when } \|y\| \geq K$$

Indeed, choosing $\widetilde{R}$ large enough and defining

$$\widetilde{F}(x) = \begin{cases} F(x) & \text{if } \|x\| \leq \widetilde{R} \\ F(x) + \gamma(\|x\| - \widetilde{R})(\mathbb{S}x - F(x)) & \text{if } \widetilde{R} \leq \|x\| \leq \widetilde{R} + 1 \\ \mathbb{S}x & \text{if } \|x\| \geq \widetilde{R} + 1 \end{cases}$$

we will have that $D \subseteq \mathcal{B}^N(0, \widetilde{R})$ and $\widetilde{F}^{-1}(0) = D$, while the cones $\mathcal{A}_F(y)$ will not be changed for $y \in \mathcal{B}^N(0, R)$.

We define the function $\mathfrak{R} \colon \mathbb{R}^{2N} \to \mathbb{R}$ as

$$\mathfrak{R}(\xi, \eta) := -\frac{c}{\varepsilon} h(\eta)$$

the function $R \colon [0, T] \times \mathbb{R}^{2N} \to \mathbb{R}$ by

$$R(t, z) := \mathfrak{R}(\mathcal{Z}_t^{-1}(z))$$

and the modified Hamiltonian $\widetilde{H} \colon [0, T] \times \mathbb{R}^{2N} \to \mathbb{R}$ as

$$\widetilde{H}(t, z) := H(t, z) + R(t, z)$$

It is a $\mathcal{C}^\infty$-smooth function, and satisfies the following properties:

(I) $\widetilde{H}(t, z + p) = \widetilde{H}(t, z),$ *if* $p \in 2\pi\mathbb{Z}^N \times \{0\}$

(II) $\widetilde{H}(t, x, y) = \frac{1}{2}\left\langle \widetilde{\mathbb{S}}y, y \right\rangle,$ *if* $\|y\| \geq R,$ *where* $\widetilde{\mathbb{S}} = -(c/\varepsilon)\mathbb{S}$

(III) $\widetilde{H}$ *and* H *coincide on the set*

$$\left\{ (t, \mathcal{Z}(t, \xi, \eta)) : t \in [0, T], \xi \in \mathbb{R}^N, \eta \in D \right\}$$

We consider the modified Hamiltonian system

$$\dot{z} = \mathcal{J}\nabla\widetilde{H}(t,z) \tag{$\widetilde{\mathrm{HS}}$}$$

and look for solutions satisfying $z(0) = z(T)$. These will be obtained as critical points of a suitably defined functional.

Let us consider the Hilbert space $H_T^{1/2}$, whose elements are those functions $z \in L^2(0,T;\mathbb{R}^{2N})$, extended by T-periodicity (in the a.e. sense), with the property that, writing the associated Fourier series

$$z(t) \sim \sum_{k=-\infty}^{+\infty} a_k e^{2\pi k i t/T}$$

one has that

$$\sum_{k=-\infty}^{+\infty} (1 + |k|)\, |a_k|^2 < +\infty$$

We refer to [HZ94, Section 3.3] for the main properties of $H_T^{1/2}$. The functions in $H_T^{1/2}$ are not necessarily continuous, but their restriction to $[0,T]$ belongs to $L^p(0,T;\mathbb{R}^{2N})$, for every $p \in [1,+\infty)$. On the other hand, let H_T^1 be the space of those functions $z \in H_T^{1/2}$ for which

$$\sum_{k=-\infty}^{+\infty} (1 + |k|^2)\, |a_k|^2 < +\infty$$

These are absolutely continuous T-periodic functions. In particular, they are such that $z(0) = z(T)$.

We define an auxiliary function $\widehat{H}\colon \mathbb{R} \times \mathbb{R}^{2N} \to \mathbb{R}$ as follows:

$$\widehat{H}(t,z) = \widetilde{H}(\tau,z) \qquad \text{with } \tau \in [0,T) \text{ and } t = \tau + kT, \text{ for some } k \in \mathbb{Z}$$

By construction, $\widehat{H}(t,z)$ is T-periodic in t, but not necessarily continuous. In view of (I) and (II) above, it is possible to define the functional $\varphi\colon H_T^{1/2} \to \mathbb{R}$ as

$$\varphi(z) = \int_0^T \left[\frac{1}{2} \langle \mathcal{J}\dot{z}(t), z(t) \rangle + \widehat{H}(t, z(t)) \right] \mathrm{d}t$$

It can be seen that it is continuously differentiable, and its critical points correspond to the weak T-periodic solutions of

$$\dot{z} = \mathcal{J}\nabla\widehat{H}(t,z) \tag{3.14}$$

Let z be a critical point of φ. Following [Rab86], we will show that the restriction of z to the closed interval $[0,T]$ is a classical solution of $(\widetilde{\mathrm{HS}})$ satisfying $z(0) = z(T)$.

Since z is a critical point of φ, we have $\langle \nabla\varphi(z), w \rangle = 0$, for every $w \in H_T^{1/2}$. Then, taking w in H_T^1, we have

$$\int_0^T \left[\langle z(t), \mathcal{J}\dot{w}(t) \rangle + \left\langle \nabla\widehat{H}(t, z(t)), w(t) \right\rangle \right] \mathrm{d}t = 0 \qquad (3.15)$$

In particular, taking as w the constant functions with all zero components except one of them, we deduce that

$$\int_0^T \nabla\widehat{H}(t, z(t))\,\mathrm{d}t = 0$$

Hence, denoting by $[\cdot]$ the mean of a function defined on $[0, T]$, we deduce

$$[\mathcal{J}\nabla\widehat{H}(\cdot, z(\cdot))] = \frac{1}{T}\int_0^T \mathcal{J}\nabla\widehat{H}(t, z(t))\,\mathrm{d}t = 0 \qquad (3.16)$$

It is known that, for every fixed vector $u \in \mathbb{R}^{2N}$ and every function $g \in L^2(0, T; \mathbb{R}^{2N})$, with $[g] = 0$, there is a unique function $v \in H_T^1$ satisfying $[v] = u$ and $\dot{v} = g$ in $L^2(0, T; \mathbb{R}^{2N})$. Hence, from (3.16) we deduce that there is a unique function $v \in H_T^1$ such that $[v] = [z]$ and $\dot{v} = \mathcal{J}\nabla\widehat{H}(\cdot, z(\cdot))$ in $L^2(0, T; \mathbb{R}^{2N})$. Therefore, for any $w \in H_T^1$, integrating by parts and using (3.15),

$$\int_0^T \langle v, \mathcal{J}\dot{w} \rangle = -\int_0^T \langle \dot{v}, \mathcal{J}w \rangle = -\int_0^T \left\langle \nabla\widehat{H}(t, z(t)), w(t) \right\rangle \mathrm{d}t = \int_0^T \langle z, \mathcal{J}\dot{w} \rangle$$

We deduce that $v = z$ in H_T^1, and

$$\dot{z}(t) = \mathcal{J}\nabla\widehat{H}(t, z(t)) \qquad (3.17)$$

for almost every $t \in [0, T]$. Moreover, since z belongs to H_T^1, it is continuous, hence $\dot{z}$ has to be continuous, too, and z satisfies (3.17) *for every* $t \in [0, T]$. Furthermore, $z(0) = z(T)$. Hence, by continuity, z is a classical solution of $(\widetilde{\mathrm{HS}})$ on $[0, T]$: when restricted to that interval, it belongs to $\mathcal{C}^1([0, T], \mathbb{R}^{2N})$. A bootstrap argument now shows that $z \in \mathcal{C}^\infty([0, T], \mathbb{R}^{2N})$.

For any $z(t) = (x(t), y(t))$ in $H_T^{1/2}$, we write $x(t) = \bar{x} + \tilde{x}(t)$, where $\bar{x} = [x] \in \mathbb{R}^N$. We thus have the decomposition $H_T^{1/2} = \mathbb{R}^N \oplus E$, where E is a Hilbert space. By (I) we can identify $\bar{x} \in \mathbb{R}^N$ with its projection on the N-torus $\mathbb{T}^N$ and define the functional $\widetilde{\varphi}\colon \mathbb{T}^N \times E \to \mathbb{R}$ as

$$\widetilde{\varphi}(\bar{x}, (\tilde{x}, y)) = \varphi(\bar{x} + \tilde{x}, y)$$

By [Szu90, Theorem 4.2] and [Szu92, Theorem 8.1], the functional $\widetilde{\varphi}$ has of at least $N+1$ critical points, and 2^N of them if all its critical points are nondegenerate. As we saw above, these critical points correspond to geometrically distinct solutions of $(\widetilde{\text{HS}})$ belonging to $\mathcal{C}^\infty([0,T],\mathbb{R}^{2N})$, satisfying $z(0) = z(T)$.

As a consequence of (III), the Hamiltonian systems (3.1) and $(\widetilde{\text{HS}})$ have the same solutions $z(t) = (x(t), y(t))$, with $t \in [0,T]$, departing with $y(0) \in D$. Thus, in order to complete the proof of Theorem 3.1, it will suffice to check that $(\widetilde{\text{HS}})$ does not have solutions $z(t) = (x(t), y(t))$, satisfying $z(0) = z(T)$, departing with $y(0) \notin D$.

We argue by contradiction, and assume that such a solution $z(t)$ exists. Let us define the $\mathcal{C}^\infty$-function $\zeta \colon [0,T] \to \mathbb{R}^{2N}$ by

$$\zeta(t) := \mathcal{Z}_t^{-1}(z(t))$$

Differentiating in the equality $z(t) = \mathcal{Z}(t, \zeta(t))$, we find

$$\dot{z}(t) = \frac{\partial \mathcal{Z}}{\partial t}(t, \zeta(t)) + \frac{\partial \mathcal{Z}}{\partial \zeta}(t, \zeta(t))\dot{\zeta}(t)$$

so that

$$\frac{\partial \mathcal{Z}}{\partial \zeta}(t, \zeta(t))\dot{\zeta}(t) = \mathcal{J}\nabla\widetilde{H}(t, z(t)) - \mathcal{J}\nabla H(t, z(t)) = \mathcal{J}\nabla R(t, z(t)) \quad (3.18)$$

By (iv) the map $\mathcal{Z}_t$ is symplectic, so

$$\frac{\partial \mathcal{Z}}{\partial \zeta}(t, \zeta(t))^* \mathcal{J} \frac{\partial \mathcal{Z}}{\partial \zeta}(t, \zeta(t)) = \mathcal{J} \qquad \text{for every } t \in \mathbb{R}$$

Hence, if we multiply both sides of 3.18 by $-\mathcal{J}(\partial\mathcal{Z}/\partial\zeta)^*\mathcal{J}$, we get

$$\dot{\zeta}(t) = \mathcal{J}\frac{\partial \mathcal{Z}}{\partial \zeta}(t, \zeta(t))^* \nabla R(t, z(t)) = \mathcal{J}\nabla\mathfrak{R}(\zeta(t))$$

where the last equality comes from the fact that $R(t, \mathcal{Z}(t, \zeta)) = \mathfrak{R}(\zeta)$. Then, recalling that $\zeta(t) = (\xi(t), \eta(t))$, we obtain

$$\dot{\xi}(t) = -\frac{c}{\varepsilon}\, F(\eta(t)) \qquad \dot{\eta}(t) = 0$$

and consequently, by (i), writing $z(t) = (x(t), y(t))$,

$$\eta(t) = \eta(0) = y(0) \qquad \xi(t) = x(0) - \frac{ct}{\varepsilon}\, F(y(0))$$

for every $t \in [0,T]$, namely

$$\zeta(t) = \left(x(0) - \frac{ct}{\varepsilon}\, F(y(0))\,, y(0) \right)$$

Being $z(t) = \mathcal{Z}(t, \zeta(t))$ and $\mathcal{Z}_T = \mathcal{P}$, we thus have

$$z(T) = \mathcal{P}\Big(x(0) - \frac{cT}{\varepsilon}\, F(y(0))\,, y(0)\Big)$$

and in particular

$$x(T) = x(0) - \frac{cT}{\varepsilon}\, F(y(0)) + \vartheta\Big(x(0) - \frac{cT}{\varepsilon}\, F(y(0)), y(0)\Big)$$

In order to obtain the desired contradiction, we shall show that $x(T) \neq x(0)$, namely,

$$\vartheta\Big(x(0) - \frac{cT}{\varepsilon}\, F(y(0)), y(0)\Big) \neq \frac{cT}{\varepsilon}\, F(y(0)) \qquad (3.19)$$

We distinguish between two situations, according to the initial point of the solution. If $0 < \|F(y(0))\| < \varepsilon$, by (3.13) we have

$$\vartheta\Big(x(0) - \frac{cT}{\varepsilon}\, F(y(0)), y(0)\Big) \notin \{\alpha F(y(0)) : \alpha \geq 0\}$$

implying (3.19). On the other hand, if $\|F(y(0))\| \geq \varepsilon$, by (3.12) we get

$$\left\|\vartheta\Big(x(0) - \frac{cT}{\varepsilon}\, F(y(0)), y(0)\Big)\right\| < cT \leq \left|\frac{cT}{\varepsilon}\, F(y(0))\right|$$

implying (3.19), again. The proof is thus completed.

3.4 A variation of Theorem 3.1

With the same strategy adopted for Theorem 3.1, we can prove the following more general result.

As before, we assume the Hamiltonian function $H\colon \mathbb{R} \times \mathbb{R}^{2N} \to \mathbb{R}$ to be $\mathcal{C}^\infty$-smooth, and T-periodic in its first variable t. Let M be an integer such that $0 \leq M < N$, and assume that $H(t, x, y)$ is 2π-periodic in $x_1, \ldots, x_N$ and in $y_1, \ldots, y_M$. We still write as in (3.2) the Poincaré map $\mathcal{P}$ associated to the system (3.1), and we define the projection $\pi\colon \mathbb{R}^N \to \mathbb{R}^{N-M}$ as

$$\pi(y_1, \ldots, y_N) = (y_{M+1}, \ldots, y_N)$$

Theorem 3.12. *Let $F = \nabla h\colon \mathbb{R}^{N-M} \to \mathbb{R}^{N-M}$ be a $\mathcal{C}^\infty$-smooth function for which there exist two constants $K > 0$ and $C > 0$ and a regular symmetric $(N - M) \times (N - M)$ matrix $\mathbb{S}$ such that*

$$\|F(w) - \mathbb{S}w\| \leq C \qquad \textit{when } \|w\| \geq K$$

and set $D := F^{-1}(0)$. If

$$\pi(\vartheta(x, y)) \notin \mathcal{A}_F(\pi(y)) \qquad \textit{for every } (x, y) \in \mathbb{R}^{N+M} \times \partial D$$

then $\mathcal{P}$ has at least $N + M + 1$ geometrically distinct fixed points, all in $\mathbb{R}^{N+M} \times D$. Moreover, if all its fixed points are non degenerate, then there are at least 2^{N+M} of them.

Proof. The proof is similar to that of Theorem 3.1, with the following changes. The construction is based on the $y_{M+1}, \ldots, y_N$ coordinates, in the sense that first we assume $H(t, x, y) = 0$ if $\|\pi(y)\| \geq R$, and later we use the function

$$\mathfrak{R}(\xi, \eta) = -\frac{c}{\varepsilon} h(\pi(\eta))$$

to define the modified Hamiltonian.

Then, when looking for the critical points of the functional φ, we use the decomposition $H_T^{1/2} = \mathbb{R}^{N+M} \oplus \widehat{E}$, where R^{N+M} is the subspace associated to the constant functions with values in $R^{N+M} \times \{0_{\mathbb{R}^{N-M}}\}$, and $\widehat{E}$ is a Hilbert space. The projection $\mathbb{R}^{N+M} \to \mathbb{T}^{N+M}$ will lead to a functional $\widetilde{\varphi} \colon \mathbb{T}^{N+M} \times \widehat{E} \to \mathbb{R}$, having at least $N + M + 1$ critical points, or at least 2^{N+M} of them if all critical points are non degenerate. With the same line of reasoning used for Theorem 3.1, it can be shown that such critical points correspond to geometrically distinct solutions of (3.1). $\qquad\square$

We notice that, if we extend Theorem 3.12 to the case $M = N$, no avoiding cones condition is required any longer and we recover a celebrated result on the existence of fixed points for a symplectic map on the torus, as conjectured by Arnold and proved by Conley and Zehnder [CZ83a]. Thus Theorem 3.12 covers the intermediate cases between this result and Theorem 3.1, corresponding to $M = 0$. We finally notice that we could have assumed the periodicity along a different basis than the usual one in $\mathbb{R}^{N+M}$. Similar situations have also been considered in [Cha89; Fel92; FM06; Fou+94; Liu89].

Chapter 4

Applications: twist at different scales

Several application of higher dimensional extensions of the Poincaré–Birkhoff Theorem have been proposed, regarding, for instance, systems associated with relativistic or mean-curvature operators [FU16a], systems of differential equations of Duffing type [BO14], superlinear systems [FS16; FU16a], systems with singularities in [FS14], and special cases of the N-vortex problem [BTK07; Bla08].

In this Chapter (cf. [FGG16]) we discuss the three main situation in which the twist can be found:

- locally: this extend the nondegeneracy perspective presented in Chapter 1;

- at an intermediate scale, as direct application of Theorem 3.1;

- globally, considering the twist generated at zero and at infinity.

4.1 Periodic perturbations of completely integrable systems

Let us consider a completely integrable Hamiltonian system on $\mathbb{T}^N \times \mathcal{D}$, where we recall that $\mathbb{T}^N$ is the N-dimensional torus $(\mathbb{R}/2\pi\mathbb{Z})^N$, and $\mathcal{D}$ is an open subset of $\mathbb{R}^N$. The continuously differentiable Hamiltonian function $\mathcal{H} \colon \mathbb{T}^N \times \mathcal{D} \to \mathbb{R}$ can therefore be written in the form $\mathcal{H}(\varphi, I) = \mathscr{K}(I)$. We recall that $I = (I_1, \dots, I_N) \in \mathcal{D}$ are the action variables, while $\varphi = (\varphi_1, \dots, \varphi_N) \in \mathbb{T}^N$ are the angle variables.

For every $I^* \in \mathcal{D}$, the torus $\mathscr{T}^* = \mathbb{T}^N \times \{I^*\}$ is invariant for the flow, and its evolution in time is determined by the associated frequency vector

$$\omega^* = (\omega_1^*, \dots, \omega_N^*) = \nabla \mathscr{K}(I^*)$$

When the components $\omega_1^*, \ldots, \omega_N^*$ are rationally independent, the solutions are *quasiperiodic* and each orbit is a dense subset of the N-torus T^*. Such tori are called *nonresonant*. Otherwise, we have a foliation in M-dimensional tori, where $M < N$ is the rational rank of the components of ω^*, and the orbits will be quasiperiodic with respect to these lower dimensional tori. A special case occurs when the components of ω^* are all pairwise commensurable: then, all the solutions on the torus are periodic with the same period, and the N-torus T^* admits a foliation in invariant 1-tori, each one defined by the orbit of a solution.

Since complete integrability reveals a lot about the behaviour of the dynamics, a natural question is: how much of this structure is preserved under a small perturbation? In particular, one could wonder whether, near an invariant torus of the unperturbed system, it is possible to find periodic or quasiperiodic solutions for the perturbed system with the same frequency.

A series of positive results are known for a large family of nonresonant tori, those with a Diophantine frequency. These results are usually collected under the name of KAM theory, recalling its main contributors A.N. Kolmogorov, V.I. Arnold and J. Moser. We remark that, beyond a nondegeneracy assumption on the torus, strong smoothness of the perturbation is always needed, cf. [Alb07; Her83; Sal04]. While these strongly nonresonant tori survive under small perturbations, the same is not true for the other tori [Bes00; MP85; Tre89], and in particular for those made of periodic solutions. Still, some traces of these tori can be found.

In the planar case, where each torus $\mathbb{T}^1$ coincides with a periodic orbit, the survival of two periodic solutions ca be directly obtained as a consequence of the Poincaré–Birkhoff theorem. The required twist condition is satisfied, in this case, under some rather weak nondegeneracy assumptions. A fainter kind of traces of an invariant torus is provided by the so called Aubry–Mather theory (cf. [Mos86], and the references therein), showing the existence of a Cantor set, called *cantorus*, that preserves, in a generalized sense, the rotational properties of the original torus.

For higher dimensional Hamiltonian systems, the problem has been solved by Bernstein and Katok [BK87] and refined by Chen [Che92]), but a strong nondegeneracy assumption, such as strict convexity, is required. In this Section we show that actually only a very weak local twist is necessary, so that the survival of $N + 1$ solution out of a perturbed N-torus can be assured also in situations when the Jacobian of $\mathscr{K}$ is degenerate or even not defined.

We are therefore interested in the case when the dynamics on the torus $\mathscr{T}^*$ consists of a family of periodic orbits with minimal period T^*. This happens if and only if there exist N integers $a_1, \ldots, a_N$ such that

$$T^* \omega_i^* = 2\pi a_i \ \text{ for every } i = 1, \ldots, N$$

and T^* is the minimum positive real number with such a property. The

integers a_i count the number of rotations made by each periodic solution around the i-th component of the torus in a period T^*; the sign of a_i describes the sense of rotation.

A standard approach to study such a system, defined on $\mathbb{T}^N \times \mathcal{D}$, is to consider its canonical lift to $\mathbb{R}^N \times \mathcal{D}$. The Hamiltonian system then becomes

$$\begin{cases} \dot{\xi} = \nabla \mathscr{K}(\eta) \\ \dot{\eta} = 0 \end{cases} \tag{4.1}$$

where $\xi = (\xi_1, \ldots, \xi_N) \in \mathbb{R}^N$ and $\eta = (\eta_1, \ldots, \eta_N) \in \mathcal{D}$. To be more precise, denoting by $\mathbb{I}_N$ the identity on $\mathbb{R}^N$ and by $P_N \colon \mathbb{R}^N \to \mathbb{T}^N$ the standard projection on the torus, the map $(P_N, \mathbb{I}_N) \colon \mathbb{R}^N \times \mathbb{R}^N \to \mathbb{T}^N \times \mathbb{R}^N$ is a local change of variables which transforms (ξ, η) into (φ, I). Each translation of 2π in the ξ_i coordinate for system (4.1) corresponds to a single rotation in the φ_i coordinate for the original system.

Let us now consider a general nearly integrable Hamiltonian system on $\mathbb{T}^N \times \mathcal{D}$, with time-dependent Hamiltonian function $\mathscr{K} \colon \mathbb{R} \times \mathbb{T}^N \times \mathcal{D} \to \mathbb{R}$, sufficiently close to $\mathscr{K}$. The canonical lift then leads to the Hamiltonian system on $\mathbb{R}^N \times \mathcal{D}$ given by

$$\begin{cases} \dot{\xi} = \nabla_\eta K(t, \xi, \eta) \\ \dot{\eta} = -\nabla_\xi K(t, \xi, \eta) \end{cases} \tag{4.2}$$

The Hamiltonian function $K \colon \mathbb{R} \times \mathbb{R}^N \times \mathcal{D} \to \mathbb{R}$ is assumed to be continuous, T-periodic in the first variable, 2π-periodic in each variable ξ_i, and continuously differentiable in $\zeta = (\xi, \eta)$.

We now fix an $I^0 \in \mathcal{D}$ and introduce some kind of nondegeneracy condition at I^0. Usually, in the literature (see, e.g., [ACE87; BK87; Che92]), it is assumed that $\mathscr{K}$ is twice continuously differentiable, and that

$$\det(\mathscr{K}''(I^0)) \neq 0 \tag{4.3}$$

Here, we only ask $\mathscr{K}$ to be once continuously differentiable, and that there exists an invertible symmetric $N \times N$ matrix $\mathbb{B}$ such that

$$0 \in \mathrm{cl} \left\{ \rho \in (0, +\infty) : \min_{\|I - I^0\| = \rho} \left\langle \nabla \mathscr{K}(I) - \nabla \mathscr{K}(I^0), \mathbb{B}(I - I^0) \right\rangle > 0 \right\} \tag{4.4}$$

where $\mathrm{cl}\, A$ denotes the closure of a set A. Notice that (4.3) implies (4.4), taking $\mathbb{B} = \mathscr{K}''(I^0)$. On the other hand, the function $\mathscr{K}(I) = \|I - I^0\|^\alpha$ satisfies (4.4), with $\mathbb{B} = \mathbb{I}$, but not (4.3), if $\alpha > 2$. Moreover, we observe

that (4.4) does not even require the local invertibility of $\nabla \mathscr{K}$. An easy example, with $N = 1$, is provided by the function $\mathscr{K}(I) = \int_0^I f(s)\,\mathrm{d}s$, with

$$
f(s) = \begin{cases} \omega^0 + |s| \sin\left(\dfrac{1}{s}\right) & \text{if } s \neq 0 \\ \omega^0 & \text{if } s = 0 \end{cases}
$$

Clearly, this function $\mathscr{K}$ is only once continuously differentiable at $I^0 = 0$, and $\nabla \mathscr{K} = f$ is not invertible, but our nondegeneracy condition (4.4) is still satisfied, with $\mathbb{B}$ being the identity on $\mathbb{R}$.

We will show that the nondegeneracy condition (4.4) extends by continuity to a neighborhood $\mathcal{U}$ of I^0. As a consequence, we will prove that, for every $I^* \in \mathcal{U}$ as above, if there exist two positive integers m^* and n^* satisfying

$$
T^* = \frac{m^* T}{n^*} \tag{4.5}
$$

then the perturbed system (4.2) has at least $N + 1$ geometrically distinct $m^* T$-periodic solutions. These solutions stay near the corresponding solutions of the unperturbed problem, and their projections on $\mathbb{T}^N \times \mathcal{D}$ will maintain the same rotational properties of $\mathscr{T}^*$.

Here is our main result.

Theorem 4.1. *Suppose that there exists $I^0 \in \mathcal{D}$ and an invertible symmetric $N \times N$ matrix $\mathbb{B}$ such that (4.4) holds. Then, for every $\sigma > 0$ there exists an open neighborhood $\mathcal{U} \subseteq \mathcal{D}$ of I^0, with the following property: given any positive integer $\overline{m}$, there exists $\varepsilon > 0$ such that, if*

$$
\|\nabla_\xi K(t, \xi, \eta)\| + \|\nabla_\eta K(t, \xi, \eta) - \nabla \mathscr{K}(\eta)\| < \varepsilon
$$
$$
\textit{for every } (t, \xi, \eta) \in [0, T] \times [0, 2\pi]^N \times \mathcal{D} \tag{4.6}
$$

then, for every $I^* \in \mathcal{U}$ being associated with an invariant torus of periodic solutions for (4.1) with frequency vector $\omega^* = (\omega_1^*, \ldots, \omega_N^*)$ and minimal period T^* satisfying (4.5) for suitable positive integers $m^* \leq \overline{m}$ and n^*, system (4.2) has at least $N + 1$ geometrically distinct $m^* T$-periodic solutions

$$
(\xi^1(t), \eta^1(t)), \ \ldots \ , (\xi^{N+1}(t), \eta^{N+1}(t))
$$

with

$$
\left\| \xi^k(t) - \xi^k(0) - t \nabla \mathscr{K}(I^*) \right\| + \left\| \eta^k(t) - I^* \right\| \leq \sigma \tag{4.7}
$$

for every $t \in [0, m^* T]$ and $k = 1, \ldots, N + 1$. Moreover, for each solution $(\xi^k(t), \eta^k(t))$, its projection on $\mathbb{T}^N \times \mathcal{D}$ makes exactly $(\omega_i^*/2\pi) m^* T$ rotations around the i-th component of the torus in a period $m^* T$, for every $i = 1, \ldots, N$.

Proof. We can assume, without loss of generality, the function $\mathscr{K}$ to be defined on the whole space $\mathbb{R}^N$. Indeed, after replacing the set $\mathcal{D}$ by a smaller open set, containing I^0, where $\mathscr{K}$ is bounded, we can construct a continuously differentiable extension of $\mathscr{K}$ on $\mathbb{R}^N$. The solutions we are interested in will nevertheless be contained in the smaller set, where $\mathscr{K}$ has not been modified. Similarly, for our purposes we can assume without loss of generality that the Hamiltonian system (4.2) is defined on $\mathbb{R} \times \mathbb{R}^N \times \mathbb{R}^N$.

Let us fix any $\sigma > 0$ such that $\mathcal{B}[I^0, \sigma] \subseteq \mathcal{D}$. By assumption (4.4), there are $\ell > 0$ and $\rho_1 \in \,]0, \sigma/4]$ such that

$$\left\| \eta - I^0 \right\| = \rho_1 \quad \implies \quad \left\langle \nabla \mathscr{K}(\eta) - \nabla \mathscr{K}(I^0), \mathbb{B}(\eta - I^0) \right\rangle \geq 4\ell$$

By continuity, there is an open neighbourhood $\mathcal{U}$ of I^0, contained in $\mathcal{B}[I^0, \rho_1]$, such that, for every $I^* \in \mathcal{U}$,

$$\left\| \eta - I^* \right\| = \rho_1 \quad \implies \quad \left\langle \nabla \mathscr{K}(\eta) - \nabla \mathscr{K}(I^*), \mathbb{B}(\eta - I^*) \right\rangle \geq 2\ell \qquad (4.8)$$

For any arbitrary $I^* \in \mathcal{U}$, with frequency vector $\omega^* = (\omega_1^*, \ldots, \omega_N^*) = \nabla \mathscr{K}(I^*)$, let us define

$$K^*(t, \xi, \eta) = K(t, \xi + \omega^* t, \eta) - \langle \omega^*, \eta \rangle$$

and consider the Hamiltonian system

$$\dot{\zeta} = \mathcal{J} \nabla_\zeta K^*(t, \zeta) \qquad (4.9)$$

Claim. *For any fixed positive real numbers $\overline{m}$ and $\bar{c}$, there exists $\varepsilon > 0$ such that, if (4.6) holds, then for every $I^* \in \mathcal{U}$, every solution $\zeta(t) = (\xi(t), \eta(t))$ of (4.9) with initial point satisfying $\|\eta(0) - I^*\| \leq \rho_1$ will be such that*

$$\left\| \xi(t) - \xi(0) - t\big[\nabla \mathscr{K}(\eta(0)) - \omega^* \big] \right\| + \|\eta(t) - \eta(0)\| \leq \bar{c}$$
$$\textit{for every } t \in [0, \overline{m}T] \quad (4.10)$$

Proof of the Claim. Arguing by contradiction, assume that there is a sequence $(I_\lambda^*)_\lambda \in \mathcal{U}$, with $\omega_\lambda^* = \nabla \mathscr{K}(I_\lambda^*)$, and a sequence $(K_\lambda)_\lambda$ of Hamiltonian functions as above (in particular, they are T-periodic in t), such that, writing

$$K_\lambda^*(t, \xi, \eta) = K_\lambda(t, \xi + \omega^* t, \eta) - \langle \omega_\lambda^*, \eta \rangle$$

one has that

$$\|\nabla_\xi K_\lambda^*(t, \xi, \eta)\| + \|\nabla_\eta K_\lambda^*(t, \xi, \eta) - \nabla \mathscr{K}(\eta) + \omega_\lambda^*\| \leq \frac{1}{\lambda}$$
$$\text{for every } (t, \xi, \eta) \in \mathbb{R} \times \mathbb{R}^N \times \mathcal{D}$$

and, correspondingly, a sequence $(\zeta^\lambda)_\lambda$, with $\zeta^\lambda = (\xi^\lambda, \eta^\lambda)$, solving $\dot\zeta^\lambda = \mathcal{J}\nabla_\zeta K_\lambda^*(t, \zeta^\lambda)$, such that $\left\|\eta^\lambda(0) - I_\lambda^*\right\| \leq \rho_1$, while (4.10) does not hold, i.e., for every λ there is a $t_\lambda \in [0, \overline{m}T]$ for which

$$\left\|\xi^\lambda(t_\lambda) - \xi^\lambda(0) - t_\lambda\left[\nabla\mathscr{K}(\eta^\lambda(0)) - \omega_\lambda^*\right]\right\| + \left\|\eta^\lambda(t_\lambda) - \eta^\lambda(0)\right\| > \bar{c} \quad (4.11)$$

Since the Hamiltonians K_λ^* are 2π-periodic in the variables $\xi_1, \ldots, \xi_N$, we can assume that $\xi^\lambda(0) \in [0, 2\pi]^N$. Hence, passing to a subsequence, $\zeta^\lambda(0)$ converges to some point $\zeta^\sharp \in [0, 2\pi]^N \times \mathcal{B}[I^0, 2\rho_1]$. Moreover, for a subsequence, I_λ^* converges to some $I^\sharp$, and $\omega_\lambda^* = \nabla\mathscr{K}(I_\lambda^*)$ converges to $\omega^\sharp = \nabla\mathscr{K}(I^\sharp)$. Finally, for a subsequence, t_λ will converge to some $t^\sharp \in [0, \overline{m}T]$. By a lemma of Kamke (cf. [Sel73]), for a further subsequence $(\zeta^{\lambda_l})_l$ we have uniform convergence on $[0, \overline{m}T]$ to the solution of

$$\begin{cases} \dot\xi = \nabla\mathscr{K}(\eta) - \omega^\sharp \\ \dot\eta = 0 \end{cases}$$

given by

$$\begin{cases} \xi(t) = \xi(0) + t(\nabla\mathscr{K}(\eta(0)) - \omega^\sharp) \\ \eta(t) = \eta(0) \end{cases}$$

On the other hand, passing to the limit in (4.11),

$$\left\|\xi(t^\sharp) - \xi(0) - t^\sharp\left[\nabla\mathscr{K}(\eta(0)) - \omega^\sharp\right]\right\| + \left\|\eta(t^\sharp) - \eta(0)\right\| \geq \bar{c} > 0$$

which is a contradiction, since the left hand side is equal to zero. The Claim is thus proved. □

We can now conclude the proof of Theorem 4.1. Let $\overline{m}$ be a fixed positive integer, and choose $\bar{c}$ such that

$$\bar{c} \leq \min\left\{\frac{T\ell}{\|\mathbb{B}\|\,\rho_1}, \frac{\sigma}{4}\right\}$$

We now focus our attention on those $I^* \in \mathcal{U}$ whose associated invariant torus is composed of periodic solutions for (4.1) with minimal period T^*, such that there exist two positive integers m^* and n^* with $m^* \leq \overline{m}$ and $T^* = m^*T/n^*$. We observe that every m^*T-periodic solution of (4.9) corresponds to an m^*T-periodic solution $(\xi(t), \eta(t))$ of (4.2), such that every $\xi_i(t)$ makes exactly $(\omega_i^*/2\pi)m^*T$ turns around the origin in the time m^*T. We will apply Corollary 3.10 in the case (T1) (cf. also [FU16a]) to system (4.9).

Let $D = \mathcal{B}[I^*, \rho_1]$, and let $\zeta(t) = (\xi(t), \eta(t))$ be a solution of (4.9), with $\eta(0) \in \partial D$, i.e. $\|\eta(0) - I^*\| = \rho_1$. Then, by (4.8) and (4.10), we get

$$\langle \xi(m^*T) - \xi(0), \mathbb{B}(\eta(0) - I^*) \rangle =$$
$$= \langle \xi(m^*T) - \xi(0) - m^*T[\nabla \mathscr{K}(\eta(0)) - \nabla \mathscr{K}(I^*)], \mathbb{B}(\eta(0) - I^*) \rangle +$$
$$+ \langle m^*T[\nabla \mathscr{K}(\eta(0)) - \nabla \mathscr{K}(I^*)], \mathbb{B}(\eta(0) - I^*) \rangle$$
$$\geq -\frac{T\ell}{\|B\| \rho_1} \|B\| \rho_1 + 2m^*T\ell \geq m^*T\ell > 0$$

We can therefore apply Corollary 3.10 in the case (T1), so to get $N + 1$ geometrically distinct m^*T-periodic solutions of (4.9),

$$\zeta^1(t) = (\xi^1(t), \eta^1(t)), \ldots, \zeta^{N+1}(t) = (\xi^{N+1}(t), \eta^{N+1}(t))$$

such that $\eta^k(0) \in D$, for every $k = 1, \ldots, N + 1$. Moreover, by (4.10), we have that $\|\eta^k(t) - I^*\| \leq \bar{c} \leq \sigma/2$, for every $t \in [0, m^*T]$. On the other hand, a continuity argument can be used, taking smaller values for $\bar{c}$ and ε, to infer that $\|\xi^k(t) - \xi^k(0) - t\nabla \mathscr{K}(I^*)\| \leq \sigma/2$, for every $t \in [0, m^*T]$. So, (4.7) holds, as well, and the proof is thus completed. $\square$

Notice that, taking $\overline{m}$ sufficiently large, it is possible to find an arbitrarily large number of values $I^* \in \mathcal{U}$ for which the assumptions of Theorem 4.1 are satisfied, thus assuring the survival of $N + 1$ subharmonic solutions from each of the corresponding invariant tori. This scenario may be compared with Birkhoff–Lewis-type results [BBV04; BL34; CZ83b], showing the existence of a family of periodic solutions with large period, accumulating towards an elliptic equilibrium. Such behaviour has been observed also in the framework of Hamiltonian PDEs [BB05; BD10].

A simple case is given by the choice $I^* = I^0$, when I^0 is associated with an invariant torus $\mathscr{T}^0$ of periodic solutions for (4.1) with frequency vector ω^0 and minimal period T^0.

Corollary 4.2. *Suppose that there exists $I^0 \in \mathcal{D}$ and an invertible symmetric $N \times N$ matrix $\mathbb{B}$ such that (4.4) holds, and that there exist two positive integers m^0 and n^0 satisfying $T^0 = m^0T/n^0$. Then, for every $\sigma > 0$ there exists $\varepsilon > 0$ such that, if*

$$\|\nabla_\xi K(t, \xi, \eta)\| + \|\nabla_\eta K(t, \xi, \eta) - \nabla \mathscr{K}(\eta)\| < \varepsilon$$
$$for\ every\ (t, \xi, \eta) \in [0, T] \times [0, 2\pi]^N \times \mathcal{D}$$

then system (4.2) has at least $N + 1$ geometrically distinct m^0T-periodic solutions

$$(\xi^1(t), \eta^1(t)), \ldots, (\xi^{N+1}(t), \eta^{N+1}(t))$$

with the same rotational properties of the torus $\mathscr{T}^0$ and such that

$$\left\|\xi^k(t) - \xi^k(0) - t\nabla \mathscr{K}(I^0)\right\| + \left\|\eta^k(t) - I^0\right\| \leq \sigma$$

for every $t \in [0, m^0T]$ and $k = 1, \ldots, N + 1$.

4.2   Twist conditions for weakly coupled period annuli

In the previous section we have described the local phenomenon of the survival of some periodic solutions of system (4.1) for the perturbed system (4.2); we now turn our attention to finding some conditions at a larger scale which guarantee the existence of multiple periodic solutions.

We still consider system (4.2) as a perturbation of system (4.1), but we now look for periodic solutions $(\xi(t), \eta(t))$ starting with $\eta(0)$ in some rectangle

$$D = [\alpha_1, \beta_1] \times \cdots \times [\alpha_N, \beta_N]$$

contained in $\mathcal{D}$; we denote the faces of this rectangle by

$$\mathcal{F}_i^- = \{\eta \in D : \eta_i = \alpha_i\} \qquad \mathcal{F}_i^+ = \{\eta \in D : \eta_i = \beta_i\}$$

Theorem 4.3. *Suppose that there exist N couples of real numbers $\omega_i^- < \omega_i^+$ such that, for every $i = 1, \ldots, N$, either*

$$\frac{\partial \mathcal{K}}{\partial \eta_i}(\eta) \begin{cases} \geq \omega_i^+ & \text{for every } \eta \in \mathcal{F}_i^- \\ \leq \omega_i^- & \text{for every } \eta \in \mathcal{F}_i^+ \end{cases} \tag{4.12a}$$

or

$$\frac{\partial \mathcal{K}}{\partial \eta_i}(\eta) \begin{cases} \leq \omega_i^- & \text{for every } \eta \in \mathcal{F}_i^- \\ \geq \omega_i^+ & \text{for every } \eta \in \mathcal{F}_i^+ \end{cases} \tag{4.12b}$$

Let $\omega^* = (\omega_1^*, \ldots, \omega_N^*)$ be the frequency vector associated to a torus $\mathscr{T}^*$ of periodic solutions of system (4.1), with minimal period T^*. If

$$\omega^* \in \Omega = (\omega_1^-, \omega_1^+) \times \cdots \times (\omega_N^-, \omega_N^+)$$

and there are two positive integers m^* and n^* such that (4.5) holds, then there exists $\varepsilon > 0$ such that every perturbed system (4.2) satisfying (4.6) has at least $N + 1$ geometrically distinct m^*T-periodic solutions

$$(\xi^1(t), \eta^1(t)), \; \ldots \;, (\xi^{N+1}(t), \eta^{N+1}(t))$$

preserving the same rotational properties of $\mathscr{T}^*$.

Proof. By the Poincaré–Miranda theorem (cf. Theorem 2.1), there exists an $I^* \in D$ such that $\omega^* = \nabla \mathcal{K}(I^*)$. We consider the Hamiltonian system

$$\dot{\zeta} = \mathcal{J} \nabla_\zeta K^*(t, \zeta) \tag{4.13}$$

with $K^*(t, \xi, \eta) = K(t, \xi + \omega^* t, \eta) - \langle \omega^*, \eta \rangle$.

Let us pick any $\rho > 0$ such that

$$\rho < \operatorname{dist}(D, \mathbb{R}^N \setminus \mathcal{D}) \qquad \text{and} \qquad \rho < m^* T \operatorname{dist}(\omega^*, \mathbb{R}^N \setminus \Omega)$$

By the same argument used in the Claim within the proof of Theorem 4.1, there is $\varepsilon_1 > 0$ such that, if (4.6) holds with $\varepsilon \in (0, \varepsilon_1)$, then every solution $\zeta(t) = (\xi(t), \eta(t))$ of (4.13) with initial point $\eta(0) \in D$ remains in $\mathbb{R}^N \times \mathcal{D}$, for $t \in [0, m^* T]$, and satisfies

$$\left\| \xi(t) - \xi(0) - t \left[\nabla \mathcal{K}(\eta(0)) - \omega^* \right] \right\| + \| \eta(t) - \eta(0) \| < \rho$$

for every $t \in [0, m^* T]$. Assume that $\eta(0) \in \partial D$; we analyse four different cases.

If $\eta_i(0) = \alpha_i$, for some $i \in \{1, \ldots, N\}$, and condition (4.12a) holds, then

$$\xi_i(m^* T) - \xi_i(0) > m^* T [\omega_i^+ - \omega_i^*] - \rho > 0$$

The same is true if $\eta_i(0) = \beta_i$ and (4.12b) holds.

If $\eta_i(0) = \alpha_i$ and condition (4.12b) holds, then

$$\xi_i(m^* T) - \xi_i(0) < m^* T [\omega_i^- - \omega_i^*] + \rho < 0$$

and the same is true if $\eta_i(0) = \beta_i$ and (4.12a) holds.

Let us define the $N \times N$ diagonal matrix $\mathbb{B}$ with, for each $i = 1, \ldots, N$, $\mathbb{B}_{ii} = -1$ when (4.12a) holds, and $\mathbb{B}_{ii} = +1$ when (4.12b) is true. The estimates above ensure us that system (4.13) satisfies all the assumptions of Corollary 3.10 in the case (T1), and the conclusion easily follows. $\qquad\square$

Let us now describe a particular situation when Theorem 4.3 can be applied, generalizing the planar setting studied in [FSZ12]. We start considering the autonomous Hamiltonian system

$$\dot{z} = \mathcal{J} \nabla \mathcal{H}(z) \tag{4.14}$$

where $\mathcal{H} \colon \mathbb{R}^{2N} \to \mathbb{R}$ is a continuously differentiable function of the special form

$$\mathcal{H}(x, y) = \mathcal{H}_1(x_1, y_1) + \cdots + \mathcal{H}_N(x_N, y_N)$$

with $x = (x_1, \ldots, x_N) \in \mathbb{R}^N$ and $y = (y_1, \ldots, y_N) \in \mathbb{R}^N$. Here we have used the notation $z = (x, y)$.

Hence, for every $i = 1, \ldots, N$, the functions $\mathcal{H}_i \colon \mathbb{R}^2 \to \mathbb{R}$ are planar Hamiltonians, and we can consider the corresponding Hamiltonian systems

$$\dot{x}_i = \frac{\partial}{\partial y_i} \mathcal{H}_i(x_i, y_i) \qquad \dot{y}_i = -\frac{\partial}{\partial x_i} \mathcal{H}_i(x_i, y_i) \tag{HS$_i$}$$

for each of which we assume the following:

- the planar system (HS$_i$) has a periodic solution $(\bar{x}_i(t), \bar{y}_i(t))$, which is non-constant and has minimal period $\overline{T}_i > 0$

- each of such solutions has a corresponding planar open tubular neighborhood $\mathscr{A}_i$ such that all the solutions of (HS$_i$) with initial point in $\mathscr{A}_i$ are periodic, and their orbits are not contractible in $\mathscr{A}_i$

- there are two positive real numbers T_i^-, T_i^+, with $T_i^- < \overline{T}_i < T_i^+$, such that the periods of the solutions in $\mathscr{A}_i$ cover the interval $[T_i^-, T_i^+]$

Let us define the set

$$\mathscr{A} = \{(x, y) \in \mathbb{R}^{2N} : (x_i, y_i) \in \mathscr{A}_i, \text{ for every } i = 1, \ldots, N\}$$

and consider the Hamiltonian system

$$\dot{z} = \mathcal{J}\nabla_z H(t, z) \tag{4.15}$$

where $H \colon \mathbb{R} \times \mathscr{A} \to \mathbb{R}$ is continuous, T-periodic in its first variable, for some $T > 0$, and has a continuous gradient with respect to its second variable $z = (x, y)$.

For every $i = 1, \ldots, N$, let us pick $T_i \in (T_i^-, T_i^+)$ for which there exist two positive integers m_i, n_i such that

$$T_i = \frac{m_i T}{n_i}$$

Denoting by $a_1, \ldots, a_N$ the minimal positive integers such that

$$a_1 \frac{m_1}{n_1} = \cdots = a_N \frac{m_N}{n_N}$$

we set

$$T^* = a_1 T_1 = \cdots = a_N T_N$$

and define the frequency vector

$$\omega^* = \frac{2\pi}{T^*}(a_1, \ldots, a_N)$$

Moreover, we choose the two least positive integers m^*, n^* such that

$$T^* = \frac{m^* T}{n^*}.$$

Theorem 4.4. *In the above setting, there exists $\varepsilon > 0$ such that every perturbed system (4.15), satisfying*

$$\|\nabla_z H(t, z) - \nabla \mathcal{H}(z)\| < \varepsilon \qquad \text{for every } (t, z) \in [0, T] \times \mathscr{A} \tag{4.16}$$

has at least $N + 1$ distinct m^*T-periodic solutions

$$z^1(t), \ldots, z^{N+1}(t)$$

whose orbits lie in $\mathscr{A}$. Moreover, for each solution $z^k(t)$, the number of rotations of the i-th component $z_i^k(t)$ along the annulus $\mathscr{A}_i$ in a period m^*T is exactly equal to n^*a_i, for every $i = 1, \ldots, N$.

Proof. By standard arguments (cf. [FSZ12]), each of the systems (HS_i) admits a canonical transformation in action-angle coordinates (φ_i, I_i). Without loss of generality we can assume that $\dot{\varphi}_i(t) > 0$, for every t. The product of all such transformations is canonical, it reduces system (4.14) to the form (4.1), and maps the set $\mathscr{A}$ onto $\mathbb{T}^N \times \mathcal{D}$, where $\mathcal{D} \subseteq \mathbb{R}^N$ is a product of open intervals.

For each $i = 1, \ldots, N$, we define α_i and β_i as the values of the I_i-coordinate associated with two solutions of (HS_i) having periods T_i^- and T_i^+, in such a way that $\alpha_i < \beta_i$, and we set

$$\omega_i^- = \frac{2\pi}{T_i^+} \qquad\qquad \omega_i^+ = \frac{2\pi}{T_i^-}$$

Theorem 4.3 then applies, and the proof is readily completed. $\qquad\square$

4.3 Weakly coupled pendulum-like systems

In this section, we consider a weakly coupled system of the type

$$\begin{cases} J\dot{z}_1 = A_1 \nabla H_1(z_1) + \mathcal{R}_1(t, z_1, \ldots, z_N) \\ \ldots \\ J\dot{z}_N = A_N \nabla H_N(z_N) + \mathcal{R}_N(t, z_1, \ldots, z_N) \end{cases} \tag{P}$$

where J is the 2×2 standard symplectic matrix, namely

$$J = \begin{pmatrix} 0 & -1 \\ 1 & 0 \end{pmatrix}$$

and $A_1, \ldots, A_N$ are positive real parameters. For every $i = 1, \ldots, N$, we assume that $H_i \colon \mathbb{R}^2 \to \mathbb{R}$ is continuously differentiable, and $\mathcal{R}_i \colon \mathbb{R} \times \mathbb{R}^{2N} \to \mathbb{R}$ is continuous, T-periodic in t and continuously differentiable in $(z_1, \ldots, z_N)$.

We assume that system (P) can be reduced to a Hamiltonian system by a linear change of variables. More precisely, there exist N invertible 2×2 matrices $\mathbb{M}_1, \ldots, \mathbb{M}_N$, having positive determinant, such that the linear operator $\mathcal{L} \colon \mathbb{R}^{2N} \to \mathbb{R}^{2N}$, defined as

$$\mathcal{L} \colon (z_1, \ldots, z_N) \mapsto (\mathbb{M}_1 z_1, \ldots, \mathbb{M}_N z_N) \tag{4.17}$$

transforms system (P) into a Hamiltonian system. With such an assumption, we will say that (P) is a *positive transformation of a Hamiltonian system*.

Let us introduce the following notation for a closed cone in $\mathbb{R}^2$ determined by two angles $\vartheta_1 < \vartheta_2$:

$$\Theta(\vartheta_1, \vartheta_2) = \{(\rho \cos \vartheta, \rho \sin \vartheta) : \rho \geq 0, \, \vartheta_1 \leq \vartheta \leq \vartheta_2\}$$

We are now ready to state the main theorem of this section.

Theorem 4.5. *Let* (P) *be a positive transformation of a Hamiltonian system. For every $i = 1, \ldots, N$, let the following assumptions hold:*

$(\mathscr{A}_1)$ *there is $C_i > 0$ such that*

$$\|\nabla H_i(w)\| \leq C_i(\|w\| + 1) \qquad \text{for every } w \in \mathbb{R}^2$$

$(\mathscr{A}_2)$ *there are $r_i > 0$ and $m_i > 0$ such that*

$$\langle \nabla H_i(w), w \rangle \geq m_i \|w\|^2 \qquad \text{for every } w \in \mathcal{B}[0, r_i]$$

$(\mathscr{A}_3)$ *for every $\sigma > 0$ there are $R_i > 0$ and $\vartheta_1^i < \vartheta_2^i$, with $\vartheta_2^i - \vartheta_1^i \leq 2\pi$, such that*

$$\sup\left\{ \frac{\langle \nabla H_i(w), w \rangle}{\|w\|^2} : w \in \Theta(\vartheta_1^i, \vartheta_2^i) \setminus \mathcal{B}(0, R_i) \right\} \leq \sigma(\vartheta_2^i - \vartheta_1^i) \quad (4.18)$$

Then, for every fixed positive integers $\nu_1, \ldots, \nu_N$, there exist $A > 0$ and $\varepsilon > 0$ such that, if $A_i \geq A$ and

$$\|\mathcal{R}_i(t, w_1, \ldots, w_N)\| \leq \varepsilon \quad \text{for every } t \in [0, T] \text{ and } w_1, \ldots, w_N \in \mathbb{R}^2,$$
$$(4.19)$$

for every $i = 1, \ldots, N$, then system (P) *has at least $N + 1$ distinct T-periodic solutions*

$$z^k(t) = (z_1^k(t), \ldots, z_N^k(t))$$

such that, for every $k = 1, \ldots, N + 1$, each planar component $z_i^k(t)$, with $i = 1, \ldots, N$, makes exactly ν_i clockwise rotations around the origin in the time interval $[0, T]$.

Some comments on the hypotheses of Theorem 4.5 are in order. Assumption $(\mathscr{A}_1)$ is needed to ensure the global existence of the solutions to the Cauchy problems associated with (P). Concerning $(\mathscr{A}_2)$, it will guarantee that the small amplitude planar components of the solutions do rotate around the origin, clockwise, with a least positive angular speed. Our hypothesis $(\mathscr{A}_3)$, on the contrary, will ensure a small rotation number for large amplitude components. It could be compared with assumption (H'_∞) in [Bos11, Theorem 4.1].

We now start the proof of Theorem 4.5. For a solution $z(t)$ of system (P) with i-th component $z_i(t) = (x_i(t), y_i(t)) \in \mathbb{R}^2 \setminus \{0\}$, for every $t \in [0, T]$, we denote by $\mathrm{rot}(z_i(t); [0, T])$ the standard clockwise winding number of the path $t \mapsto z_i(t)$ around the origin, namely

$$\mathrm{rot}(z_i(t); [0, T]) = \frac{1}{2\pi} \int_0^T \frac{\langle J\dot{z}_i(t), z_i(t) \rangle}{\|z_i(t)\|^2} \, \mathrm{d}t$$

Our first lemma concerns solutions $z(t)$ whose i-th component $z_i(t)$ is small. We assume without loss of generality that $H_i(0) = 0$, and consider the level set

$$\Gamma_i^h = \{w \in \mathbb{R}^2 : H_i(w) = h\}$$

By $(\mathscr{A}_2)$, if $h > 0$ is sufficiently small, then Γ_i^h is a strictly star-shaped Jordan curve around the origin. We will denote by D_i^h the bounded, closed and connected region of $\mathbb{R}^2$ with $\partial D_i^h = \Gamma_i^h$.

Lemma 4.6. *For any $i = 1, \ldots, N$ and every positive integer ν_i, if $(\mathscr{A}_1)$ and $(\mathscr{A}_2)$ hold, there exist three positive constants $\bar{A}_i$, $\bar{\varepsilon}_i$ and $\bar{h}_i$ such that, if $A_i \geq \bar{A}_i$, $h \in (0, \bar{h}_i]$ and*

$$\|\mathcal{R}_i(t, w_1, \ldots, w_N)\| \leq \bar{\varepsilon}_i \quad \text{for every } t \in [0, T] \text{ and } w_1, \ldots, w_N \in \mathbb{R}^2 \quad (4.20)$$

then any solution $z(t)$ to (P) with $z_i(0) \in \Gamma_i^h$ satisfies

$$\mathrm{rot}(z_i(t); [0, T]) > \nu_i$$

Proof. Let $i \in \{1, \ldots, N\}$ and ν_i be fixed. We can choose $h > 0$ and $\hat{r} \in (0, r_i)$, where r_i is as in assumption $(\mathscr{A}_2)$, in such a way that

$$\mathcal{B}(0, \hat{r}) \subset D_i^h \subset D_i^{2h} \subset D_i^{3h} \subset \mathcal{B}(0, r_i) \tag{4.21}$$

We now claim that, if (4.20) holds with a suitable choice of $\bar{\varepsilon}_i$, then, for every solution $z(t)$ of (P), with $z_i(0) \in \Gamma_i^{2h}$, one has

$$h < H_i(z_i(t)) < 3h, \quad \text{for every } t \in [0, T]$$

Indeed, set

$$C = \max\{\|\nabla H_i(w)\| : w \in \mathcal{B}[0, r_i]\} \qquad \bar{\varepsilon}_i = \frac{h}{2CT}$$

and assume by contradiction that $z_i(0) \in \Gamma_i^{2h}$ and there exists $t_1 \in [0, T]$ such that $h < H_i(z_i(t)) < 3h$ for every $t \in [0, t_1)$, and either $H_i(z_i(t_1)) = h$, or $H_i(z_i(t_1)) = 3h$. In view of (4.21),

$$\left| \frac{\mathrm{d}}{\mathrm{d}t} H_i(z_i(t)) \right| = |\langle J\nabla H_i(z_i(t)), A_i\nabla H_i(z_i(t)) + \mathcal{R}_i(t, z_1, \ldots, z_N) \rangle|$$

$$= |\langle J\nabla H_i(z_i(t)), \mathcal{R}_i(t, z_1, \ldots, z_N) \rangle| \leq C\bar{\varepsilon}_i = \frac{h}{2T}$$

for every $t \in [0, t_1]$, so that

$$|H_i(z_i(t_1)) - H_i(z_i(0))| \leq \frac{h}{2T}t_1 < h$$

a contradiction.

Consequently, if $z_i(0) \in \Gamma_i^{2h}$, we have that

$$\hat{r} < \|z_i(t)\| \leq r_i \qquad \text{for every } t \in [0, T]$$

so that the rotation number of $z_i(t)$ around the origin is well defined. Writing $z_i(t)$ in polar coordinates, namely

$$z_i(t) = (\rho_i(t) \cos \vartheta_i(t), \rho_i(t) \sin \vartheta_i(t))$$

using $(\mathscr{A}_2)$ and (4.20) we thus have

$$-\vartheta_i'(t) = \frac{\langle J\dot{z}_i(t), z_i(t)\rangle}{\|z_i(t)\|^2}$$
$$= \frac{\langle A_i \nabla H_i(z_i(t)) + \mathcal{R}_i(t, z_1, \ldots, z_N), z_i(t)\rangle}{\|z_i(t)\|^2} \geq A_i m_i - \frac{\bar{\varepsilon}_i}{\hat{r}}$$

Choosing finally

$$\bar{A}_i = \frac{2\pi \hat{r} \nu_i + \bar{\varepsilon}_i T}{m_i \hat{r} T}$$

we easily conclude. □

Now we need a control on the rotation number of the large planar components of the solutions.

Lemma 4.7. *For any $i = 1, \ldots, N$, let $\bar{A}_i$ and $\bar{\varepsilon}_i$ be as in Lemma 4.6, and assume that $A_i \geq \bar{A}_i$ and (4.20) holds. Then, there exists $\overline{R}_i > 0$ such that any solution $z(t)$ of (P) with $\|z_i(0)\| \geq \overline{R}_i$ satisfies*

$$\text{rot}(z_i(t); [0, T]) < 1$$

Proof. Fix $\sigma = 1/(2A_iT)$ and let $R_i > 0$ and $\vartheta_1^i < \vartheta_2^i$, with $\vartheta_2^i - \vartheta_1^i \leq 2\pi$, be as in $(\mathscr{A}_3)$. Choose $\widehat{R}_i \geq R_i$ such that

$$\widehat{R}_i > \frac{2\bar{\varepsilon}_i T}{\vartheta_2^i - \vartheta_1^i}$$

In view of assumption $(\mathscr{A}_1)$, there is $\overline{R}_i \geq \widehat{R}_i$ such that, if $\|z_i(0)\| \geq \overline{R}_i$, then $\|z_i(t)\| \geq \widehat{R}_i$, for every $t \in [0, T]$; in particular, the rotation number of $z_i(t)$ is well defined. Let us assume, by contradiction, that $\|z_i(0)\| \geq \overline{R}_i$ and $\text{rot}(z_i(t); [0, T]) \geq 1$; then, writing

$$z_i(t) = (\rho_i(t) \cos \vartheta_i(t), \rho_i(t) \sin \vartheta_i(t))$$

as long as $\vartheta_i(t) \in \Theta(\vartheta_1^i, \vartheta_2^i)$, since $\rho_i(t) \geq \widehat{R}_i \geq R_i$, we can use (4.18) and (4.20) to obtain

$$
\begin{aligned}
-\vartheta_i'(t) &= \frac{\langle A_i \nabla H_i(z_i(t)) + \mathcal{R}_i(t, z_1, \ldots, z_N), z_i(t) \rangle}{\|z_i(t)\|^2} \\
&\leq A_i \frac{1}{2 A_i T}(\vartheta_2^i - \vartheta_1^i) + \frac{\bar{\varepsilon}_i}{\widehat{R}_i} < \frac{\vartheta_2^i - \vartheta_1^i}{T}
\end{aligned}
$$

Consequently, the time needed to clockwise cross the sector $\Theta(\vartheta_1^i, \vartheta_2^i)$ is greater than T, a contradiction. $\qquad\square$

Proof of Theorem 4.5. For any $i \in \{1, \ldots, N\}$, let $\bar{A}_i > 0$ and $\bar{\varepsilon}_i > 0$ be as in Lemma 4.6, and set

$$
A = \max\{\bar{A}_i : i = 1, \ldots, N\} \qquad \varepsilon = \min\{\bar{\varepsilon}_i : i = 1, \ldots, N\}
$$

Take $A_i \geq A$ and assume that (4.19) holds. Then, take $\overline{R}_i$ as in Lemma 4.7, for every $i = 1, \ldots, N$, and consider the annulus $\mathscr{A}_i = \mathcal{B}(0, \overline{R}_i) \setminus D_i^{\bar{h}_i}$. Recall that, taking $\bar{h}_i > 0$ sufficiently small, the inner boundary of $\mathscr{A}_i$ is star-shaped. Then, by Lemmas 4.6 and 4.7, for every solution $z(t)$ of (P), if $z_i(0)$ belongs to the inner boundary of $\mathscr{A}_i$, then $z_i(t)$ makes more than ν_i clockwise rotations around the origin in the time T, while, if $\|z_i(0)\| = \overline{R}_i$, it makes less than one clockwise turn in the same time.

We now use the fact that (P) is a *positive transformation of a Hamiltonian system*, and consider the linear transformation $\mathcal{L}$ defined in (4.17). Being all matrices $\mathbb{M}_i$ invertible with positive determinant, the set

$$
\mathscr{A} = \mathcal{L}(\mathscr{A}_1 \times \cdots \times \mathscr{A}_N)
$$

is thus of the type $\widetilde{\mathscr{A}_1} \times \cdots \times \widetilde{\mathscr{A}_N}$, where each $\widetilde{\mathscr{A}_i}$ is a planar annulus with star-shaped boundaries with respect to the origin. Since the change of variables preserves the above described rotational properties of the solutions, we can apply Corollary 3.10 in the case (T1) (cf. also [FU16a]) to the Hamiltonian system obtained from (P) by the change of variables given by $\mathcal{L}$. We thus obtain at least $N + 1$ distinct T-periodic solutions

$$
\tilde{z}^k(t) = (\tilde{z}_1^k(t), \ldots, \tilde{z}_N^k(t))
$$

such that, for every $k = 1, \ldots, N+1$, each component $\tilde{z}_i^k(t)$, with $i = 1, \ldots, N$, makes exactly ν_i clockwise rotations around the origin in the time interval $[0, T[$. Setting

$$
z^k(t) = (\mathbb{M}_1^{-1} \tilde{z}_1^k(t), \ldots, \mathbb{M}_N^{-1} \tilde{z}_N^k(t))
$$

we obtain the solutions of (P) we are looking for, and the proof is thus completed. $\qquad\square$

Remark 4.8. Theorem 4.5 exploits a gap between the rotation numbers of the solutions at zero and at infinity. With reference to the assumption at infinity, another possibility could be to replace $(\mathscr{A}_3)$ with the requirement that, for some $i \in \{1, \ldots, N\}$, the system $J\dot{z}_i = \nabla H_i(z_i)$ has a homoclinic orbit surrounding the origin (in the spirit of [FZ97, Theorem 3.3]). Indeed, by continuity, small perturbations of trajectories next to the homoclinic would have small rotation number, since the homoclinic spends an infinite time to rotate around the origin. In this setting, assuming moreover $(\mathscr{A}_2)$, it would then be possible to construct the gap which allows to apply Corollary 3.10 in the case (T1) taking a level curve of H_i sufficiently near the homoclinic orbit as outer boundary of the required annulus in the i-th planar component. The same line of thought can be also adapted when the homoclinic is replaced by heteroclinics. One could also combine assumptions at infinity like $(\mathscr{A}_3)$ for some indices $i_1, \ldots, i_r \in \{1, \ldots, N\}$ and existence of homoclinics for the other indices $i \in \{1, \ldots, N\} \setminus \{i_1, \ldots, i_r\}$. We omit the details for briefness.

As a particular case, we can deal with a system of scalar second order equations like

$$\begin{cases} \ddot{x}_1 + A_1^2 f_1(x_1) = \dfrac{\partial \mathcal{W}}{\partial x_1}(t, x_1, \ldots, x_N) \\ \ldots \\ \ddot{x}_N + A_N^2 f_N(x_N) = \dfrac{\partial \mathcal{W}}{\partial x_N}(t, x_1, \ldots, x_N) \end{cases} \tag{4.22}$$

where the continuous function $\mathcal{W} \colon \mathbb{R} \times \mathbb{R}^N \to \mathbb{R}$ is T-periodic in t, and continuously differentiable in $(x_1, \ldots, x_N)$. Indeed, we can write the equivalent system

$$\begin{cases} -\dot{y}_i = A_i \, f_i(x_i) - \dfrac{1}{A_i} \dfrac{\partial \mathcal{W}}{\partial x_i}(t, x_1, \ldots, x_n) \\ \dot{x}_i = A_i \, y_i \end{cases} \qquad i = 1, \ldots, N$$

which is in the form (P), with $z_i = (x_i, y_i)$, taking

$$H_i(x_i, y_i) = \frac{1}{2} y_i^2 + F_i(x_i)$$

where F_i is a primitive of f_i, and

$$\mathcal{R}_i(t, x_1, y_1, \ldots, x_N, y_N) = -\frac{1}{A_i} \begin{pmatrix} \frac{\partial \mathcal{W}}{\partial x_i}(t, x_1, \ldots, x_n) \\ 0 \end{pmatrix}$$

Notice that (4.22) is a *positive transformation of a Hamiltonian system*, with the linear function $\mathcal{L}$ in (4.17) given by

$$\mathbb{M}_i = \begin{pmatrix} 1 & 0 \\ 0 & A_i \end{pmatrix} \qquad i = 1, \ldots, N$$

As a consequence, we have the following statement, where, for simplicity, we only consider the case $\nu_1 = \cdots = \nu_N = 1$.

Corollary 4.9. *Assume that the continuous functions $f_i \colon \mathbb{R} \to \mathbb{R}$ satisfy*

$$\liminf_{s \to 0} \frac{f_i(s)}{s} > 0 \qquad\qquad \lim_{s \to +\infty} \frac{f_i(s)}{s} = 0$$

Moreover, for every $i = 1, \ldots, N$, let $K_i > 0$ be such that

$$\left| \frac{\partial \mathcal{W}}{\partial x_i}(t, x_1, \ldots, x_n) \right| \le K_i \quad \text{for every } t \in [0, T] \text{ and } x_1, \ldots, x_N \in \mathbb{R} \quad (4.23)$$

Then, there exists $\bar{A} > 0$ such that, if $A_i \ge \bar{A}$ for every $i = 1, \ldots, N$, system (4.22) has at least $N + 1$ distinct periodic solutions

$$x^k(t) = (x_1^k(t), \ldots, x_N^k(t))$$

with minimal period T. Moreover, for every $k = 1, \ldots, N+1$, each component $x_i^k(t)$, with $i = 1, \ldots, N$, has exactly two simple zeros in the interval $[0, T]$.

Proof. First, we notice that $(\mathscr{A}_1)$ is fulfilled, in view of the growth assumption on the nonlinearities. Let us now check $(\mathscr{A}_2)$. We know that there are $\alpha_i > 0$ and $\beta_i > 0$ such that

$$0 < |s| < \beta_i \quad \Longrightarrow \quad \frac{f_i(s)}{s} \ge \alpha_i$$

Then, if $\|(x_i, y_i)\| \le \beta_i$,

$$\frac{\langle \nabla H_i(x_i, y_i), (x_i, y_i) \rangle}{\|(x_i, y_i)\|^2} = \frac{x_i f_i(x_i) + y_i^2}{x_i^2 + y_i^2} \ge \min\{\alpha_i, 1\} > 0$$

as desired.

We now verify $(\mathscr{A}_3)$. Fix $\sigma \in (0, \pi)$, and take $\vartheta_1^i = 0$, $\vartheta_2^i = \sigma/2$. Writing

$$z_i = (x_i, y_i) = (\rho_i \cos \vartheta_i, \rho_i \sin \vartheta_i)$$

we have that, if $z_i \in \Theta(0, \sigma/2)$, then

$$\frac{\langle \nabla H_i(z_i), z_i \rangle}{\|z_i\|^2} = \frac{(\rho_i \cos \vartheta_i) f_i(\rho_i \cos \vartheta_i) + (\rho_i \sin \vartheta_i)^2}{\rho_i^2}$$

$$\le \sin^2 \vartheta_i + \left| \frac{f_i(\rho_i \cos \vartheta_i)}{\rho_i \cos \vartheta_i} \right| \le \frac{\sigma^2}{4} + \left| \frac{f_i(\rho_i \cos \vartheta_i)}{\rho_i \cos \vartheta_i} \right|$$

Taking $R_i > 0$ large enough, if $z_i \in \Theta(0, \sigma/2) \setminus \mathcal{B}(0, R_i)$, then

$$\frac{\langle \nabla H_i(z_i), z_i \rangle}{\|z_i\|^2} \le \frac{\sigma^2}{4} + \frac{\sigma^2}{4} = \sigma(\vartheta_2^i - \vartheta_1^i)$$

The proof is thus completed, noticing that it suffices to choose A_i large enough in order to make $\mathcal{R}_i(t, z_1, \ldots, z_N)$ as small as desired. $\qquad \square$

As an example, Corollary 4.9 directly applies to the following system of N coupled pendulums,

$$
\begin{cases}
\ddot{x}_1 + A_1^2 \sin x_1 = \dfrac{\partial \mathcal{W}}{\partial x_1}(t, x_1, \ldots, x_N) \\
\ldots \\
\ddot{x}_N + A_N^2 \sin x_N = \dfrac{\partial \mathcal{W}}{\partial x_N}(t, x_1, \ldots, x_N)
\end{cases}
$$

where $\frac{\partial \mathcal{W}}{\partial x_i}(t, x_1, \ldots, x_N)$ is continuous and bounded, for $i = 1, \ldots, N$, and the constants $A_1, \ldots, A_N$ are large enough. We are thus able to recover the results obtained in [FZ97], by the use of the Poincaré–Birkhoff theorem, for a single equation modelling a forced pendulum having a very small length.

Part II

Directional friction in bio-inspired locomotion

Chapter 5

Crawling motility and directional friction

5.1 Motivation

The study of locomotion of biological organisms and bio-mimetic engineered replicas is receiving considerable and increasing attention in the recent literature [Ale03; Arr+12b; AD14; CBH05; DT12; DeS+13; Dre+05; FT04; Lai+10; Tan+12; VTT15]. In several cases, such as motility at the micron scale accomplished by unicellular organisms, or such as the ability to navigate on rough terrains exhibited by insects, worms, snakes, etc., Nature has elaborated strategies that surpass those achievable through current engineering design. The combination of quantitative observations, theoretical and computational modelling, design and optimization of bio-inspired artefacts is however leading to fast progress both in the understanding of the options Nature has selected and optimized through evolution, and on the possibility of replicating them (or even improving upon them) in man-made devices.

For example, the swimming strategies of unicellular organisms can be understood, starting from videos of their motion captured with a microscope and processed with machine-learning techniques [Arr+12b], by using tools from geometric control theory [ADL08; Alo+13a]. In fact, self-propulsion at low Reynolds numbers [Pur77] arises from non-reciprocal looping in the space of shape parameters [ADL08; Arr+12b], it can be replicated by using actuation strategies that can induce non-reciprocal shape changes [Dre+05; Alo+13b], and optimized by solving optimal control problems [ADL08; Alo+13a].

Crawling motility on solid substrates of some model organisms (snails, earthworms, etc.) can be understood using similar techniques. In the case of crawlers exploiting dry friction, or lubricating fluid layers with complex rheology (such as the mucus secreted by snails [Den80; CBH05]), resistance forces are nonlinear functions of the sliding velocity and locomotion is typically accomplished through stick-and-slip. Even when resistance forces are linear

in the sliding velocity, if they also depend on the size of the contact region, then locomotion is still possible, provided that more elaborate strategies are employed [DT12; DeS+13; NTD14]. These are very similar to those that are effective in low Reynolds number swimming, and show that the transition between crawling and swimming motility is much more blurred than what was previously thought.

Such results may provide a useful theoretical framework on the way of a more detailed understanding of crawling motility of metastatic tumor cells, neuronal growth cones etc., see, e.g., [FT04; Car+11]. In addition, they may provide valuable new concepts in applications, by helping the practical design of a new generation of soft bio-inspired robots ranging from crawlers able to advance on rough terrains, to microscopic devices that may navigate inside the human body for diagnostic or therapeutic purposes [AD14; Dre+05; GF09; Zha+09].

In this second part of the thesis, we carry on this line of investigation by focusing on the role and effect of a directionality in the friction. By this, we mean a situation in which the resistance force is not odd in the velocity: this may arise, for instance, when the substrate is hairy or it is shaped as a ratchet, or else when the interaction with the substrate is mediated by oblique flexible filaments or bristles (so that, if one reverses the sign of the velocity and moves against the grain, then the resistance force does not only change in sign, but may also change in magnitude). Concrete examples of such biological or bio-inspired directional surfaces are reviewed, e.g., in [HSD12]. In Nature, such effect is accomplished for instance by the *setæ* of the earthworm; several mechanism are also exploited by crawling robots to obtain this kind of asymmetry, cf. [ND14; Vik+15].

Regarding the shape-change strategies adopted by the crawler, our focus will be on the minimal mechanisms needed to make (efficient) self-propulsion possible. Thus our starting point will be reciprocal shape changes (i.e., a very restrictive class of periodic histories of shape change, obtained by tracing backward and forward an open curve in shape space); these can be easily accomplished by natural or artificial actuation: the breathing motion of a balloon (or of a bio-membrane) inflated and deflated by cyclic variations of (osmotic) pressure, or the motion of a specimen of a stimulus-responsive material (e.g., a shape-memory alloy) under cyclic actuation (e.g., temperature change) are all relevant examples. The conditions under which such oscillatory motions can be rectified to produce non zero net displacements has been the object of several studies, see, e.g., [MDC04; DT12; GHM13; CD15]. However, as we will show, in general they do not produce a complete motility (e.g., moving both forward and backward), so the next step will be to consider crawlers made by two of such segment. Such modular structure, with each single element capable of contractions and elongations, is frequent in crawlers [Men+06; Man+14]. In addition, in this Chapter (cf. [GND14]) we study the motion produced by the propagation of travelling waves of contraction or
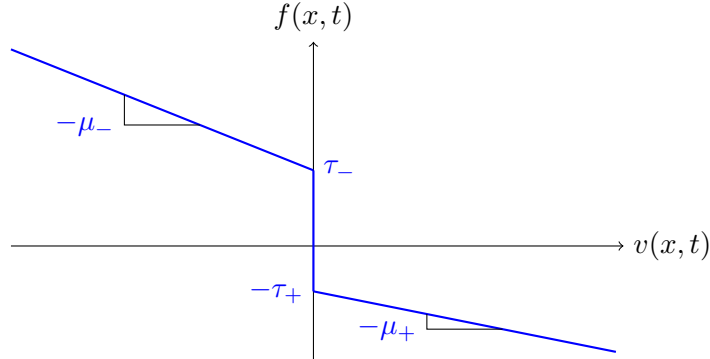
Figure 5.1: The general force-velocity law (5.1) for friction used in this chapter.

extension, which is another typical strategy for self-propulsion in biology.

5.2 Crawling with prescribed shape: formulation

Let us denote with $f(x,t)$ the friction force per unit (current) length exerted by the surface on the crawler. As anticipated, we will focus on *directional friction*, meaning that the friction exerted on the crawler at one point depends (only) on the velocity at that point according to a force-velocity law that is not odd in the velocity. A relevant example is the following one-dimensional force-velocity law of *Bingham*-type

$$f(x,t) = \begin{cases} \tau_- - \mu_- v(x,t) & \text{if } v(x,t) < 0 \\ \tau \in [-\tau_+, \tau_-] & \text{if } v(x,t) = 0 \\ -\tau_+ - \mu_+ v(x,t) & \text{if } v(x,t) > 0 \end{cases} \tag{5.1}$$

where $\tau_-, \tau_+, \mu_-, \mu_+$ are all non-negative material parameters[1], see Fig. 5.1.

There are two interesting special cases of (5.1), obtained by setting either $\mu_+ = \mu_- = 0$, or $\tau_+ = \tau_- = 0$. We refer to them as the *dry friction* and the *Newtonian friction* case, respectively, because they are reminiscent of the tangential forces arising either from dry friction, or from the drag due to a Newtonian viscous fluid, see Fig. 5.2. In the case of dry friction, the force depends only on the sign of the velocity ($\mu_+ = \mu_- = 0$), whereas in the Newtonian case there are no yield forces ($\tau_+ = \tau_- = 0$), so that friction depends linearly on speed through a coefficient determined by the direction of motion.

We study a straight, one-dimensional crawler moving along a straight line. Let the coordinate X describe the crawler's body in the reference configuration. The left end of the body is denoted with $X_1 = 0$, while the

---

[1]We exclude the trivial case when all the parameters vanish ($\mu_+ = \mu_- = \tau_+ = \tau_- = 0$) and therefore no frictional interaction with the substrate occurs.

(a) *Dry friction* (b) *Newtonian friction*
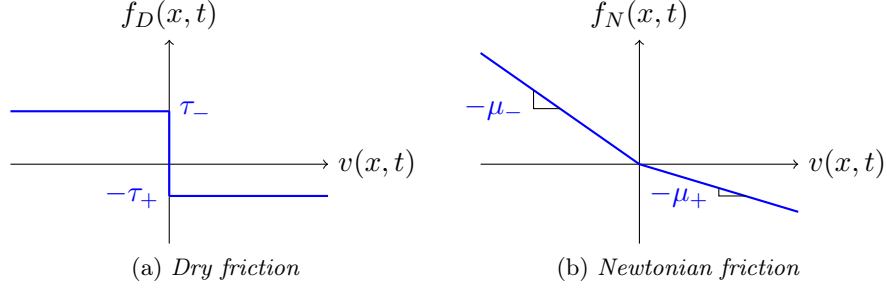
Figure 5.2: Two special cases of the force-velocity law (5.1) of Fig. 5.1.

right end with $X_2 = L$, where L is the reference length. The motion of the crawler is described by the function

$$x(X, t) = x_1(t) + s(X, t) \qquad (5.2)$$

where $x_1(t) = x(X_1, t)$ is the current position of the left end of the crawler (similarly, we define $x_2(t) = x(X_2, t)$ as the current position of the right end), while the arc-length $s(X, t)$, which is the current distance of point X from the left end, describes its shape in the deformed configuration. By definition we have $s(0, t) = 0$, while, denoting with a prime the derivative with respect to X, we guarantee that the deformation described by (5.2) is one-to-one for every t by assuming that

$$s'(X, t) > 0 \qquad (5.3)$$

The length $l(t)$ of the crawler at time t is given by

$$l(t) = \int_0^L s'(X, t) \, dX$$

and the Eulerian velocity $v(x, t)$ at position x of the crawler and time t reads

$$v(x, t) = \dot{x}(X_x, t) = \dot{x}_1(t) + \dot{s}(X_x, t) \qquad (5.4)$$

where $X_x = s^{-1}(x - x_1(t), t)$.

We assume that the crawler is able to control its shape, namely, to freely prescribe $s(X, t)$ subject only to the constraint (5.3). Moreover, we neglect inertia and make use of the force balance

$$F(t) = \int_0^{l(t)} f(x_1(t) + s, t) \, ds = 0 \qquad (5.5)$$

to obtain the velocity $\dot{x}_1(t)$ at the left hand side of the crawler.

5.3 Crawling with two shape parameters

In this section, we restrict our study to the case of a model crawler composed by two segments, namely, $\overline{X_1 X^*}$ and $\overline{X^* X_2}$, each of which is allowed to deform only affinely. Therefore, the shape of the crawler can be described by just two parameters, such as the current lengths of the two segments $l_1(t) = x^*(t) - x_1(t)$ and $l_2(t) = x_2(t) - x^*(t)$, where $x^*(t) = x(X^*, t)$. We shall consider in the following two special cases of these systems, particularly relevant to crawling on directional surfaces.

Crawling with only one shape parameter: breathers

We start by considering a simpler crawler made of a single segment that can only deform affinely, so that $s(X, t)$ can be expressed as a function of the current length $l(t)$ in the following way

$$s(X, t) = \frac{X}{L} l(t) \tag{5.6}$$

This model can also be obtained as a special case of the two-segment crawler subject to the additional constraint

$$\frac{\dot{l}_1(t)}{l_1(t)} = \frac{\dot{l}_2(t)}{l_2(t)} \tag{5.7}$$

By making use of equations (5.4) and (5.6), the velocity is obtained as

$$v(x_1(t) + s, t) = \dot{x}_1(t) + \frac{s}{l(t)} \dot{l}(t) \tag{5.8}$$

a linear function of the arc-length $s \in [0, l(t)]$ vanishing at one point at most for $\dot{l}(t) \neq 0$. This implies that the force balance can be satisfied only if the velocity (and hence the force) assumes different signs along the crawler. More precisely, we argue from (5.8) that:

- if $\dot{l}(t) > 0$ (elongation), then $\dot{x}_1 < 0$ and $\dot{x}_2 > 0$;

- if $\dot{l}(t) < 0$ (contraction), then $\dot{x}_1 > 0$ and $\dot{x}_2 < 0$.

We conclude that the two ends of the crawler always move in opposite directions, and there exists $\bar{s}(t) \in (0, l(t))$ such that $v(\bar{s}(t), t) = 0$. By equation (5.8) we get

$$\bar{s}(t) = -\frac{\dot{x}_1(t) l(t)}{\dot{l}(t)} \tag{5.9}$$

To justify the interest of one-segment crawlers (breathers) on directional surfaces, let us briefly consider the case of interactions which are odd function of the velocity, i.e., interactions such that $f(-v) = -f(v)$. By using the

force balance (5.5) and equation (5.8), it can be easily shown that $\bar{s}(t) = l(t)/2$. From equation (5.9) we get $\dot{x}_1(t) = -\dot{l}(t)/2$, and thereby breathing deformation modes always lead to zero net displacement, when performed on homogeneous surfaces which are not directional.

Consider now the directional law of equation (5.1): the frictional force acting at one point of the crawler depends on whether its distance from x_1 is smaller or larger than $\bar{s}$. For convenience, we establish that the parameters (τ_1, μ_1) describe the forces acting on the left side of $x_1 + \bar{s}$, and (τ_2, μ_2) those acting on the right side. Explicitly, we set

$$(\tau_1, \mu_1) = \begin{cases} (\tau_-, \mu_-) & \text{if } \dot{l} > 0 \\ (-\tau_+, \mu_+) & \text{if } \dot{l} < 0 \end{cases} \quad \text{and} \quad (\tau_2, \mu_2) = \begin{cases} (-\tau_+, \mu_+) & \text{if } \dot{l} > 0 \\ (\tau_-, \mu_-) & \text{if } \dot{l} < 0 \end{cases}$$
(5.10)

so that the total force acting on the crawler reads

$$F(t) = \int_0^{\bar{s}} \left[\tau_1 - \mu_1 \left(\dot{x}_1 + \frac{s\dot{l}}{l} \right) \right] \mathrm{d}s + \int_{\bar{s}}^l \left[\tau_2 - \mu_2 \left(\dot{x}_1 + \frac{s\dot{l}}{l} \right) \right] \mathrm{d}s =$$

$$= (\mu_2 - \mu_1)\bar{s} \left(\dot{x}_1 + \frac{\bar{s}\dot{l}}{2l} \right) - \mu_2 l \left(\dot{x}_1 + \frac{\dot{l}}{2} \right) - (\tau_2 - \tau_1)\bar{s} + \tau_2 l \quad (5.11)$$

Replacing expression (5.9) for $\bar{s}$ and dividing by l, the force balance $F(t) = 0$ leads to the following equation for $\dot{x}_1$

$$\frac{(\mu_1 - \mu_2)}{2\dot{l}} \dot{x}_1^2 + \left(\frac{\tau_2 - \tau_1}{\dot{l}} - \mu_2 \right) \dot{x}_1 - \frac{\mu_2 \dot{l}}{2} + \tau_2 = 0 \quad (5.12)$$

In the special case of $\mu_1 = \mu_2 = \mu$, equation (5.12) becomes linear and its solution reads

$$\dot{x}_1 = - \left(1 + \frac{\tau_1 + \tau_2}{\tau_2 - \tau_1 - \mu\dot{l}} \right) \frac{\dot{l}}{2} \quad (5.13)$$

whereas, for $\mu_1 \neq \mu_2$, equation (5.12) is quadratic with discriminant

$$\Delta = \mu_1 \mu_2 + \frac{(\tau_2 - \tau_1)^2}{\dot{l}^2} + \frac{2}{\dot{l}} (\mu_2 \tau_1 - \mu_1 \tau_2) \quad (5.14)$$

The first two terms of the RHS of (5.14) are both nonnegative and, having excluded the null friction case, at least one of them is positive. The two parameters τ_1 and τ_2, when non zero, have respectively the same and the opposite sign of $\dot{l}$, so also the third term is nonnegative and equation (5.12) has two distinct real solutions

$$\dot{x}_1^\pm = \frac{\mu_2 + \frac{\tau_1 - \tau_2}{\dot{l}} \pm \sqrt{\Delta}}{\mu_1 - \mu_2} \dot{l} = C^\pm \dot{l}$$

(a) *Case $\dot{l} > 0$*
(b) *Case $\dot{l} < 0$*
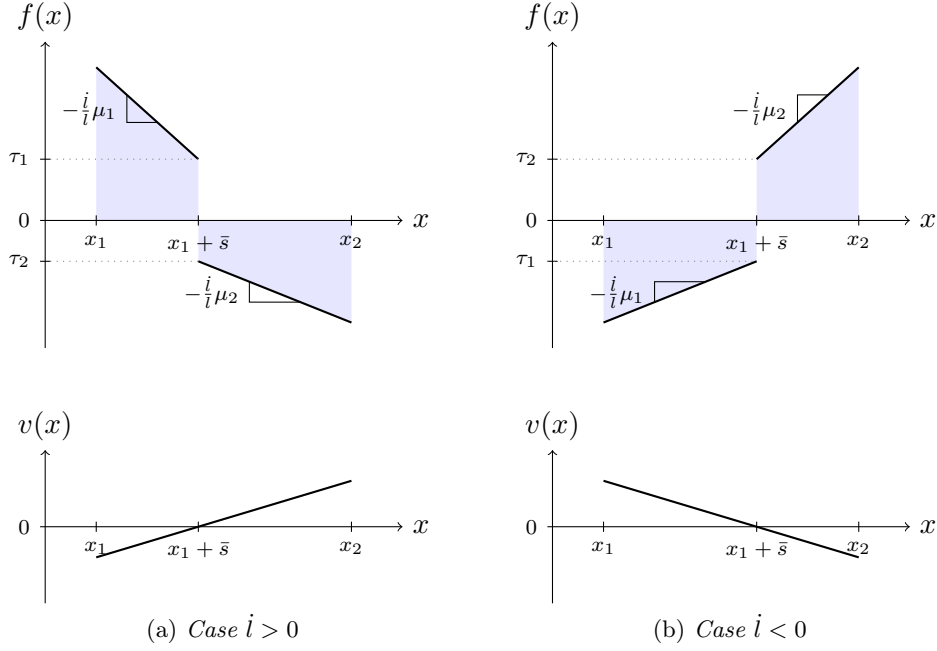
Figure 5.3: The velocity $v(x)$ and the force per unit current length $f(x)$ along a breather in the extensile and contractive case.

In view of (5.9), however, any admissible solution must satisfy

$$C^\pm = \frac{\dot{x}_1^\pm}{\dot{l}} = -\frac{\bar{s}}{l} \in (-1, 0)$$

and we claim that, for any choice of the parameters, this condition is satisfied only by the solution $\dot{x}_1^-$. We start by observing that the following estimate holds for Δ

$$\left(\min\{\mu_1, \mu_2\} + \frac{\tau_1 - \tau_2}{l}\right)^2 < \Delta < \left(\max\{\mu_1, \mu_2\} + \frac{\tau_1 - \tau_2}{l}\right)^2 \qquad (5.15)$$

If $\mu_1 < \mu_2$, then by (5.15) we see that both C^- and C^+ are negative, but $C^- > -1$ while $C^+ < -1$. On the other hand, if $\mu_1 > \mu_2$, applying again (5.15), we have $C^- \in (-1, 0)$ while $C^+ > 0$.

We can assume, without loss of generality, that

$$\mu_- > \mu_+, \text{ if } \mu_- \neq \mu_+ \qquad \text{or that} \qquad \tau_- \geq \tau_+, \text{ if } \mu_- = \mu_+ \qquad (5.16)$$

Indeed, this amount to fixing the orientation of the x axis so that the positive direction is the one of least frictional resistance, in the sense specfied by (5.16). The expressions for the velocity $\dot{x}_1(t)$ as a function of the rate of shape change are presented in Table 5.1.

Table 5.1: Expressions of $\dot{x}_1(t)$ for the one-segment crawler in the extensile and contractive case.

$\mu_- = \mu_+ = \mu,\ \tau_- \geq \tau_+$	$\mu_- > \mu_+$
$\dot{l}(t) > 0:\quad \left(\dfrac{\tau_- - \tau_+}{\tau_- + \tau_+ + \mu\left\|\dot{l}\right\|} - 1\right)\dfrac{\left\|\dot{l}\right\|}{2}$	$\dfrac{\mu_+ + \frac{\tau_- + \tau_+}{\|\dot{l}\|} - \sqrt{\mu_-\mu_+ + \frac{(\tau_- + \tau_+)^2}{\dot{l}^2} + \frac{2}{\|\dot{l}\|}(\mu_-\tau_+ + \mu_+\tau_-)}}{\mu_- - \mu_+}\left\|\dot{l}\right\|$
$\dot{l}(t) < 0:\quad \left(\dfrac{\tau_- - \tau_+}{\tau_- + \tau_+ + \mu\left\|\dot{l}\right\|} + 1\right)\dfrac{\left\|\dot{l}\right\|}{2}$	$\dfrac{\mu_- + \frac{\tau_- + \tau_+}{\|\dot{l}\|} - \sqrt{\mu_-\mu_+ + \frac{(\tau_- + \tau_+)^2}{\dot{l}^2} + \frac{2}{\|\dot{l}\|}(\mu_-\tau_+ + \mu_+\tau_-)}}{\mu_- - \mu_+}\left\|\dot{l}\right\|$

It is interesting to notice that the velocity $\dot{x}_1(t)$ is invariant if we multiply the force-velocity law (5.1) by a positive factor. Furthermore, $\dot{x}_1(t)$ does not depend explicitly on the length $l(t)$, but just on its time derivative $\dot{l}(t)$.

It is also interesting to remark that, for the special cases of dry friction ($\mu_- = \mu_+ = 0$) and Newtonian friction ($\tau_- = \tau_+ = 0$), $\dot{x}_1(t)$ becomes linear in $|\dot{l}|$. Hence, in these situations, the displacement produced by any history of shape changes depends on the path traced in the configuration space, but not on the speed at which it is executed. In particular, the displacement produced in a cycle composed of a monotone elongation (resp. contraction) followed by a monotone return to the initial length is a linear function of the length increase (resp. decrease), through a coefficient determined by the force-velocity laws. We now examine these cases in more detail.

Dry friction   To analyze the case of dry friction, we introduce the dimensionless parameter $\alpha = \tau_-/(\tau_- + \tau_+) \in (0,1)$, such that the orientation assumption $\tau_- \geq \tau_+$ implies $\alpha \geq 1/2$ and the formula for the velocity $\dot{x}_1(t)$ reads

$$\dot{x}_1(t) = \begin{cases} -(1-\alpha)\dot{l}(t) < 0 & \text{if } \dot{l}(t) > 0 \quad \text{(elongation)} \\ -\alpha\dot{l}(t) > 0 & \text{if } \dot{l}(t) < 0 \quad \text{(contraction)} \end{cases} \tag{5.17}$$

The net displacement of the single-segment crawler, arising from a T-periodic shape change, can be computed by integration of equation (5.17) upon definition of $l(t)$ for $t \in [0,T]$. Let us consider the following example. The length of the crawler first increases (resp. decreases) monotonically from L to $L + \delta$, and then decreases (resp. increases) from $L + \delta$ to L, with δ a positive (resp. negative) quantity. An example of such T-periodic shape function is given by $l(t) = L + \delta \sin^2(\pi t/T)$, and the net advancement after one stretching cycle simply follows as

$$\Delta_D x_1 = (2\alpha - 1)\,|\delta| \tag{5.18}$$

This is proportional to the peak extension (or contraction) δ experienced by the crawler, through the non-negative coefficient $2\alpha - 1 < 1$. This coefficient approaches 1 when α tends to 1, and this occurs in the case of infinite contrast between the frictional resistances in the easy and hard directions ($\tau_-/\tau_+ \to \infty$). In this idealised case there is no back-sliding, and all the available extension/contraction of the crawler's body is converted into "useful" displacement, as it is commonly assumed in the classical literature (see e.g., [Ale03; Qui99]). We finally remark that in the limiting case of $\tau_- = \tau_+$ the net advancement $\Delta_D x_1$ vanishes as $\alpha = 1/2$.

Newtonian friction For the analysis of the Newtonian case, we introduce the dimensionless parameter $\beta = \sqrt{\mu_-/\mu_+} \in (0, +\infty)$ (note that we restrict to $\beta > 1$ in view of the orientation assumption on the x axis, $\mu_- > \mu_+$). Setting $\tau_- = \tau_+ = 0$ in Table 5.1 we obtain

$$\dot{x}_1(t) = \begin{cases} -\dfrac{1}{\beta+1}\dot{l}(t) < 0 & \text{if } \dot{l}(t) > 0 \quad \text{(elongation)} \\[2mm] -\dfrac{\beta}{\beta+1}\dot{l}(t) > 0 & \text{if } \dot{l}(t) < 0 \quad \text{(contraction)} \end{cases} \tag{5.19}$$

We now consider the time-periodic shape change previously assumed for the case of dry friction, that is, a monotone expansion-contraction between lengths L and $L + \delta$. The net displacement after one period reads

$$\Delta_N x_1 = \left(-\frac{1}{\beta+1} + \frac{\beta}{\beta+1}\right)|\delta| = \frac{\beta-1}{\beta+1}|\delta| \tag{5.20}$$

This is again proportional to the maximum change in length δ experienced by the crawler through the positive coefficient $(\beta-1)/(\beta+1) \in (0,1)$. The limiting case of infinite contrast between the frictional resistances in the easy and hard directions ($\tau_-/\tau_+ \to \infty$, and hence $\beta \to +\infty$) leads to $\Delta_N x_1 \to \delta$. Furthermore, in the limiting case of $\mu_- = \mu_+$ the net advancement $\Delta_N x_1$ vanishes, since $\beta = 1$.

Crawling with only one shape parameter: constant length crawlers

We turn now our attention to another special case of two-segment crawler, arising from the additional constraint of constant total length, i.e.,

$$l_1(t) + l_2(t) = L$$

In this context, the shape of the crawler can be described by only one parameter, say, $l_1(t)$, and the arc-length $s(X,t)$ reads as

$$s(X,t) = \begin{cases} \dfrac{X}{X^*}l_1(t) & \text{if } X \in [0, X^*] \\[3mm] l_1(t) + \dfrac{L - l_1(t)}{L - X^*}(X - X^*) & \text{if } X \in (X^*, L] \end{cases}$$

Moreover, we have that $\dot{x}_2(t) = \dot{x}_1(t) + \dot{l}_1(t) + \dot{l}_2(t) = \dot{x}_1(t)$ and the Eulerian velocity at point $x = x_1(t) + s$ and time t reads

$$
v(x_1(t) + s, t) = \begin{cases} \dot{x}_1(t) + \dfrac{s}{l_1(t)}\dot{l}_1(t) & \text{if } s \in [0, l_1(t)] \\[2ex] \dot{x}_1(t) + \dfrac{L - s}{L - l_1(t)}\dot{l}_1(t) & \text{if } s \in (l_1(t), L] \end{cases} \tag{5.21}
$$

We notice from equation (5.21) that the velocity equals zero in two points at most. As already observed for the one-segment crawler, the force balance can be satisfied only if the velocity assumes both signs along the crawler, so that there must exist two points $\bar{s}_1(t) \in (0, l_1(t))$ and $\bar{s}_2(t) \in (l_1(t), L)$ where the velocity vanishes. From equation (5.21) we conclude that

$$
\bar{s}_1(t) = -\frac{\dot{x}_1(t)l_1(t)}{\dot{l}_1(t)} \qquad \text{and} \qquad \bar{s}_2(t) = L + \frac{\dot{x}_1(t)(L - l_1(t))}{\dot{l}_1(t)}
$$

and we further observe that the following relation holds between $\bar{s}_1(t)$ and $\bar{s}_2(t)$

$$
\bar{s}_2(t) = L - \frac{L - l_1(t)}{l_1(t)}\bar{s}_1(t) \tag{5.22}
$$

For a two-segment, constant length crawler, the velocity assumes one sign in the interval $(\bar{s}_1(t), \bar{s}_2(t))$, and the other one outside that interval. We adapt the definition of (τ_1, μ_1) and (τ_2, μ_2) given above by replacing $\dot{l}$ with $\dot{l}_1$ in (5.10). Thus (τ_2, μ_2) refer to the interval $(\bar{s}_1(t), \bar{s}_2(t))$, while (τ_1, μ_1) are the friction parameters in $[0, \bar{s}_1(t))$ and $(\bar{s}_2(t), L]$. With these positions, the total force acting on the crawler is

$$
F(t) = \int_0^{\bar{s}_1}\left[\tau_1 - \mu_1\left(\dot{x}_1 + \frac{s\,\dot{l}_1}{l_1}\right)\right] ds + \int_{\bar{s}_1}^{l_1}\left[\tau_2 - \mu_2\left(\dot{x}_1 + \frac{s\,\dot{l}_1}{l_1}\right)\right] ds +
$$

$$
+ \int_{l_1}^{\bar{s}_2}\left[\tau_2 - \mu_2\left(\dot{x}_1 + \frac{(L - s)\dot{l}_1}{L - l_1}\right)\right] ds + \int_{\bar{s}_2}^{L}\left[\tau_1 - \mu_1\left(\dot{x}_1 + \frac{(L - s)\dot{l}_1}{L - l_1}\right)\right] ds
$$

and, using equation (5.22), the force balance $F(t) = 0$ can be written as

$$
\left(1 + \frac{L - l_1}{l_1}\right)\left\{\int_0^{\bar{s}_1}\left[\tau_1 - \mu_1\left(\dot{x}_1 + \frac{s\,\dot{l}_1}{l_1}\right)\right] ds + \int_{\bar{s}_1}^{l_1}\left[\tau_2 - \mu_2\left(\dot{x}_1 + \frac{s\,\dot{l}_1}{l_1}\right)\right] ds\right\} = 0 \tag{5.23}
$$

Comparing the last equation with (5.11), we notice that the force balance on the whole crawler is satisfied if and only if it is independently satisfied on
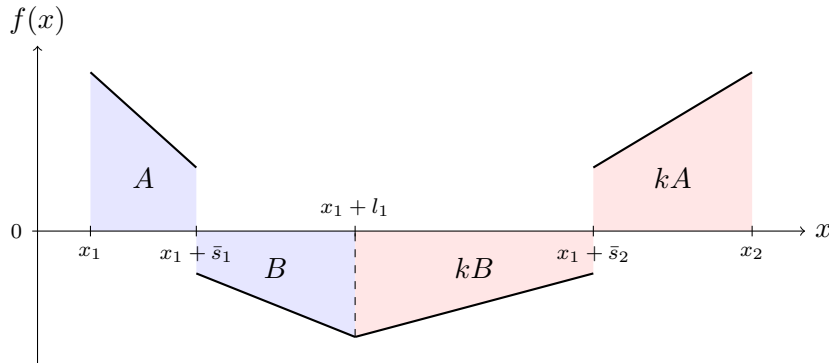
Figure 5.4: Graphical interpretation of equation (5.23). The two integrals in (5.23) correspond respectively to A and B, while $k = (L - l_1)/l_1$. The force balance on the whole crawler is $(1 + k)(A + B) = 0$. It can be satisfied if and only if $A + B = 0$, that is exactly the force balance on the first segment.

each of the two segments, assuming no exchange of force between them (see also Fig. 5.4). This means that a two-segment crawler with constant length is equivalent to two adjacent but independent one-segment crawlers that are "well coordinated" (as a consequence of the constant total length constraint): they move remaining adjacent, neither pushing nor pulling each other.

It follows that the motion of x_1 can be obtained by applying the results for single-segment crawlers to the first segment alone. In particular, the expressions for $\dot{x}_1(t)$ of Table 5.1 and equations (5.17) and (5.19) hold for the two-segment crawler with constant length if we replace $\dot{l}(t)$ with $\dot{l}_1(t)$. Equations (5.18) and (5.20) also hold if we consider a periodic motion where the first segment experiences a monotone elongation-contraction between lengths L_1 and $L_1 + \delta$, being L_1 the reference length of the first segment.

A composite stride for a two-segment crawler

We notice that the two examples of periodic shape change considered so far, each of which exploits just one shape parameter, both produce a positive displacement, namely, a net displacement in the direction of least frictional resistance. We would like to investigate whether, by suitably composing these "elementary" shape changes, we can obtain a net displacement in the direction of maximal frictional resistance, i.e., a negative displacement in view of our orientation assumption (5.16). We will determine below the conditions under which this "riding against the largest friction" is indeed possible.

Given any $\delta, \lambda > 0$ and $h > 1$, we define the following points in the (l_1, l_2)
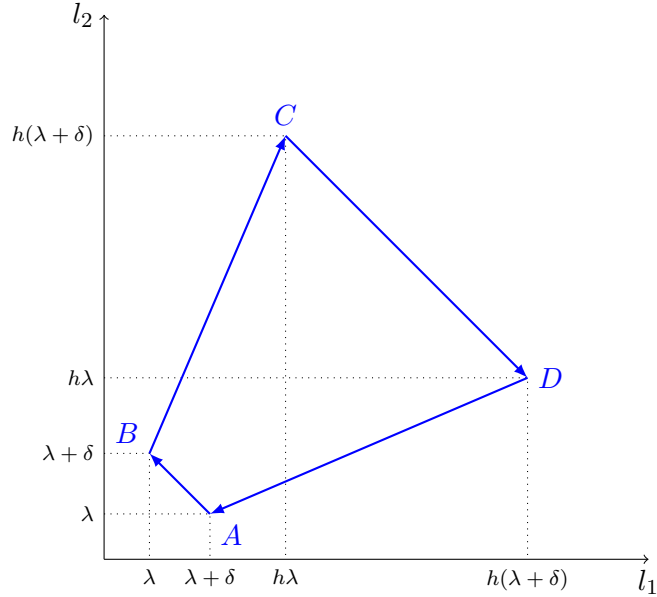
Figure 5.5: An example of periodic shape change for a two-parameters crawler.

shape parameters space

$$A = (\lambda + \delta, \lambda) \qquad\qquad B = (\lambda, \lambda + \delta)$$
$$C = (h\lambda, h(\lambda + \delta)) \qquad\qquad D = (h(\lambda + \delta), h\lambda)$$

We shall now explore the case of shape changes arising from the closed polygonal chain with vertices A, B, C and D, see Fig. 5.5.

Dry Friction   In order to compute the net displacement arising from the closed loop depicted in Fig. 5.5, it is useful to first notice that:

- the two segments $A \rightarrow B$ and $C \rightarrow D$ keep the total length $l_1 + l_2$ of the crawler constant, so that, in view of equation (5.23), their contributions to the displacement can be evaluated by means of equation (5.17) applied to the first segment only;

- the two stride paths $B \rightarrow C$ and $D \rightarrow A$ satisfy condition (5.7), so that their "breathing" contributions to the displacement can be evaluated by means of equation (5.17) applied to the crawler as a whole.

Specifically, the four contributions to the displacement read

$$\Delta_D^{AB} = \alpha \, \delta$$

$$\Delta_D^{BC} = -(1 - \alpha)(h - 1)(2\lambda + \delta)$$

$$\Delta_D^{CD} = -(1 - \alpha)h \, \delta$$

$$\Delta_D^{DA} = -\alpha(1 - h)(2\lambda + \delta)$$

and thereby the net displacement $\Delta_D x_1$ produced after one cycle is

$$\Delta_D x_1 = \alpha \left[4\lambda(h - 1) + \delta(3h - 1) \right] - 2\lambda(h - 1) - \delta(2h - 1)$$

A negative net displacement, $\Delta_D x_1 < 0$, can therefore be obtained only if

$$2\alpha - 1 < \cfrac{1}{\cfrac{4\lambda}{\delta} + \cfrac{3h - 1}{h - 1}} < \frac{1}{3}$$

where the upper bound can be approached when $h \to +\infty$ and $\lambda/\delta \to 0$. It turns out that, in this limit case, a negative displacement is possible only if $\alpha < 2/3$, i.e., only if $\tau_-/\tau_+ < 2$.

Newtonian friction To explore the case of Newtonian friction, we proceed just as in the case of dry friction, but using equation (5.19) instead. The four contributions to the displacement read now

$$\Delta_N^{AB} = \frac{\beta}{\beta + 1} \delta$$

$$\Delta_N^{BC} = -\frac{1}{\beta + 1}(h - 1)(2\lambda + \delta)$$

$$\Delta_N^{CD} = -\frac{1}{\beta + 1}h \, \delta$$

$$\Delta_N^{DA} = -\frac{\beta}{\beta + 1}(1 - h)(2\lambda + \delta)$$

and thereby the net displacement $\Delta_N x_1$ produced after one cycle is

$$\Delta_N x_1 = \frac{\beta}{\beta + 1} \left[2\lambda(h - 1) + \delta h \right] - \frac{1}{\beta + 1} \left[2\lambda(h - 1) + \delta(2h - 1) \right]$$

We thus obtain a negative net displacement, $\Delta_N x_1 < 0$, only if

$$\beta - 1 < \cfrac{1}{\cfrac{2\lambda}{\delta} + \cfrac{h}{h - 1}} < 1$$

where the upper bound can be approached for $h \to +\infty$ and $\lambda/\delta \to 0$. Thus, in this limit case, a negative displacement is possible only if $\beta < 2$, i.e., only if the ratio of $\mu_-/\mu_+ < 4$.

5.4 Crawling with square waves

The purpose of this section is to extend our analyses by exploring the case of shape changes arising from extension (or contraction) travelling waves. In particular, we consider a square stretching wave of width $\delta < L$ and amplitude ε, travelling rightwards along the crawler with speed $c > 0$. The shape $s(X, t)$ is assumed to be $(L + \delta)/c$ periodic in the time variable t, and defined as follows

$$
s(X,t) = \begin{cases}
\begin{rcases}
X(1+\varepsilon) & \text{for } X \in [0, ct) \\
X + \varepsilon\,ct & \text{for } X \in [ct, L]
\end{rcases} & \text{if } t \in [0, \delta/c) \\[2ex]
\begin{rcases}
X & \text{for } X \in [0, ct-\delta) \\
X + \varepsilon(X + \delta - ct) & \text{for } X \in [ct-\delta, ct) \\
X + \varepsilon\,\delta & \text{for } X \in [ct, L]
\end{rcases} & \text{if } t \in [\delta/c, L/c) \\[3ex]
\begin{rcases}
X & \text{for } X \in [0, ct-\delta) \\
X + \varepsilon(X + \delta - ct) & \text{for } X \in [ct-\delta, L]
\end{rcases} & \text{if } t \in [L/c, (L+\delta)/c)
\end{cases}
\tag{5.24}
$$

so that the current length of the crawler reads

$$
l(t) = \begin{cases}
L + \varepsilon\,ct & \text{if } t \in [0, \delta/c), \\
L + \varepsilon\,\delta & \text{if } t \in [\delta/c, L/c) \\
L + \varepsilon(L + \delta - ct) & \text{if } t \in [L/c, (L+\delta)/c)
\end{cases}
$$

Therefore, by making use of equations (5.4) and (5.24), we obtain the Eulerian velocity at point $x = x_1(t) + s$ as

$$
v(x,t) = \begin{cases}
\begin{rcases}
\dot{x}_1(t) & \text{for } s \in [0, (1+\varepsilon)ct) \\
\dot{x}_1(t) + \varepsilon\,c & \text{for } s \in [(1+\varepsilon)ct, L + \varepsilon\,ct]
\end{rcases} & \text{if } t \in [0, \delta/c) \\[2ex]
\begin{rcases}
\dot{x}_1(t) & \text{for } s \in [0, ct-\delta) \\
\dot{x}_1(t) - \varepsilon\,c & \text{for } s \in [ct-\delta, ct+\varepsilon\,\delta) \\
\dot{x}_1(t) & \text{for } s \in [ct+\varepsilon\,\delta, L + \varepsilon\,\delta]
\end{rcases} & \text{if } t \in [\delta/c, L/c) \\[3ex]
\begin{rcases}
\dot{x}_1(t) & \text{for } s \in [0, ct-\delta) \\
\dot{x}_1(t) - \varepsilon\,c & \text{for } s \in [ct-\delta, L + \varepsilon(L+\delta-ct)]
\end{rcases} & \text{if } t \in [L/c, (L+\delta)/c)
\end{cases}
\tag{5.25}
$$

We focus now our attention on the case of extension waves, such that $\varepsilon > 0$. The case of contraction waves, with $-1 < \varepsilon < 0$, can be treated similarly. From equation (5.25) we observe that, at any time t, the velocity along the crawler can assume only two values: a certain velocity $\nu(t)$ at the points where no deformation occurs ($s'(X, t) = 1$) and a lower velocity $\nu(t) - \varepsilon\,c$ at the points experiencing elongation ($s'(X, t) = 1 + \varepsilon$). Obviously, force balance dictates that $\nu(t) \geq 0$ for extension waves (resp. $\nu(t) \leq 0$ for contraction waves) and, in principle, two qualitatively different situations are possible: if $\nu(t) = 0$, then a stick-slip behaviour takes place (with "slipping" occurring in the elongating part, with velocity $-\varepsilon\,c$, and "sticking" elsewhere), whereas for $\nu(t) \neq 0$ sliding occurs throughout the crawler.

Furthermore, we notice that for extension waves the velocity $\nu(t)$ is restricted to $\nu(t) \leq \varepsilon\,c$ (resp. $\nu(t) \geq \varepsilon\,c$ for contraction waves), and that the choice of $\nu(t) = \varepsilon\,c$ is compatible with the force balance only when the part of crawler being stretched is sufficiently large with respect to its total length. In fact, let us consider the time interval $t \in [0, \delta/c)$, during which the extension wave enters the crawler at its left end. For any time t such that

$$c\,t < L\frac{\tau_+ + \mu_+ \varepsilon\,c}{(1 + \varepsilon)\tau_- + \tau_+ + \mu_+ \varepsilon\,c}$$

the following estimate applies to the total force $F(t)$ acting on the crawler

$$F(t) = \int\limits_0^{(1+\varepsilon)c\,t} \tau(s,t)\,\mathrm{d}s - (L - c\,t)(\tau_+ + \mu_+ \varepsilon\,c) \leq (1+\varepsilon)\tau_- c\,t - (L - c\,t)(\tau_+ + \mu_+ \varepsilon\,c) < 0$$

and thus the force balance does not hold. In other words, an "inverted" stick-slip crawler, where sticking occurs along the deformed part and slipping along the other one, is in general not admissible in the context of our analysis, where the stride is given by equation (5.24). The only exception is the trivial case of $\tau_+ = \mu_+ = 0$.

In the following sections we shall assume that, for a given crawler, only one of the two modes of locomotion can be activated, and we will separately consider *stick-slip* crawlers ($\nu(t) = 0$) and *sliding* crawlers ($\nu(t) \neq 0$).

Stick-slip crawlers

We first explore the case of stick-slip crawlers, such that the Ansatz $\nu(t) = 0$ for every t yields

$$\dot{x}_1(t) = \begin{cases} -\varepsilon\,c & \text{for } t \in [0, \delta/c) \\ 0 & \text{for } t \in [\delta/c, (L + \delta)/c) \end{cases} \tag{5.26}$$

and time integration of (5.26) in the interval $t \in [0, (L + \delta)/c)$ immediately leads to the expression

$$\Delta x_1 = -\varepsilon\,\delta \tag{5.27}$$

for the net displacement after one period of the square wave.

We just need to check the compatibility of the Ansatz with the force balance. To this end, we compute the overall force exerted on the crawler,

which, for an extension wave ($\varepsilon > 0$), reads

$$
F(t) = \begin{cases}
(\tau_- + \mu_- \varepsilon c)(1+\varepsilon)ct + \displaystyle\int_{(1+\varepsilon)ct}^{L+\varepsilon ct} \tau(s,t)\,\mathrm{d}s & \text{for } t \in [0, \delta/c) \\[4ex]
\displaystyle\int_0^{ct-\delta} \tau(s,t)\,\mathrm{d}s + (\tau_- + \mu_- \varepsilon c)(1+\varepsilon)\delta + \displaystyle\int_{ct+\varepsilon\delta}^{L+\varepsilon\delta} \tau(s,t)\,\mathrm{d}s & \text{for } t \in [\delta/c, L/c) \\[4ex]
\displaystyle\int_0^{ct-\delta} \tau(s,t)\,\mathrm{d}s + (\tau_- + \mu_- \varepsilon c)(1+\varepsilon)(L - ct + \delta) & \text{for } t \in [L/c, (L+\delta)/c)
\end{cases}
$$

$$(5.28)$$

and we further notice that the most restrictive condition to $F(t) = 0$ is given by the middle term of (5.28), which specifically requires

$$
\delta \le \frac{\tau_+ L}{(\tau_- + \mu_- \varepsilon\, c)(1+\varepsilon) + \tau_+} = \delta_+^{\max} \tag{5.29}
$$

The case of contraction waves ($-1 < \varepsilon < 0$) can be studied similarly and leads to the following restriction on δ

$$
\delta \le \frac{\tau_- L}{(\tau_+ - \mu_+ \varepsilon\, c)(1+\varepsilon) + \tau_-} = \delta_-^{\max} \tag{5.30}
$$

We notice that $\tau_+ = 0$ implies $\delta_+^{\max} = 0$ and, likewise, $\tau_- = 0$ implies $\delta_-^{\max} = 0$. Therefore, no stick-slip behaviour can occur on a Newtonian substrate and the largest achievable displacement, at fixed ε, is given by $-\varepsilon\, \delta_\pm^{\max}$.

The displacement (5.27) produced by an elongation wave spanning the crawler's body once is always negative (opposite to the wave direction), whereas it is always positive (concordant to the wave direction) for a contraction wave. Furthermore, we observe that the net advancement $\Delta x_1 \to \delta$ in the limit $\varepsilon \to -1$, and, as we will see, this is a feature in common with sliding crawlers. This is due to the fact that, as $\varepsilon \to -1$, the portion of crawler experiencing deformation collapses to a single point: the force balance is then trivially satisfied, with no friction being exerted, and the resulting motion is determined exclusively by geometrical reasons, rather than dynamical ones.

Dry friction   The coefficients μ_+ and μ_- play only a minor role in stick-slip crawling. In fact, they only reduce the set of admissible square waves, see equations (5.29)-(5.30), and hence the maximum achievable displacement. Thus, dry friction is an ideal environment to study stick-slip behaviour. By making use of (5.27) and equations (5.29)-(5.30), the maximum achievable advancement for a traveling wave of fixed ε is obtained as

$$
\Delta_D x_1 = \begin{cases}
-\dfrac{\varepsilon(1-\alpha)}{1+\varepsilon\alpha} L & \text{for } \varepsilon > 0 \;\; \text{(extension wave)} \\[3ex]
-\dfrac{\varepsilon\alpha}{1+\varepsilon(1-\alpha)} L & \text{for } -1 < \varepsilon < 0 \;\; \text{(contraction wave)}
\end{cases}
\tag{5.31}
$$
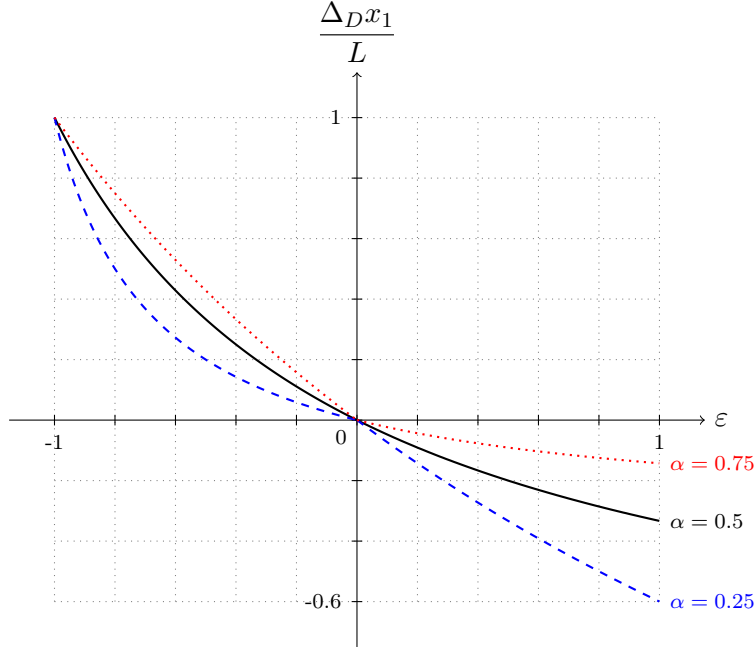
Figure 5.6: Maximum displacement $\Delta_D x_1/L$ for a stick-slip crawler in the case of dry friction as a function of $\varepsilon \in (-1, 1)$ and for $\alpha = \{0.25, 0.5, 0.75\}$.

The maximum displacement after one stretching cycle is shown in Fig. 5.6 in dimensionless form as a function of ε and for $\alpha = \{0.25, 0.5, 0.75\}$. The net advancement is always negative (positive) for extension (resp. contraction) waves, and its magnitude decreases (resp. increases) as α is increased.

Sliding crawlers

We turn now to the case of sliding crawlers, so that no stick-slip behaviour can occur and $\nu(t) > 0$ for $t \neq n(L+\delta)/c$ with n integer (at these times no deformation takes place and the velocity vanishes everywhere along the crawler). Specifically, we consider extensional waves ($\varepsilon > 0$) and study separately the force balance equation in the following three stages of deformation.

Stage A: $t \in (0, \delta/c)$ During this first time interval the square wave enters the crawler at its left end. As already discussed in section 5.4, force balance requires that $0 < \nu(t) < \varepsilon c$ and hence the velocity of the left end of the crawler is restricted to $-\varepsilon c < \dot{x}_1(t) < 0$. Thus, the force balance equation becomes

$$[\tau_- - \mu_- \dot{x}_1(t)](1 + \varepsilon)ct - [\tau_+ + \mu_+(\dot{x}_1(t) + \varepsilon c)](L - ct) = 0 \qquad (5.32)$$

from which we get

$$\dot{x}_1(t) = \frac{\tau_-(1+\varepsilon)c\,t - (\tau_+ + \mu_+\varepsilon c)(L - c\,t)}{\mu_-(1+\varepsilon)c\,t + \mu_+(L - c\,t)} \tag{5.33}$$

Taking into account the restrictions upon $\dot{x}_1(t)$, the solution (5.33) is admissible only if

$$\tau_+ = 0 \qquad \text{and} \qquad \delta < \frac{\mu_+\varepsilon c}{\mu_+\varepsilon c + \tau_-(1+\varepsilon)}\,L \tag{5.34}$$

and we notice that this implies $\mu_+ \neq 0$, for else $\delta = 0$ and no motion occurs.

Hereafter we assume[2] that $(1+\varepsilon)\mu_- \neq \mu_+$, and integration of (5.33) in the time interval $t \in (0, \delta/c)$ immediately provides the expression of the first contribution to the displacement, namely,

$$\Delta x_1^a = \frac{\delta[(1+\varepsilon)\tau_- + \mu_+\varepsilon c]}{c[(1+\varepsilon)\mu_- - \mu_+]} + \frac{L(1+\varepsilon)(\tau_- + \mu_-\varepsilon c)\mu_+}{c[(1+\varepsilon)\mu_- - \mu_+]^2} \ln\left[\frac{L\mu_+}{\delta(1+\varepsilon)\mu_- + (L-\delta)\mu_+}\right] \tag{5.35}$$

Stage B: $t \in [\delta/c, L/c)$.   At any instant of this interval, the square wave of width δ is entirely contained within the crawler's body. The restrictions on $\dot{x}_1(t)$ become $0 < \dot{x}_1(t) < \varepsilon\,c$ and, therefore, the force balance reads

$$[\tau_- - \mu_-(\dot{x}_1(t) - \varepsilon c)](1+\varepsilon)\delta - [\tau_+ + \mu_+\dot{x}_1(t)](L - \delta) = 0$$

from which we get

$$\dot{x}_1(t) = \frac{(\tau_- + \mu_-\varepsilon c)(1+\varepsilon)\delta - \tau_+(L - \delta)}{\mu_-(1+\varepsilon)\delta + \mu_+(L - \delta)} \tag{5.36}$$

This solution is admissible under conditions (5.34), and its time integration in the interval $t \in [\delta/c, L/c)$ yields the second contribution to the displacement as

$$\Delta x_1^b = \frac{\delta(L-\delta)(\tau_- + \mu_-\varepsilon c)(1+\varepsilon)}{\delta(1+\varepsilon)\mu_- c + (L-\delta)\mu_+ c} \tag{5.37}$$

---

[2]For $(1+\varepsilon)\mu_- = \mu_+$, the displacement (5.35) in the first interval must be replaced by

$$\Delta x_1^a = -\varepsilon\delta + \frac{\delta^2\varepsilon}{2L} + \frac{\delta^2(1+\varepsilon)\tau_-}{2L\mu_+ c} \tag{5.35*}$$

and the displacement (5.39) in the third interval by

$$\Delta x_1^c = \frac{\delta^2\varepsilon}{2L} + \frac{\delta^2(1+\varepsilon)\tau_-}{2L\mu_+ c} \tag{5.39*}$$

so that the overall displacement after one period, instead of (5.40), becomes

$$\Delta x_1 = -\varepsilon\delta + \frac{\delta^2\varepsilon}{L} + \frac{\delta^2(1+\varepsilon)\tau_-}{L\mu_+ c} + \frac{\delta(L-\delta)(\tau_- + \mu_-\varepsilon c)(1+\varepsilon)}{\delta(1+\varepsilon)\mu_- c + (L-\delta)\mu_+ c} \tag{5.40*}$$

Stage C: $t \in [L/c, (L+\delta)/c)$.   During the last time interval the square wave leaves the crawler at its right end. The velocity $\dot{x}_1(t)$ is again restricted to $0 < \dot{x}_1(t) < \varepsilon c$ and the equation for the force balance yields

$$[\tau_- - \mu_-(\dot{x}_1(t) - \varepsilon c)](1+\varepsilon)(L - ct + \delta) - [\tau_+ + \mu_+\dot{x}_1(t)](ct - \delta) = 0$$

from which we get

$$\dot{x}_1(t) = \frac{(\tau_- + \mu_-\varepsilon c)(1+\varepsilon)(L - ct + \delta) - \tau_+(ct - \delta)}{\mu_-(1+\varepsilon)(L - ct + \delta) + \mu_+(ct - \delta)} \tag{5.38}$$

Also in this case the solution is admissible under conditions (5.34), and integration in the time interval $t \in [L/c, (L+\delta)/c)$ leads to the third contribution of the displacement as

$$\Delta x_1^c = \frac{\delta(1+\varepsilon)(\tau_- + \mu_-\varepsilon c)}{c[(1+\varepsilon)\mu_- - \mu_+]} + \frac{L(1+\varepsilon)(\tau_- + \mu_-\varepsilon c)\mu_+}{c[(1+\varepsilon)\mu_- - \mu_+]^2} \ln\left[\frac{L\mu_+}{(1+\varepsilon)\delta\mu_- + (L-\delta)\mu_+}\right] \tag{5.39}$$

In conclusion, the total net advancement Δx_1, arising from an extensional wave spanning the crawler's body once, is computed adding equations (5.35), (5.37) and (5.39), leading to

$$\Delta x_1 = \frac{\delta\varepsilon[(1+\varepsilon)\mu_- + \mu_+]}{(1+\varepsilon)\mu_- - \mu_+} + \frac{2\delta(1+\varepsilon)\tau_-}{c[(1+\varepsilon)\mu_- - \mu_+]} + \frac{\delta(L-\delta)(\tau_- + \mu_-\varepsilon c)(1+\varepsilon)}{\delta(1+\varepsilon)\mu_- c + (L-\delta)\mu_+ c} +$$

$$+ \frac{2L(1+\varepsilon)(\tau_- + \mu_-\varepsilon c)\mu_+}{c[(1+\varepsilon)\mu_- - \mu_+]^2} \ln\left[\frac{L\mu_+}{\delta(1+\varepsilon)\mu_- + (L-\delta)\mu_+}\right] \tag{5.40}$$

The same reasoning holds also in the context of contraction waves $(-1 < \varepsilon < 0)$. In that case, $\varepsilon c < \nu(t) < 0$ and the formulae above can still be applied, provided that we replace τ_- with $-\tau_+$ and μ_- with μ_+. In particular, we remark that the admissibility conditions (5.34) are replaced in the contractive case by

$$\tau_- = 0 \qquad \text{and} \qquad \delta < \frac{\mu_-\varepsilon c}{\mu_-\varepsilon c - \tau_+(1+\varepsilon)} L \tag{5.41}$$

The restrictions on the width δ and on the substrate rheology deserve particular attention and are summarized in Table 5.2. In fact, considering the case of an extension (contraction) wave, we may observe that *sliding* crawling requires a vanishing value of τ_+ (resp. τ_-), whereas *stick-slip* crawling is feasible only if $\tau_+ \neq 0$ (resp. $\tau_- \neq 0$). In other words, the two modes of locomotion ("sliding" and "stick-slip" crawling) are mutually exclusive, in the sense that they are not compatible with the same choice of wave and substrate parameters.

Table 5.2: Admissibility restrictions on the width δ and on the substrate rheology.

	stick-slip crawling	sliding crawling
$\varepsilon > 0:$	$\delta \leq \dfrac{\tau_+ L}{(\tau_- + \mu_- \varepsilon\, c)(1 + \varepsilon) + \tau_+},\ \tau_+ \neq 0$	$\tau_+ = 0,\ \delta < \dfrac{\mu_+ \varepsilon c}{\mu_+ \varepsilon c + \tau_-(1 + \varepsilon)} L,\ \mu_+ \neq 0$
$\varepsilon < 0:$	$\delta \leq \dfrac{\tau_- L}{(\tau_+ - \mu_+ \varepsilon\, c)(1 + \varepsilon) + \tau_-},\ \tau_- \neq 0$	$\tau_- = 0,\ \delta < \dfrac{\mu_- \varepsilon c}{\mu_- \varepsilon c - \tau_+(1 + \varepsilon)} L,\ \mu_- \neq 0$

Newtonian friction   The admissibility conditions (5.34) and (5.41) are quite strict, see also the right column of Table 5.2. Indeed, sliding crawling by means of both extension and contraction waves is feasible only for a purely Newtonian rheology ($\tau_- = \tau_+ = 0$), and this is also the only case where δ can freely vary in the interval $(0, L)$. In this context, the net displacement Δx_1 for an extension wave becomes

$$\Delta_N x_1 = \frac{\delta \varepsilon [(1 + \varepsilon)\beta^2 + 1]}{(1 + \varepsilon)\beta^2 - 1} + \frac{\delta(L - \delta)(1 + \varepsilon)\varepsilon\beta^2}{\delta(1 + \varepsilon)\beta^2 + (L - \delta)} +$$

$$+ \frac{2L(1 + \varepsilon)\varepsilon\beta^2}{[(1 + \varepsilon)\beta^2 - 1]^2} \ln\left[\frac{L}{\delta(1 + \varepsilon)\beta^2 + (L - \delta)}\right]$$

and the formula for contraction waves can be obtained by replacing β with $1/\beta$.

The displacement attained after one stretching cycle is shown in Fig. 5.7 as a function of ε for the choice $\delta/L = 0.25$ and for $\beta^2 = \{0.25, 0.5, 1, 2, 4\}$. A lower friction in the direction of wave propagation ($\beta \geq 1$) always leads to a positive displacement, whereas a negative displacement is possible, for sufficiently small values of ε, when friction is lower in the opposite direction ($\beta < 1$). Furthermore, the displacement always tends to δ as $\varepsilon \to -1$, and tends to $+\infty$ as $\varepsilon \to +\infty$. A decrease of β enlarges the range of the values of ε that produce a negative displacement.
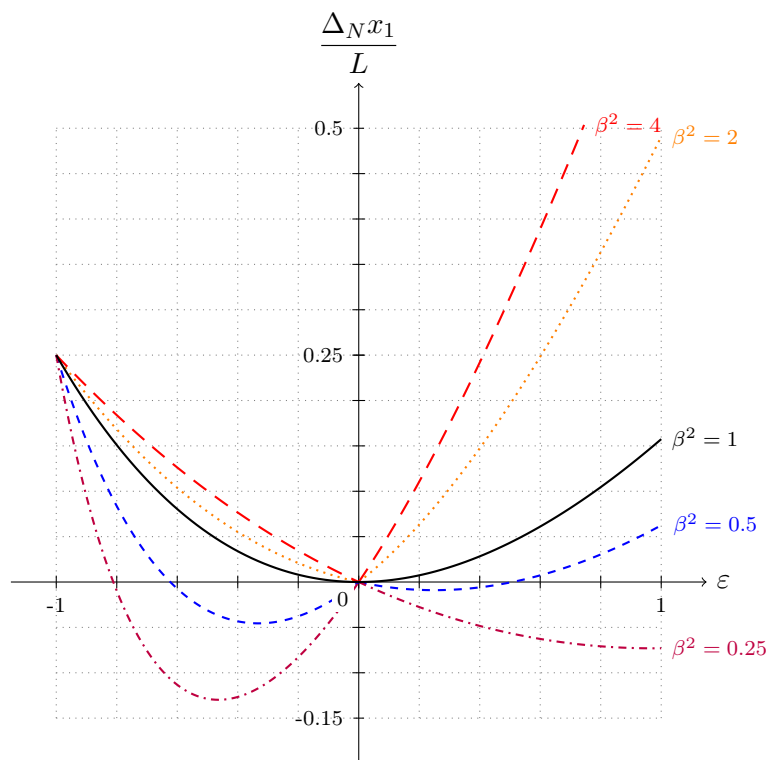
Figure 5.7: Maximum displacement $\Delta_N x_1/L$ for a sliding crawler in the case of Newtonian friction as a function of $\varepsilon \in (-1, 1)$ for the choice $\delta/L = 0.25$ and for $\beta^2 = \{0.25, 0.5, 1, 2, 4\}$.

Chapter 6

Nematic elastomer strips as soft crawlers

From this Chapter, we plan to introduce an elastic body as a key element of our analysis. Recalling our interest in having a minimal mechanism for locomotion, possibly also suitable to miniaturization, and the importance in this framework of reciprocal shape change, we discuss as our first model the behaviour of a strip of nematic elastomer, on which we can induce a periodic sequence of contractions and elongations (cf [DGN15]).

This situation can be associated to the spontaneous deformation accompanying either the nematic-to-isotropic transition (which can be induced by increasing the temperature past the phase transition temperature, or by irradiation with UV light in the case of photosensitive elastomers), or the isotropic-to-nematic transition induced by cooling a specimen initially in the isotropic state. Alternatively, it can be the spontaneous deformation accompanying a director reorientation in a nematic specimen (say, from perpendicular to parallel to the crawler axis, that can be induced by the application of a suitably oriented electric field).

We remark also that our model we are going to develop, based on energy (6.4), could be applied also to active strips made of other active materials (e.g., soft electroactive polymers, but also hard materials such as electrostrictive, ferroelectric, ferromagnetic, and ferroelastic solids). As we will see in the sequel, larger spontaneous strains lead to larger achievable displacements and locomotion is possible only if the spontaneous strains are sufficiently large, in a sense made precise by inequalities (6.34) and (6.57) below. For this reason, we suggest, as most natural candidate material, Liquid Crystal Elastomers (LCE), that provide the key example of a soft active material exhibiting large spontaneous strain. Indeed, the spontaneous extension accompanying the isotropic-to-nematic transition can be as large as 300%, cf. [WT03]. In light of this, we put no restrictions on the magnitude of the spontaneous strain, which can be arbitrarily large.

6.1   A first toy model of crawler

We consider the model crawler shown in Fig. 6.1 and denote the position of its points through a one-to-one function $\chi(X,t)$ mapping the reference configuration $[X_1, X_2]$ (more concretely, $X_1 = 0$ and $X_2 = L$, L being the reference length of the crawler) onto the deformed configuration $[x_1(t), x_2(t)]$ where

$$\begin{cases} x_1(t) = \chi(X_1, t) = X_1 + u(X_1, t) = u_1(t) \\ x_2(t) = \chi(X_2, t) = X_2 + u(X_2, t) = L + u_2(t) \end{cases} \tag{6.1}$$

Here $u(X,t)$ is the displacement at point X and time t defined by

$$u(X,t) = x - X = \chi(X,t) - X \tag{6.2}$$

whereas $u_1(t)$ and $u_2(t)$ are the displacements at time t of the two end points. We will denote with primes and dots the partial derivatives with respect to space and time, respectively, according to

$$u'(X,t) := \frac{\partial}{\partial X} u(X,t) \qquad \dot{u}(X,t) := \frac{\partial}{\partial t} u(X,t) \tag{6.3}$$
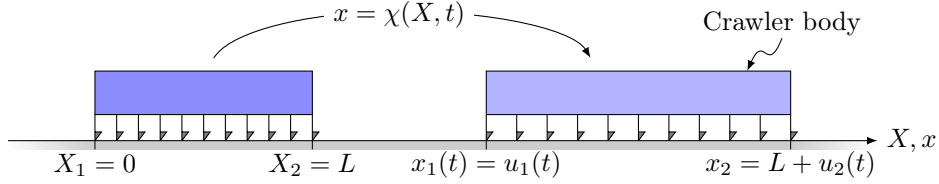
Figure 6.1: A sketch of the one-dimensional crawler analysed in this study. The model accounts only for horizontal displacements along the X coordinate, whereas the system exploits directional frictional interactions with a solid substrate either at its extremities (case of interactions only at the extremities) or along its body length (case of distributed interactions, shown in the figure).

The body of the crawler is elastic and we assume that its configurational energy is given by

$$\mathcal{E}(u,t) = \int_0^L \frac{K}{2} \left(\varepsilon_u(X,t) - \varepsilon_\mathrm{o}(X,t) \right)^2 \mathrm{d}X \tag{6.4}$$

where

$$\varepsilon_u(X,t) = u'(X,t) \tag{6.5}$$

is the strain, $K > 0$ is the 1D elastic modulus (with dimension of force since $K = EA$, where E is Young's modulus and A the cross-sectional area), and

Figure 6.2: Force-velocity law (a) and dissipation (b) in the case of frictional, directional forces acting only at the extremities of the crawler.

$\varepsilon_\mathrm{o}(X, t)$ is the spontaneous, or stress-free strain at X and t. We assume that $-1 < \varepsilon_\mathrm{o} < +\infty$ and refer to ε_o as the *active distortion*: in analogy with thermal dilatation, it is the spontaneous strain (i.e., the one in the absence of stress) associated with a phase transition.

The tension $T(X, t)$ at any crawler section X and time t is given by

$$T(X, t) = K \left(u'(X, t) - \varepsilon_\mathrm{o}(X, t) \right) = K u'(X, t) + T^a(X, t) \qquad (6.6)$$

and is the 1D analogue of the first Piola-Kirchhoff stress. The term $T^a(X, t) = -K\varepsilon_\mathrm{o}(X, t)$ can be regarded as the *active* part of the internal tension, in analogy with the *active stress* used to model biological matter as an active gel [Mar+13].

Frictional forces arising from directional interactions with a solid substrate act on the crawler. These are either concentrated at the two ends or distributed along the crawler body, see the sketch of Fig. 6.1.

In the case of frictional forces acting only at the two ends of the crawler X_i $(i = 1, 2)$, these are given by

$$F_i(t) = F(\dot{u}_i(t)) \quad \text{where } F(v) \in \begin{cases} \{F_-\} & \text{if } v < 0 \\ [-F_+, F_-] & \text{if } v = 0 \\ \{-F_+\} & \text{if } v > 0 \end{cases} \qquad (6.7)$$

and $F_- > F_+ > 0$ are threshold forces to be overcome for sliding to occur to the left or to the right, respectively, see Fig. 6.2a. The assumption $F_- > F_+$ simply means that we have chosen to orient the x-axis so that the positive direction is the one of easy sliding. We remark that the notation $F(v) \in \{F_-\}$ means $F(v) = F_-$, which occurs if $v < 0$. Likewise, the notation $F(v) \in \{-F_+\}$ means $F(v) = -F_+$, which occurs if $v > 0$. If instead $v = 0$, then $F(v)$ can take any value in the interval $[-F_+, F_-]$. We also notice that the contribution of the end frictional forces to the rate of energy dissipation reads

$$-\sum_{i=1}^{2} F_i(t)\dot{u}_i(t) = \sum_{i=1}^{2} \mathcal{D}(\dot{u}_i(t)) \qquad (6.8)$$

where the dissipation $\mathcal{D}(v) := F_+ (v)^+ - F_- (v)^-$ has been introduced with $(v)^\pm := \frac{1}{2}(v \pm |v|)$, such that in the notation of convex analysis we can write

$$-F(v) \in \frac{\partial}{\partial v} \mathcal{D}(v) = \begin{cases} \{-F_-\} & \text{if } v < 0 \\ [-F_-, F_+] & \text{if } v = 0 \\ \{F_+\} & \text{if } v > 0 \end{cases} \qquad (6.9)$$

where $\frac{\partial}{\partial v} \mathcal{D}(v)$ is the sub-differential of $\mathcal{D}$ at v, see Fig. 6.2b.

(a)

(b)
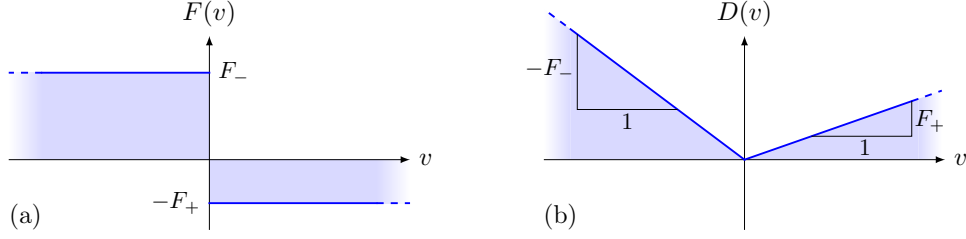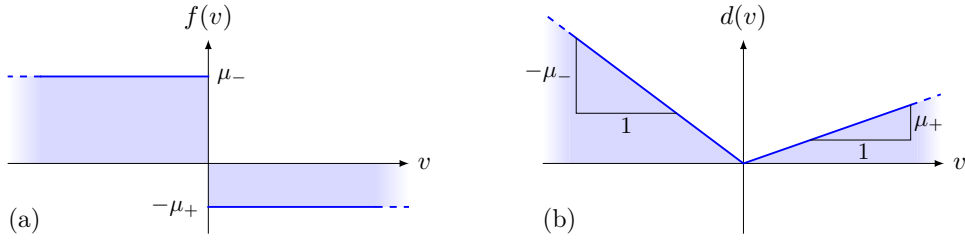
Figure 6.3: Force-velocity law (a) and dissipation (b) in the case of frictional, directional forces distributed along the crawler body.

In the case of distributed interactions, the frictional force per unit reference length is given by

$$f(X,t) = f(\dot{u}(X,t)), \text{ where } f(v) \in \begin{cases} \{\mu_-\} & \text{if } v < 0 \\ [-\mu_+, \mu_-] & \text{if } v = 0 \\ \{-\mu_+\} & \text{if } v > 0 \end{cases} \qquad (6.10)$$

and $\mu_- > \mu_+ > 0$ are threshold forces per unit reference length to be overcome for sliding to occur, see Fig. 6.3a. As before, $f(v) \in \{\mu_-\}$ means $f(v) = \mu_-$, which occurs if $v < 0$. Likewise, $f(v) \in \{-\mu_+\}$ means $f(v) = -\mu_+$, which occurs if $v > 0$. If instead $v = 0$, then $f(v)$ can take any value in the interval $[-\mu_+, \mu_-]$. The contribution of the distributed frictional forces to the rate of energy dissipation is now

$$-\int_0^L f(X,t)\dot{u}(X,t)\, \mathrm{d}X = \int_0^L d(\dot{u}(X,t))\, \mathrm{d}X \qquad (6.11)$$

where the dissipation per unit reference length $d(v) := \mu_+ (v)^+ - \mu_- (v)^-$ has been introduced, again with $(v)^\pm := \frac{1}{2}(v \pm |v|)$, such that in the notation of convex analysis we can write

$$-f(v) \in \frac{\partial}{\partial v} d(v) = \begin{cases} \{-\mu_-\} & \text{if } v < 0 \\ [-\mu_-, \mu_+] & \text{if } v = 0 \\ \{\mu_+\} & \text{if } v > 0 \end{cases} \qquad (6.12)$$

where $\frac{\partial}{\partial v}d(v)$ is the sub-differential of d at v, see Fig. 6.3b.

We consider a history of active distortions $\varepsilon_{\mathrm{o}}(X,T)$ varying in time sufficiently slowly, so that the crawler evolves quasi-statically through a sequence of equilibrium states. The governing equations are then obtained by neglecting inertia in the balance of linear momentum, and read

$$T'(X,t) + f(\dot{u}(X,t)) = 0 \tag{6.13}$$

together with the boundary conditions for the tension at the crawler extremities

$$\begin{cases} T(0,t) = -F_1(t) = -F(\dot{u}_1(t)) \\ T(L,t) = F_2(t) = F(\dot{u}_2(t)) \end{cases} \tag{6.14}$$

By making use of (6.9) and (6.12), the balance of linear momentum can be rewritten as

$$T'(X,t) \in \frac{\partial}{\partial v}d\left(\dot{u}(X,t)\right), \tag{6.15}$$

whereas the boundary conditions at the two extremities become

$$\begin{cases} T(0,t) \in \frac{\partial}{\partial v}\mathcal{D}\left(\dot{u}_1(t)\right) \\ T(L,t) \in -\frac{\partial}{\partial v}\mathcal{D}\left(\dot{u}_2(t)\right) \end{cases} \tag{6.16}$$

Integrating (6.13), and using the boundary conditions (6.14), we obtain the global force balance for the crawler, namely

$$F(\dot{u}_1(t)) + F(\dot{u}_2(t)) + \int_0^L f(\dot{u}(X,t))\,\mathrm{d}X = 0 \tag{6.17}$$

6.2 Formulation of the motility problem

We formulate our motility problem as follows. Given the initial state of the system through the assignment of the initial position and tension, e.g., $u(X,0) \equiv 0$, and $T(X,0) \equiv 0$, we look for the history of displacements $t \mapsto u(X,t)$ and tensions $t \mapsto T(X,t)$ corresponding to a given periodic time history of spatially constant active distortions, $t \mapsto \varepsilon_{\mathrm{o}}(X,t) \equiv \varepsilon_{\mathrm{o}}(t)$. In particular, we are interested in the asymptotic average speed of the crawler

$$\lim_{t\to+\infty} \frac{u(X^*,t)}{t} \tag{6.18}$$

where X^* is an arbitrarily chosen point. We consider in particular the time history of active distortions given by the 2τ-periodic sawtooth graph of Fig. 6.4, defined on $[0,2\tau]$ as

$$\varepsilon_{\mathrm{o}}(t) = \begin{cases} \alpha t & \text{for } t \in [0,\tau] \\ \alpha(2\tau - t) & \text{for } t \in [\tau,2\tau] \end{cases} \tag{6.19}$$

and then extended 2τ-periodically for $t \geq 0$. We denote the maximum distortion encountered as

$$\varepsilon_{\mathrm{o}}^{\max} := \alpha\tau \tag{6.20}$$
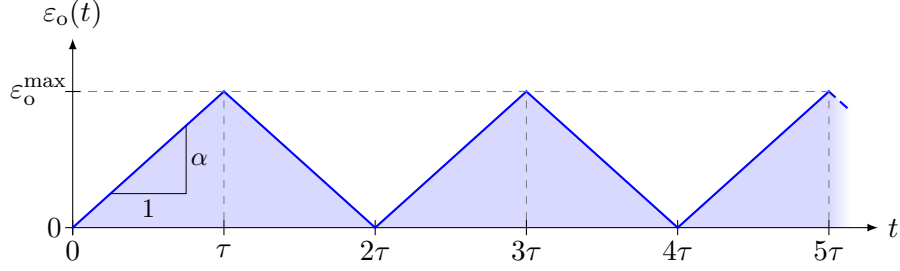
Figure 6.4: Time history of 2τ-periodic, sawtooth active distortions applied to the crawler.

Friction only at the ends

Here, since $f \equiv 0$, we have that the internal tension $T(X, t)$ is independent of the coordinate X. It follows from (6.6) that also $u'(X, t)$ is independent of X, and the expression (6.4) for the energy reduces to

$$\mathcal{E}_r(u_1(t), u_2(t), t) = \frac{KL}{2} \left(\frac{u_2(t) - u_1(t)}{L} - \varepsilon_{\mathrm{o}}(t) \right)^2 \tag{6.21}$$

Furthermore, the evolution equations (6.16) simplify to

$$\begin{cases} T(0, t) = -\frac{\partial}{\partial u_1}\mathcal{E}_r(u_1(t), u_2(t), t) \in \frac{\partial}{\partial v}\mathcal{D}\left(\dot{u}_1(t)\right) \\[2mm] -T(L, t) = -\frac{\partial}{\partial u_2}\mathcal{E}_r(u_1(t), u_2(t), t) \in \frac{\partial}{\partial v}\mathcal{D}\left(\dot{u}_2(t)\right) \end{cases} \tag{6.22}$$

and, at times when sliding occurs, these can be written as equalities

$$\begin{cases} -\frac{\partial}{\partial u_1}\mathcal{E}_r(u_1(t), u_2(t), t) = \frac{\partial}{\partial v}\mathcal{D}\left(\dot{u}_1(t)\right) & \text{if } \dot{u}_1 \neq 0 \\[2mm] -\frac{\partial}{\partial u_2}\mathcal{E}_r(u_1(t), u_2(t), t) = \frac{\partial}{\partial v}\mathcal{D}\left(\dot{u}_2(t)\right) & \text{if } \dot{u}_2 \neq 0 \end{cases} \tag{6.23}$$

Denoting now by

$$F_{\mathrm{fric}}^i := \frac{\partial}{\partial \dot{u}_i}\sum_{j=1}^{2}\mathcal{D}(\dot{u}_j(t)) \quad \text{and} \quad F_{\mathrm{el}}^i := \frac{\partial}{\partial u_i}\mathcal{E}_r(u_1(t), u_2(t), t) \tag{6.24}$$

the *frictional* and *elastic* forces at the i-th end (i=1,2), we recover the interpretation of the evolution equations (6.23) above as force balances at the two

ends, on each of which the total force consists of an elastic and of a frictional contribution, namely

$$F_{\text{el}}^i + F_{\text{fric}}^i = 0 \qquad (6.25)$$

We recall that we are working in the quasi-static regime, hence neglecting inertial forces. Alternatively, by multiplying each of the equations above by $\dot{u}_i$ we obtain

$$-\frac{\partial}{\partial u_i}\mathcal{E}_r\,\dot{u}_i = F_{\text{fric}}^i\,\dot{u}_i \qquad (6.26)$$

and we can interpret the evolution equations as the statement that the system evolves in such a way that the energy dissipation rate always match the rate of release of elastic energy.

Only distributed friction

Here there are no concentrated frictional forces at the two ends, recall the sketch of Fig. 6.1, so that equations (6.16) simply reduce to

$$\begin{cases} T(0,t) = 0\,, \\ T(L,t) = 0\,, \end{cases} \qquad (6.27)$$

and provide the boundary conditions for the tension field

$$T(X,t) = K(u'(X,t) - \varepsilon_{\text{o}}(t)) \qquad (6.28)$$

which satisfies the evolution equation (6.15), namely,

$$T'(X,t) \in \begin{cases} \{-\mu_-\} & \text{if } \dot{u}(X,t) < 0 \\ [-\mu_-, \mu_+] & \text{if } \dot{u}(X,t) = 0 \\ \{\mu_+\} & \text{if } \dot{u}(X,t) > 0 \end{cases} \qquad (6.29)$$

By substituting (6.28) into (6.29), we see that, in this case, the evolution equations take the form of a differential inclusion for the displacement field $u(X,t)$.

6.3 Friction only at the ends

We solve in this section the evolution problem for the case in which frictional forces act only at the two ends. This can be considered as a warm up for the more difficult case in which distributed frictional forces act along the crawler body.

Evolution equations

We recall that, in this case, the internal tension $T(X,t)$ is independent of X and given by

$$T(t) = K \left(\frac{u_2(t) - u_1(t)}{L} - \varepsilon_o(t) \right) \tag{6.30}$$

The equations governing the evolution of the system are (6.22), and they can be conveniently recast as

$$\dot{u}_1(t) = 0 \qquad \dot{u}_2(t) = 0 \qquad \text{if} \begin{cases} T(t) \in (F_+, F_+) \\ T(t) = F_+ \text{ and } \dot{\varepsilon}_o(t) \geq 0 \\ T(t) = -F_+ \text{ and } \dot{\varepsilon}_o(t) \leq 0 \end{cases} \tag{6.31}$$

corresponding to the case of stationarity of the two crawler extremities,

$$\dot{u}_1(t) = \alpha L \quad \dot{u}_2(t) = 0 \qquad \text{if } T(t) = F_+ \text{ and } \dot{\varepsilon}_o(t) < 0 \tag{6.32}$$

corresponding to the case of slip for the left hand side of the crawler and stationarity of the other one, and finally

$$\dot{u}_1(t) = 0 \quad \dot{u}_2(t) = \alpha L \qquad \text{if } T(t) = -F_+ \text{ and } \dot{\varepsilon}_o(t) > 0 \tag{6.33}$$

corresponding to the case of stationarity for the left hand side of the crawler and slip of the other one.

Solution of the motility problem

We recall that the initial conditions are $u_1(0) = u_2(0) = 0$ and $T(0) = 0$, and we consider the case of sufficiently large distortion, namely we assume that

$$\varepsilon_o^{\max} > \frac{2F_+}{K} \tag{6.34}$$

We will show that the motion of the crawler is characterized by a preliminary transient phase for $t \in [0, \tau]$, followed by a 2τ-periodic behaviour for $t > \tau$, with a constant forward displacement of the crawler in each period. An important role in our analysis will be played by the time constant

$$t_d = \frac{2F_+}{K\alpha} \tag{6.35}$$

and we notice that our assumption (6.34) is equivalent to $t_d < \tau$.

Interval $0 \leq t < t_d/2$.   During this time interval $\dot{\varepsilon}_o(t) = \alpha > 0$ and $T(t) > -F_+$, so that we are in case (6.31). The two ends of the crawler are stationary $(\dot{u}_1(t) = \dot{u}_2(t) = 0)$, such that

$$u_1(t) = u_2(t) = 0 \tag{6.36}$$

and the tension in the crawler varies linearly in time as

$$T(t) = -K\alpha t \tag{6.37}$$

reaching the critical value $T(t_d/2) = -F_+$ at the end of the interval.

Interval $t_d/2 \leq t < \tau$. In this time interval we still have $\dot{\varepsilon}_o(t) = \alpha > 0$, but now $T(t) = -F_+$, so we are in situation (6.33). The first end is stationary ($\dot{u}_1(t) = 0$) while the second one moves keeping the tension constant ($\dot{u}_2(t) = \alpha L$), leading to

$$u_1(t) = 0 \qquad u_2(t) = \alpha L \left(t - \frac{t_d}{2} \right) \tag{6.38}$$

At the end of the time interval we have that $T(\tau) = -F_+$ and

$$u_1(\tau) = 0 \qquad u_2(\tau) = \alpha L \left(\tau - \frac{t_d}{2} \right) \tag{6.39}$$

Interval $\tau \leq t < \tau + t_d$. During this time interval $\dot{\varepsilon}_o(t) = -\alpha < 0$ and $T(t) < F_+$, so we are again in situation (6.31). The two ends are stationary ($\dot{u}_1(t) = \dot{u}_2(t) = 0$) and therefore at time $t = \tau + t_d$ the position of the crawler is given by (6.39). The tension instead increases linearly according to

$$T(t) = -F_+ + K\alpha \left(t - \tau \right) \tag{6.40}$$

reaching at the end of this time interval the other critical value $T(\tau + t_d) = F_+$.

Interval $\tau + t_d \leq t < 2\tau$. In this time interval we still have $\dot{\varepsilon}_o(t) = -\alpha < 0$, but now $T(t) = F_+$, so we are in situation (6.32). The second end is stationary ($\dot{u}_2(t) = 0$) while the first one moves keeping the tension constant ($\dot{u}_1(t) = \alpha L$), leading to

$$u_1(t) = \alpha L(t - \tau - t_d) \qquad u_2(t) = \alpha L \left(\tau - \frac{t_d}{2} \right) \tag{6.41}$$

At the end of the time interval we have that $T(2\tau) = F_+$ and

$$u_1(2\tau) = \alpha L(\tau - t_d) \qquad u_2(2\tau) = \alpha L \left(\tau - \frac{t_d}{2} \right) \tag{6.42}$$

Interval $2\tau \leq t < 2\tau + t_d$. During this time interval $\dot{\varepsilon}_o(t) = \alpha > 0$ and $T(t) > -F_+$, so that we are in case (6.31). The two ends are stationary ($\dot{u}_1(t) = \dot{u}_2(t) = 0$) and so at $t = 2\tau + t_d$ the position of the crawler is still the one of (6.42). The tension decreases linearly according to

$$T(t) = F_+ - K\alpha(t - 2\tau) \tag{6.43}$$

and reaches at the end of the time interval the critical value of $T(2\tau + t_d) = -F_+$.

In this time interval we observe a behaviour similar to that of the first interval $0 < t < t_d/2$, but in this case we have a greater initial tension (F_+ instead of 0), so we need twice the time to reach the critical tension $-F_+$.

Interval $2\tau + t_d \leq t < 3\tau$. In this time interval we still have $\dot{\varepsilon}_o(t) = \alpha > 0$, but now $T(t) = -F_+$, so we are in situation (6.33). The first end is stationary $(\dot{u}_1(t) = 0)$ while the second one moves keeping the tension constant $(\dot{u}_2(t) = \alpha L)$, leading to

$$u_1(t) = \alpha L(\tau - t_d) \qquad u_2(t) = \alpha L \left(\tau - \frac{t_d}{2} \right) + \alpha L(t - 2\tau - t_d) \qquad (6.44)$$

At the end of the time interval we have that $T(3\tau) = -F_+$ and

$$u_1(3\tau) = \alpha L(\tau - t_d) \qquad u_2(3\tau) = \alpha L \left(2\tau - \frac{3t_d}{2} \right) \qquad (6.45)$$
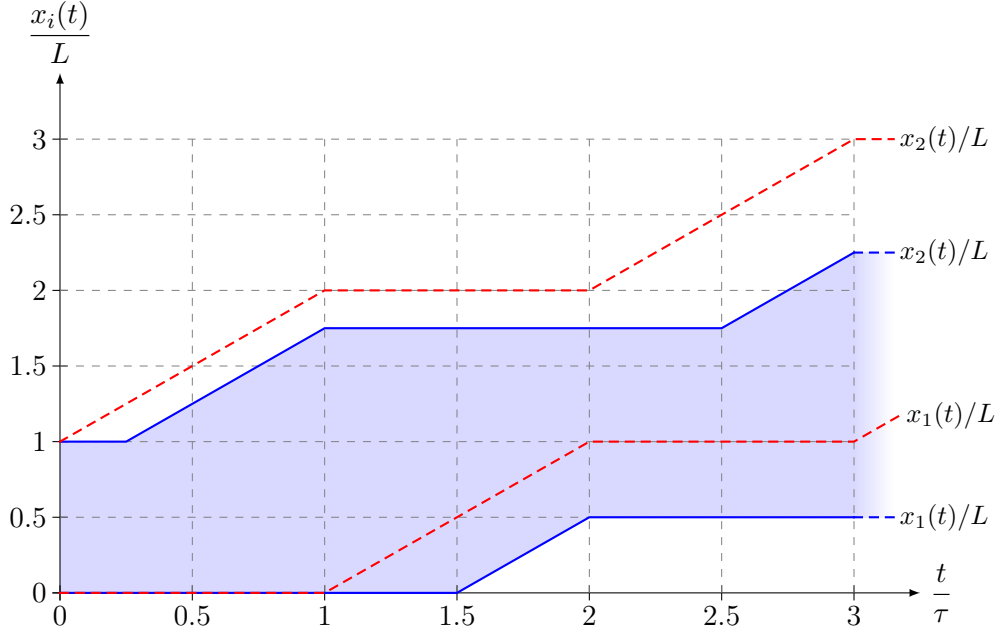
Figure 6.5: Position of the crawler extremities $x_i(t)$ during a time interval of 3τ and for a maximum distortion $\varepsilon_o^{\max} = 1$. Two cases are shown to stress the effect on the displacements of the crawler stiffness, and these correspond to $t_d/\tau = 1/2$ (or equivalently to $F_+/K = \varepsilon_o^{\max}/4$, blue solid curves), and $t_d/\tau = 0$ (or equivalently to $F_+/K = 0$, red dashed curves). Notice the piecewise linear time history of the displacements, which arises from the frictional, directional nature of the interactions with the substrate. At any time, the current length $l(t)$ of the crawler body (highlighted in the figure for the case of $t_d/\tau = 1/2$) can be inferred from the vertical distance between the two curves.

The position of the crawler extremities $x_i(t)$ is depicted in Fig. 6.5 for a time interval of 3τ and for the case of $\varepsilon_o^{\max} = 1$. Specifically, two cases are shown to stress the effect on the displacements of the crawler stiffness,

and these correspond to $t_d/\tau = 1/2$ (blue solid curves), and $t_d/\tau = 0$ (red dashed curves). We observe that the state of the crawler at time $t = 3\tau$ corresponds to that at time $t = \tau$ except for a translation of $\alpha L(\tau - t_d)$. Since the dynamics of the crawler is translation-invariant, the solution will repeat 2τ-periodically the behaviour found in $[\tau, 3\tau]$. We can thus easily find the position of the crawler at any positive integer multiple of τ, namely, for any integer $m > 0$,

$$u_1(2m\tau) = m\alpha L(\tau - t_d) \qquad , u_2(2m\tau) = m\alpha L(\tau - t_d) + \alpha L\frac{t_d}{2}$$

and

$$u_1((2m+1)\tau) = m\alpha L(\tau - t_d) \qquad u_2((2m+1)\tau) = (m+1)\alpha L(\tau - t_d) + \alpha L\frac{t_d}{2}$$

Thus, the net displacement in one stretching cycle, corresponding to a time interval $\Delta t = 2\tau$, reads

$$\alpha L(\tau - t_d) = L\left(\varepsilon_{\mathrm{o}}^{\max} - \frac{2F_+}{K}\right) \tag{6.46}$$

The equation above shows that, at fixed F_+ and K, the achievable displacement increases when $\varepsilon_{\mathrm{o}}^{\max}$ increases and no displacement is possible if the material exhibits spontaneous strains whose maximal magnitude does not satisfy inequality (6.34).

Finally, we notice that the crawler will be elongated in comparison to the initial length L, oscillating between a minimum length

$$l(2m\tau) = L\left(1 + \frac{F_+}{K}\right) \tag{6.47}$$

and a maximum length

$$l((2m + 1)\tau) = L\left(1 + \varepsilon_{\mathrm{o}}^{\max} - \frac{F_+}{K}\right) \tag{6.48}$$

6.4 Distributed friction

In the previous section, the case of a crawler has been addressed that exploits frictional, directional interactions at its ends only. We extend now our study to the case in which distributed frictional forces act along the crawler body.

Evolution equations

We recall from Section 6.2 the evolution equations, namely,

$$T'(X, t) \in \begin{cases} \{-\mu_-\} & \text{if } \dot{u}(X, t) < 0 \\ [-\mu_-, \mu_+] & \text{if } \dot{u}(X, t) = 0 \\ \{\mu_+\} & \text{if } \dot{u}(X, t) > 0 \end{cases} \tag{6.49}$$

where the tension $T(X,t)$ is given by

$$T(X,t) = K(u'(X,t) - \varepsilon_\mathrm{o}(t)) \tag{6.50}$$

It follows from equation (6.50) that

$$\dot{T}(X_0,t) = -K\dot{\varepsilon}_\mathrm{o}(t) \qquad \text{if } \dot{u}(X,t) = 0 \text{ for every } X \in N_0(X_0) \tag{6.51}$$

i.e., in a neighbourhood N_0 of X_0. Additionally, we have the boundary conditions at the crawler extremities, such that at any time

$$\begin{cases} T(0,t) = 0 \\ T(L,t) = 0 \end{cases} \tag{6.52}$$

Solution of the motility problem

For the solution of the problem, it is expedient to introduce two special points, namely

$$X_L = \frac{\mu_+}{\mu_- + \mu_+}L \qquad X_R = \frac{\mu_-}{\mu_- + \mu_+}L \tag{6.53}$$

We first notice that

$$X_L + X_R = L \tag{6.54}$$

and set

$$x_L(t) = X_L + u_L(t) \qquad x_R(t) = X_R + u_R(t) \tag{6.55}$$

where $u_L(t) = u(X_L,t)$ and $u_R(t) = u(X_R,t)$. We further notice that we can relate the positions at time t of every couple of points X_A and X_B through

$$u(X_B,t) = u(X_A,t) + \int_{X_A}^{X_B} \left(\varepsilon_\mathrm{o}(t) + \frac{1}{K}T(X,t) \right) \mathrm{d}X \tag{6.56}$$

which follows from (6.50), by solving for u' and then integrating with respect to X.

Similarly to the case of localized interactions, recall condition (6.34), we assume that the active distortions are sufficiently large, and in fact require that

$$\varepsilon_\mathrm{o}^{\max} > \frac{\mu_+}{K}L \tag{6.57}$$

For our analysis, it is also useful to introduce two special time values, namely,

$$t_c = \frac{\mu_+ L}{K\alpha} \qquad t_c^* = \frac{\mu_-}{\mu_- + \mu_+}\frac{\mu_+ L}{K\alpha} \tag{6.58}$$

and we notice that our assumption of large distortion is equivalent to $t_c < \tau$.

In what follows, we will seek solutions by using an ansatz on $\dot{u}(X,t)$. Namely, we assume that the interval $[0,L]$ is partitioned into three, possibly

empty, disjoint sub-intervals $I_L(t) \cup I_0(t) \cup I_R(t) = [0, L]$ (written in order from left to right) with either

$$
\begin{cases}
\dot{u}(X,t) < 0 & \text{for } X \in I_L(t) \\
\dot{u}(X,t) = 0 & \text{for } X \in I_0(t) \qquad \text{if } \dot{\varepsilon}_\mathrm{o}(t) > 0 \\
\dot{u}(X,t) > 0 & \text{for } X \in I_R(t)
\end{cases}
\tag{6.59}
$$

i.e., for a positive incremental distortion, or

$$
\begin{cases}
\dot{u}(X,t) > 0 & \text{for } X \in I_L(t) \\
\dot{u}(X,t) = 0 & \text{for } X \in I_0(t) \qquad \text{if } \dot{\varepsilon}_\mathrm{o}(t) < 0 \\
\dot{u}(X,t) < 0 & \text{for } X \in I_R(t)
\end{cases}
\tag{6.60}
$$

i.e., for a negative incremental distortion. We assume that $I_0(t)$ is a closed interval and consequently that $I_L(t)$ and $I_R(t)$ have an open end. The critical times $m\tau$, where $\dot{\varepsilon}_\mathrm{o}$ is not defined, will be studied as extreme points of prescribed time sub-intervals and thus the partition of the Ansatz will be be assigned only as (left or right) limit, in accordance with the instance considered.

Combining the Ansatz with (6.49) and the boundary conditions (6.52) we deduce that, if $\dot{\varepsilon}_\mathrm{o}(t) > 0$, then

$$
I_L(t) \subseteq [0, X_L) \qquad I_R(t) \subseteq (X_L, L] \tag{6.61}
$$

and the tension satisfies

$$
\begin{cases}
T(X,t) = -\mu_- X & \text{if } X \in I_L(t) \\
T(X,t) \geq -\mu_- X & \text{if } X \in I_0(t) \cap [0, X_L] \\
T(X,t) \geq \mu_+(X - L) & \text{if } X \in I_0(t) \cap [X_L, L] \\
T(X,t) = \mu_+(X - L) & \text{if } X \in I_R
\end{cases}
\tag{6.62}
$$

In the two middle conditions of (6.62), equality holds only on the boundary of I_0 in accordance with the continuity of T. On the other hand, for the interior points of I_0 the inequality is always strict, for else there would be a contradiction with (6.51). In the extreme case $I_0(t) = \{X_L\}$, the tension reaches everywhere its minimum admissible value

$$
T_{\min}(X) = \begin{cases}
-\mu_- X & \text{if } 0 \leq X \leq X_L \\
\mu_+(X - L) & \text{if } X_L \leq X \leq L
\end{cases}
\tag{6.63}
$$

and the whole crawler is extending, with each point moving away from the only stationary point X_L. We remark that, once this tension configuration is reached, we will have $T(X,t) = T_{\min}(X)$ as long as $\dot{\varepsilon}_\mathrm{o}(t) > 0$, with the crawler elongating according to (6.50). In fact, any change in the tension would be in contradiction with (6.49).

A similar reasoning is applicable in the case of a negative incremental distortion. In fact we argue that, if $\dot{\varepsilon}_{\mathrm{o}}(t) < 0$, then

$$I_L(t) \subseteq [0, X_R) \qquad I_R(t) \subseteq (X_R, L] \tag{6.64}$$

and the tension satisfies

$$\begin{cases} T(X,t) = \mu_+ X & \text{if } X \in I_L(t) \\ T(X,t) \le \mu_+ X & \text{if } X \in I_0(t) \cap [0, X_R] \\ T(X,t) \le -\mu_-(X - L) & \text{if } X \in I_0(t) \cap [X_R, L] \\ T(X,t) = -\mu_-(X - L) & \text{if } X \in I_R \end{cases} \tag{6.65}$$

As in the previous case, the inequalities are strict in the interior of $I_0(t)$, whereas the equality holds on the boundary of $I_0(t)$. In the limit case $I_0(t) = \{X_R\}$, the tension reaches everywhere its maximum admissible value

$$T_{\max}(X) = \begin{cases} \mu_+ X & \text{if } 0 \le X \le X_R \\ -\mu_-(X - L) & \text{if } X_R \le X \le L \end{cases} \tag{6.66}$$

and the whole crawler is contracting around the only stationary point X_R. The crawler will keep this tension configuration, i.e. $T(X,t) = T_{\max}(X)$, as long as $\dot{\varepsilon}_{\mathrm{o}}(t) < 0$, contracting accordingly.

As in the case of friction only at the ends, we will show that the motion is characterized by a preliminary transient phase for $t \in [0, \tau]$, followed by a 2τ-periodic behaviour for $t > \tau$, with a constant forward displacement of the crawler in each period.

Interval $0 \le t < t_c^*$. We recall the initial conditions, namely $u(X, 0) = 0$ and $T(X, 0) = 0$. For (6.62), at the beginning of the time interval the crawler is stationary, i.e. $I_0(0) = [0, L]$, and so at every point X the tension decreases according to (6.51), until it reaches the critical value of $T_{\min}(X)$, such that point X starts to move, see Fig. 6.6a. Explicitly, we have that

$$T(X,t) = \begin{cases} -\mu_- X & \text{if } 0 \le X < c_1 t \quad \text{i.e., if } X \in I_L(t) \\ -K\alpha t & \text{if } c_1 t \le X \le L - c_2 t \quad \text{i.e., if } X \in I_0(t) \\ \mu_+(X - L) & \text{if } L - c_2 t < X \le L \quad \text{i.e., if } X \in I_R(t) \end{cases} \tag{6.67}$$

where the two velocities c_1 and c_2 have been introduced as

$$c_1 = \frac{K\alpha}{\mu_-}, \quad c_2 = \frac{K\alpha}{\mu_+} \tag{6.68}$$

At the end of the time interval, we have $T(X, t_c^*) = T_{\min}(X)$. We also notice that during the whole interval $X_L \in I_0(t)$, that means that $\dot{u}_L \equiv 0$ and so

$$u_L(t_c^*) = 0 \tag{6.69}$$

Hence, by using equations (6.54) and (6.56), we obtain the expressions for the displacement of the crawler extremities at time t_c^*

$$\begin{cases} u_1(t_c^*) = -\alpha t_c^* X_L + \dfrac{\mu_-}{2K} X_L^2 \\[2mm] u_2(t_c^*) = \alpha t_c^* X_R - \dfrac{\mu_+}{2K} X_R^2 \end{cases} \tag{6.70}$$

and of point X_R, namely

$$u_R(t_c^*) = \alpha t_c^* (X_R - X_L) - \frac{\mu_+}{2K}(X_R^2 - X_L^2) \tag{6.71}$$

Interval $t_c^* \leq t < \tau$. At time $t = t_c^*$, the tension has reached its minimum value (6.63) everywhere along the crawler, and we still have $\dot{\varepsilon}_o(t) > 0$ until the end of the interval, so, as we have anticipated, the tension remains constant, i.e. $T(X,t) = T_{\min}(X)$, and the crawler elongates until $t = \tau$. Moreover, the point X_L stands still and so

$$u_L(\tau) = u_L(t_c^*) = 0 \tag{6.72}$$

Since the tension is known, see Fig. 6.6b, we can find the displacement of other points at time $t = \tau$ by comparison with $u_L(\tau)$ and using the condition (6.56). In this way, we immediately get the displacements of the extremities, namely

$$\begin{cases} u_1(\tau) = -\varepsilon_o^{\max} X_L + \dfrac{\mu_-}{2K} X_L^2 \\[2mm] u_2(\tau) = \varepsilon_o^{\max} X_R - \dfrac{\mu_+}{2K} X_R^2 \end{cases} \tag{6.73}$$

and also of point X_R

$$u_R(\tau) = \varepsilon_o^{\max}(X_R - X_L) - \frac{\mu_+}{2K}(X_R^2 - X_L^2) \tag{6.74}$$

Interval $\tau \leq t < \tau + t_c$. During this time interval the crawler is subject to a negative incremental distortion, i.e. $\dot{\varepsilon}_o(t) < 0$, so we are in the case (6.65). At the beginning of the interval the crawler is stationary, and so the tension at each point X increases according to (6.51), until it reaches the maximum admissible value of $T_{\max}(X)$, such that point X begins to move, see Fig. 6.6c. Explicitly, we have now that

$$T(X,t) = \begin{cases} \mu_+ X & \text{if } 0 \leq X < c_3(t - \tau) \\ K\alpha(t - \tau) - \mu_- X & \text{if } c_3(t - \tau) \leq X \leq X_L \\ K\alpha(t - \tau) + \mu_+(X - L) & \text{if } X_L \leq X \leq L - c_3(t - \tau) \\ -\mu_-(X - L) & \text{if } L - c_3(t - \tau) < X \leq L \end{cases} \tag{6.75}$$

where the first and the last interval correspond respectively to $I_L(t)$ and $I_R(t)$, whereas the union of the other two is $I_0(t)$, and c_3 has been introduced as

$$c_3 = \frac{K\alpha}{\mu_- + \mu_+} \tag{6.76}$$

At the end of the time interval we have $T(X, \tau + t_c) = T_{\max}(X)$. Furthermore, we remark that during the whole interval we also have $[X_L, X_R] \subseteq I_0(T)$, since all the points of this subinterval reach the critical tension $T_{\max}(X)$ simultaneously at $t = \tau + t_c$. It follows that X_L and X_R are stationary $(\dot{u}_L \equiv \dot{u}_R \equiv 0)$ and thus

$$u_L(\tau + t_c) = u_L(\tau) \qquad u_R(\tau + t_c) = u_R(\tau) \tag{6.77}$$

It turns out that the displacements of the two end points can be obtained from $u_L(\tau + t_c)$ and $u_R(\tau + t_c)$ by using (6.56), namely

$$\begin{cases} u_1(\tau + t_c) = -(\varepsilon_o^{\max} - \alpha t_c)X_L - \dfrac{\mu_+}{2K}X_L^2 \\[2mm] u_2(\tau + t_c) = u_R(\tau + t_c) + (\varepsilon_o^{\max} - \alpha t_c)X_L + \dfrac{\mu_-}{2K}X_L^2 \end{cases} \tag{6.78}$$

Interval $\tau + t_c \leq t < 2\tau$. At time $t = \tau + t_c$, the tension has reached its maximum value (6.66) everywhere along the crawler, and we still have $\dot{\varepsilon}_o(t) < 0$ until the end of the interval, so the tension remains constant, i.e. $T(X,t) = T_{\max}(X)$, and the crawler contracts until time $t = 2\tau$. Furthermore, point X_R stands still and so we immediately get

$$u_R(2\tau) = u_R(\tau + t_c^*) = \varepsilon_o^{\max}(X_R - X_L) - \frac{\mu_+}{2K}(X_R^2 - X_L^2) \tag{6.79}$$

Since the tension is known, see Fig. 6.6d, we can find the displacement of other points at $t = 2\tau$ by comparison with $u_R(2\tau)$ and using (6.56). In fact, the displacements of the extremities read

$$\begin{cases} u_1(2\tau) = u_R(2\tau) - \dfrac{\mu_+}{2K}X_R^2 \\[2mm] u_2(2\tau) = u_R(2\tau) + \dfrac{\mu_-}{2K}X_L^2 \end{cases} \tag{6.80}$$

whereas for point X_L we get

$$u_L(2\tau) = u_R(2\tau) - \frac{\mu_+}{2K}(X_R^2 - X_L^2) = \varepsilon_o^{\max}(X_R - X_L) - \frac{\mu_+}{K}(X_R^2 - X_L^2) \tag{6.81}$$

Interval $2\tau \leq t < 2\tau + t_c$. During this time interval, the crawler is again subject to a incremental positive distortion, i.e. $\dot{\varepsilon}_o(t) > 0$, and so we are in the case (6.62). The crawler is stationary at the beginning of the interval, and consequently the tension at each point X decreases according to (6.51),

until it reaches the minimum admissible value $T_{\min}(X)$, such that point X begins to move, see Fig. 6.6e. Explicitly, we have that

$$
T(X,t) = \begin{cases}
-\mu_- X & \text{if } 0 \leq X < c_3(t - 2\tau) \\
-K\alpha(t - 2\tau) + \mu_+ X & \text{if } c_3(t - 2\tau) \leq X \leq X_R \\
-K\alpha(t - 2\tau) - \mu_-(X - L) & \text{if } X_R \leq X \leq L - c_3(t - 2\tau) \\
\mu_+(X - L) & \text{if } L - c_3(t - 2\tau) < X \leq L
\end{cases}
$$

where the first and the last interval correspond to $I_L(t)$ and $I_R(t)$, respectively.

At the end of this time interval we have $T(X, 2\tau + t_c) = T_{\min}(X)$. We further underline that during the whole time interval we have $[X_L, X_R] \subseteq I_0(T)$. Specifically, points X_L and X_R are stationary during this interval ($\dot{u}_L \equiv \dot{u}_R \equiv 0$) and thus

$$
u_L(2\tau + t_c) = u_L(2\tau), \quad u_R(2\tau + t_c) = u_R(2\tau) \tag{6.82}
$$

Again, the displacements of the end points can be conveniently computed by means of (6.56), namely

$$
\begin{cases}
u_1(2\tau + t_c) = u_L(2\tau + t_c) - \alpha t_c X_L + \dfrac{\mu_-}{2K} X_L^2 \\[2mm]
u_2(2\tau + t_c) = u_R(2\tau + t_c) + \alpha t_c X_L - \dfrac{\mu_+}{2K} X_L^2
\end{cases} \tag{6.83}
$$

Interval $2\tau + t_c \leq t < 3\tau$. This time interval is qualitatively similar to the interval $t_c^* \leq t < \tau$, but, since $t_c^* < t_c$, it is shorter. We still have that $\dot{\varepsilon}_o(t) > 0$, and the tension is constant in time and equals its minimum admissible value, i.e. $T(X, t) = T_{\min}(X)$, see Fig. 6.6f. Therefore, the crawler elongates during this interval, with X_L as a single stationary point, such that

$$
u_L(3\tau) = u_L(2\tau + t_c) = \varepsilon_o^{\max}(X_R - X_L) - \frac{\mu_+}{K}(X_R^2 - X_L^2) \tag{6.84}
$$

As for the previous time intervals, the displacements of the extremities can be easily computed by making use of (6.56), namely

$$
\begin{cases}
u_1(3\tau) = u_L(3\tau) - \varepsilon_o^{\max} X_L + \dfrac{\mu_-}{2K} X_L^2 \\[2mm]
u_2(3\tau) = u_L(3\tau) + \varepsilon_o^{\max} X_R - \dfrac{\mu_+}{2K} X_R^2
\end{cases} \tag{6.85}
$$

whereas the displacement of point X_R at time $t = 3\tau$ reads

$$
u_R(3\tau) = u_L(3\tau) + \varepsilon_o^{\max}(X_R - X_L) - \frac{\mu_+}{2K}(X_R^2 - X_L^2) \tag{6.86}
$$

The position of the crawler extremities $x_i(t)$ is depicted in Fig. 6.7 during a time interval of 3τ for the case of $\varepsilon_o^{\max} = 1$ and for a ratio of $\mu_+/\mu_- = 1/5$.

Specifically, two cases are shown to stress the effect on the displacements of the crawler stiffness, and these correspond to $\mu_- L/K = 5/2$ (blue solid curves), and $\mu_- L/K = 0$ (red dashed curves). We notice that the state of the crawler at time $t = 3\tau$ corresponds to that at time $t = \tau$ except for a translation of $u_L(3\tau) - u_L(\tau) = u_L(3\tau)$. Since the dynamic of the crawler is translation-invariant, the behaviour found in the interval $[\tau, 3\tau]$ will repeat 2τ-periodically. Furthermore, the asymptotic displacement produced in a 2τ-cycle can be reformulated as

$$u(X, 3\tau) - u(X, \tau) = \left(\varepsilon_o^{\max} - \frac{\mu_+ L}{K} \right) \frac{\mu_- - \mu_+}{\mu_- + \mu_+} L \qquad (6.87)$$

To understand the meaning of the result above, we first recall that we have required the maximum distortion to satisfy the condition $\varepsilon_o^{\max} > \mu_+ L/K$. In fact, it can be easily shown that, otherwise, no net displacement can be extracted on average from periodic shape changes.

The displacement (6.87) produced in a cycle is actually linear with respect to the body length (and therefore scale invariant) if instead of the distortion ε_o we consider the distortion excess over the critical threshold of $\mu_+ L/K$. The quadratic part of (6.87) is only due to the fact that, keeping constant the other parameters, the distortion needed to produce some net motion linearly increases with the crawler length. Finally, we observe that the length of the crawler oscillates between a minimum value that is reached at times that are even multiples of τ, namely

$$l(2m\tau) = L + \frac{\mu_- \mu_+ L^2}{2K(\mu_- + \mu_+)} \qquad (6.88)$$

and a maximum value that, instead, is reached at times that are odd multiples of τ,

$$l((2m + 1)\tau) = L + \left(\varepsilon_o^{\max} - \frac{\mu_- \mu_+ L}{2K(\mu_- + \mu_+)} \right) L \qquad (6.89)$$

6.5 Final remarks

Compared to the results of the previous chapter, here we consider, similarly, the system as subject to a spatially uniform time-history of distortion, but now we do not assume the shape of the crawler to be known a-priori. Instead, the configuration of the crawler is an *emergent* property which arises from the coupled nonlinear system consisting of the crawler force-generating mechanism, its passive elasticity and the external frictional forces. This approach has allowed us, in particular, to determine the axial forces acting along the body of the crawler: this is a quantity of great mechanical relevance in assessing the propensity of the system towards buckling, when compressions are generated during the locomotion process.

While our analysis has focused mostly on some of the theoretical challenges that our model crawler raises, it already provides clues that may guide practical design. For example, (6.46) implies that no net displacement can be achieved unless the available spontaneous strains are large enough that inequality (6.34) is satisfied. Using order of magnitude estimates for the geometric and material parameters involved, namely, $F_+ = 0.45\,\text{N}$ (as in [ND14]) and $K = 10^2\,\text{N}$ (arising from $K = EA$, with Young modulus $E = 1$ MPa and area $A = 10^{-4}\,\text{m}^2$ for a cross-section of $1 \times 1\,\text{cm}^2$) we obtain that the minimal magnitude of the active strains to produce non-zero displacements is around 1%. In these circumstances, using Euler formula for the buckling of a column, one would estimate that strips can safely locomote without buckling provided that their length L is below 10 cm. Smaller scale cross sections (in particular smaller thicknesses) will presumably require contact interactions with smaller F_+.

Our quasi-static approximation may need to be reconsidered in some applications, where stick-slick phenomena may lead to oscillations, or even in the interest of exploring dynamic effects that may lead to additional locomotion mechanisms. This occurs, for example, in the case liquid drops moving on a vibrated substrate where the complex shape dynamics of the drop may lead to reversal of the direction of motion as the frequency and amplitude of vibration of the substrate are varied [CCD15]. It has been suggested in [CD15] that a similar effect can also occur in bristle-legged-robots locomoting on a rigid substrate when actuated by rotary motors or by a vibrating internal mass.

Having in mind the key example of LCEs as material for our strip, we briefly comment our choice, in expression (6.4) to use a quadratic energy density. This assumption was led by a search for simplicity; more realistic (Ogden-type) expressions to explore the regime of large induced stresses are discussed in [DT09; AD11]. In fact, expression (6.4) for the energy is the 1D, small strain version of the energy proposed by Warner, Terentjev and collaborators [BTW93; VWT96; WT03], and thoroughly discussed by DeSimone and coworkers in a series of papers [DeS99; DD00; DD02; CDD02b; CDD02a; AD12]. The emergence of (6.4) as the small strain limit of the Warner-Terentjev energy has been discussed on the basis of both formal Taylor expansion and Gamma-convergence arguments in [DT09; CD11; AD11].

Evolution equations through an incremental, variational principle

The evolution equations solved in Sections 6.3 and 6.4 can be obtained from an incremental variational principle, as we show below. For the discrete case this approach will be discussed in the next Chapter in a more abstract and general way. Here we propose a direct derivation, that covers also the continuous case.

We consider the history of prescribed states of spontaneous distortions $t \mapsto \varepsilon_{\mathrm{o}}(t)$ given in Section 6.2, and assume that the displacement field $X \mapsto u(X,t)$ is known at time t. We look for the displacement and tension at time $t + dt$ by seeking solutions of the following incremental minimization problem. Find $X \mapsto u(X, t + dt)$ as

$$u(X, t + dt) = \mathrm{argmin}_v \left\{ \mathcal{E}(v, t + dt) + \mathrm{diss}(v, u(\cdot, t)) + \mathrm{Diss}(v, u(\cdot, t)) \right\}$$
(6.90)

where $\mathcal{E}$ is the elastic energy defined in (6.4) and

$$\mathrm{diss}(v, u(\cdot, t)) := \int\limits_0^L \left\{ \mu_+ \left(v(X) - u(X, t) \right)^+ - \mu_- \left(v(X) - u(X, t) \right)^- \right\} \mathrm{d}X$$

whereas

$$\mathrm{Diss}(v, u(\cdot, t)) := F_+ \left(v_1 - u_1(t) \right)^+ - F_- \left(v_1 - u_1(t) \right)^- +$$
$$+ F_+ \left(v_2 - u_2(t) \right)^+ - F_- \left(v_2 - u_2(t) \right)^-$$

Here we have set $v_1 := v(X_1 = 0)$ and $v_2 := (X_2 = L)$. Once $u(X, t + dt)$ is known, we can find $T(X, t + dt)$ using (6.6), namely

$$T(X, t) = K \left(u'(X, t) - \varepsilon_{\mathrm{o}}(X, t) \right)$$

We consider the case of distributed friction first. We check for solutions of the form $u(X, t + dt) = u(X, t) + \dot{u}(X, t)\, dt$ and assume that $X \mapsto \dot{u}(X, t)$ is continuous.

Let us first prove (6.49) for every point $x_0 \in (0, L)$ and for every time t such that $\dot{u}(X, t) \geq 0$ in a neighbourhood $N_{x_0}^+$ of x_0. Using minimality of $u(X, t + dt)$ against $v_\eta(X) := u(X, t) + \dot{u}(X, t)\, dt + \eta \varphi(X)$, with $\eta \geq 0$ an arbitrary non-negative scalar, and $\varphi(X) \geq 0$ an arbitrary non-negative $\mathcal{C}^\infty$ function with compact support in $N_{x_0}^+$, we obtain

$$\mathcal{E}(u(\cdot, t + dt), t + dt) + \mathrm{diss}(u(\cdot, t) + \dot{u}(X, t)\, dt, u(\cdot, t)) \leq$$
$$\leq \mathcal{E}(u(\cdot, t + dt) + \eta \varphi(\cdot), t + dt) + \mathrm{diss}(u(\cdot, t) + \dot{u}(X, t)\, dt + \eta \varphi(\cdot), u(\cdot, t))$$

and, in turn,

$$I_\varphi(\eta) := \mathcal{E}(u(\cdot, t + dt) + \eta \varphi(\cdot), t + dt) - \mathcal{E}(u(\cdot, t + dt)t + dt) + \eta \int\limits_{N_{x_0}^+} \mu_+ \varphi(x)\, \mathrm{d}X \geq 0$$

for every $\eta \geq 0$ and $\varphi \geq 0$. Moreover, $I_\varphi(0) = 0$ for every φ. It follows that

$$\frac{\mathrm{d}}{\mathrm{d}\eta} I_\varphi(\eta)|_{\eta = 0^+} = \int\limits_{N_{x_0}^+} [-K(u' - \varepsilon_{\mathrm{o}})' + \mu_+] \varphi\, \mathrm{d}X \geq 0 \qquad (6.91)$$

for every φ, and since we can take an arbitrarily small neighbourhood $N_{x_0}^+$, we obtain that, for every $x_0 \in (0, L)$ with $\dot{u}(X, t) \geq 0$ in a neighbourhood $N_{x_0}^+$,

$$-T'(x_0, t + \mathrm{d}t) + \mu_+ \geq 0 \tag{6.92}$$

If, in particular, $\dot{u}(x_0, t) > 0$, then there exists a neighbourhood $N_{x_0}^+$ where $\dot{u}(X, t) > 0$ and we can take η of unrestricted sign in the argument above. This leads to strict equality to zero in (6.91) and hence

$$-T'(x_0, t + \mathrm{d}t) + \mu_+ = 0 \quad \text{at any } x_0 \in (0, L) \text{ with } \dot{u}(x_0, t) > 0 \tag{6.93}$$

Similar arguments at a point $x_0 \in (0, L)$ such that either $\dot{u}(x_0, t) \leq 0$, or $\dot{u}(x_0, t) < 0$, show that, for every $x_0 \in (0, L)$ with $\dot{u}(X, t) \leq 0$ in a neighbourhood $N_{x_0}^-$,

$$-T'(x_0, t + \mathrm{d}t) - \mu_- \leq 0 \tag{6.94}$$

and that

$$-T'(x_0, t + \mathrm{d}t) - \mu_- = 0 \quad \text{at any } x_0 \in (0, L) \text{ with } \dot{u}(x_0, t) < 0 \tag{6.95}$$

We exclude from our analysis the points where $\dot{u}$ changes sign. Since $\dot{u}$ is continuous, those point are at most countably many and thus negligible. Hence, putting (6.92)-(6.95) together, and using (6.12), we obtain (6.15), namely,

$$T'(X, t) \in \frac{\partial}{\partial v} d\left(\dot{u}(X, t)\right) \tag{6.96}$$

Now we derive the boundary conditions (6.52). Given our solution $u(X, t + \mathrm{d}t) = u(X, t) + \dot{u}(X, t)\,\mathrm{d}t$, we define $N^+ = \{X \in [0, L] \colon \dot{u}(X, t) > 0\}$ and $N^- = \{X \in [0, L] \colon \dot{u}(X, t) < 0\}$. Let $\varphi(X) \geq 0$ be a non-negative $\mathcal{C}^\infty$ function on $[0, L]$ such that $\varphi(L) > 0$ and $\varphi(0) = 0$. For every η we set

$$\mathcal{A}(\eta) = \begin{cases} \{X \in N^+ \colon \dot{u}(X, t)\,\mathrm{d}t + \eta\varphi(X) < 0\} & \text{if } \eta < 0 \\ \emptyset & \text{if } \eta = 0 \\ \{X \in N^- \colon \dot{u}(X, t)\,\mathrm{d}t + \eta\varphi(X) > 0\} & \text{if } \eta > 0 \end{cases}$$

We have that $|\mathcal{A}(\eta)| \to 0$ for $\eta \to 0$. We repeat the minimality argument used previously and obtain

$$I_\varphi(\eta) := \mathcal{E}(u(\cdot, t + \mathrm{d}t) + \eta\varphi(\cdot), t + \mathrm{d}t) - \mathcal{E}(u(\cdot, t + \mathrm{d}t)t + \mathrm{d}t) +$$

$$+ \eta \int_{N_L^+} \mu_+\varphi(x)\,\mathrm{d}X + \eta \int_{N_L^-} \mu_-\varphi(x)\,\mathrm{d}X + \mathcal{R}(\eta) \geq 0$$

where

$$\mathcal{R}(\eta) = \int_{\mathcal{A}(\eta)} (\mu_- + \mu_+)\,|\dot{u}(X, t)\,\mathrm{d}t + \eta\varphi(X)|\,\mathrm{d}X$$

We observe that

$$|\mathcal{R}(\eta)| \le |\eta| \, |\mathcal{A}(\eta)| \left| (\mu_- + \mu_+) \max_{X \in [0,L]} \varphi(X) \right|$$

from which it follows that

$$\frac{\mathrm{d}}{\mathrm{d}\eta} \mathcal{R}(\eta)|_{\eta=0} = 0$$

From this condition and the minimality of $I_\varphi(0)$ we obtain

$$0 = \frac{\mathrm{d}}{\mathrm{d}\eta} I_\varphi(\eta)|_{\eta=0} = \int_{N_L^+} [-T(X, t + \mathrm{d}t) + \mu_+]\varphi(x)\,\mathrm{d}X +$$

$$+ \int_{N_L^-} [-T(X, t + \mathrm{d}t) - \mu_-]\varphi(x)\,\mathrm{d}X + T(L)\varphi(L) - T(0)\varphi(0)$$

The two integrals are both equal to zero because the integrands vanish in view of (6.93) and (6.95). Since $\varphi(L) = 0$ and $\varphi(0) > 0$, we get $T(0) = 0$. To obtain the second boundary condition $T(L) = 0$ it suffices to consider instead test functions $\varphi(X) \ge 0$ such that $\varphi(L) > 0$ and $\varphi(0) = 0$.

We now consider the case of friction concentrated at the two ends. Since $d \equiv 0$ implies that $T(X, t)$ is now independent of X and, since ε_{o} is spatially uniform, the function $X \mapsto u(X, t)$ is affine and the incremental minimization problem (6.90) can be reduced to

$$\mathbf{u}(t + \mathrm{d}t) = \mathrm{argmin}_{\mathbf{v}} \left\{ \mathcal{E}_r(\mathbf{v}, t + \mathrm{d}t) + \mathrm{Diss}(\mathbf{v}, \mathbf{u}(t)) \right\} \qquad (6.97)$$

where $\mathbf{u}(t) := (u_1(t), u_2(t))$ and $\mathbf{v}(t) := (v_1(t), v_2(t))$, whereas

$$\mathcal{E}_r(\mathbf{v}, t) := \frac{1}{2} KL \left(\frac{v_2 - v_1}{L} - \varepsilon_{\mathrm{o}}(t) \right)^2 \qquad (6.98)$$

and

$$\mathrm{Diss}(\mathbf{v}, \mathbf{u}(t)) = F_+ \left(v_1 - u_1(t) \right)^+ - F_- \left(v_1 - u_1(t) \right)^- +$$
$$+ F_+ \left(v_2 - u_2(t) \right)^+ - F_- \left(v_2 - u_2(t) \right)^-$$

Following similar arguments to those used above for the case of distributed friction, we obtain (6.22), namely,

$$\begin{cases} T(0, t) = -\dfrac{\partial}{\partial u_1} \mathcal{E}_r(\mathbf{u}(t), t) \in \dfrac{\partial}{\partial u_1} \mathcal{D}\left(\dot{u}_1(t)\right) \\[3mm] -T(L, t) = -\dfrac{\partial}{\partial u_2} \mathcal{E}_r(\mathbf{u}(t), t) \in \dfrac{\partial}{\partial \dot{u}_2} \mathcal{D}\left(\dot{u}_2(t)\right) \end{cases} \qquad (6.99)$$

We remark in conclusion that the general case in which both distributed and concentrated frictional forces are present can be obtained by combining equations (6.96) and (6.99).
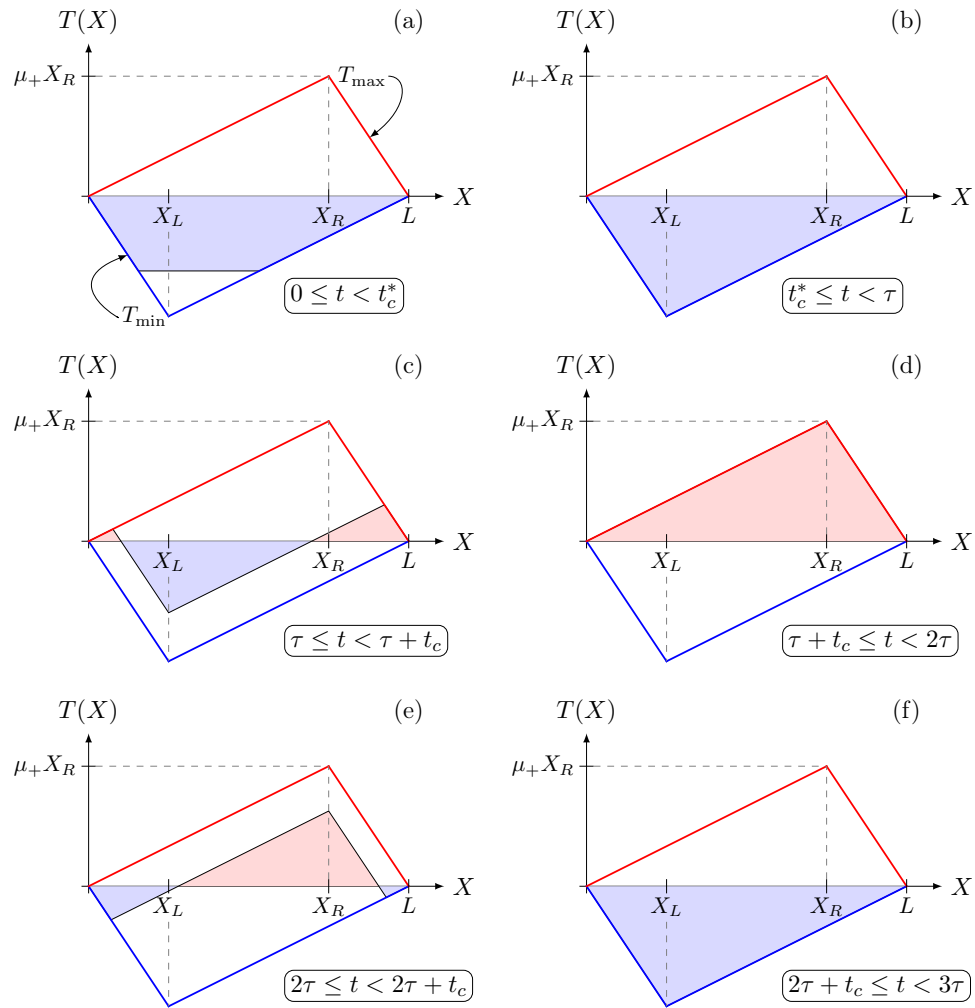
Figure 6.6: Tension $T(X)$ along the crawler body during distinct time intervals for the case of distributed, directional friction. Notice that the tension stays always bounded and oscillates between the maximum and the minimum admissible values of $T_{\max}$ and $T_{\min}$, respectively.
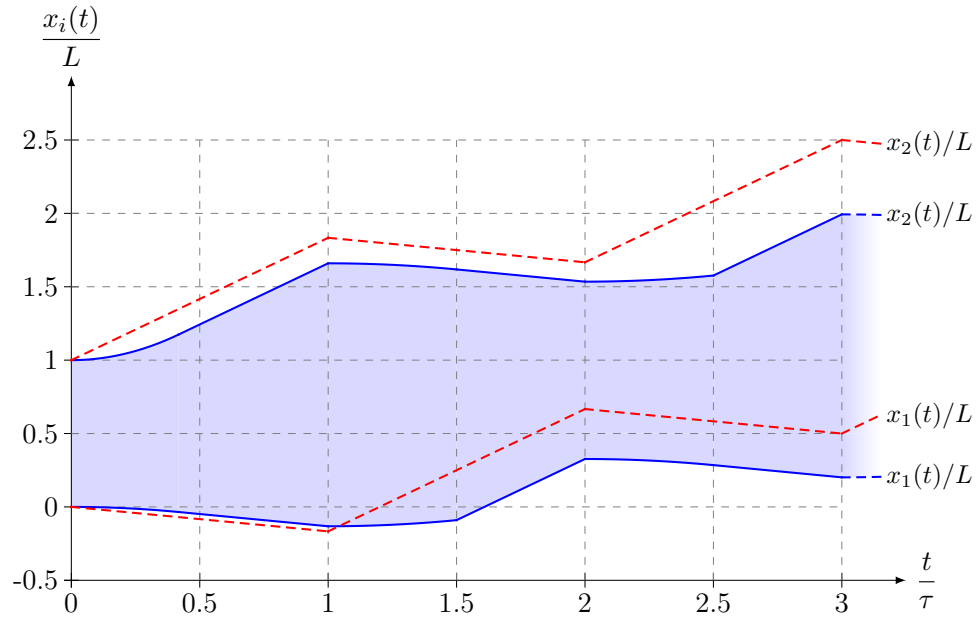
Figure 6.7: Position of the crawler extremities $x_i(t)$ during a time interval of 3τ for a maximum distortion $\varepsilon_\text{o}^\text{max} = 1$ and for a ratio of $\mu_+/\mu_- = 1/5$. Two cases are shown to stress the effect on the displacements of the crawler stiffness, and these correspond to $\mu_- L/K = 5/2$ (blue solid curves), and $\mu_- L/K = 0$ (red dashed curves). Notice that for the case of distributed friction, a significant back-sliding of x_1 takes place irrespective of the crawler stiffness K. At any time, the current length $l(t)$ of the crawler body (highlighted in the figure for the case of $\mu_- L/K = 5/2$) can be inferred from the vertical distance between the two curves.

Chapter 7

Stasis domains and slip surfaces

In this Chapter (cf. [GD16b]) we develop the derivation of the equation
of motion proposed at the conclusion of Chapter 6 in the more abstract
and general framework of rate-independent systems. Then, we illustrate
the situation by analysing in detail the motility of a crawler consisting of
two active elastic segments, resting on three supports providing directional
frictional interactions. Such a model is the natural extension of the discrete
model discussed in the previous Chapter, and, compared to that case, we
find that, for a suitable range of the friction parameters, specific choices of
the actuation strategy can lead to net displacements also in the direction of
higher friction.

Moreover, we show that the behaviour of the system is governed by
the tensions arising in the elastic segments, and that the resulting laws of
motion are entirely analogous to the flow rules typical of elasto-plasticity. In
particular, there are convex domains in the plane of the internal tensions
(*stasis domains*, the analog of elastic domains) corresponding to which no
sliding of the supports can take place. Only when the tensions reach the
boundaries of these domains (*slip surfaces*, the analog of yield surfaces),
sliding of the supports, and hence motion of the segments can occur.

7.1   An abstract approach to crawling

We consider the quasi-static evolution of a mechanical systems, i.e. our crawler,
characterized as follows. The position of the body of crawler at each time is
described by a vector $x = x(t) \in X$, where X is a n-dimensional real vector
space, that means $X \cong \mathbb{R}^n$. We assume that the space X is the product of
two subspaces $X \cong Y \times Z$, so that we can identify each vector x with the
couple (y, z), where $y \in Y \cong \mathbb{R}^d$ and $z \in Z \cong \mathbb{R}^{n-d}$, with $d \in \{1, 2, \ldots, n\}$.
We denote with $\pi_Y \colon X \to Y$ and $\pi_Z \colon X \to Z$ the projections of a vector
$x \in X$ on Y and Z.

This decomposition has to be interpreted as follows. The value d is the

dimension of the space where the crawler moves, so $d = 1$ if it moves along a line, $d = 2$ if it moves on a surfaces, etc. The vector $y \in Y \cong \mathbb{R}^d$ is associated to a generic description of the position of the crawler, e.g. the position of its head or of its center of mass. The vector $z \in Z$ instead describes the shape of the crawler. In this way, it is evident how the absolute position x of the different parts of the body of the crawler is equivalently described by the absolute position y of a specific point, together with the relative positions z, with respect to that point, of the other parts of the crawler.

Since we are assuming the quasi-static approximation, the evolution of the system is governed by the balance of the forces acting on the systems, that can be grouped in two families: configurational or Eshelby-like forces, and frictional forces.

In our models the configurational energy $\mathcal{E}$ is invariant for translations of the crawler, meaning that it depends only on the shape z and on a time-dependent load exerted by the crawler itself. We assume that the energy takes the form

$$\mathcal{E}(t, x) = \langle \mathbb{A}x, x \rangle - \langle x, \ell(t) \rangle \tag{7.1}$$

where $\mathbb{A} \colon X \to X$ is symmetric positive-semidefinite, with $\ker \mathbb{A} = Y$, while $\ell(t) \colon [0, T] \to Z$ is continuously differentiable.[1]

Moreover, we can define a symmetric linear positive definite operator $A \colon Z \to Z$ such that $A = \mathbb{A}|_Z$.

We assume a rate-indepent dissipation, that in our case can be view as considering Coulomb dry friction, so that the forces are described by a dissipation potential $\mathcal{D} \colon \mathbb{R}^n \to \mathbb{R}$, that we assume convex (and so continuous), coercive and positively homogeneous of degree 1.

Thus the evolution of the system is described by the force balance

$$0 \in \partial \mathcal{D}(\dot{x}(t)) + D_x \mathcal{E}(t, x) \tag{7.2}$$

where D_x denotes the gradient with respect to the x variables, while $\partial \mathcal{D}$ is the subdifferential of $\mathcal{D}$. We say that a function $x \colon [0, T] \to X$, differentiable for almost all $t \in (0, T)$, is a *solution* of the problem (7.2) with starting point x_0 if $x(0) = x_0$ and $x(t)$ satisfies (7.2) for almost all $t \in (0, T)$.

Since $\mathcal{D}$ is positively homogeneous of degree 1, we have that $\partial \mathcal{D}(\xi) \subseteq \partial \mathcal{D}(0)$, where $\partial \mathcal{D}(0)$ is convex and compact, by the convexity and coercivity of $\mathcal{D}$.[2] We immediately see that

$$-D_x \mathcal{E}(t, x) \in \partial \mathcal{D}(\dot{x}(t)) \subseteq \partial \mathcal{D}(0)$$

---

[1] Actually, as we will show in Section 7.3, it is possible to extend the same argument to continuous, piecewise continuously differentiable functions ℓ.

[2] We remark that, strictly speaking, the subdifferential consists of elements of the dual space $(\mathbb{R}^n)^*$, but since we are working with finite dimensional spaces we implicitly adopt the usual identification of the elements of the dual with vectors of the space.

and in particular that the initial point x_0 must satisfy

$$-D_x\mathcal{E}(0, x_0) \in \subseteq \partial\mathcal{D}(0) \tag{7.3}$$

We will call such initial points x_0 *admissible* for the problem.

The evolution of systems of this form, frequently referred as *rate-independent systems*, is a very well studied problem (see [MT04; Mie15]). Indeed, it is known that the differential inclusion (7.2) admits always at least a solution for every admissible initial point. However nothing can be said about its uniqueness: indeed, as we show below, a additional "symmetry breaking" condition is required to assure that exists only one solution, whereas counterexamples with multiple solution can be constructed in the other cases.

Let us proceed by casting system (7.2), in the form of a variational inequality, a classical way to write rate-independent systems

For a given external load $\ell(t)$, the evolution $z(t), y(t)$ of our system is obtained as a solution of the variational inequality

$$\langle Az(t) - \ell(t), w - \dot{z}(t)\rangle + \mathcal{D}(w, v) - \mathcal{D}(\dot{z}(t), \dot{y}(t)) \geq 0 \tag{VI}$$

for every $(w, v) \in \mathbb{R}^{n-d} \times \mathbb{R}^d$, where we write $\mathcal{D}(w, v)$ meaning $\mathcal{D}((w, v))$. In particular this must hold for $w = \dot{z}(t)$, for which we get

$$\mathcal{D}(\dot{z}(t), v) - \mathcal{D}(\dot{z}(t), \dot{y}(t)) \geq 0 \qquad \text{for every } v \in \mathbb{R}^d \tag{7.4}$$

We now make state our *symmetry breaking* assumption.

(SB) *For every $w \in \mathbb{R}^{n-d}$ there exists a unique $v_{\min} = v_{\min}(w) \in \mathbb{R}^d$ such that*
$$\mathcal{D}(w, v) - \mathcal{D}(w, v_{\min}) \geq 0 \qquad \text{for every } v \in \mathbb{R}^d$$

We notice that, if (SB) holds, then the displacement $\dot{y}(t)$ can be recovered as a function of the shape change $\dot{z}(t)$, namely

$$\dot{y}(t) = v_{\min}(\dot{z}(t)) \tag{7.5}$$

We also remark that $v_{\min}$ is positively homogeneous of degree 1.

We can use the notion of $v_{\min}$ to reduce the dimension of the problem associated to the variational inequality (VI), leading to

$$\langle Az(t) - \ell(t), w - \dot{z}(t)\rangle + \mathcal{D}_{\mathrm{sh}}(w) - \mathcal{D}_{\mathrm{sh}}(\dot{z}(t)) \geq 0 \quad \text{for every } w \in \mathbb{R}^{n-d} \tag{RVI}$$

where $\mathcal{D}_{\mathrm{sh}}$ is the "shape-restricted" dissipation, i.e. the dissipation after minimization with respect to translations of the crawler,

$$\mathcal{D}_{\mathrm{sh}}(w) = \mathcal{D}(w, v_{\min}(w)) \tag{7.6}$$

This allows us to study the system for the shape changes alone and then recover the displacement $y(t)$ of the crawler through the relationship (7.5).

Before discussing existence and uniqueness of the solutions for our problem, let us notice that $\mathcal{D}_{\text{sh}}$ is convex (and therefore continuous) and positively homogeneous of degree 1. To show this, we recall that $w \mapsto v_{\min}(w)$ is positively homogeneous of degree 1. Hence, for $\lambda > 0$

$$\mathcal{D}_{\text{sh}}(\lambda w) = \mathcal{D}(\lambda w, v_{\min}(\lambda w)) = \mathcal{D}(\lambda w, \lambda v_{\min}(w)) = \lambda \mathcal{D}(w, v_{\min}(w)) = \lambda \mathcal{D}_{\text{sh}}(w)$$

Regarding the convexity of $\mathcal{D}_{\text{sh}}$, we observe that for every $0 \leq \lambda \leq 1$, writing $w_\lambda = \lambda w + (1 - \lambda \bar{w})$, we have

$$\begin{aligned}
\lambda \mathcal{D}_{\text{sh}}(w) + (1 - \lambda)\mathcal{D}_{\text{sh}}(\bar{w}) &\geq \lambda \mathcal{D}(w, v_{\min}(w)) + (1 - \lambda)\mathcal{D}(\bar{w}, v_{\min}(\bar{w})) \\
&\geq \mathcal{D}(w_\lambda, \lambda v_{\min}(w) + (1 - \lambda)v_{\min}(\bar{w})) \\
&\geq \mathcal{D}(w_\lambda, v_{\min}(w_\lambda)) = \mathcal{D}_{\text{sh}}(w_\lambda)
\end{aligned} \tag{7.7}$$

Let us recall that the subdifferential of $\mathcal{D}_{\text{sh}}$ in $\bar{w}$ is defined as

$$\partial \mathcal{D}_{\text{sh}}(\bar{w}) = \{\xi \in \mathbb{R}^2 \colon \mathcal{D}_{\text{sh}}(w) \geq \mathcal{D}_{\text{sh}}(\bar{w}) + \langle \xi, w - \bar{w} \rangle \text{ for every } w \in \mathbb{R}^{n-d}\}$$

Setting $C^* = \partial \mathcal{D}_{\text{sh}}(0)$, we observe that C^* is convex and satisfies

$$\mathcal{D}_{\text{sh}}(w) = \max_{\xi \in C^*} \langle \xi, w \rangle \tag{7.8}$$

The reduced variational inequality (RVI) can be restated in the *subdifferential formulation* of the problem, namely

$$0 \in \partial \mathcal{D}_{\text{sh}}(\dot{z}(t)) + D_z \mathcal{E}(t, z(t)) \tag{SF}$$

where, since the energy $\mathcal{E}$ depends only on the shape z and not on the displacement y, by a slight abuse of notation we write $\mathcal{E}(t, z)$ with the obvious meaning. Also for the reduced problem, we can identify the admissibility condition for the initial point, namely

$$-D_z \mathcal{E}(0, z_0) \in C^* \tag{7.9}$$

We notice that this condition is actually equivalent to (7.3). We observe that, decomposing (7.3) in the shape and displacement components, the displacement part does not depend on the data and sets the constraint $-D_y \mathcal{E} = 0$, but the intersection of $\partial \mathcal{D}$ with the subspace $\{y = 0\}$ corresponds exactly to C^*.

Compared with the starting problem (7.2), the shape-restricted problem (SF) has strongly convex energy, and so we can apply the following result, providing also uniqueness (cf. [Mie05, Theorem 2.1]).

Theorem 7.1. *Given $\ell \in \mathcal{C}^1([0, \mathcal{T}], \mathbb{R}^{n-d})$ and $z_0 \in A^{-1}(\ell(0) - C^*)$, there exists a unique function $z \in \mathcal{C}^{\text{Lip}}([0, \mathcal{T}], \mathbb{R}^2)$, with $z(0) = z_0$ and such that the shape-restricted variational inequality* (RVI) *is satisfied for almost all $t \in [0, \mathcal{T}]$.*

We remark that once again that the symmetry breaking assumption (SB), allowing the dimensional reduction, is actually necessary to attain uniqueness, as shown below by Remark 7.2.
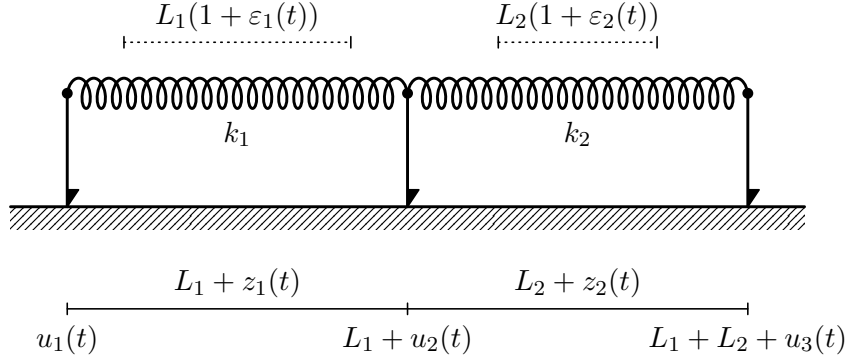
Figure 7.1: The model of our crawler. The dotted lines represent the rest lengths of the two springs.

7.2 Motility of a two-segment crawler

The crawler: formulation of the problem

We now see how the framework presented in the previous section applies to a model of crawler, such as that represented in Figure 7.1. The crawler is composed of two adjacent rods, identified in the reference configuration by the segments $[X_1, X_2]$ and $[X_2, X_3]$. We assume $X_1 = 0$, $X_2 = L_1$ and $X_2 = L_1 + L_2$, so that L_1 and L_2 are the reference lengths of the two rods. A point X of the crawler is mapped to the point $x = \chi(X, t)$ in the deformed configuration and thus its displacement is $u(X, t) = \chi(X, t) - X$. It is useful to set $u_1(t) = u(X_1, t)$, $u_2(t) = u(X_2, t)$ and $u_3(t) = u(X_3, t)$.

We denote the derivatives with respect to space and time with a prime and a dot, respectively,

$$u'(X,t) = \frac{\partial}{\partial X} u(X,t) \qquad \dot{u}(X,t) = \frac{\partial}{\partial t} u(X,t) \qquad (7.10)$$

The crawler interacts with the substrate only through three rigid legs located at X_1, X_2 and X_3. These interactions are described by the (directional) friction law

$$F_i(t) = F(X_i, t) \in \begin{cases} \{F_-\} & \text{if } \dot{u}_i(t) < 0 \\ [-F_+, F_-] & \text{if } \dot{u}_i(t) = 0 \\ \{-F_+\} & \text{if } \dot{u}_i(t) > 0 \end{cases} \qquad (7.11)$$

where $i = 1, 2, 3$. We assume that

$$F_- > F_+ > 0 \qquad (7.12)$$

This means that the absolute value of the friction force is not constant and depends on the direction of motion; moreover the coordinates are chosen so that negative velocities generate greater friction.

The two rods are assumed to be elastic, with stiffnesses k_1, k_2, and subject to an active distortion $\varepsilon_0(X, t)$. We assume that the distortion is uniform along each rod so that

$$\varepsilon_0(X, t) = \begin{cases} \varepsilon_1(t) & \text{if } X \in (0, L_1) \\ \varepsilon_2(t) & \text{if } X \in (L_1, L_1 + L_2) \end{cases} \tag{7.13}$$

The rest length of the two rods is thus $(1 + \varepsilon_1(t))L_1$ and $(1 + \varepsilon_2(t))L_2$, respectively.

Internal energy and dissipation

We describe the state of the crawler with two parameters $z = (z_1, z_2)^t$ associated with its shape and a parameter y that identifies its position. More precisely, we set

$$z_1(t) = u_2(t) - u_1(t) \qquad z_2(t) = u_3(t) - u_2(t) \qquad y(t) = u_2(t) \tag{7.14}$$

The stored energy of the crawler is given by

$$\mathcal{E} = \frac{k_1}{2} \int_0^{L_1} (u'(X, t) - \varepsilon_1)^2 \, \mathrm{d}X + \frac{k_2}{2} \int_{L_1}^{L_1 + L_2} (u'(X, t) - \varepsilon_2)^2 \, \mathrm{d}X$$

$$= \frac{k_1 L_1}{2} \left[\frac{u_2(t) - u_1(t)}{L_1} - \varepsilon_1(t) \right]^2 + \frac{k_2 L_2}{2} \left[\frac{u_3(t) - u_2(t)}{L_2} - \varepsilon_2(t) \right]^2$$

$$= \frac{1}{2} \langle Az(t), z(t) \rangle - \langle \ell(t), z(t) \rangle + c(t) \tag{7.15}$$

where we have used the fact that minimal energy leads to $X \mapsto u'(x, t)$ constant along each of the two rods, and we have set

$$A = \begin{pmatrix} \frac{k_1}{L_1} & 0 \\ 0 & \frac{k_2}{L_2} \end{pmatrix} \qquad\qquad \ell(t) = \begin{pmatrix} k_1 \varepsilon_1(t) \\ k_2 \varepsilon_2(t) \end{pmatrix}$$

$$c(t) = \frac{k_1 L_1 \varepsilon_1(t)^2}{2} + \frac{k_2 L_2 \varepsilon_2(t)^2}{2}$$

We thus see that, for a prescribed active distortion $\varepsilon(t)$, the internal energy of the crawler depends only on time and on the shape $z(t)$, allowing us to write from now on $\mathcal{E} = \mathcal{E}(t, z(t))$.

The dissipation produced by the displacement $u_i \mapsto u_i + v_i$ of a single contact point is

$$d(v_i) = v_i^+ F_+ - v_i^- F_- \tag{7.16}$$

where

$$v_i^+ = \begin{cases} v_i & \text{if } v_i \geq 0 \\ 0 & \text{if } v_i < 0 \end{cases} \qquad \text{and} \qquad v_i^- = \begin{cases} v_i & \text{if } v_i \leq 0 \\ 0 & \text{if } v_i > 0 \end{cases} \tag{7.17}$$

and therefore the dissipation produced by a shape change $z \mapsto z + w$ and a position change $y \mapsto y + v$ is

$$\mathcal{D}(w, v) = d(v - w_1) + d(v) + d(v + w_2) \tag{7.18}$$

We observe that $\mathcal{D}$ is convex and positively homogeneous of degree 1.

We now want to indentify when the symmetry break condition (SB) is satisfied. First of all we observe that $\mathcal{D}(\bar{w}, \cdot)$ is differentiable everywhere except on the finite set $\{\bar{w}_1, 0, -\bar{w}_2\}$. A straightforward computation shows that (SB) is equivalent to assume

$$F_- \neq 2F_+ \qquad\qquad F_- \neq F_+ \qquad\qquad 2F_- \neq F_+ \tag{7.19}$$

Indeed, such conditions ensure that

$$\frac{\partial \mathcal{D}(\bar{w}, v)}{\partial v} \neq 0 \qquad \text{for every } \bar{w} \in \mathbb{R}^2 \text{ and every } v \in \mathbb{R} \setminus \{\bar{w}_1, 0, -\bar{w}_2\} \tag{7.20}$$

that, for the convexity of $\mathcal{D}(\bar{w}, \cdot)$ implies the existence of a unique minimum attained at $v = v_{\min}(\bar{w}) \in \{\bar{w}_1, 0, -\bar{w}_2\}$. We remark that, assuming (7.12), we already excluded the last two conditions in (7.19), so it remains only $F_- \neq 2F_+$, that from now on will be assumed true. With simple considerations on the sign of the derivative we can determine the exact value of $v_{\min}$. Precisely

$$v_{\min}(\bar{w}) = \begin{cases} \max\{\bar{w}_1, 0, -\bar{w}_2\} & \text{if } F_- > 2F_+ \\ \text{middle}(\bar{w}_1, 0, -\bar{w}_2) & \text{if } 2F_+ > F_- > F_+ \end{cases} \tag{7.21}$$

where we have introduced a 'middle' function that returns

- if its three arguments have all different values, the one with the middle value;

- if at least two arguments have the same value, that value.

More pragmatically, we order the triplet $(\bar{w}_1, 0, -\bar{w}_2)$ and pick the middle element. The behaviour of $v_{\min}$ according to the values of the friction force is illustrated in Figure 7.2.

Remark 7.2. We now show that, when assumption (7.19) does not hold, it is possible to find multiple solutions for problem (VI). Let us set $F_- = 2F_+$ and assume that, at the initial time $t = 0$, the state of the crawler is such that both the springs are in the state of maximum compression, namely

$$\frac{k_1}{L_1}(z_1 - L_1\varepsilon_1) = -F_- \qquad\qquad \frac{k_2}{L_2}(z_2 - L_2\varepsilon_2) = -F_+$$

We consider an external load such that, for $t \in [0, \mathbb{T}]$, we have $\dot{\varepsilon}_1(t) > 0$ and $\dot{\varepsilon}_2(t) = 0$. Under this conditions, the system has infinite solutions, identified by the parameter $\mu \in [0, 1]$ and defined by

$$\dot{u}_1(t) = -\mu L_1\dot{\varepsilon}_1(t) \qquad\qquad \dot{u}_2(t) = \dot{u}_3(t) = (1 - \mu)L_1\dot{\varepsilon}_1(t)$$

(a) *Case $F_- > 2F_+$.* (b) *Case $2F_+ > F_- > F_+$.*
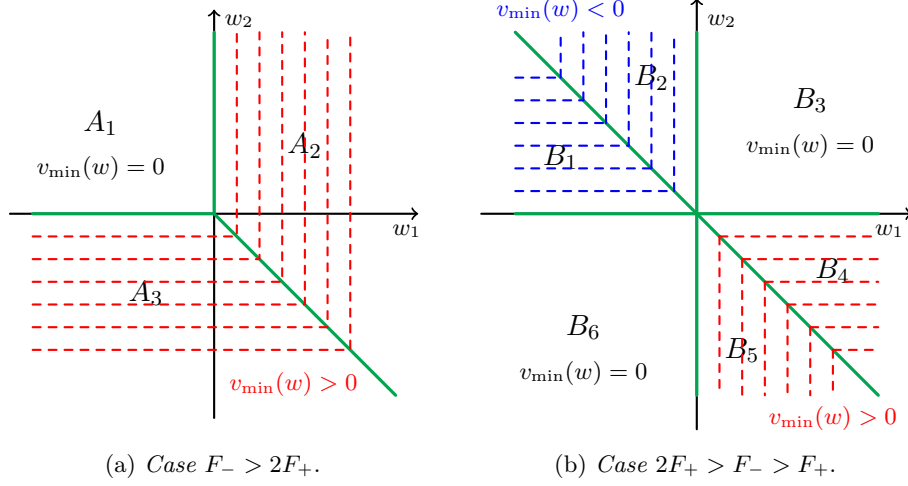
Figure 7.2: Contour plot (dashed) of the function $v_{\min}(w)$ for different choices of the friction parameters.

The shape-dependent dissipation

In the previous section we check that the framework of Section 7.1 is satisfied, so that we can apply Theorem 7.1 and get the existence and uniqueness of the evolution of the systems, provided admissible initial data. From now on our plan is to study the nature of such solutions.

Our next step is therefore to study the restricted dissipation $\mathcal{D}_{\mathrm{sh}}$ and express more explicitly its differential. We consider separately the two cases $F_- > 2F_+$ and $2F_+ > F_- > F_+$, since a different behaviour is observed.

Case $F_- > 2F_+$

We divide the plane into three regions A_1, A_2 and A_3, as shown in Figure 7.3.

(A_1) This is the region defined by $w_1 \leq 0 \leq w_2$, that implies $v_{\min}(w) = 0$ and

$$\mathcal{D}_{\mathrm{sh}}(w) = (-w_1 + w_2)F_+ = \langle \alpha_1, w \rangle \qquad \text{where } \alpha_1 = \begin{pmatrix} -F_+ \\ F_+ \end{pmatrix}$$

(A_2) Here we have $w_1 \geq 0$ and $-w_2 \leq w_1$, so $v_{\min}(w) = w_1$ and

$$\mathcal{D}_{\mathrm{sh}}(w) = (2w_1 + w_2)F_+ = \langle \alpha_2, w \rangle \qquad \text{where } \alpha_2 = \begin{pmatrix} 2F_+ \\ F_+ \end{pmatrix}$$

(A_3) Here we have $w_2 \leq 0$ and $-w_2 \geq w_1$, so $v_{\min}(w) = -w_2$ and

$$\mathcal{D}_{\mathrm{sh}}(w) = (-w_1 - 2w_2)F_+ = \langle \alpha_3, w \rangle \qquad \text{where } \alpha_3 = \begin{pmatrix} -F_+ \\ -2F_+ \end{pmatrix}$$

The subdifferential of $\mathcal{D}_{\text{sh}}$ in the origin is the convex hull generated by $\alpha_1, \alpha_2, \alpha_3$ (cf. Fig. 7.5), namely

$$C_A^* = \partial\mathcal{D}_{\text{sh}}(0) = \text{conv}\{\alpha_1, \alpha_2, \alpha_3\} \tag{7.22}$$

If $w \in \text{int } A_i$, then $\partial\mathcal{D}_{\text{sh}}(w) = \alpha_i$, whereas if $w \in A_i \cap A_j \setminus \{0\}$, then $\partial\mathcal{D}_{\text{sh}}(w) = \overline{\alpha_i\alpha_j}$, where the latter denotes the edge of C_A^* having endpoints α_i and α_j, namely $\overline{\alpha_i\alpha_j} = \text{conv}\{\alpha_i, \alpha_j\}$.
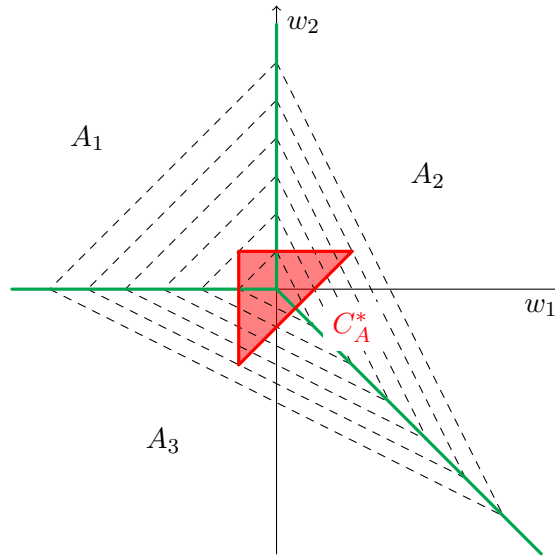
Figure 7.3: Case $F_- > 2F_+$. The three regions A_1, A_2 and A_3, the contour lines of $\mathcal{D}_{\text{sh}}$ (dashed) and its subdifferential at the origin C_A^* (red).

Case $2F_+ > F_- > F_+$

In this case we have to divide the plane into six different regions, as shown in Figure 7.4.

(B_1) Here $w_1 \leq -w_2 \leq 0$ and so $v_{\min}(w) = -w_2$. In this region we have

$$\mathcal{D}_{\text{sh}}(w) = (-w_1-w_2)F_+ + (w_2)F_- = \langle\beta_6, w\rangle \qquad \text{where } \beta_1 = \begin{pmatrix} -F_+ \\ -F_+ + F_- \end{pmatrix}$$

(B_2) Here $-w_2 \leq w_1 \leq 0$ holds, so $v_{\min}(w) = w_1$. In this region we have

$$\mathcal{D}_{\text{sh}}(w) = (w_1+w_2)F_+ + (-w_1)F_- = \langle\beta_4, w\rangle \qquad \text{where } \beta_2 = \begin{pmatrix} F_+ - F_- \\ F_+ \end{pmatrix}$$

(B_3) Here $-w_2 \le 0 \le w_1$ holds, so $v_{\min}(w) = 0$. In this region we have

$$\mathcal{D}_{\mathrm{sh}}(w) = (w_2)F_+ + (w_1)F_- = \langle \beta_2, w \rangle \qquad \text{where } \beta_3 = \begin{pmatrix} F_- \\ F_+ \end{pmatrix}$$

(B_4) Here $0 \le -w_2 \le w_1$ holds, so $v_{\min}(w) = -w_2$. In this region we have

$$\mathcal{D}_{\mathrm{sh}}(w) = (-w_2)F_+ + (w_1+w_2)F_- = \langle \beta_5, w \rangle \qquad \text{where } \beta_4 = \begin{pmatrix} F_- \\ -F_+ + F_- \end{pmatrix}$$

(B_5) Here $0 \le w_1 \le -w_2$ holds, so $v_{\min}(w) = w_1$. In this region we have

$$\mathcal{D}_{\mathrm{sh}}(w) = (w_1)F_+ + (-w_1-w_2)F_- = \langle \beta_3, w \rangle \qquad \text{where } \beta_5 = \begin{pmatrix} F_+ - F_- \\ -F_- \end{pmatrix}$$

(B_6) Here $w_1 \le 0 \le -w_2$ holds, so $v_{\min}(w) = 0$. In this region we have

$$\mathcal{D}_{\mathrm{sh}}(w) = (-w_1)F_+ + (-w_2)F_- = \langle \beta_1, w \rangle \qquad \text{where } \beta_6 = \begin{pmatrix} -F_+ \\ -F_- \end{pmatrix}$$

The subdifferential of $\mathcal{D}_{\mathrm{sh}}$ in the origin is

$$C_B^* = \partial \mathcal{D}_{\mathrm{sh}}(0) = \mathrm{conv}\{\beta_1, \beta_2, \beta_3, \beta_4, \beta_5, \beta_6\} \tag{7.23}$$

If $w \in \mathrm{int}\, B_i$, then $\partial \mathcal{D}_{\mathrm{sh}}(w) = \beta_i$, whereas if $w \in B_i \cap B_j \setminus \{0\}$, then $\partial \mathcal{D}_{\mathrm{sh}}(w) = \overline{\beta_i \beta_j}$, using the notation we introduced in the previous case.

Stasis domains and the laws of motion

We observe that the gradient of $\mathcal{E}$ with respect to the z-coordinates corresponds to the vector composed by the tensions of the two springs, i.e.

$$D_z \mathcal{E}(t, z(t)) = Az(t) - \ell(t) = \begin{pmatrix} \frac{k_1}{L_1}\left(z_1(t) - \varepsilon_1(t)L_1\right) \\ \frac{k_2}{L_2}\left(z_2(t) - \varepsilon_2(t)L_2\right) \end{pmatrix} = \begin{pmatrix} T_1(t) \\ T_2(t) \end{pmatrix} = T(t)$$
$$\tag{7.24}$$

Thus, from (SF), we have

$$-T(t) \in \partial \mathcal{D}_{\mathrm{sh}}(\dot z(t)) \tag{7.25}$$

We can distinguish between three different situations.

- If $\dot z(t) = 0$, then $-T(t) \in C^*$.

- If $\dot z(t) \in \mathrm{int}\, A_i$ for some i, then $-T(t) = \alpha_i$. Similarly, if $\dot z(t) \in \mathrm{int}\, B_i$ for some i, then $-T(t) = \beta_i$.

- If $\dot z(t) \in A_i \cap A_j \setminus \{0\}$ for some $i \ne j$, then $-T(t) \in \overline{\alpha_i \alpha_j}$. Similarly, if $\dot z(t) \in B_i \cap B_j \setminus \{0\}$ for some $i \ne j$, then $-T(t) \in \overline{\beta_i \beta_j}$.
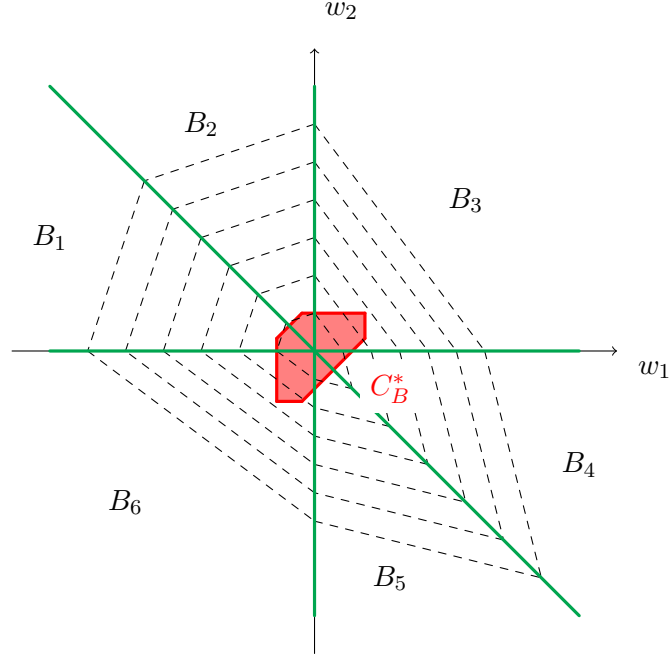
Figure 7.4: Case $2F_+ > F_- > F_+$. The six regions $B_1,\ldots B_6$, the contour lines of $\mathcal{D}_{\mathrm{sh}}$ (dashed) and its subdifferential at the origin C_B^* (red).

This gives us a first description of the behaviour of our system. The tensions of the springs are allowed to change only within the set $-C^*$, that we call *stasis domain*, in analogy with the elastic domains used in elasto-plasticity. Shape changes, and therefore motion, can occur only if the tensions have values on the boundary of $-C^*$, to which we refer as *slip surface*.

The next step is to use the information contained in (7.25), combined with the definition of $T(t)$, to recover how variations in the active distortion produce shape changes. The best way to do that is to work in terms of the tension state of the crawler $T(t)$ instead of the shape state $z(t)$.

First of all we notice that, by differentiating (7.24), we get

$$\dot{T}_1(t) = -k_1\dot{\varepsilon}_1(t) + \frac{k_1}{L_1}\dot{z}_1(t) \tag{7.26a}$$

$$\dot{T}_2(t) = -k_2\dot{\varepsilon}_2(t) + \frac{k_2}{L_2}\dot{z}_2(t) \tag{7.26b}$$

If $-T(t) \in \mathrm{int}\, C^*$, from (7.25) we have $\dot{z}(t) = 0$ and the previous equations reduce to

$$\dot{T}_1(t) = -k_1\dot{\varepsilon}_1(t) \qquad \dot{T}_2(t) = -k_2\dot{\varepsilon}_2(t) \tag{7.27}$$
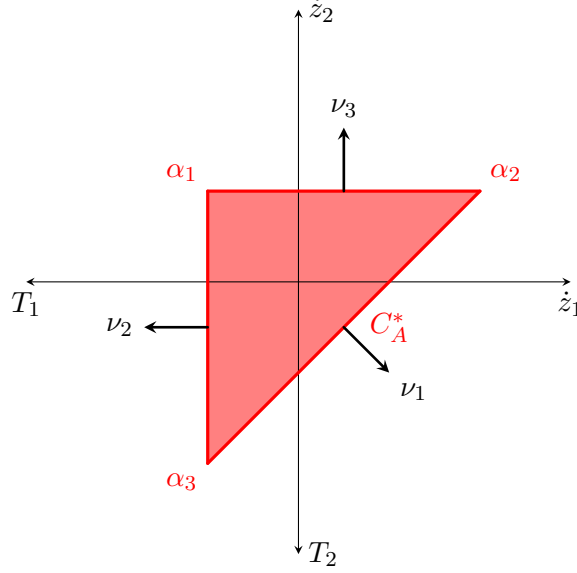
Figure 7.5: Case $F_- > 2F_+$. The stasis domain $-C_A^* = -\partial \mathcal{D}_{\mathrm{sh}}(0)$.

that describe the evolution of the system. On the other end, when $T(t)$ lies on the boundary of $-C^*$, the behaviour of the system is less trivial. We will discuss first the simpler case $F_- > 2F_+$ and then consider the second case $2F_+ > F_- > F_+$.

Case $F_- > 2F_+$

First of all let us introduce the unit vectors

$$\nu_1 = \frac{1}{\sqrt{2}} \begin{pmatrix} 1 \\ -1 \end{pmatrix} \qquad \nu_2 = \begin{pmatrix} -1 \\ 0 \end{pmatrix} \qquad \nu_3 = \begin{pmatrix} 0 \\ 1 \end{pmatrix}$$

that are the outer unit normals to C_A^* respectively along the edges $\overline{\alpha_2\alpha_3}$, $\overline{\alpha_3\alpha_1}$ and $\overline{\alpha_1\alpha_2}$. The constraint $-T(t) \in C_A^*$ implies that, if T is differentiable at time t, then

$$\left\langle \dot{T}(t), \nu_1 \right\rangle = 0 \qquad\qquad \text{if } -T(t) \in \overline{\alpha_2\alpha_3}$$

$$\left\langle \dot{T}(t), \nu_2 \right\rangle = 0 \qquad\qquad \text{if } -T(t) \in \overline{\alpha_3\alpha_1} \qquad (7.28)$$

$$\left\langle \dot{T}(t), \nu_3 \right\rangle = 0 \qquad\qquad \text{if } -T(t) \in \overline{\alpha_1\alpha_2}$$

If one of the scalar products were positive, then the tension should have been outside the stasis domain C_A^* for the times immediately before, and similarly,

if one of them were negative, the tension would be outside C_A^* for the times immediately after.

Let us note that condition 7.28 can be expressed in a more concise way as

$$-T(t) \in N_{C_A^*}(T(t)) \tag{7.29}$$

where $N_C(T)$ denotes the normal cone to the convex set C at the point T. This is also a classical way to approach the problem (RVI), usually known as *differential inclusion* formulation [MT04; Mie05].

Following this same line of thought, each of the constraints could be decoupled into two inequalities on the increments of T, one for the past and one for the future, without requiring the differentiability of T. However, for our purposes, we will work under the assumptions of Theorem 7.1, that guarantees the Lipschitz continuity of the tension $T(t)$, so that the times when $T(t)$ is not differentiable can be neglected for the study of the motion.

A consequence of (7.28) is that, when we reach an edge, either the tension is differentiable, that implies $\left\langle \dot{\ell}(t), \nu_i \right\rangle = 0$ and thus means that $\varepsilon(t)$ is in a certain sense "well calibrated", or we have a time t of non-differentiability for $T(t)$ and $z(t)$, corresponding to an abrupt transition between rest and motion.

If $-T(t)$ lies on one on the vertices of C_A^*, then two of the constraints of (7.28) are satisfied simultaneously, leading to

$$\dot{z}_1(t) = L_1 \dot{\varepsilon}_1(t) \qquad\qquad \dot{z}_2(t) = L_2 \dot{\varepsilon}_2(t) \tag{7.30}$$

We also recall that, by (7.25), we know that $\dot{z}(t) \in A_i$; combining this with (7.30) we see that, to keep that tension configuration, the derivative of the active distortion must lie in a specific cone. In more detail, we have the following situation.

- If $-T(t) = \alpha_1$, then by (7.28) we have $\dot{z}_1(t) \leq 0 \leq \dot{z}_2(t)$ (i.e. $\dot{z}(t) \in A_1$), that implies $\dot{v}(t) = 0$ and

$$\dot{\varepsilon}_1(t) \leq 0 \leq \dot{\varepsilon}_2(t)$$

  The resulting motion of the crawler is

$$\dot{u}_1(t) = -L_1 \dot{\varepsilon}_1(t) \geq 0 \qquad \dot{u}_2(t) = 0 \qquad \dot{u}_3(t) = L_2 \dot{\varepsilon}_2(t) \geq 0$$

- If $-T(t) = \alpha_2$, then $\dot{z}_1(t) \geq 0$ and $\dot{z}_1(t) \geq -\dot{z}_2(t)$, so that $\dot{v}(t) = \dot{z}_1(t)$ and

$$\dot{\varepsilon}_1(t) \geq 0 \qquad \text{and} \qquad \dot{\varepsilon}_2(t) \geq -\frac{L_1}{L_2}\dot{\varepsilon}_1(t)$$

  The resulting motion of the crawler is

$$\dot{u}_1(t) = 0 \qquad\qquad\qquad \dot{u}_2(t) = L_1 \dot{\varepsilon}_1(t) \geq 0$$
$$\dot{u}_3(t) = L_1 \dot{\varepsilon}_1(t) + L_2 \dot{\varepsilon}_2(t) \geq 0$$

- If $-T(t) = \alpha_3$, then $\dot{z}_2(t) \leq 0$ and $\dot{z}_1(t) \leq -\dot{z}_2(t)$, so that $\dot{v}(t) = -\dot{z}_2(t)$ and

$$\dot{\varepsilon}_2(t) \leq 0 \qquad \text{and} \qquad \dot{\varepsilon}_1(t) \leq -\frac{L_2}{L_1}\dot{\varepsilon}_2(t)$$

The resulting motion of the crawler is

$$\dot{u}_1(t) = -L_1\dot{\varepsilon}_1(t) - L_2\dot{\varepsilon}_2(t) \geq 0 \qquad \dot{u}_2(t) = -L_2\dot{\varepsilon}_2(t) \geq 0$$
$$\dot{u}_3(t) = 0$$

If $-T(t)$ lies in the interior of one on the edges of C_A^*, then condition (7.28) gives us only one constraint. However a second constraint is obtained by (7.25), since we know that, if $-T(t) \in \text{int}\,\overline{\alpha_i\alpha_j}$, then $\dot{z}(t) \in A_i \cap A_j$. In more detail, we have the following situation.

- If $-T(t) \in \overline{\alpha_1\alpha_2}$ then we have $\dot{v}(t) = 0$ and

$$\dot{z}_1(t) = 0 \qquad\qquad \dot{z}_2(t) = L_2\dot{\varepsilon}_2(t) \geq 0$$
$$\dot{T}_1(t) = -k_1\dot{\varepsilon}_1(t) \qquad\qquad \dot{T}_2(t) = 0$$

The resulting motion of the crawler is

$$\dot{u}_1(t) = \dot{u}_2(t) = 0 \qquad\qquad \dot{u}_3(t) = L_2\dot{\varepsilon}_2(t) \geq 0$$

- If $-T(t) \in \overline{\alpha_3\alpha_1}$ then we have $\dot{v}(t) = 0$ and

$$\dot{z}_1(t) = -L_1\dot{\varepsilon}_1(t) \geq 0 \qquad\qquad \dot{z}_2(t) = 0$$
$$\dot{T}_1(t) = 0 \qquad\qquad \dot{T}_2(t) = -k_2\dot{\varepsilon}_2(t)$$

The resulting motion of the crawler is

$$\dot{u}_1(t) = -L_1\dot{\varepsilon}_1(t) \geq 0 \qquad\qquad \dot{u}_2(t) = \dot{u}_3(t) = 0$$

- If $-T(t) \in \overline{\alpha_2\alpha_3}$, differently from the two previous cases, we observe changes on the tension and length of both segments; however this happens in a coordinated fashion, namely,

$$\dot{z}_1(t) = -\dot{z}_2(t) = \dot{v}(t) = \frac{k_1\dot{\varepsilon}_1(t) - k_2\dot{\varepsilon}_2(t)}{\frac{k_1}{L_1} + \frac{k_2}{L_2}} \geq 0$$

that gives the condition $\dot{\varepsilon}_1(t) \geq \frac{k_2}{k_1}\dot{\varepsilon}_2(t)$ for the admissible active distortion. The tension evolves according to

$$\dot{T}_1(t) = \dot{T}_2(t) = -\frac{L_1\dot{\varepsilon}_1(t) + L_2\dot{\varepsilon}_2(t)}{\frac{L_1}{k_1} + \frac{L_2}{k_2}}$$

The resulting motion of the crawler is

$$\dot{u}_1(t) = \dot{u}_3(t) = 0 \qquad\qquad \dot{u}_2(t) = \frac{k_1\dot{\varepsilon}_1(t) - k_2\dot{\varepsilon}_2(t)}{\frac{k_1}{L_1} + \frac{k_2}{L_2}} \geq 0$$
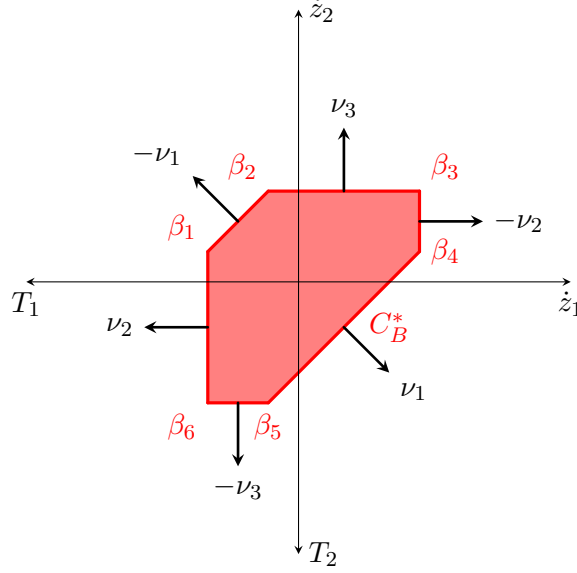
Figure 7.6: Case $2F_+ > F_- > F_+$. The stasis domain $-C_B^* = -\partial\mathcal{D}_{\mathrm{sh}}(0)$.

Case $2F_+ > F_- > F_+$

As in the previous case, we want to exploit the constraint $-T(t) \in C_B^*$ to deduce a condition on $\dot{T}(t)$. We observe that ν_1, ν_2 and ν_3 are the outer unit normals respectively to the edges $\overline{\beta_4\beta_5}$, $\overline{\beta_6\beta_1}$ and $\overline{\beta_2\beta_3}$, but also the inner unit normals to the edges $\overline{\beta_1\beta_2}$, $\overline{\beta_3\beta_4}$ and $\overline{\beta_5\beta_6}$. Thus we have, analogously to (7.28),

$$\left\langle \dot{T}(t), \nu_1 \right\rangle = 0 \qquad\qquad \text{if } -T(t) \in \overline{\beta_4\beta_5} \cup \overline{\beta_1\beta_2}$$
$$\left\langle \dot{T}(t), \nu_2 \right\rangle = 0 \qquad\qquad \text{if } -T(t) \in \overline{\beta_6\beta_1} \cup \overline{\beta_3\beta_4} \qquad (7.31)$$
$$\left\langle \dot{T}(t), \nu_3 \right\rangle = 0 \qquad\qquad \text{if } -T(t) \in \overline{\beta_2\beta_3} \cup \overline{\beta_5\beta_6}$$

As before, when $-T(t)$ lies in one on the vertices of C_B^*, two of the constraints of (7.31) are satisfied simultaneously and therefore

$$\dot{z}_1(t) = L_1\dot{\varepsilon}_1(t) \qquad\qquad \dot{z}_2(t) = L_2\dot{\varepsilon}_2(t) \qquad (7.32)$$

Similarly to the previous case, if $-T(t) \in \beta_i$, then by (7.25) we have $\dot{z}(t) \in B_i$, leading to the following situation.

- If $-T(t) = \beta_1$, then by (7.28) we have $\dot{z}_1(t) \leq -\dot{z}_2(t) \leq 0$, that implies $\dot{v}(t) = -\dot{z}_2(t)$ and requires, when $T(t)$ is differentiable, that

$$\dot{\varepsilon}_2(t) \geq 0 \qquad\qquad \dot{\varepsilon}_1(t) \leq -\frac{L_2}{L_1}\dot{\varepsilon}_2(t)$$

  The resulting motion of the crawler is

$$\dot{u}_1(t) = -L_1\dot{\varepsilon}_1(t) - L_2\dot{\varepsilon}_2(t) \geq 0 \quad \dot{u}_2(t) = -L_2\dot{\varepsilon}_2(t) \leq 0 \quad \dot{u}_3(t) = 0$$

- If $-T(t) = \beta_2$, then we have $-\dot{z}_2(t) \leq \dot{z}_1(t) \leq 0$, so that $\dot{v}(t) = \dot{z}_1(t)$ and

$$\dot{\varepsilon}_1(t) \leq 0 \qquad\qquad \dot{\varepsilon}_2(t) \geq -\frac{L_1}{L_2}\dot{\varepsilon}_1(t)$$

  The resulting motion of the crawler is

$$\dot{u}_1(t) = 0 \quad \dot{u}_2(t) = L_1\dot{\varepsilon}_1(t) \leq 0 \quad \dot{u}_3(t) = L_1\dot{\varepsilon}_1(t) + L_2\dot{\varepsilon}_2(t) \geq 0$$

- If $-T(t) = \beta_3$, then we have $\dot{z}_1(t) \geq 0$ and $\dot{z}_2(t) \geq 0$, so that $\dot{v}(t) = 0$ and

$$\dot{\varepsilon}_1(t) \geq 0 \qquad\qquad \dot{\varepsilon}_2(t) \geq 0$$

  The resulting motion of the crawler is

$$\dot{u}_1(t) = -L_1\dot{\varepsilon}_1(t) \leq 0 \qquad \dot{u}_2(t) = 0 \qquad \dot{u}_3(t) = L_2\dot{\varepsilon}_2(t) \geq 0$$

- If $-T(t) = \beta_4$, then by (7.28) we have $\dot{z}_1(t) \geq -\dot{z}_2(t) \geq 0$, so that $\dot{v}(t) = -\dot{z}_2(t)$ and

$$\dot{\varepsilon}_2(t) \leq 0 \qquad\qquad \dot{\varepsilon}_1(t) \geq -\frac{L_2}{L_1}\dot{\varepsilon}_2(t)$$

  The resulting motion of the crawler is

$$\dot{u}_1(t) = -L_1\dot{\varepsilon}_1(t) - L_2\dot{\varepsilon}_2(t) \leq 0 \quad \dot{u}_2(t) = -L_2\dot{\varepsilon}_2(t) \geq 0 \quad \dot{u}_3(t) = 0$$

- If $-T(t) = \beta_5$, then we have $-\dot{z}_2(t) \geq \dot{z}_1(t) \geq 0$, so that $\dot{v}(t) = \dot{z}_1(t)$ and

$$\dot{\varepsilon}_1(t) \geq 0 \qquad\qquad \dot{\varepsilon}_2(t) \leq -\frac{L_1}{L_2}\dot{\varepsilon}_1(t)$$

  The resulting motion of the crawler is

$$\dot{u}_1(t) = 0 \quad \dot{u}_2(t) = L_1\dot{\varepsilon}_1(t) \geq 0 \quad \dot{u}_3(t) = L_1\dot{\varepsilon}_1(t) + L_2\dot{\varepsilon}_2(t) \leq 0$$

- If $-T(t) = \beta_6$, then we have $\dot{z}_1(t) \leq 0$ and $\dot{z}_2(t) \leq 0$, so that $\dot{v}(t) = 0$ and

$$\dot{\varepsilon}_1(t) \leq 0 \qquad\qquad \dot{\varepsilon}_2(t) \leq 0$$

  The resulting motion of the crawler is

$$\dot{u}_1(t) = -L_1 \dot{\varepsilon}_1(t) \geq 0 \qquad \dot{u}_2(t) = 0 \qquad \dot{u}_3(t) = L_2 \dot{\varepsilon}_2(t) \leq 0$$

As in the previous case, when $-T(t)$ lies in the interior of one on the edges of C_B^*, only one constraint is given by condition (7.31), but a second one is recovered by (7.25), using the fact that if $-T(t) \in \operatorname{int} \overline{\beta_i \beta_j}$, then $\dot{z}(t) \in B_i \cap B_j$. The pairs of opposite edges are characterized by the same behaviour of the crawler, but associated with shape variations of opposite sign. In more detail, we have the following situation.

- If $-T(t) \in \overline{\beta_2 \beta_3} \cup \overline{\beta_5 \beta_6}$ then we have $\dot{v}(t) = 0$ and

$$\begin{aligned} \dot{z}_1(t) &= 0 & \dot{z}_2(t) &= L_2 \dot{\varepsilon}_2(t) \\ \dot{T}_1(t) &= -k_1 \dot{\varepsilon}_1(t) & \dot{T}_2(t) &= 0 \end{aligned}$$

  so that it is required that $\varepsilon_2(t) \geq 0$ if $-T(t) \in \overline{\beta_2 \beta_3}$, whereas $\varepsilon_2(t) \leq 0$ if $-T(t) \in \overline{\beta_5 \beta_6}$. The resulting motion of the crawler is

$$\dot{u}_1(t) = \dot{u}_2(t) = 0 \qquad \dot{u}_3(t) = L_2 \dot{\varepsilon}_2(t) \begin{cases} \geq 0 & \text{if } -T(t) \in \overline{\beta_2 \beta_3} \\ \leq 0 & \text{if } -T(t) \in \overline{\beta_5 \beta_6} \end{cases}$$

- If $-T(t) \in \overline{\beta_3 \beta_4} \cup \overline{\beta_6 \beta_1}$ then we have $\dot{v}(t) = 0$ and

$$\begin{aligned} \dot{z}_1(t) &= -L_1 \dot{\varepsilon}_1(t) & \dot{z}_2(t) &= 0 \\ \dot{T}_1(t) &= 0 & \dot{T}_2(t) &= -k_2 \dot{\varepsilon}_2(t) \end{aligned}$$

  so that it is required that $\varepsilon_2(t) \geq 0$ if $-T(t) \in \overline{\beta_6 \beta_1}$, whereas $\varepsilon_2(t) \leq 0$ if $-T(t) \in \overline{\beta_3 \beta_4}$. The resulting motion of the crawler is

$$\dot{u}_2(t) = \dot{u}_3(t) = 0 \qquad \dot{u}_1(t) = -L_1 \dot{\varepsilon}_1(t) \begin{cases} \geq 0 & \text{if } -T(t) \in \overline{\beta_6 \beta_1} \\ \leq 0 & \text{if } -T(t) \in \overline{\beta_3 \beta_4} \end{cases}$$

- The third case $-T(t) \in \overline{\beta_1 \beta_2} \cup \overline{\beta_4 \beta_5}$, is characterized by a coordinated change in the tension and length of both segments, more precisely

$$\dot{z}_1(t) = -\dot{z}_2(t) = \dot{v}(t) = \frac{k_1 \dot{\varepsilon}_1(t) - k_2 \dot{\varepsilon}_2(t)}{\frac{k_1}{L_1} + \frac{k_2}{L_2}}$$

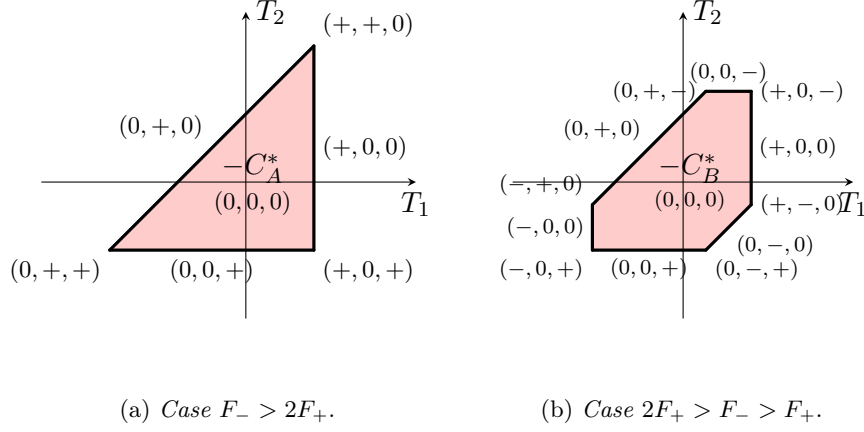(a) *Case $F_- > 2F_+$.*   (b) *Case $2F_+ > F_- > F_+$.*

Figure 7.7: Qualitative summary of the motility results of section 7.2. Each triple is placed in the interior, on an edge or on a vertex of the stasis domain $-C^*$ and describes the admissible directions of displacement for the three legs while the crawler keeps that tension configuration. A plus denotes a positive displacement, a minus a negative one and a zero that that leg must remain steady. For instance the triple $(+, 0, -)$ near a vertex indicates that, for that value of the tension $T(t)$, we have $\dot{u}_1(t) \geq 0$, $\dot{u}_2(t) = 0$ and $\dot{u}_3(t) \leq 0$.

that gives, for the admissible active distortion, the condition $\dot{\varepsilon}_1(t) \geq \frac{k_2}{k_1}\dot{\varepsilon}_2(t)$ if $-T(t) \in \overline{\beta_4\beta_5}$ and $\dot{\varepsilon}_1(t) \leq \frac{k_2}{k_1}\dot{\varepsilon}_2(t)$ if $-T(t) \in \overline{\beta_1\beta_2}$. The tension configuration evolves according to

$$\dot{T}_1(t) = \dot{T}_2(t) = -\frac{L_1\dot{\varepsilon}_1(t) + L_2\dot{\varepsilon}_2(t)}{\frac{L_1}{k_1} + \frac{L_2}{k_2}}$$

The resulting motion of the crawler is

$$\dot{u}_1(t) = \dot{u}_3(t) = 0 \quad \dot{u}_2(t) = \frac{k_1\dot{\varepsilon}_1(t) - k_2\dot{\varepsilon}_2(t)}{\frac{k_1}{L_1} + \frac{k_2}{L_2}} \begin{cases} \geq 0 & \text{if } -T(t) \in \overline{\beta_4\beta_5} \\ \leq 0 & \text{if } -T(t) \in \overline{\beta_1\beta_2} \end{cases}$$

7.3　Motility analysis and crawling strategies

A qualitative description of the results of the previous section is illustrated in Figure 7.7. The two possibilities considered for the relative magnitude of the friction forces determine very different motile behaviours of the crawler.

If $F_- > 2F_+$, the legs of the crawler can move only forward. The set $-C_A^*$ of the admissible tension configurations scales with F_+, but it is independent of the value of F_-.

If $2F_+ > F_- > F_+$, each leg of the crawler can move both forward and backward. The precise shape of the stasis domain $-C_B^*$ depends on the ratio F_+/F_-, although it is always a hexagon with parallel opposite edges oriented

as in Figure 7.6. If the ratio F_+/F_- is fixed, then $-C_B^*$ scales homothetically with the magnitude of the friction coefficients; if instead we fix the value of F_+, then $-C_B^*$ shrinks as F_- tends to F_+.

To truly understand the motility of our crawler, we have to consider the effects of a periodic active distortion $\varepsilon(t)$. As a corollary of Theorem 7.1, we are granted the existence of a unique Lipschitz continuous displacement $u(X,t)$ for any given continuous and piecewise continuously differentiable active distortion $\varepsilon \colon [0, \mathcal{T}] \to \mathbb{R}^2$.

We now discuss the main qualitative behaviour of such motility strategies and then present some illustrative examples. To simplify the computation, we assume $k_1 = k_2 = k$ and $L_1 = L_2 = L$.

To produce a non-null translation of the crawler that repeats itself in each period, sufficiently large excursions in the stasis domain are necessary. More precisely, during every period the tension $T(t)$ has to reach all the three edges of $-C_A^*$ (if $F_- > 2F_+$) or a suitable triple of non adjacent edges of $-C_B^*$ (if $2F_+ > F_- > F_+$). Since a certain amount of excursion in the active distortion is spent in crossing $-C^*$, allowing larger fluctuations in $\varepsilon(t)$ permits more performant motility strategies, because in this way a larger amount of the active distortion is spent moving the legs.

In the case $F_- > 2F_+$, an effective motility strategy can be achieved even by activating only one of the segments, for instance by setting $\varepsilon_2 \equiv 0$ and assuming a sufficiently large sawtooth oscillation for ε_1. This strategy can be compared to a one-segment crawler experiencing the same sawtooth fluctuations, as that studied in Chapter 6 (cf. [DGN15, Sec. 4]). Indeed, the one-segment crawler results more efficient: it requires a lower minimal amplitude $\Delta\varepsilon$ of the sawtooth ($\Delta\varepsilon > 2F_+/k$ instead of $\Delta\varepsilon > 3F_+/k$), it produces a greater displacement after one cycle ($\Delta u = (\Delta\varepsilon - 2F_+/k)L$ instead of $\Delta u = (\Delta\varepsilon - 3F_+/k)L$) and it is effective also in the case $2F_+ > F_- > F_+$. For such friction ratios a two-segment crawler, performing the sawtooth strategy above, has a zero net displacement after one cycle.

We remark that in all the situations above, net displacements are possible only in the direction of lower friction. To achieve a *complete motility*, i.e. to be able to move also backwards (against the higher friction) using periodic shape changes, we need to consider the case $2F_+ > F_- > F_+$ and strategies that fully exploit two shape parameters. This minimality of two shape parameters for a complete motility belongs to folklore knowledge for unidimensional locomotors (cf. for instance [Arr+12a; DT12; GND14; MD15]). The ability of our two-segment crawler to effectively move in both directions, assuming a small friction asymmetry, is illustrated by the following strategies.

We consider the periodic change in the active distortion illustrated in Figure 7.8, recalling that $2F_+ > F_- > F_+$. We set the times so that the period is $\mathcal{T} = 3\tau$ and divide the evolution of $\varepsilon(t)$ into three phases, described
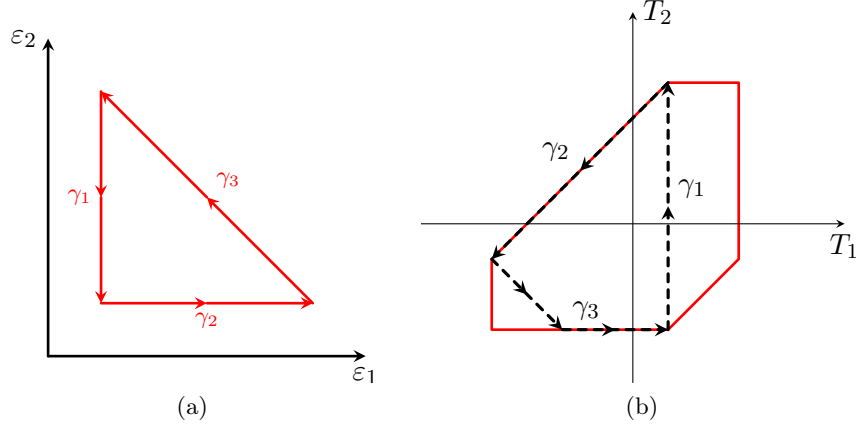
Figure 7.8: Active distortion strategy (7.33) and associated evolution of the tension.

as follows.

$$\dot{\varepsilon}_1(t) = \begin{cases} 0 & \text{if } 0 < t < \tau \\ \eta & \text{if } \tau < t < 2\tau \\ -\eta & \text{if } 2\tau < t < 3\tau \end{cases} \qquad \dot{\varepsilon}_2(t) = \begin{cases} -\eta & \text{if } 0 < t < \tau \\ 0 & \text{if } \tau < t < 2\tau \\ \eta & \text{if } 2\tau < t < 3\tau \end{cases} \qquad (7.33)$$

where $\eta > 0$ is a given parameter. We require that $\eta\tau k > F_+ + F_-$, to ensure sufficiently large distortions. Note that, since our system is rate independent, what really affects the resulting displacement is not η but the increment $\eta\tau$ of the active distortion; actually, any other smooth time reparametrization of the curve in Figure 7.8 (a) would produce exactly the same displacement after each period.

The behaviour of the system in the first period depends on the initial state; however after the first period we always reach the same tension configuration $T(3\tau) = -\beta_2$. Since we are interested in the long term behaviour, we assume $T(0) = -\beta_2$ and so avoid the initial adjustment period.

We now describe the behaviour in the three phases (see Fig. 7.8).

(γ_1) For $0 < t < \frac{F_+ + F_-}{\eta k}$ the three legs are steady and T_2 increases from $-F_+$ to F_-. Then, for $\frac{F_+ + F_-}{\eta k} < t < \tau$ the tension are constant but the third leg moves backwards with $\dot{u}_3(t) = -\eta L$.

(γ_2) For $\tau < t < \frac{4F_- - 2F_+}{\eta k}$ the tension evolves from $-\beta_5$ to $-\beta_4$ along the corresponding edge of $-C_B^*$. At the same time, the middle leg moves forward with $\dot{u}_2(t) = -\frac{\eta L}{2}$. Once the tension edge $-\beta_4$ is reached, for $\frac{4F_- - 2F_+}{\eta k} < t < 2\tau$ the tension is constant, the middle leg is again steady while the first leg moves backwards with $\dot{u}_1(t) = -\eta L$.

(γ_3) For $2\tau < t < \frac{2F_+ - F_-}{k}$, T_1 increases and T_2 decreases at the same rate, until they reach the edge of $-C_B^*$. Then, for $\frac{2F_+ - F_-}{k} < t < \frac{3F_- - 3F_+}{k}$

the tension evolves along the edge until it reaches the vertex $-\beta_2$. In this time interval the third leg advances with $\dot{u}_3(t) = L\eta$. Finally, in the last interval $\frac{3F_- - 3F_+}{k} < t < 3\tau$, the tension is constant, the third leg is again steady and the middle leg moves backwards with $\dot{u}_2(t) = -L\eta$.

The sum of these actions produces in a period the displacement

$$\Delta^- u = L\left(\eta\mathcal{T} - \frac{4F_- - 2F_+}{k}\right) \tag{7.34}$$

We notice that the strategy we just presented could be slightly improved by suitably modifying $\varepsilon(t)$, for instance in a way to avoid the temporary forward movement of two of the legs. However these changes require an a priori knowledge of all the parameters of the systems, so that the strategy is, in a certain sense, calibrated to the situation, for instance requiring changes in $\dot{\varepsilon}(t)$ exactly at the moment when the tension reaches the slip surface, i.e. the boundary of $-C_B^*$. The strategy we presented instead shows the same behaviour for every choice of the parameters, provided that the assumption of large distortions is satisfied. Moreover we remark that such improvements of the strategy decrease only the numerator of the negative term inside the brackets in (7.34), so the main term is untouched and any improvement becomes negligible for large distortions $\eta\mathcal{T}$ or large stiffness k.

The history of active distortion (7.33) was also chosen to show a backward movement of the crawler, that corresponds to proceeding in the direction of higher friction. A simple strategy to move forwards is given by the time reverse of strategy (7.33), namely

$$\dot{\varepsilon}_1(t) = \begin{cases} \eta & \text{if } 0 < t < \tau \\ -\eta & \text{if } \tau < t < 2\tau \\ 0 & \text{if } 2\tau < t < 3\tau \end{cases} \qquad \dot{\varepsilon}_2(t) = \begin{cases} -\eta & \text{if } 0 < t < \tau \\ 0 & \text{if } \tau < t < 2\tau \\ \eta & \text{if } 2\tau < t < 3\tau \end{cases} \tag{7.35}$$

Also in this case, after a preliminary stage, the tension configuration at the beginning of each period stabilizes to $T = -\beta_2$, that will be the starting condition in our analysis. The evolution of the tension is shown in Figure 7.9. After a period the displacement produced is

$$\Delta^+ u = L\left(\eta\mathcal{T} - \frac{5F_+ - F_-}{2k}\right) \tag{7.36}$$

We have that

$$\Delta^+ u - \Delta^- u = \frac{9}{2}L(F_- - F_+) > 0 \tag{7.37}$$

and so there is an advantage when moving in the direction of lower friction. This advantage becomes null as the ratio F_+/F_- tends to one, while it increases to a constant when we approximate the threshold case $F_+/F_- = 2$.

We notice that the difference $\Delta^+ u - \Delta^- u$ between the displacement produced by our twin strategies does not depend on the amplitude $\eta\mathcal{T}$ of the distortion. This means that, if the crawler can produce only small distortions, but slightly greater than the lower threshold $(F_+ + F_-)/k$, then a very large number of iterations of the first strategy is necessary to obtain a negative displacement equal to the positive one produced by a cycle of the second strategy. On the other hand, if the crawler can produce very large distortions (i.e. $\eta\mathcal{T} \to \infty$) the outcomes of the two strategies become comparable, in the sense that the ratio $\Delta^+ u / \Delta^- u$ tends to one.

We remark that reversing the strategy does not always reverse also the direction of motion, as it happens in the example above. A counterexample is given by the simple strategy

$$\dot{\varepsilon}_1(t) = \begin{cases} \eta & \text{if } 0 < t < \tau \\ 0 & \text{if } \tau < t < 2\tau \\ -\eta & \text{if } 2\tau < t < 3\tau \end{cases} \qquad \dot{\varepsilon}_2(t) = \begin{cases} 0 & \text{if } 0 < t < \tau \\ \eta & \text{if } \tau < t < 2\tau \\ -\eta & \text{if } 2\tau < t < 3\tau \end{cases} \qquad (7.38)$$

and its time-reverse, for sufficiently large distortions, namely $\eta\mathcal{T} > 3F_- k$. Both stategy (7.38) and its reverse produce the same, positive displacement after a period, equal to

$$\Delta u = L\frac{2F_- - F_+}{k} \qquad (7.39)$$

We notice that in this case the displacement is independent of the distortion $\eta\mathcal{T}$, while with the previous strategies we had an asympotically linear growth in terms of $\eta\mathcal{T}$. The inefficiency of this strategies with respect to (7.35) can be seen intuitively also by looking at the behaviour of the crawler during a cycle. The first and the third legs perform both a forward and a backward movement, of amplitude growing with $\eta\mathcal{T}$, that almost cancel each other out, leaving only the final displacement Δu.

We conclude by remarking that the abstract setup of Section 7.1 can be applied to analogous crawlers composed by a larger number of segments. Increasing the number of legs enlarges the range of friction ratios under which motility in both directions is possible from $F_+ < F_- < 2F_+$ to $F_+ < F_- < NF_+$. Intuitively, a N-segment crawler can move each leg backwards one by one, by leaning against the other $N - 1$ legs, resulting in a strategy that generalizes (7.33). However also the number of critical friction ratios, to be avoided in order to satisfy (SB), increases with N, and with it increases also the number of different scenarios that appear by varying the friction ratio, and a complete and detailed description of a generic evolution problem becomes soon burdensome.
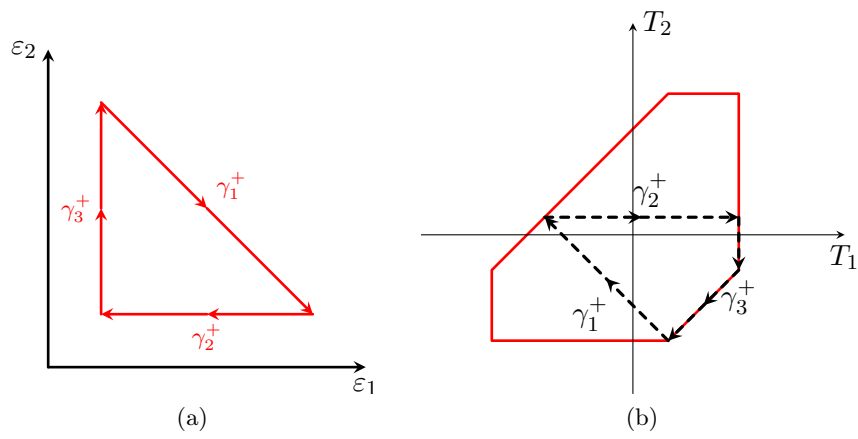
Figure 7.9: Active distortion strategy (7.35) and associated evolution of the tension.

Chapter 8

On the genesis of directional friction

8.1 Introduction

Modelling frictional interactions is a challenging task, both for the variety of behaviours experimentally observed, and for the relevance of such phenomena in the study and control of mechanical devices. The common strategy consists of a multiscale approach, where the frictional behaviour is an emergent macroscopic property of mechanical interactions between the asperities of the two surfaces occurring at microscale [AS08]. Such interactions are often described by modelling the asperities with simple mechanical systems, such as springs and bristles [DB11; Can+95; HF91].

A classical example of such multiscale approach is the Prandtl-Tomlinson model, developed to explain the genesis of Coulomb dry friction [Pop10; PG14]. The model considers the motion of a point mass along a sinusoidal potential, subject to an external driving force and a viscous damping, showing convergence to a dry friction behaviour when the sinusoidal oscillations decrease homothetically. This scenario can be related to the interaction of a single asperity of the upper surface with a rigid rough lower surface. Such representation applies also to the interaction of the cantilever with the surface in a friction force microscope.

In this Chapter we follow this multiscale paradigm to propose an explanation of the genesis of a directional asymmetry in the coefficients of Coulomb dry friction, in situations where the interaction between the two surfaces is mediated by bristle-like elements (cf [GD16a]).

Our starting point is the paper [Mie12] by Mielke. Here, it is shown that the quasi-static behaviour of a family of Prandtl–Tomlinson-like systems, in which the fluctuation in the potential decreases homothetically, converge to that of a particle subject to dry friction. Moreover, the leftwards and rightwards friction coefficients coincide with the minimum and maximum of

the derivative of the oscillating potential. In this way, a directionality in the friction is produced simply by assuming a suitable asymmetry in the potential. As we discuss in Section 8.4, a key element in this approach is the change in the nature of the dissipation, from viscous in the approximating systems to rate-independent in the limit one.

We apply these ideas to study the limit behaviour of systems characterized by a mediating, bristle-like element, interacting with a wiggly surface whose periodic fluctuations scale homothetically to zero. In this way the wiggly potential is generated by the small oscillations in the mediating element, induced by the fluctuations of the surface. Moreover an asymmetry in the wiggly potential can be simply produced by an asymmetry in the mediating element (e.g. the inclination of a bristle), also in the case of a symmetric surface.

In order to apply Mielke's approach to our problem, we need to extend his framework to more general families of approximating systems, in which the scaling of the wiggly potential is no longer homothetic, but contains also a nonlinear term (cf. eq. (8.5)). This is our first result, presented in Section 8.2 (Theorem 8.1), and constitutes the abstract contribution of this Chapter.

From the point of view of applications, our main result is to provide some physical insight into the origin of directional friction. This is obtained by constructing some concrete examples of simple mechanical systems producing, in the limit, directional dry friction, and by interpreting the origin of this frictional asymmetry in terms of the parameters characterizing each example.

The friction coefficients we obtain are the product of two factors. The first one is "geometric": it contains the asymmetry of the system and is determined only by the roughness of the surface and by the angle of the mediating bristle-like element. The second factor is instead "energetic": it depends on the limit energetic state of the mediating element, but not on the direction of motion. This last coefficient is proportional to the normal force exerted, at the limit, by the mediating element on the surface. In this way we recover the classical structure of Coulomb friction law, where the friction force is the product of a coefficient characteristic of the surfaces and the modulus of the normal forces exchanged between them.

Our results are then used to discuss the *with the nap/against the nap* asymmetry. As we will argue better in Section 8.3, our intuition of such asymmetry actually includes under the same name several distinct phenomena, producing the same kind of directionality. Despite the complex behaviour that can be showed by a bristle, our "angular spring" model of Section 8.3 can be used to outline two fundamental effects, corresponding to changes in the two factors that characterize the friction coefficients. The *geometric effect* occurs when the bristle keeps the same configuration during the two phases (with and against the nap), and the directionality is due to the inclination of the bristle, that in this way "perceives" a symmetric fluctuation of the

surface as asymmetric. The *energetic effect* applies to situations where the configuration of the bristle flips when the velocity changes sign, so that the tip of the bristle is always behind its root with respect to the direction of motion. In this case the geometric component is unchanged, but the bristle switches between two different energetic states, exerting a different normal force on the surface.

Finally, we notice that the behaviour of the "angular spring" model of Section 8.3 has a close resemblance to that observed experimentally for the robotic crawler developed in [ND14]. There, slanted bristles, interacting with a groove-textured surface, are used to obtain net displacement, when the body of the crawler performs a cycle of elongation and contraction. The bristle-surface interaction produces an oscillatory friction force, and it is shown that the system can be effectively discussed considering supports moving on a flat surface and experiencing a constant average friction force. Such result supports our approach and encourages a future experimental validation of the predictions of our models.

8.2 Abstract setting

In this section we show that the evolution of a prototype one dimensional rate independent system, with energy $\mathcal{E}$ and a dissipation potential $\mathcal{R}$ positively homogeneous of degree 1, can be constructed as the limit of the evolutions of a family of systems $(\mathcal{E}_\varepsilon, \mathcal{R}_\varepsilon)$, where $\mathcal{E}_\varepsilon = \mathcal{E} + V_\varepsilon$, with V_ε an oscillatory ("wiggly") small perturbation, and $\mathbb{R}_\varepsilon$ is a small viscous dissipation potential. The system $(\mathcal{E}_\varepsilon, \mathcal{R}_\varepsilon)$ will describe a motion on an undulatory surface with vanishing small roughness, while the system $(\mathcal{E}, \mathcal{R})$ describes motion on a flat surface with directional dry friction.

Let us therefore consider a mechanical system having internal energy

$$\mathcal{E}(t, z) = \Phi(z) - \ell(t)z \tag{8.1}$$

where $t \in [0, T]$ represent the time and $z \in \mathbb{R}$ is a one-dimensional state variable. We assume that $\Phi \in \mathcal{C}^2(\mathbb{R}, \mathbb{R})$ is a uniformly convex function, while $\ell \in \mathcal{C}^1([0, T], \mathbb{R})$. The dissipative effects of a change in the state of the system is described by the dissipation potential

$$\mathcal{R}(v) = \begin{cases} \rho_+ v & \text{for } v \geq 0 \\ \rho_- v & \text{for } v \leq 0 \end{cases} \tag{8.2}$$

where $\rho_- < 0$ and $\rho_+ > 0$ are suitable constants. We consider the quasi-static evolution of the system, described by

$$0 \in \partial_{\dot{z}} \mathcal{R}(\dot{z}) + D_z \mathcal{E}(t, z) \tag{8.3}$$

where the dot ˙ denotes the derivative with respect to the time variable t, $\partial_{\dot{z}}$ denotes the subdifferential with respect to $\dot{z}$ and D_z denotes the derivative in the z variable (below also denoted briefly, when not ambiguous, with a prime $'$).

Similarly we introduce the following family of perturbed systems depending on a small parameter ε. The energy of these systems is obtained by adding to $\mathcal{E}$ a small wiggly perturbation. More precisely we have

$$\mathcal{E}_\varepsilon(t, z) = \Phi(z) - \ell(t)z + V_\varepsilon(z) \tag{8.4}$$

with

$$V_\varepsilon(z) = \varepsilon W\left(\frac{z}{\varepsilon}\right) + \varepsilon^2 Q\left(\varepsilon; \frac{z}{\varepsilon}\right) \tag{8.5}$$

Here $W \in \mathcal{C}^2(\mathbb{R}, \mathbb{R})$ is a 1-periodic (non-constant) function; whereas $Q \colon (0, \varepsilon_Q) \times \mathbb{R} \to \mathbb{R}$, for some $\varepsilon_Q > 0$, is 1-periodic and $\mathcal{C}^2$ in the second variable. Moreover we assume the existence of two positive constants $C_{Q,0}$ and $C_{Q,1}$ such that, for every $0 < \varepsilon < \varepsilon_Q$ and for every $y \in \mathbb{R}$ we have

$$|Q(\varepsilon; y)| < C_{Q,0} \qquad\qquad \left|Q'(\varepsilon; y)\right| < C_{Q,1} \tag{8.6}$$

where the prime $'$ denotes the derivative with respect to the second variable y.

The systems are subject to a viscous friction, described by the Rayleigh dissipation potential

$$\mathcal{R}_\varepsilon(\dot{z}) = \frac{\varepsilon^\gamma}{2}\dot{z}^2 \qquad \text{for some } \gamma > 0 \tag{8.7}$$

and their (quasi-static) evolution is described by the equation

$$0 = D_{\dot{z}}\mathcal{R}_\varepsilon(\dot{z}) + D_z\mathcal{E}_\varepsilon(t, z) \tag{8.8}$$

We are going to show that the behaviour of the system (8.3) is approximated, for $\varepsilon \to 0$, by that of the systems (8.8). To do so, a last assumption is needed, in order to link the two situations. Namely, we require

$$\rho_+ = \max W'(z) > 0 \qquad\qquad \rho_- = \min W'(z) < 0 \tag{8.9}$$

We are now ready to state the main result of this section.

Theorem 8.1. *In the framework described above, let $z_\varepsilon \colon [0, T] \to \mathbb{R}$ be a family of solutions of* (8.8), *such that*

$$z_\varepsilon(0) \to z^0 \in (\Phi')^{-1}\left([\ell(0) - \rho_+, \ell(0) - \rho_-]\right) \tag{8.10}$$

Then, the differential inclusion (8.3) *has a unique solution $\bar{z} \colon [0, T] \to \mathbb{R}$ for the initial conditions $\bar{z}(0) = z^0$. Moreover, for $\varepsilon \to 0$, this solution satisfies*

$$z_\varepsilon \to \bar{z} \qquad \text{in } \mathcal{C}^0([0, T]) \tag{8.11}$$

$$\int_{t_1}^{t_2} 2\mathcal{R}_\varepsilon(\dot{z}_\varepsilon(t))\,\mathrm{d}t \to \int_{t_1}^{t_2} \mathcal{R}(\dot{\bar{z}}(t))\,\mathrm{d}t \qquad \text{for every } 0 \leq t_1 < t_2 \leq T \tag{8.12}$$

Theorem 8.1 is proved in Section 8.5, through a convergence strategy illustrated in Section 8.4. Let us remark that the right term in (8.10) is well defined since, being Φ uniformly convex, it follows that Φ' is globally invertible with range equal to $\mathbb{R}$.

For our application, it is useful to study an apparently more general situation and show that it actually falls in the framework of Theorem 8.1. Let us consider a function $\mathcal{F} \in \mathcal{C}^3([-\delta_\mathcal{F}, \delta_\mathcal{F}], \mathbb{R})$ defined in a neighbourhood of zero and such that

$$\mathcal{F}'(0) = \alpha \neq 0 \tag{8.13}$$

Let $\mathcal{W} \in \mathcal{C}^2(\mathbb{R}, \mathbb{R})$ be a 1-periodic (non-constant) function and set

$$\mu_+ = \max \mathcal{W}'(z) > 0 \qquad\qquad \mu_- = \min \mathcal{W}'(z) < 0 \tag{8.14}$$

We consider also a function $\mathcal{Q} \colon (0, \tilde{\varepsilon}_\mathcal{Q}) \times \mathbb{R} \to \mathbb{R}$, defined for some $\tilde{\varepsilon}_\mathcal{Q} > 0$, and such that it is 1-periodic and $\mathcal{C}^2$ in the second variable. We assume that there exist two positive constants $\tilde{C}_{\mathcal{Q},0}$ and $\tilde{C}_{\mathcal{Q},1}$ such that, for every $0 < \varepsilon < \tilde{\varepsilon}_\mathcal{Q}$ and for every $y \in \mathbb{R}$, we have

$$|\mathcal{Q}(\varepsilon; y)| < \tilde{C}_{\mathcal{Q},0} \qquad\qquad \left|\mathcal{Q}'(\varepsilon; y)\right| < \tilde{C}_{\mathcal{Q},1} \tag{8.15}$$

Let $\varepsilon_\mathcal{F}$ be small enough to satisfy $\varepsilon_\mathcal{F} \|\mathcal{W}\|_\infty + \varepsilon_\mathcal{F}^2 \tilde{C}_{\mathcal{Q},0} < \delta_\mathcal{F}$. We now consider, for every positive $\varepsilon < \min\{\varepsilon_\mathcal{F}, \varepsilon_\mathcal{Q}\}$, the general wiggly potential $\mathcal{V}_\varepsilon$ defined as

$$\mathcal{V}_\varepsilon(z) = \mathcal{F}\left[\varepsilon\mathcal{W}\left(\frac{z}{\varepsilon}\right) + \varepsilon^2 \mathcal{Q}\left(\varepsilon; \frac{z}{\varepsilon}\right)\right] - \mathcal{F}(0) \tag{8.16}$$

Lemma 8.2. *In the framework above, for every wiggly potential $\mathcal{V}_\varepsilon$ of the form (8.16) there exist two suitable functions W and Q, such that $\mathcal{V}_\varepsilon$ can be written in the form (8.5) for sufficiently small $\varepsilon > 0$. Moreover we have $W(y) = \alpha\mathcal{W}(y)$ and therefore*

$$\begin{array}{ll} \rho_+ = \alpha\mu_+ \\ \rho_- = \alpha\mu_- \end{array} \quad \text{if } \alpha > 0 \qquad \left(\text{resp.} \quad \begin{array}{ll} \rho_+ = -\alpha\mu_- \\ \rho_- = -\alpha\mu_+ \end{array} \quad \text{if } \alpha < 0\right) \tag{8.17}$$

Proof. We recall that, expanding $\mathcal{F}$ as a Taylor series, we have

$$\mathcal{F}(u) - \mathcal{F}(0) = \alpha u + \frac{\mathcal{F}''(0)}{2} u^2 + h(u) u^2 \tag{8.18}$$

with $\lim_{u \to 0} h(u) = 0$. Moreover, since $\mathcal{F} \in \mathcal{C}^3$, it can be shown that $h \in \mathcal{C}^1$ and $h'(0) = \mathcal{F}'''(0)/6$. Thus, applying this expansion to (8.16), we get

$$\mathcal{V}_\varepsilon(z) = \varepsilon W\left(\frac{z}{\varepsilon}\right) + \varepsilon^2 Q\left(\varepsilon; \frac{z}{\varepsilon}\right)$$

where we set $W(y) = \alpha\mathcal{W}(y)$ and

$$Q(\varepsilon; y) = \alpha\mathcal{Q}(\varepsilon; y) + \frac{\mathcal{F}''(0)}{2}\mathcal{W}(y)^2 + \varepsilon^2 \frac{\mathcal{F}''(0)}{2}\mathcal{Q}(\varepsilon; y)^2 +$$
$$+ h\left(\varepsilon\mathcal{W}(y) + \varepsilon^2\mathcal{Q}(y)\right)\left[\mathcal{W}(y) + \varepsilon\mathcal{Q}(\varepsilon; y)\right]^2$$

All the desired properties of W follow from their analogous ones for $\mathcal{W}$. To recover the desired estimates on Q and Q', we notice that, for any arbitrary $C_h > 0$, we can find ε_h such that

$$
\begin{aligned}
&\left| h\left(\varepsilon\mathcal{W}(y) + \varepsilon^2\mathcal{Q}(y)\right)\right| < C_h \\
&\left| h'\left(\varepsilon\mathcal{W}(y) + \varepsilon^2\mathcal{Q}(y)\right)\right| < |\mathcal{F}'''(0)| + 1
\end{aligned}
\qquad \text{for every } y \in \mathbb{R} \text{ and } \varepsilon \in (0, \varepsilon_h)
$$

Thus, for every for every positive $\varepsilon < \min\{1, \varepsilon_\mathcal{F}, \varepsilon_\mathcal{Q}, \varepsilon_h\}$, we have

$$
|Q(\varepsilon; y)| \le C_{Q,0} := \alpha\tilde{C}_{\mathcal{Q},0} + \frac{\mathcal{F}''(0)}{2}\left\|\mathcal{W}\right\|_\infty^2 + \frac{\mathcal{F}''(0)}{2}\tilde{C}_{\mathcal{Q},0}^2 + C_h\left(\left\|\mathcal{W}\right\|_\infty + \tilde{C}_{\mathcal{Q},0}\right)^2
$$

The twice continuous differentiability of Q follows from those of $\mathcal{Q}$ and $\mathcal{W}$, recalling also that $h(u)u^2$ is twice continuously differentiable in u. Moreover we have the estimate

$$
\begin{aligned}
\left|Q'(\varepsilon; y)\right| \le C_{Q,1} := {}& \alpha\tilde{C}_{\mathcal{Q},1} + \mathcal{F}''(0)\left\|\mathcal{W}\right\|_\infty\left\|\mathcal{W}'\right\|_\infty + \mathcal{F}''(0)\tilde{C}_{\mathcal{Q},0}\tilde{C}_{\mathcal{Q},1} + \\
&+ (\mathcal{F}'''(0) + 1)\left(\left\|\mathcal{W}\right\|_\infty + \tilde{C}_{\mathcal{Q},0}\right)^2 + \\
&+ C_h\left(\left\|\mathcal{W}\right\|_\infty + \tilde{C}_{\mathcal{Q},0}\right)\left(\left\|\mathcal{W}'\right\|_\infty + \tilde{C}_{\mathcal{Q},1}\right)
\end{aligned}
$$

$\square$

The form (8.16) of $\mathcal{V}_\varepsilon$ is interesting from a physical point of view, since it highlights the role of two different elements in our applications. Formula (8.17) shows that the effective friction $\rho_\pm$ in the $\varepsilon \to 0$ limit is the product of two quantities: $\mu_\pm$ associated to $\mathcal{W}$ and α associated to $\mathcal{F}$. On one hand the "geometric" coefficients μ_+, μ_- are related to the (directional) roughness of the surface, as perceived by the geometry of the system. On the other hand, the "energetic" coefficient α is associated to a "tension" in the element that mediates the frictional interaction.

This duality is quite central in our applications. Firstly, this distinction reinforces the resemblance with Coulomb's classical formulation of dry friction, where the friction intensity depends both on a coefficient, related to the properties of the interacting surfaces, and on the normal force exerted by each surface on the other one. Remarkably, in our models, the term α is proportional to the normal force exerted, in the limit case, on the surface by the mediating element.

Moreover, when discussing the *with the nap/ against the nap* asymmetry in Section 8.3, we will see that it can be produced by two distinct effects: a geometric effect, given by the intrinsic asymmetry of the system, as captured by the coefficients $\mu_\pm$, and a energetic effect, where we observe a change of the configuration of the system between the two phases (with and against the nap), producing a change in the value of α.

8.3 Modelling

In this section we discuss three different models to obtain directional dry friction as the limit of the effects of an interaction with a surface having vanishingly small roughness, with the mediation of a hair/bristle-like element. We remind that, as in the previous section, we are assuming quasi-static evolution.

The limit system We characterize a frictional interaction governed by dry friction through a system, illustrated in Figure 8.1, consisting of a horizontal spring, that evolves as follows. The position of one end of the spring is controlled by the function $q \in \mathcal{C}^1([0,T],\mathbb{R})$; the second end of the spring, with position $u(t)$, is free to move and interacts with the surface, according to the force-velocity law

$$f^{\mathrm{lim}}(\dot{u}) = \begin{cases} -\rho_+ < 0 & \text{if } \dot{u} > 0 \\ \rho \in [-\rho_+, -\rho_-] & \text{if } \dot{u} = 0 \\ -\rho_- > 0 & \text{if } \dot{u} < 0 \end{cases} \tag{8.19}$$

Thus the limit system has dissipation potential (8.2) and internal energy

$$\mathcal{E} = \frac{k_h}{2} \left(L_h^{\mathrm{rest}} - q(t) + u \right)^2 + \mathrm{const.} \tag{8.20}$$

where k_h and L_h^{rest} are respectively the elastic constant and the rest length of the spring.

The state of the system will be described by a coordinate z of the form $z(t) = u(t) + c$. The constant c, introduced for technical reasons, has different values in the models and can be thought as a gap between the position $u(t)$ of the second end of the spring and the position $z(t)$ at which, in the $\varepsilon \to 0$ limit, the bristle-like mediating element interacts with the surface, cf. Figure 8.1. Thus the energy $\mathcal{E}$ can be written in the form (8.1) by setting

$$\Phi(z) = \frac{k_h}{2} z^2 \qquad\qquad \ell(t) = k_h(q(t) - L_h^{\mathrm{rest}}) \tag{8.21}$$

and neglecting a remaining term $r(t)$, depending only on the time t, since it does not affect the dynamics (8.3). We also remark that the change of variable to z does not alter the dissipative terms, since $\dot{u} = \dot{z}$. Finally, we mention [Ale16], where a similar model was used to study discontinuous evolutions.

The approximating systems In the approximating systems, we imagine that the surface in no longer flat, but has a small, ε-periodic perturbation of the form

$$w_\varepsilon(x) = \varepsilon w \left(\frac{x}{\varepsilon} \right) \tag{8.22}$$
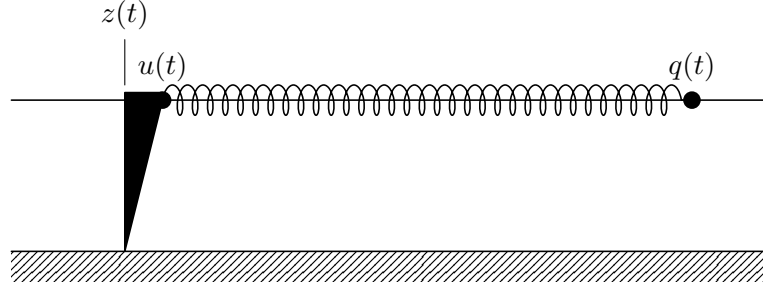
Figure 8.1: The limit system.

where $w \in \mathcal{C}^2(\mathbb{R}, \mathbb{R})$ is a 1-periodic (non-constant) function. Moreover we define

$$\omega_+ = \max w'(x) > 0 \qquad\qquad \omega_- = \min w'(x) < 0 \qquad (8.23)$$

The approximating systems are still characterized by a horizontal spring as in the limit model. However, the interaction with the surface is no longer subject to dry friction, but mediated by a new element, that ideally plays the role of a hair or a bristle, attached to the end $u(t)$ of the horizontal spring. This element has, up to a constant, an internal energy V_ε as in (8.16), that depends only on u and on the magnitude of the perturbation ε. Finally, the only dissipative force acting on the system is a (vanishing) viscous force

$$f_\varepsilon^{\mathrm{vis}}(\dot u) = -\varepsilon^\gamma \dot u \qquad (8.24)$$

so that the Rayleigh dissipation potential of the system is given by (8.7).

In the following we discuss three different models for this mediating element. In the first model, the mediating element is a vertical spring. The second model is actually a generalization of the first one, since in this case the spring forms a constant angle ϑ with the vertical axis. In the third model the mediating element is a straight rigid bar with constant length, but now the angle with the vertical axis can change and is influenced by an angular spring.

First model: vertical spring

In our first model the mediating element (bristle) is a vertical spring, with horizontal position $u(t)$, as illustrated in Figure 8.2. One end of the spring has fixed height, while the height of the other end follows the fluctuation of the surface, in such a way that the length of the spring is

$$L(u) = h - w_\varepsilon(u)$$
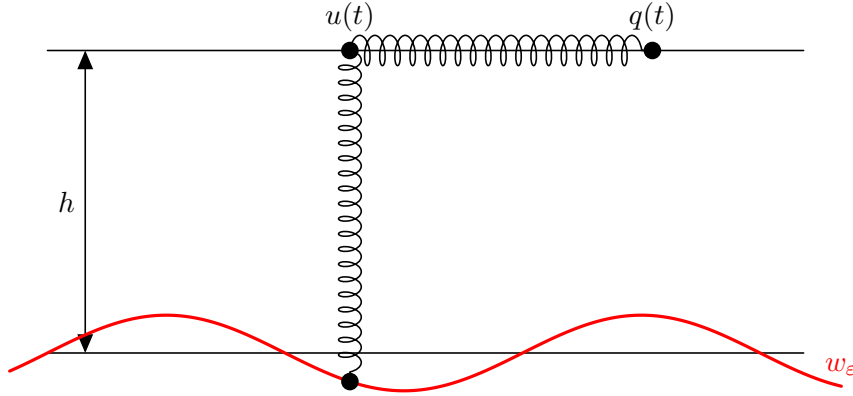
Figure 8.2: First model: vertical spring

Let $k > 0$ and L^{rest} be respectively the elastic constant and the rest length of the spring. Setting $z(t) = u(t)$, the energy of the vertical spring is

$$\frac{k}{2} \left(L^{\mathrm{rest}} - h + w_\varepsilon(z) \right)^2 = \mathcal{F}(\varepsilon \mathcal{W}(\tfrac{z}{\varepsilon})) = V_\varepsilon(z) + \mathcal{F}(0)$$

where $\mathcal{W}(y) = w(y)$ and $\mathcal{F}(y) = \frac{k}{2} \left(L^{\mathrm{rest}} - h + y \right)^2$, so that we have

$$\alpha = \mathcal{F}'(0) = k(L^{\mathrm{rest}} - h) \qquad \mu_+ = \omega_+ \qquad \mu_- = \omega_-$$

We require

$$L^{\mathrm{rest}} \neq h$$

so that $\alpha \neq 0$ and (8.13) is satisfied. We notice that, for instance, setting $L^{\mathrm{rest}} > h$ means that the spring is always compressed.

In this way all the requirements of Lemma 8.2 are satisfied, and therefore we can apply Theorem 8.1 to obtain the desired behaviour for the limit system. In this way, for a compressed spring, we recover a sort of Coulomb law, since the friction coefficients are proportional to the normal force exerted by the spring on the surface, that, in the limit, is exactly equal to α. Moreover, if the profile of the fluctuations is asymmetric, in the sense that $\omega_+ \neq \omega_-$, then also the friction is asymmetric.

Second model: slanted spring

Our second model generalizes the first one, since in this case we consider a slanted spring forming a fixed angle $0 < \vartheta < \pi/2$ with the vertical axis, as illustrated in Figure 8.3. As before, one end of the spring has fixed height and horizontal position $u(t)$. In this case, however, the horizontal position of the
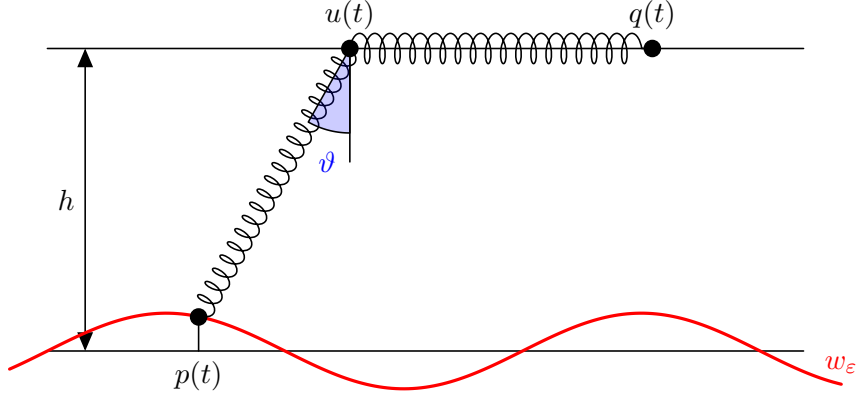
Figure 8.3: Second model: slanted spring

second end will be different from $u(t)$ and denoted with $p(t)$. We therefore have

$$\frac{u - p}{h - w_\varepsilon(p)} = \tan \vartheta \tag{8.25}$$

We can express explicitly u as a function of p as

$$u - h \tan \vartheta = p - w_\varepsilon(p) \tan \vartheta \tag{8.26}$$

We require

$$\omega_+ < \cot \vartheta \tag{8.27}$$

so that $w'_\varepsilon(p) \tan \vartheta < \omega_+ \tan \vartheta < 1$ and therefore $p_\varepsilon(u)$ is a one-to-one correspondence. The length of the spring is thus

$$L = \sqrt{(u - p)^2 + (h - w_\varepsilon(p))^2} = \frac{u - p}{\sin \vartheta} = \frac{h - w_\varepsilon(p)}{\cos \vartheta} \tag{8.28}$$

For our purposes, it is convenient to adopt the variable

$$z = u - h \tan \vartheta$$

to represent the state of the system. Setting

$$g(p) = p - w(p) \tan \vartheta$$

we notice, for every choice of $\varepsilon > 0$, the function g relates $z(t)$ with $p(t)$ through the one-to-one correspondences

$$\frac{z(t)}{\varepsilon} = g\left(\frac{p(t)}{\varepsilon}\right)$$

The bijectivity of g follows from (8.27) since

$$g'(p) = 1 - w'(p) \tan \vartheta > 0$$

The inverse function g^{-1} is twice continuously differentiable and such that $g^{-1}(z + 1) = g^{-1}(z) + 1$ for every $z \in \mathbb{R}$.

We set

$$\mathcal{W}(z) = w\left(g^{-1}(z)\right) \qquad\qquad \mathcal{Q}(\varepsilon; z) = 0$$

and

$$\mathcal{F}(y) = \frac{k}{2}\left(L^{\text{rest}} - \frac{h-y}{\cos\vartheta}\right)^2$$

so that, up to a constant, the internal energy of the slanted spring is given by $\mathcal{V}_\varepsilon(z) = \mathcal{F}(\varepsilon\mathcal{W}(z/\varepsilon))$ of the form (8.16).

We now want to determine the coefficients $\rho_\pm$. Since

$$\alpha = \frac{k}{\cos\vartheta}\left(L^{\text{rest}} - \frac{h}{\cos\vartheta}\right) \tag{8.29}$$

it remains to find μ_+ and μ_-. Since this involves the derivative of g^{-1}, difficulties may arise trying a direct computation, since g cannot be always inverted explicitly and thus, in general, $\mathcal{W}$ may not be explicitly determined. Such is the case, for instance, of a sinusoidal choice of w, for which the inversion of g leads to the well studied problem of the inverse Kepler equation [AKN06b].

However, for our purpose, the full knowledge of the fluctuation profile as perceived by the slanted spring, i.e. the explicit form of $\mathcal{W}$, is not necessary, since we are only interested in the minimum and maximum of $\mathcal{W}'$. Such values can be computed without inverting g explicitly. Since the same issue will arise also in the next model, we summarize the result in the following lemma.

Lemma 8.3. *Let $w \in \mathcal{C}^2(\mathbb{R}, \mathbb{R})$, be a 1-periodic function with $\omega_+ = \max w'(z) > 0$ and $\omega_- = \min w'(z) < 0$. For some constant a, with $\omega_-^{-1} < -a < \omega_+^{-1}$, we consider*

$$g(p) = p + aw(p) > 0 \qquad\qquad \mathcal{W}(z) = w\left(g^{-1}(z)\right)$$

Then

$$\mu_+ = \max \mathcal{W}'(z) = \frac{\omega_+}{1 + a\omega_+} \qquad \mu_- = \min \mathcal{W}'(z) = \frac{\omega_-}{1 + a\omega_-} \tag{8.30}$$

Proof. For any fixed $\bar{z} \in \mathbb{R}$, let us define $\bar{p} = g^{-1}(\bar{z})$. We have

$$\mathcal{W}'(\bar{z}) = w'(\bar{p}) \cdot (g^{-1})'(\bar{z}) = w'(\bar{p})\frac{1}{g'(\bar{p})} = \frac{w'(\bar{p})}{1 + aw'(\bar{p})} \tag{8.31}$$

Since g is a bijection and the function $y \mapsto \dfrac{y}{1 + ay}$ is increasing monotone for $y \in [\omega_-, \omega_+]$, we get

$$\mu_+ = \max_{\bar{z}\in\mathbb{R}} W'(\bar{z}) = \max_{\bar{p}\in\mathbb{R}} \frac{w'(\bar{p})}{1 + aw'(\bar{p})} = \frac{\omega_+}{1 + a\omega_+}$$

$$\mu_- = \min_{\bar{z}\in\mathbb{R}} W'(\bar{z}) = \min_{\bar{p}\in\mathbb{R}} \frac{w'(\bar{p})}{1 + aw'(\bar{p})} = \frac{\omega_-}{1 + a\omega_-}$$

$\square$
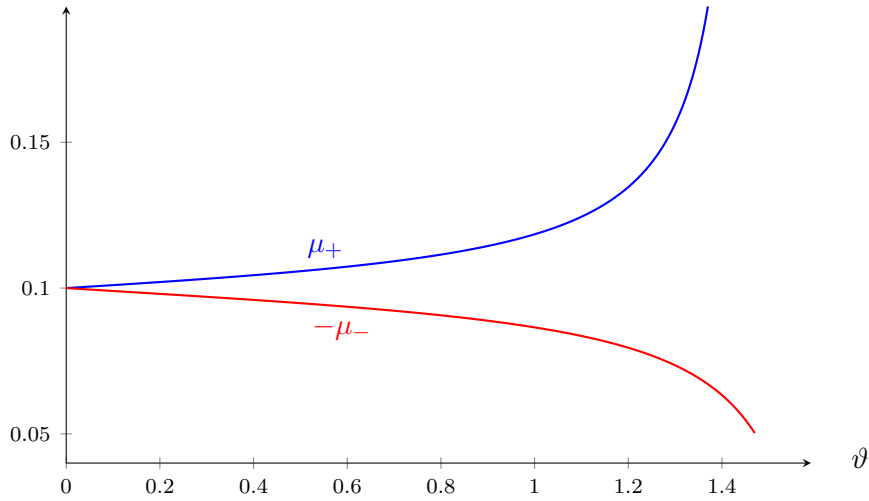
Figure 8.4: Behaviour of μ_+ and μ_- in the second model as a function of ϑ. We are setting $\omega_+ = -\omega_- = 0.1$, so that by (8.27) the admissible domain is $0 < \vartheta < \mathrm{arccot}\, 0.1$.

Thus, for our second model, we have

$$\mu_+ = \frac{\omega_+}{1 - \omega_+ \tan \vartheta} \qquad\qquad \mu_- = \frac{\omega_-}{1 - \omega_- \tan \vartheta} \qquad (8.32)$$

We notice that, for $\vartheta = 0$, we recover the situation of the first model, as expected. The behaviour of the coefficient as function of ϑ is illustrated in Figure 8.4.

Thus all the requirements of Lemma 8.2 are satisfied, and Theorem 8.1 can be applied. We also observe from (8.29) that the coefficient α is proportional to the normal force exerted by the spring on flat surface at $\varepsilon = 0$, by a factor $1/\cos^2 \vartheta$.

We notice that, for this model, we have $\rho_+ > -\rho_-$, meaning that the friction opposing a rightward movement ($\dot{u} > 0$) is greater than the one corresponding to a leftward movement ($\dot{u} < 0$). This is exactly the opposite of what we usually experience in the *with the nap/against the nap* asymmetry, for which, as we will discuss in the last part of this Section, other explanations can be found.

Remarkably, such a "reversed" with the nap/against the nap asymmetry has been observed in experiments dealing with friction force microscopy on molecular monolayers [KS04; Lil+98]; the resemblance with such situations suggests a possible connection.

Third model: angular spring

In this model, the mediating element consists of a straight rigid rod with length L, as illustrated in Figure 8.5. One end of the rod has constant height
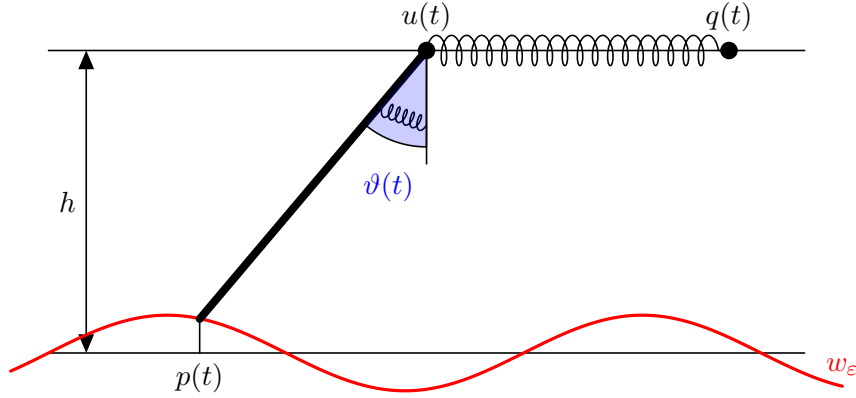
Figure 8.5: Third model: angular spring, for $\vartheta^{\text{rest}} = 0$

and horizontal position $u(t)$. The rod can rotate around this end and we denote with $\vartheta > 0$ the angle formed with the vertical axis. We denote with $p(t)$ the horizontal coordinate of the second end of the rod and assume that the systems is oriented so that $p < u$. Denoting with h the distance between the first end of the rod and the limit flat surface, we require $L > h$, so that, for sufficiently small oscillations w_ε, the rod can always touch the surface. We define

$$\vartheta^{\text{lim}} = \arccos \frac{h}{L} > 0 \tag{8.33}$$

as the angle of the rod when it touches the flat surfaces in the limit $\varepsilon \to 0$. The rod has an angular spring with rest angle ϑ^{rest}. We assume

$$\vartheta^{\text{lim}} > \vartheta^{\text{rest}} > -\frac{\pi}{2} \tag{8.34}$$

The internal energy of the spring is

$$\frac{k}{2} \left(\vartheta - \vartheta^{\text{rest}} \right)^2$$

Since the surface acts as a constraint on the system and we consider quasi-static motion, for each value of u, we deduce that the rod assumes the minimum angle possible $\vartheta = \vartheta(u)$, touching the surface.

We require, for every $x \in \mathbb{R}$,

$$-\tan \vartheta^{\text{lim}} < w'(x) < \cot \vartheta^{\text{lim}} \tag{8.35}$$

For ε sufficiently small, the right inequality assures that the rod touches the wiggly surface only with its second end, whereas the left inequality implies that, when $u(t)$ changes, then also $p(t)$ changes, but without jumps. Thus,

since the second end of the rod touches the surface, we can deduce the following relationships:

$$L = \sqrt{(u-p)^2 + (h - w_\varepsilon(p))^2} = \frac{u - p}{\sin \vartheta} = \frac{h - w_\varepsilon(p)}{\cos \vartheta} \qquad (8.36)$$

From this, can express explicitly $\vartheta(t)$ as a function of $p(t)$, namely

$$\vartheta(t) = \arccos \frac{h - w_\varepsilon(p(t))}{L} \qquad (8.37)$$

Let us introduce the new variable

$$z(t) = u(t) - \sqrt{L^2 - h^2} \qquad (8.38)$$

We now want to show that $w_\varepsilon(p(t))$ can be expressed as a function of $z(t)$ of the form

$$w_\varepsilon(p(t)) = \varepsilon \mathcal{W}\left(\frac{z(t)}{\varepsilon}\right) + \varepsilon^2 \mathcal{Q}\left(\varepsilon; \frac{z(t)}{\varepsilon}\right)$$

with $\mathcal{W}$ and $\mathcal{Q}$ as in (8.16); in this way also $\vartheta(t)$ can be expressed as a function of $z(t)$.

From (8.36) we can express $z(t)$ as a function of $p(t)$, as

$$z(t) = p(t) + A(w_\varepsilon(p(t))) \qquad (8.39)$$

where

$$A(y) = \sqrt{L^2 - (h-y)^2} - \sqrt{L^2 - h^2}$$

We notice that $A(0) = 0$ and $A'(y) = \frac{h - y}{\sqrt{L^2 - (h-y)^2}}$. Equation (8.39) gives a one-to-one correspondence between $z(t)$ and $p(t)$, since

$$\frac{\mathrm{d}z}{\mathrm{d}p} = 1 + A'(w_\varepsilon(p))w'\left(\frac{p}{\varepsilon}\right) = 1 + (\cot \vartheta)w'\left(\frac{p}{\varepsilon}\right) > 0 \qquad (8.40)$$

for ε sufficiently small. The last inequality follows from the fact that, for $\varepsilon \to 0$, we have $\|w_\varepsilon\|_\infty \to 0$ and $\vartheta \approx \vartheta^{lim}$. Hence, by (8.35), we can find ε_ϑ such that, for $\varepsilon < \varepsilon_\vartheta$, we always have $\cot \vartheta > 0$.

Let us denote $Z = z/\varepsilon$ and $P = p/\varepsilon$. From (8.39), we get a twice continuously differentiable bijection $Z = G(\varepsilon; P)$, that can be decomposed as

$$G(\varepsilon; P) = G_0(P) + \varepsilon G_R(\varepsilon; P)$$

where

$$G_0(P) = P + \frac{h}{\sqrt{L^2 - h^2}} w(P) = P + (\cot \vartheta^{\mathrm{lim}})w(P)$$

and $G_R(\varepsilon; P)$ is 1-periodic and twice continuously differentiable in P; moreover G_R and its derivative in P are uniformly bounded for ε sufficiently small.

From (8.40) we know that $D_P G(\varepsilon; P) > 0$ for every $P \in \mathbb{R}$; thus, for each $\varepsilon < \varepsilon_\vartheta$, the function $G(\varepsilon; \cdot)$ has a twice continuously differentiable inverse $H(\varepsilon; \cdot)$, so that $P = H(\varepsilon, Z)$. The function H can be written in the form

$$H(\varepsilon; Z) = H_0(Z) + \varepsilon H_R(\varepsilon; Z)$$

Here H_0 is twice continuously differentiable, 1-periodic in Z and there are two positive constants C_H and ε_H such that

$$\begin{aligned} |H_R(\varepsilon; Z)| &< C_H \\ |D_Z H_R(\varepsilon; Z)| &< C_H \end{aligned} \qquad \text{for every } Z \in \mathbb{R} \text{ and every } \varepsilon \in (0, \varepsilon_H)$$

A straightforward computation shows that $H_0 = G_0^{-1}$.

Let us notice that, since that, since w is periodic and twice continuously differentiable, there exists a continuously differentiable function $h_w \colon \mathbb{R} \times \mathbb{R} \to R$, 1-periodic and such that

$$w(x + \varepsilon) = w(x) + \varepsilon h_w(\varepsilon; x)$$

Moreover there exist two positive constants C_w and ε_w such that

$$\begin{aligned} |h_w(\varepsilon; x)| &< C_w \\ |D_x h_w(\varepsilon; x)| &< C_w \end{aligned} \qquad \text{for every } x \in \mathbb{R} \text{ and every } \varepsilon \in (0, \varepsilon_w)$$

Thus we have

$$\begin{aligned} w(P) &= w\left(H_0(Z) + \varepsilon H_R(\varepsilon; Z)\right) \\ &= w(H_0(Z)) + \varepsilon h_w(\varepsilon H_R(\varepsilon; Z); H_0(Z)) H_R(\varepsilon; Z) \end{aligned}$$

We set

$$\begin{aligned} \mathcal{W}(y) &= w(H_0(y)) \\ \mathcal{Q}(\varepsilon; y) &= h_w(\varepsilon H_R(\varepsilon; y); H_0(y)) H_R(\varepsilon; y) \\ \mathcal{F}(y) &= \frac{k}{2}\left(\arccos \frac{h - y}{L} - \vartheta^{\text{rest}}\right)^2 \end{aligned}$$

and observe the energy of the angular spring is, up to a constant, expressed by a function $\mathcal{V}_\varepsilon(z)$ of the form (8.16), with constants $\tilde{C}_{\mathcal{Q},0} = C_w C_H$, $\tilde{C}_{\mathcal{Q},1} = C_w C_H(\|H_0'\|_\infty + 1)$ and $\varepsilon_\mathcal{Q} = \min\{\varepsilon_\vartheta, \varepsilon_H, \varepsilon_w\}$.

We obtain that

$$\alpha = \mathcal{F}'(0) = \frac{k}{\sqrt{L^2 - h^2}}(\vartheta^{\text{lim}} - \vartheta^{\text{rest}}) \tag{8.41}$$

so that, by (8.34), the assumption (8.13) is satisfied, as are also the other requirements of Lemma 8.2. Thus Theorem 8.1 gives the desired behaviour for $\varepsilon \to 0$.
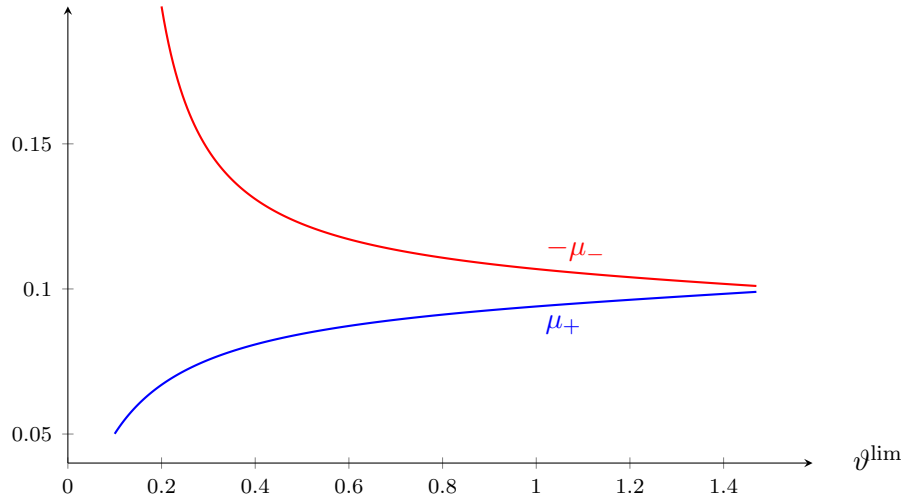
Figure 8.6: Behaviour of μ_+ and μ_- in the third model as a function of ϑ^{lim}. We are setting $\omega_+ = -\omega_- = 0.1$, so that by (8.35) the admissible domain is $\arctan 0.1 < \vartheta^{\mathrm{lim}} < \mathrm{arccot}\, 0.1$.

As in the previous model, in general G cannot be inverted explicitly. However we can apply Lemma 8.3 to recover the coefficients μ_+, μ_-. We have

$$\mu_+ = \frac{\omega_+}{1 + \omega_+ \cot \vartheta^{\mathrm{lim}}} \qquad \mu_- = \frac{\omega_-}{1 + \omega_- \cot \vartheta^{\mathrm{lim}}} \qquad (8.42)$$

where we recall that $\cot \vartheta^{\mathrm{lim}} = \frac{h}{\sqrt{L^2 - h^2}}$. The behaviour of the coefficient as a function of ϑ^{lim} is illustrated in Figure 8.6.

Interpretation of the *with the nap/against the nap* effect.

A hairy surface is a common denominator of many situations where we experience a directionality in the friction: stroking a cat, rubbing a brush with slanted bristles, using climbing skins for backcountry skiing or brushing napped fabric. Although we intuitively gather all this instances under the same name of *with the nap/against the nap* asymmetry, what we are actually considering is family of different phenomena, all producing the same kind of directional effect. For instance, in some situations there is no significant change in the bristle configuration between the two phases (e.g., rubbing gently a hard brush), while in others large deformations of the bristles occur and we observe a dramatic change in their configuration passing from one direction to the other one (e.g., stroking a cat).

Clearly a comprehensive and complete characterization of all these with the nap/against the nap phenomena would require a sophisticated modelling of the mechanical behaviour of a bristle. Yet, with the help of the "angular spring" model, we can easily identify two fundamental effects that are involved. The

geometric one is a direct application of the angular spring model, and holds for sufficiently rigid bristles, remaining straight also under small compressions. The energetic one instead applies to flexible bristles, buckling very easily when compressed.

Geometric effect   From (8.42), we obtain that, for the angular spring model, we have $\rho_+ > -\rho_-$, meaning that the friction opposing a rightward movement ($\dot{u} > 0$) is smaller than the one corresponding to a leftward movement ($\dot{u} < 0$). This is exactly what we expect by the with the nap/against the nap effect.

However, it is not obvious that a bristle should always behave as a rigid bar with an angular spring. Indeed, especially during strokes against the nap, the rod is subject to a longitudinal compression, that could produce buckling in a flexible bar, invalidating the model. An estimate of the axial tension along the bar, obtained by considering the limit case when the lower end of the bar moves on a flat surface experiencing dry friction, is

$$ T = -\frac{k}{L}(\vartheta^{\mathrm{lim}} - \vartheta^{\mathrm{rest}})\cot\vartheta^{\mathrm{lim}} + \frac{\rho_\pm}{\sin\vartheta^{\mathrm{lim}}} \tag{8.43} $$

where $\rho_\pm$ depends on the direction of motion. We observe that during a stroke against the nap (so $\rho_\pm = \rho_- < 0$) the bar is always compressed ($T < 0$), however this tension is small when the bristle oscillates near its rest position ($\vartheta^{\mathrm{lim}} \approx \vartheta^{\mathrm{rest}}$) and the friction coefficients are small. This situation suits well to the motion of a hard brush rubbed gently on a smooth surface.

Energetic effect   When the critical load for buckling is too low, the above description is no longer valid, but we can still apply the "angular spring" model when the bristle is subject to traction. The following interpretation of the with the nap/against the nap effect is based on such assumption.

When moved with the nap, the hair is rotated in the same direction of its rest angle, as shown in Figure 8.7(a), so that the angular spring is only slightly stretched. On the other hand, when the hair is moved against the nap, it is rotated in the opposite direction of its rest position, as shown in Figure 8.7(b); in this way the angular spring is much more stretched than in the previous case. Another way to describe this scenario is to notice that the tip of the hair is always behind its root, with respect to the direction of motion.

Hence, if we report both situations to the framework of our"angular spring" model (as done in Figure 8.7), we observe that the two cases share the same coefficient μ_+, while we have a change in the coefficient α, since the rest angle of the hair changes. In case of *with the nap* motion, the rest angle of the hair is $\vartheta_{\mathrm{with}} > 0$. On the other hand, the case of *against the nap* motion corresponds to $\vartheta_{\mathrm{against}} = -\vartheta_{\mathrm{with}} < 0$.

(a) *With the nap.*   (b) *Against the nap.*
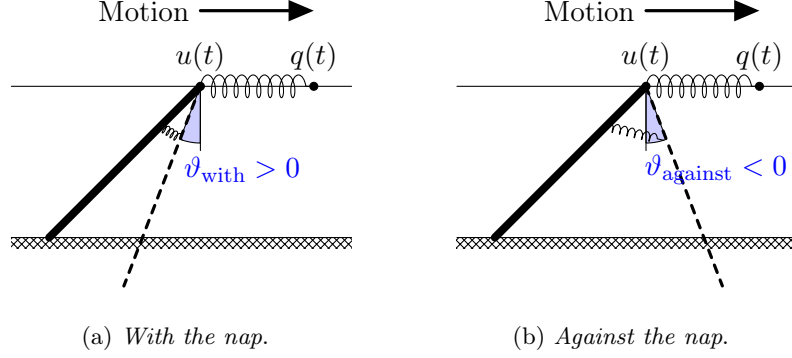
Figure 8.7: Energetic interpretation of the *with the nap/against the nap* asymmetry. The dashed line represent the rest angle of the bar.

In this way we can immediately recover the friction coefficients using (8.41) and (8.42). We get

$$\rho_{\text{with}} = \frac{\mu_+}{\tan \vartheta^{\text{lim}}}(\vartheta^{\text{lim}} - \vartheta_{\text{with}})$$
$$\rho_{\text{against}} = \frac{\mu_+}{\tan \vartheta^{\text{lim}}}(\vartheta^{\text{lim}} - \vartheta_{\text{against}}) = \frac{\mu_+}{\tan \vartheta^{\text{lim}}}(\vartheta^{\text{lim}} + \vartheta_{\text{with}})$$

where we trivially have $\rho_{\text{against}} > \rho_{\text{with}}$, in agreement with our common experience of the phenomenon.

We now analyse the compatibility of this interpretation with the tension of the bristle during the motion. We notice that, since in both phases we have $\rho_\pm = \rho_+$, the last term in (8.43) gives always a positive contribution to the tension. Thus, if the surface is quite rough (ρ_+ large) and the bristle flexible (k/L small), the rod is subject to traction, so that our model provides a good approximation.

We remark that this energetic interpretation requires a transitional phase, where the bristle is strongly deformed, to account for the change of configuration occurring when the direction of motion is inverted. Since we assume a small critical load and high friction, we expect this transition to be triggered by buckling when the direction is changed, and that, afterwards, a sufficiently long motion in same same direction restores the bristle to a stable straight state, as those we discussed above.

8.4   Convergence structure

The main issue in Section 8.2 is the change in the nature of the dissipation: in the approximating systems $(\mathcal{E}_\varepsilon, \mathcal{R}_\varepsilon)$ we have a viscous drag (i.e. the dissipation potential $\mathcal{R}_\varepsilon$ is quadratic), whereas in the limit system it is rate independent (i.e. the dissipation potential $\mathcal{R}_\varepsilon$ is positively homogeneous of degree 1). Such

a situation has been successfully addressed in continuum mechanics, showing that rate-independent plasticity can be obtained as limit of a chain of viscous bistable springs [MT12; PT05]. Here we follow the recent approach by Mielke [Mie12] (cf. also [Mie15]), based on the De Giorgi's $(\mathcal{R}, \mathcal{R}^*)$ formulation, also called *energy-dissipation principle*.

We begin by recalling some known facts about the Legendre transform (cf. for instance [RW98]).

Legendre transform and De Giorgi's $(\mathcal{R}, \mathcal{R}^*)$ formulation Let us consider a function $\Psi \colon \mathbb{R} \to \mathbb{R} \cup \{+\infty\}$ that is proper (i.e. not identically $+\infty$), lower semi-continuous and convex . The Legendre transform $\Psi^* \colon \mathbb{R} \to \mathbb{R} \cup \{+\infty\}$ of Ψ is defined as

$$\Psi^*(\xi) = \sup_{x \in X} \left[\xi x - \Psi(x) \right]$$

The function Ψ^* is proper, lower semi-continuous and convex; moreover we have $(\Psi^*)^* = \Psi$.

We now briefly recall some well-known properties of the Legendre transform. The Fenchel estimate states that, for every $x \in \mathbb{R}$ and $\xi \in X\mathbb{R}$, we have

$$\Psi(x) + \Psi^*(\xi) \geq \xi x \tag{8.44}$$

The case when the equality holds is characterized by the Legendre-Fenchel equivalence:

$$\xi \in \partial\Psi(x) \quad \Longleftrightarrow \quad x \in \partial\Psi^*(\xi) \quad \Longleftrightarrow \quad \Psi(x) + \Psi^*(\xi) = \xi x \tag{8.45}$$

Let us now consider the problem

$$0 \in \partial_{\dot{z}}\tilde{\mathcal{R}}(\dot{z}) + D_z\tilde{\mathcal{E}}(t, z) \tag{8.46}$$

where $\tilde{\mathcal{E}} \in \mathcal{C}^1([0, T] \times \mathbb{R}, \mathbb{R})$ and $\tilde{\mathcal{R}} \colon \mathbb{R} \to \mathbb{R}$ is a convex function. A solution of the problem is a function $z \colon [0, T] \to \mathbb{R}$ that satisfies (8.46) for almost every $t \in [0, T]$. Note that this framework covers both the wiggly systems (8.8) and the limit system (8.3).

Let us therefore define $\tilde{\mathcal{R}}^* \colon \mathbb{R} \to \mathbb{R} \cup \{+\infty\}$ as the Legendre transform of the function $\tilde{\mathcal{R}}$. First of all, let us notice that, by the Legendre-Fenchel equivalence (8.45), the inclusion (8.46) is equivalent to

$$\left(\dot{z}(t), -D_z\tilde{\mathcal{E}}(t, z(t)) \right) \in \tilde{\mathcal{C}}_{\Psi+\Psi^*} = \left\{ (x, \xi) \colon \Psi(x) + \Psi^*(\xi) = \xi x \right\} \tag{8.47}$$

De Giorgi's $(\mathcal{R}, \mathcal{R}^*)$ formulation of the problem consists in the following sufficient condition for being a solution of (8.46).

Proposition 8.4. *A function* $z\colon [0,T] \to \mathbb{R}$ *is a solution of* (8.46) *if and only if it satisfies*

$$\tilde{\mathcal{E}}(T, z(T)) + \int_0^T \left[\tilde{\mathcal{R}}(\dot{z}(s)) + \tilde{\mathcal{R}}^*\left(-D_z\tilde{\mathcal{E}}(s, z(s))\right)\right] \mathrm{d}s \leq$$

$$\leq \tilde{\mathcal{E}}(0, z(0)) + \int_0^T \partial_t\tilde{\mathcal{E}}(s, z(s))\, \mathrm{d}s \tag{8.48}$$

We now prove a slightly more general proposition, suitable to our purposes. Let us replace the integral dissipation term in the left-hand side of (8.48) with a term of the form

$$\tilde{\mathcal{D}}(z) = \int_0^T \tilde{\mathcal{M}}(\dot{z}(s), -D_z\tilde{\mathcal{E}}(s, z))\, \mathrm{d}s \tag{8.49}$$

where we require

$$\tilde{\mathcal{M}}(x, \xi) \geq \xi x \qquad \text{for every } x \in \mathbb{R},\ \xi \in \mathbb{R} \tag{8.50}$$

Moreover let us define the set

$$\tilde{\mathcal{C}}_{\mathcal{M}} = \left\{(x, \xi)\colon \tilde{\mathcal{M}}(x, \xi) = \xi x\right\} \tag{8.51}$$

Proposition 8.5. *A function* $z\colon [0,T] \to \mathbb{R}$ *satisfies*

$$\tilde{\mathcal{E}}(T, z(T)) + \tilde{\mathcal{D}}(z) \leq \tilde{\mathcal{E}}(0, z(0)) + \int_0^T \partial_t\tilde{\mathcal{E}}(s, z(s))\, \mathrm{d}s \tag{8.52}$$

if and only if it satisfies

$$\left(\dot{z}(t), -D_z\tilde{\mathcal{E}}(t, z(t))\right) \in \tilde{\mathcal{C}}_{\mathcal{M}} \qquad \text{for almost every } t \in [0,T] \tag{8.53}$$

Proof. Using the chain rule, we get that the estimate (8.52) is equivalent to

$$\int_0^T \tilde{\mathcal{M}}(\dot{z}(s), -D_z\tilde{\mathcal{E}}(s, z))\, \mathrm{d}s \leq -\int_0^T D_z\tilde{\mathcal{E}}(s, z(s))\dot{z}(s)\, \mathrm{d}s$$

Looking at estimate (8.50), we get that (8.52) is true if and only if equality in (8.50) holds for almost every $t \in [0,T]$. □

We remark that Proposition 8.5 applies to the case $\tilde{\mathcal{M}}(x, \xi) = \mathcal{R}(x) + \mathcal{R}^*(\xi)$. Thus Proposition 8.4 follows as an immediate corollary, since, as we have seen, the Legendre-Fenchel equivalence implies the equivalence between (8.46) and (8.47).

Convergence structure Our strategy to prove Theorem 8.1 is to consider the convergence of the systems only once they have been reformulated in the form (8.48).

Let us consider a family of energy functions $\mathcal{E}_\varepsilon \in \mathcal{C}^1([0,T] \times \mathbb{R}, \mathbb{R})$, and the corresponding dissipation functionals $\mathcal{D}_\varepsilon$ of the form

$$\mathcal{D}_\varepsilon(z) = \int_0^T \mathcal{M}_\varepsilon(\dot{z}(s), -D_z\mathcal{E}_\varepsilon(s,z)) \, ds \tag{8.54}$$

where $\mathcal{M}_\varepsilon(x,\xi) \geq \xi x$ for every $x \in \mathbb{R}$, $\xi \in \mathbb{R}$. We are given a family of functions $z_\varepsilon \colon [0,T] \to \mathbb{R}$ that solve the associated evolution problems, i.e. each z_ε satisfies the estimate

$$\mathcal{E}_\varepsilon(T, z(T)) + \mathcal{D}_\varepsilon(z) \leq \mathcal{E}_\varepsilon(0, z(0)) + \int_0^T \partial_t \mathcal{E}_\varepsilon(s, z(s)) \, ds \tag{8.55}$$

Then, we consider a limit energy function $\mathcal{E} \in \mathcal{C}^1([0,T] \times \mathbb{R}, \mathbb{R})$, and a limit dissipation functional $\mathcal{D}$ of the form

$$\mathcal{D}(z) = \int_0^T \mathcal{M}(\dot{z}(s), -D_z\mathcal{E}(s,z)) \, ds \tag{8.56}$$

where $\mathcal{M}(x,\xi) \geq \xi x$ for every $x \in \mathbb{R}$, $\xi \in \mathbb{R}$. We define

$$\mathcal{C}_\mathcal{M} = \{(x,\xi) \colon \mathcal{M}(x,\xi) = \xi x\} \tag{8.57}$$

Proposition 8.6. *Let $\mathcal{E}_\varepsilon, \mathcal{D}_\varepsilon, z_\varepsilon, \mathcal{E}$ and $\mathcal{D}$ be as above. Assume that there exists a continuous function $\bar{z} \colon [0,T] \to R$ such that $z_\varepsilon \to \bar{z}$ in $\mathcal{C}([0,T], \mathbb{R})$. Suppose that, for every $t \in [0,T]$, the following estimates hold*

$$\mathcal{E}(t, \bar{z}(t)) \leq \liminf_{\varepsilon \to 0} \mathcal{E}_\varepsilon(t, z_\varepsilon(t))$$

$$\partial_t \mathcal{E}(t, \bar{z}(t)) = \lim_{\varepsilon \to 0} \partial_t \mathcal{E}_\varepsilon(t, z_\varepsilon(t))$$

$$\mathcal{D}(\bar{z}) \leq \liminf_{\varepsilon \to 0} \mathcal{D}_\varepsilon(z_\varepsilon)$$

and moreover

$$\mathcal{E}(0, \bar{z}(0)) = \lim_{\varepsilon \to 0} \mathcal{E}_\varepsilon(0, z_\varepsilon(0)) \tag{8.58}$$

Then $\bar{z}$ is a solution of the problem

$$\left(\dot{\bar{z}}(t), -D_z\tilde{\mathcal{E}}(t, \bar{z}(t)) \right) \in \mathcal{C}_\mathcal{M} \qquad \text{for almost every } t \in [0,T] \tag{8.59}$$

Proof. The convergence assumptions, applied to (8.55), lead to the estimate

$$\mathcal{E}(T, \bar{z}(T)) + \mathcal{D}(\bar{z}) \leq \mathcal{E}(0, \bar{z}(0)) + \int_0^T \partial_t \mathcal{E}(s, \bar{z}(s)) \, ds \tag{8.60}$$

The thesis follows from Proposition 8.5. $\qquad\qquad\square$

8.5   Proof of Theorem 8.1

We now implement the convergence strategy of Section 8.4 to the situation described in Section 8.2, in order to prove Theorem 8.1. From now on the symbols $\mathcal{E}, \mathcal{E}_\varepsilon, \mathcal{R}, \mathcal{R}_\varepsilon$, etc. have the same properties and meaning considered in Section 8.2. In addition, we assume that the hypothesis (8.10) of Theorem 8.1 holds.

Our plan is to apply Proposition 8.6. To begin, we recall the definition (8.7) of $\mathcal{R}_\varepsilon$ and define $\mathcal{D}_\varepsilon$ and $\mathcal{M}_\varepsilon$ by setting

$$\mathcal{M}_\varepsilon(v, \xi) = \mathcal{R}_\varepsilon(v) + \mathcal{R}_\varepsilon^*(\xi) = \frac{\varepsilon^\gamma v^2}{2} + \frac{\xi^2}{2\varepsilon^\gamma} \tag{8.61}$$

By Proposition 8.4, each function z_ε satisfies the estimate (8.55).

The reformulation of the limit system requires a little more attention. Let us first define the set $\Omega_0 = [\rho_-, \rho_+]$ and denote, for any set $A \subseteq \mathbb{R}$,

$$\chi_A(\xi) = \begin{cases} 0 & \text{for } \xi \in A \\ +\infty & \text{for } \xi \notin A \end{cases} \tag{8.62}$$

To define the functions $\mathcal{D}$ and $\mathcal{M}$, instead of the trivial choice associated to De Giorgi's formulation of problem (8.3), we set

$$\mathcal{M}(v, \xi) = |v| \, K(\xi) + \chi_{\Omega_0}(\xi) \tag{8.63}$$

where

$$K(\xi) = \int_0^1 \left| \xi - W'(y) \right| \mathrm{d}y \tag{8.64}$$

Since W' is continuous, 1-periodic with zero average and has image Ω_0, we deduce that $K(\xi) > |\xi|$ if $\xi \in \operatorname{int} \Omega_0$, whereas $K(\xi) = |\xi|$ if $\xi \notin \operatorname{int} \Omega_0$. As a consequence, we obtain the desired estimate $\mathcal{M}(x, \xi) \geq \xi x$. Moreover we have

$$\mathcal{C}_\mathcal{M} = (\{0\} \times \Omega_0) \cup ((-\infty, 0) \times \{\rho_-\}) \cup ((0, +\infty) \times \{\rho_+\}) \tag{8.65}$$

Recalling the definition (8.2) of $\mathcal{R}$, we have $\mathcal{R}^*(\xi) = \chi_{\Omega_0}(\xi)$, and so $\mathcal{C}_\mathcal{M} = \mathcal{C}_{\mathcal{R}+\mathcal{R}^*}$. This means that, by Proposition 8.4, problem (8.59) is equivalent to (8.3).

To apply Proposition 8.6 and complete the proof of Theorem 8.1, it is left to prove

- the existence of a limit function $\bar{z}$, such that $z_\varepsilon \to \bar{z}$ in $\mathcal{C}([0, T], \mathbb{R})$;

- that the estimate $\mathcal{D}(\bar{z}) \leq \liminf_{\varepsilon \to 0} \mathcal{D}_\varepsilon(z_\varepsilon)$ holds.

These will be the subjects of the next two subsections.

Convergence of the solutions

Preliminary notation   Without loss of generality, we restrict our discussion to the interval $\varepsilon \in (0, \bar{\varepsilon}]$, where $\bar{\varepsilon}$ is sufficiently small to satisfy $\bar{\varepsilon} < \min\{1, \varepsilon_Q\}$. We set $\beta = \min\{1, \gamma\}$ and notice that, for the values of ε considered, we have $\varepsilon^\beta = \max\{\varepsilon, \varepsilon^\gamma\}$.

Let us also introduce the following notations for some recurrent constants. We call Λ_ℓ the Lipschitz constant of ℓ. By the uniform convexity of Φ, we can find a constant $\varphi > 0$ such that $\Phi''(z) > \varphi$ for all $z \in \mathbb{R}$. Since W and its first derivative are bounded, we denote

$$C_{W,0} = \|W\|_\infty \qquad\qquad C_{W,1} = \|W'\|_\infty$$

Strip of admissible solutions   Let us now define $\tilde{z}_\pm \colon [0, T] \to \mathbb{R}$ as

$$\tilde{z}_-(t) = (\Phi')^{-1}(\ell(t) - \rho_+) \qquad \tilde{z}_+(t) = (\Phi')^{-1}(\ell(t) - \rho_-) \qquad (8.66)$$

We recall that this definition is well-posed since, by the uniform convexity of Φ, Φ' is globally invertible and $\operatorname{Im}\Phi' = \mathbb{R}$. Since the image of ℓ is bounded, by compactness arguments, we also have

$$C_\pm = \max\{\|\dot{\tilde{z}}_+\|_\infty, \|\dot{\tilde{z}}_-\|_\infty\} < +\infty$$

We notice that condition (8.10) can be restated by writing $z^0 \in [\tilde{z}_-(0), \tilde{z}_+(0)]$. Moreover, looking carefully at the inclusion (8.3), we observe that the solution $\bar{z}$ is bounded between $\tilde{z}_-$ and $\tilde{z}_+$, and the current state can possibly change (i.e. $\dot{\bar{z}}(t) \neq 0$) only if $\bar{z} = \tilde{z}_-$ (and therefore $\dot{\bar{z}}(t) \geq 0$) or $\bar{z} = \tilde{z}_+$ (and therefore $\dot{\bar{z}}(t) \leq 0$). The strip $[\tilde{z}_-(t), \tilde{z}_+(t)]$ gives the evolution of the elastic domains of the limit system.

Hence, we define the distance at each time t of a solution z_ε of (8.8) from this region, by setting

$$\delta_\varepsilon(t) = \operatorname{dist}(z_\varepsilon(t), [\tilde{z}_-(t), \tilde{z}_+(t)])$$

Notice that (8.10) implies $\delta_\varepsilon(0) \to 0$ for $\varepsilon \to 0$.

Estimates on z_ε   Let us recall that, by (8.8), the solution z_ε satisfies

$$\varepsilon^\gamma \dot{z}_\varepsilon(t) = -\Phi'(z_\varepsilon(t)) - W'\left(\frac{z_\varepsilon(t)}{\varepsilon}\right) - \varepsilon Q'\left(\varepsilon; \frac{z_\varepsilon(t)}{\varepsilon}\right) + \ell(t) \qquad (8.67)$$

The value of $\delta_\varepsilon(t)$ is controlled by the following estimate.

Lemma 8.7. *There exists a constant $C_0 > 0$ such that, for every $t \in [0, T]$ and $\varepsilon \in (0, \bar{\varepsilon})$, we have*

$$\delta_\varepsilon(t) \leq \delta_\varepsilon(0)e^{-\varphi t/\varepsilon^\gamma} + \varepsilon^\beta C_0 \qquad (8.68)$$

Moreover, if $t \in [0, T]$ is such that $\delta_\varepsilon(t) > \varepsilon^\beta C_0$, we have that $\dot{\delta}_\varepsilon(t) < 0$.

Proof. If $z_\varepsilon(t) \in (\tilde{z}_-(t), \tilde{z}_+(t))$, then the estimate follows immediately. Let us now consider the case $z_\varepsilon(t) \geq \tilde{z}_+(t)$. We have

$$
\begin{aligned}
\varepsilon^\gamma \dot{\delta}_\varepsilon &= \varepsilon^\gamma \dot{z}_\varepsilon - \varepsilon^\gamma \dot{\tilde{z}}_+ \\
&\leq -\Phi'(z_\varepsilon) - W'\left(\frac{z}{\varepsilon}\right) - \varepsilon Q'\left(\varepsilon; \frac{z}{\varepsilon}\right) + \Phi'(\tilde{z}_+) + \rho_- + \varepsilon^\gamma C_\pm \\
&\leq -\Phi'(z_\varepsilon) + \Phi'(\tilde{z}_+) + \varepsilon C_{Q,1} + \varepsilon^\gamma C_\pm \\
&\leq -\varphi \delta_\varepsilon + \varepsilon C_{Q,1} + \varepsilon^\gamma C_\pm \\
&\leq -\varphi \delta_\varepsilon + C_1 \varepsilon^\beta
\end{aligned}
$$

where $C_1 = C_\pm + C_{Q,1}$. The same estimate can be obtained analogously in the case $z_\varepsilon(t) \geq \tilde{z}_+(t)$. Thus the required estimate for δ_ε follows, by a suitable application of Gronwall's Lemma, for with $C_0 = C_1/\varphi$. $\qquad\square$

Let us notice that, combining Lemma 8.7 with assumption (8.10) and the Lipschitz continuity of $\tilde{z}_\pm$, it can be shown that all the solutions z_ε are bounded within an interval $[z_{\min}, z_{\max}]$. By compactness, in this interval the function Φ' is Lipschitz continuous with Lipschitz constant $\Lambda_{\Phi'}$.

Lemma 8.8. *For every $C_2 > 0$, there exists $C_3 > 0$ such that, for every $\varepsilon \in (0, \bar{\varepsilon})$ and every solutions z_ε of (8.8), if*

$$
\delta_\varepsilon(t_0) \leq \varepsilon^\beta C_2 \qquad \text{for some } t_0 \in [0, T] \tag{8.69}
$$

then

$$
|z_\varepsilon(t) - z_\varepsilon(t_0)| \leq \varepsilon^\beta C_3 \qquad \text{for every } t \in I_\varepsilon^0 = [t_0, t_0 + \varepsilon^\beta] \cap [0, T]
$$

Proof. Let us set

$$
b_\varepsilon(z) = -\Phi'(z) - V_\varepsilon'(z)
$$

We plan to find two points ζ_- and ζ_+ such that

$$
z_\varepsilon(t_0) - \varepsilon^\beta C_3 \leq \zeta_- \leq z_\varepsilon(t_0) \leq \zeta_+ \leq z_\varepsilon(t_0) + \varepsilon^\beta C_3
$$

and, for every $t \in I_\varepsilon^0$,

$$
b_\varepsilon(\zeta_-) + \ell(t) > 0 \qquad \text{and} \qquad b_\varepsilon(\zeta_+) + \ell(t) < 0
$$

This last condition implies that every solution of (8.8) starting at t_0 inside the interval $[\zeta_-, \zeta_+]$ cannot cross its boundary in the time interval I_ε^0.

We present the proof only for ζ_+, since ζ_- can be found similarly. Let $y_+ \in \mathbb{R}$ be any point such that $W'(y_+) = \rho_+$; we will look for $\zeta_+ \in y_+ + \varepsilon \mathbb{Z}$, so that $W'(\zeta_+) = \rho_+$. We know that, for every $t \in I_\varepsilon^0$,

$$
\begin{aligned}
\ell(t) &\leq \ell(t_0) + \Lambda_\ell(t - t_0) \leq \Phi'(\tilde{z}_-(t_0)) + \rho_+ + \varepsilon^\beta \Lambda_\ell \\
&\leq \Phi'(z_\varepsilon(t_0)) + \varepsilon^\beta \Lambda_{\Phi'} C_2 + \rho_+ + \varepsilon^\beta \Lambda_\ell
\end{aligned}
$$

Thus we have

$$b_\varepsilon(\zeta_+) + \ell(t) \leq -\Phi'(\zeta_+) - \rho_+ + \varepsilon C_{Q,1} + \Phi'(z_\varepsilon(t_0)) + \varepsilon^\beta C_2 \Lambda_{\Phi'} + \rho_+ + \varepsilon^\beta \Lambda_\ell$$
$$\leq -(\zeta_+ - z_\varepsilon(t_0))\varphi + \varepsilon^\beta C_4$$

where $C_4 = C_{Q,1} + \Lambda_{\Phi'} C_2 + \Lambda_\ell$. Therefore we take the smallest value $\zeta_+ \in y_+ + \varepsilon\mathbb{Z}$ satisfying $\zeta_+ > z_\varepsilon(t_0) + \frac{\varepsilon^\beta C_4}{\varphi}$. This choice gives one part of the thesis with $C_3 = 1 + C_4/\varphi$.

We proceed similarly for ζ_- and conclude the proof. $\qquad\square$

Lemma 8.9. *There exists a constant $C > 0$ such that, for every $s, t \in [0, T]$, the following estimate holds:*

$$|z_\varepsilon(t) - z_\varepsilon(s)| \leq C(\delta_\varepsilon(0) + |t - s| + \varepsilon^\beta) \tag{8.70}$$

Proof. Using Lemma 8.7 we can characterize the possible behaviours of z_ε.

If $\delta_\varepsilon(0) \leq 2\varepsilon^\beta C_0$, then $\delta_\varepsilon(t) \leq 2\varepsilon^\beta C_0$ for every $t \in [0, T]$. In this case the assumptions (8.69) of Lemma 8.8 are satisfied for every $t_0 \in [0, T]$ by taking $C_2 = 2C_0$. Now, for every $s, t \in [0, T]$, we set $k \in \mathbb{N}$ such that $|t - s|/\varepsilon^\beta \leq k < |t - s|/\varepsilon^\beta + 1$. We can therefore construct a partition $s = \tau_0 < \tau_1 < \cdots < \tau_{k-1} < \tau_k = t$, such that, for every $i = 1, \dots, k$, we have $\tau_i - \tau_{i-1} < \varepsilon^\beta$. Thus we have

$$|z_\varepsilon(t) - z_\varepsilon(s)| \leq \sum_{i=1}^k |z_\varepsilon(\tau_i) - z_\varepsilon(\tau_{i-1})| \leq C_3 k \varepsilon^\beta \leq C_3(|t - s| + \varepsilon^\beta) \tag{8.71}$$

where C_3 is given by Lemma 8.8 and does not depend on ε.

On the other hand, if $\delta_\varepsilon(0) > 2\varepsilon^\beta C_0$, Lemma 8.7 shows that the solution z_ε monotonically gets closer to the strip $[\tilde{z}_-, \tilde{z}_+]$, and *possibly* at some time t_ε satisfies $\delta_\varepsilon(t_\varepsilon) = 2\varepsilon^\beta C_0$, so that $\delta_\varepsilon(t) \leq 2\varepsilon^\beta C_0$ for every $t \in [t_\varepsilon, T]$. For $s, t \in [0, t_\varepsilon]$ (or in $[0, T]$ if there is no such t_ε), we have the estimate

$$|z_\varepsilon(t) - z_\varepsilon(s)| \leq \delta_\varepsilon(0) + C_\pm |t - s| \tag{8.72}$$

If there is a $t_\varepsilon \in [0, T]$ as above, since $\delta_\varepsilon(t) \leq 2\varepsilon^\beta C_0$ for every $t \in [t_\varepsilon, T]$ we can proceed as in the first part of the proof and the estimate (8.71) holds for every $s, t \in [t_\varepsilon, T]$.

We set $C = C_3 + C_\pm + 1$ and the proof is completed by combining (8.71) and (8.72), possibly splitting the estimate in two parts if $s < t_\varepsilon < t$. $\qquad\square$

Convergence of the solutions z_ε By Lemma 8.9 we obtain the equicontinuity of the family of functions $z_\varepsilon \colon [0, T] \to \mathbb{R}$, for $\varepsilon \in (0, \bar{\varepsilon}]$. By the Ascoli-Arzelà Theorem we can find a subsequence $(z_{\varepsilon_i})_{i \in \mathbb{N}}$ with $\varepsilon_i \to 0$ for which there exists a continuous function $\bar{z} \colon [0, T] \to \mathbb{R}$ such that $z_{\varepsilon_i} \to \bar{z}$

uniformly in $\mathcal{C}([0,T])$. A second consequence of Lemma 8.9 is that $\bar{z}$ is Lipschitz continuous with constant C, that is $|\bar{z}(t) - \bar{z}(s)| < C\,|t - s|$ for every $s, t \in [0,T]$.

It remains to show that $\bar{z}$ is a solution of (8.3) and that actually the whole sequence z_ε converges to $\bar{z}$, not only a subsequence z_{ε_i}. We will address these issues in the last step of the proof.

Estimate on the dissipation functionals

Let us write

$$\eta_\varepsilon(t) = -\Phi'(z_\varepsilon(t)) + \ell(t)$$

$$u_\varepsilon(t) = W'\left(\frac{z_\varepsilon(t)}{\varepsilon}\right) + \varepsilon Q'\left(\varepsilon; \frac{z_\varepsilon(t)}{\varepsilon}\right)$$

$$\xi_\varepsilon(t) = \eta_\varepsilon(t) - u_\varepsilon(t)$$

Lemma 8.10. *Let $z_\varepsilon, \bar{z} \in W^{1,1}([0,T])$ and $\eta_\varepsilon, \bar{\eta} \in \mathcal{C}^0([0,T])$ be such that, for $\varepsilon \to 0$,*

$$z_\varepsilon \to \bar{z} \qquad \text{and} \qquad \eta_\varepsilon \to \bar{\eta} \qquad \text{in } \mathcal{C}^0([0,T]).$$

Then

$$\liminf_{\varepsilon \to 0} \int\limits_0^T \mathcal{M}_\varepsilon\big(\dot{z}_\varepsilon(t), \xi_\varepsilon(t)\big)\,\mathrm{d}t \geq \int\limits_0^T \mathcal{M}\big(\dot{\bar{z}}(t), \eta(t)\big)\,\mathrm{d}t \qquad (8.73)$$

Proof. Let us define the interval

$$\Omega_\varepsilon = [\rho_- - \varepsilon C_{Q,1}\,,\ \rho_+ + \varepsilon C_{Q,1}]$$

so that $u_\varepsilon \in \Omega_\varepsilon$ and $\Omega_0 = [\rho_-, \rho_+]$, as defined above. We recall that $\xi_\varepsilon = \eta_\varepsilon - u_\varepsilon$, implying $|\xi_\varepsilon| \geq \mathrm{dist}(\eta_\varepsilon, \Omega_\varepsilon)$.

We therefore obtain the following lower bound for $\mathcal{M}_\varepsilon$:

$$\begin{aligned}
\mathcal{M}_\varepsilon(v, \xi_\varepsilon) &= \frac{\varepsilon^\gamma v^2}{2} + \frac{(1 - \varepsilon^{\frac{\gamma}{2}})\xi_\varepsilon^2}{2\varepsilon^\gamma} + \frac{\varepsilon^{\frac{\gamma}{2}}\xi_\varepsilon^2}{2\varepsilon^\gamma} \\
&\geq (1 - \varepsilon^{\frac{\gamma}{2}})\,|v|\,|\xi_\varepsilon| + \frac{1}{2\varepsilon^{\frac{\gamma}{2}}}\left[\mathrm{dist}(\eta_\varepsilon, \Omega_\varepsilon)\right]^2
\end{aligned} \qquad (8.74)$$

We now derive two separate estimates for the two terms of the right hand side of (8.74).

For the second term, we observe that

$$\liminf_{\varepsilon \to 0} \frac{1}{2\varepsilon^{\frac{\gamma}{2}}}\left[\mathrm{dist}(\eta_\varepsilon, \Omega_\varepsilon)\right]^2 \geq \chi_{\Omega_0}(\eta) \qquad (8.75)$$

so, by Fatou's Lemma, we obtain

$$\liminf_{\varepsilon \to 0} \int_0^T \frac{1}{2\varepsilon^{\frac{\gamma}{2}}} \left[\mathrm{dist}(\eta_\varepsilon(t), \Omega_\varepsilon)\right]^2 \mathrm{d}t \geq \int_0^T \chi_{\Omega_0}(\eta(t)) \,\mathrm{d}t \tag{8.76}$$

To study the integral of the remaining term in (8.74), let us consider the integral

$$\mathcal{D}_\varepsilon^{(1)} = \int_0^T |\dot{z}_\varepsilon(t)| \, |\xi_\varepsilon(t)| \,\mathrm{d}t \tag{8.77}$$

We define, for every integer $n > (\bar{\varepsilon})^{-1}$ and $j \in \{1, 2, \ldots, n\}$, the time interval

$$I_j^n = \left[\frac{j-1}{n}T, \frac{j}{n}T\right) \tag{8.78}$$

to which we associate the value

$$h_j^n(y) = \inf\left\{\left|\eta_{\tilde{\varepsilon}}(s) - W'(y) - \tilde{\varepsilon}Q'(\tilde{\varepsilon}; y)\right|, \quad \text{for } s \in I_j^n, \, \tilde{\varepsilon} \in \left(0, \frac{1}{n}\right)\right\}$$

We remark that h_j^n is periodic with period 1. We also notice that, by definition, for every $t \in I_j^n$ and every $\varepsilon \in \left(0, \frac{1}{n}\right)$ we have $|\xi_\varepsilon(t)| > h_j^n\left(\frac{z_\varepsilon(t)}{\varepsilon}\right)$. Thus, for each $\varepsilon < \frac{1}{n}$,

$$\mathcal{D}_\varepsilon^{(1)} \geq \sum_{j=1}^n \int_{I_j^n} |\dot{z}_\varepsilon(t)| \, h_j^n\left(\frac{z_\varepsilon(t)}{\varepsilon}\right) \mathrm{d}t$$

Let us now consider the case $z(\frac{j-1}{n}T) < z(\frac{j}{n}T)$. We have

$$\int_{I_j^n} |\dot{z}_\varepsilon(t)| \, h_j^n\left(\frac{z_\varepsilon(t)}{\varepsilon}\right) \mathrm{d}t \geq \int_{z_\varepsilon(\frac{j-1}{n}T)}^{z_\varepsilon(\frac{j}{n}T)} h_j^n\left(\frac{z}{\varepsilon}\right) \mathrm{d}z$$

$$\xrightarrow{\varepsilon \to 0} \quad \left[z\left(\frac{j}{n}T\right) - z\left(\frac{j-1}{n}T\right)\right] \int_0^1 h_j^n(y) \,\mathrm{d}y$$

since, due to the periodicity of h_j^n, for $\varepsilon \to 0$ the integral of $h_j^n(z/\varepsilon)$ on a given interval tends to the integral of the average value of h_j^n. Arguing similarly for $z(\frac{j-1}{n}T) > z(\frac{j}{n}T)$, we get

$$\liminf_{\varepsilon \to 0} \int_{I_j^n} |\dot{z}_\varepsilon(t)| \, h_j^n\left(\frac{z_\varepsilon(t)}{\varepsilon}\right) \mathrm{d}t \geq \left|z\left(\frac{j}{n}T\right) - z\left(\frac{j-1}{n}T\right)\right| \int_0^1 h_j^n(y) \,\mathrm{d}y \tag{8.79}$$

Let z_n be the piecewise affine interpolant such that $z_n(\frac{j}{n}T) = z(\frac{j}{n}T)$ for every $j + 0, 1, \ldots, n$. We define $k_n(t)$ as the average of h_j^n, where j is the one such that $t \in I_j^n$, that means

$$k_n(t) = \int\limits_0^1 h_j^n(y) \, \mathrm{d}y \qquad \text{for } \frac{j-1}{n}T \le t < \frac{j}{n}T$$

Thus, summing the estimates (8.79) for $j + 1, \ldots, n$, we get

$$\liminf_{\varepsilon \to 0} \mathcal{D}_\varepsilon^{(1)} \ge \sum_{j=1}^n \left| z\left(\tfrac{j}{n}T\right) - z\left(\tfrac{j-1}{n}T\right) \right| \int\limits_0^1 h_j^n(y) \, \mathrm{d}y = \int\limits_0^T k_n(t) \, |\dot{z}_n(t)| \, \mathrm{d}t$$

Since we assumed that $z \in W^{1,1}([0,T])$, we know that $\dot{z}_n \to \dot{z}$ strongly in $L^1([0,T])$ for $n \to \infty$. Moreover, the uniform convergence $(\eta_\varepsilon, z_\varepsilon) \to (\eta, \bar{z})$ assures us that $k_n(t) \to K(\eta(t))$ uniformly. Thus we get

$$\liminf_{\varepsilon \to 0} \mathcal{D}_\varepsilon^{(1)} \ge \int\limits_0^T |\dot{z}(t)| \, K(\eta(t)) \, \mathrm{d}t \tag{8.80}$$

The proof is completed combining the estimates (8.76) and (8.80). $\qquad \square$

Completion of the proof

At the end of the first subsection of the proof, we have shown that there exist a subsequence $(z_{\varepsilon_i})_{i \in \mathbb{N}}$ with $\varepsilon_i \to 0$ and a continuous function $\bar{z} \colon [0,T] \to \mathbb{R}$ such that $z_{\varepsilon_i} \to \bar{z}$ uniformly in $\mathcal{C}([0,T])$. Setting $\bar{\eta}(t) = -\Phi'(\bar{z}(t)) + \ell(t)$, we can apply Lemma 8.10 to the subsequence z_{ε_i} and get that

$$\liminf_{i \to \infty} \mathcal{D}_{\varepsilon_i}(z_{\varepsilon_i}) \le \mathcal{D}(\bar{z})$$

We can therefore apply Proposition 8.6 to find that $\bar{z}$ is a solution of (8.59) for $\bar{z}(0) = z_0$ and so, as we have seen, of (8.3).

It is however well known in literature that problem (8.3) has only one solution for each choice of z_0 (cf. [Mie05; MR15]). This implies that actually the whole sequence z_ε converges to $\bar{z}$. Suppose by contradiction that there exists a subsequence $(z_{\varepsilon_k})_{k \in \mathbb{N}}$ with $\varepsilon_k \to 0$ such that $\|z_{\varepsilon_k} - \bar{z}\|_\infty > \bar{\delta}$, for some $\bar{\delta} > 0$ and every $k \ge 0$. Then we can repeat the same reasoning done for z_ε, to find a function $\hat{z} \in \mathcal{C}([0,T,])$, and a subsequence of z_{ε_k} that converges to $\hat{z}$. But, proceeding as above, $\hat{z}$ must be a solution of (8.59) with $\hat{z}(0) = z_0$, and so, because of the uniqueness of the solutions, $\hat{z} = \bar{z}$, contradicting $\|z_{\varepsilon_k} - \bar{z}\|_\infty > \bar{\delta}$.

To complete the proof, it remains only to prove (8.12). Let us first notice that, since (8.8) gives $\varepsilon^\gamma \dot{z}_\varepsilon(t) = \xi_\varepsilon(t)$, a straightforward computation shows

that $\mathcal{R}_\varepsilon(\dot{z}_\varepsilon(t)) = \mathcal{R}_\varepsilon^*(\xi_\varepsilon(t))$ for almost every $t \in [0, T]$. Moreover, since $\mathcal{R}_\varepsilon(\dot{z}_\varepsilon(t)) + \mathcal{R}_\varepsilon^*(\xi_\varepsilon(t)) = \dot{z}_\varepsilon(t)\xi_\varepsilon(t)$ for almost every t, by the chain rule we get, for every $0 \le t_1 < t_2 \le T$,

$$\int_{t_1}^{t_2} 2\mathcal{R}_\varepsilon(z_\varepsilon(s)) \, \mathrm{d}s = \mathcal{E}_\varepsilon(t_2, z_\varepsilon(t_2)) - \mathcal{E}_\varepsilon(t_1, z_\varepsilon(t_1)) + \int_{t_1}^{t_2} \dot{\ell}(s)z_\varepsilon(s) \, \mathrm{d}s$$

On the other hand, for the limit system, since $-D_z\mathcal{E}(t, \bar{z}(t)) \in \Omega_0$, it follows that $\mathcal{R}^*(-D_z\mathcal{E}(t, \bar{z}(t))) = 0$ for almost every $t \in [0, T]$. Thus, again by the chain rule

$$\int_{t_1}^{t_2} \mathcal{R}(\bar{z}(s)) \, \mathrm{d}s = \mathcal{E}(t_2, \bar{z}(t_2)) - \mathcal{E}(t_1, \bar{z}(t_1)) + \int_{t_1}^{t_2} \dot{\ell}(s)\bar{z}(s) \, \mathrm{d}s$$

Since, for $\varepsilon \to 0$, we have $z_\varepsilon \to \bar{z}$ uniformly and $\mathcal{E}_\varepsilon(t, z_\varepsilon(t)) \to \mathcal{E}(t, \bar{z}(t))$ for every $t \in [0, T]$, it follows that

$$\int_{t_1}^{t_2} 2\mathcal{R}_\varepsilon(\dot{z}_\varepsilon(s)) \, \mathrm{d}s \to \int_{t_1}^{t_2} \mathcal{R}(\dot{\bar{z}}(s)) \, \mathrm{d}s \qquad \text{for every } 0 \le t_1 < t_2 \le T$$

and the proof is complete.

Bibliography

Bibliography of Part I

[Abb01]   A. Abbondandolo. *Morse theory for Hamiltonian systems*. CRC Press, 2001.

[AC84]   J.-P. Aubin and A. Cellina. *Differential inclusions*. Set-valued maps and viability theory. Springer-Verlag, Berlin, 1984.

[ACE87]   A. Ambrosetti, V. Coti Zelati, and I. Ekeland. "Symmetry breaking in Hamiltonian systems". *Journal of differential equations* 67.2 (1987), pp. 165–184.

[AKN06a]   V. I. Arnold, V. V. Kozlov, and A. I. Neishtadt. *Mathematical aspects of classical and celestial mechanics*. Third edition. Vol. 3. Encyclopaedia of Mathematical Sciences. [Dynamical systems. III], Translated from the Russian original by E. Khukhro. Springer-Verlag, Berlin, 2006.

[Alb07]   J. Albrecht. "On the existence of invariant tori in nearly-integrable Hamiltonian systems with finitely differentiable perturbations". *Regular and Chaotic Dynamics. International Scientific Journal* 12.3 (2007), pp. 281–320.

[Ama82]   H. Amann. "A note on degree theory for gradient mappings". *Proceedings of the American Mathematical Society* 85.4 (1982), pp. 591–595.

[AO98]   J. Alonso and R. Ortega. "Roots of Unity and Unbounded Motions of an Asymmetric Oscillator". *Journal of Differential Equations* 143.1 (1998), pp. 201–220.

[Are07]   H. Aref. "Point vortex dynamics: a classical mathematics playground". *Journal of Mathematical Physics* 48.6 (2007), pp. 065401, 23.

[AZ80]   H. Amann and E. Zehnder. "Nontrivial solutions for a class of nonresonance problems and applications to nonlinear differential equations". *Annali della Scuola Normale Superiore di Pisa-Classe di Scienze* 7.4 (1980), pp. 539–603.

[BB05]   D. Bambusi and M. Berti. "A Birkhoff-Lewis-type theorem for some Hamiltonian PDEs". *SIAM Journal on Mathematical Analysis* 37.1 (2005), 83–102 (electronic).

[BBV04]   M. Berti, L. Biasco, and E. Valdinoci. "Periodic orbits close to elliptic tori and applications to the three-body problem". *Annali della Scuola Normale Superiore di Pisa. Classe di Scienze. Serie V* 3.1 (2004), pp. 87–138.

[BCW05]   D. Blackmore, J. Champanerkar, and C. Wang. "A generalized Poincaré-Birkhoff theorem with applications to coaxial vortex ring motion". *Discrete and Continuous Dynamical Systems B* 5 (2005), pp. 15–48.

[BD10]   L. Biasco and L. Di Gregorio. "A Birkhoff-Lewis type theorem for the nonlinear wave equation". *Archive for Rational Mechanics and Analysis* 196.1 (2010), pp. 303–362.

[Ben05]   G. Benettin. "The elements of Hamiltonian perturbation theory". In: *Hamiltonian systems and Fourier analysis*. Adv. Astron. Astrophys. Camb. Sci. Publ., Cambridge, 2005, pp. 1–98.

[Bes00]   U. Bessi. "An analytic counterexample to the KAM theorem". *Ergodic Theory and Dynamical Systems* 20.2 (2000), pp. 317–333.

[BGG85]   G. Benettin, L. Galgani, and A. Giorgilli. "Poincaré's nonexistence theorem and classical perturbation theory for nearly integrable Hamiltonian systems". In: *Advances in nonlinear dynamics and stochastic processes (Florence, 1985)*. World Sci. Publishing, Singapore, 1985, pp. 1–22.

[BK87]   D. Bernstein and A. Katok. "Birkhoff periodic orbits for small perturbations of completely integrable Hamiltonian systems with convex Hamiltonians". *Inventiones Mathematicae* 88.2 (1987), pp. 225–241.

[BK97]   H. Ben-El-Mechaiekh and W. Kryszewski. "Equilibria of set-valued maps on nonconvex domains". *Transactions of the American Mathematical Society* 349.10 (1997), pp. 4159–4179.

[BL34]   G. D. Birkhoff and D. C. Lewis. "On the periodic motions near a given periodic motion of a dynamical system". *Annali di Matematica Pura ed Applicata* 12.1 (1934), pp. 117–133.

[Bla08]   D. Blackmore. "Nonintegrable perturbations of two vortex dynamics". In: *IUTAM Symposium on Hamiltonian Dynamics, Vortex Structures, Turbulence*. Springer. 2008, pp. 331–340.

[BO14]   A. Boscaggin and R. Ortega. "Monotone twist maps and periodic solutions of systems of Duffing type". *Mathematical Proceedings of the Cambridge Philosophical Society* 157.2 (2014), pp. 279–296.

[Bos11]   A. Boscaggin. "Subharmonic solutions of planar Hamiltonian systems: a rotation number approach". *Advanced Nonlinear Studies* 11.1 (2011), pp. 77–103.

[BTK07]   D. Blackmore, L. Ting, and O. Knio. "Studies of perturbed three vortex dynamics". *Journal of Mathematical Physics* 48.6 (2007), pp. 065402, 30.

[Car82]   P. H. Carter. "An improvement of the Poincaré-Birkhoff fixed point theorem". *Transactions of the American Mathematical Society* 269.1 (1982), pp. 285–299.

[CC07]   A. Celletti and L. Chierchia. "KAM stability and celestial mechanics". *Memoirs of the American Mathematical Society* 187.878 (2007).

[Cel10]   A. Celletti. *Stability and chaos in celestial mechanics*. Springer-Verlag, Berlin; published in association with Praxis Publishing Ltd., Chichester, 2010.

[Cha89]   K.-C. Chang. "On the periodic nonlinearity and the multiplicity of solutions". *Nonlinear Analysis. Theory, Methods and Applications* 13.5 (1989), pp. 527–537.

[Che92]   W. F. Chen. "Birkhoff periodic orbits for small perturbations of completely integrable Hamiltonian systems with nondegenerate Hessian". In: *Twist mappings and their applications*. Vol. 44. IMA Vol. Math. Appl. Springer, New York, 1992, pp. 87–94.

[Chi87]   C. Chicone. "The monotonicity of the period function for planar Hamiltonian vector fields". *Journal of Differential Equations* 69.3 (1987), pp. 310–321.

[ĆK06]   A. Ćwiszewski and W. Kryszewski. "The constrained degree and fixed-point index theory for set-valued maps". *Nonlinear Analysis, Theory, Methods and Applications* 64.12 (2006), pp. 2643–2664.

[Cla90]   F. H. Clarke. *Optimization and nonsmooth analysis*. Second edition. Society for Industrial and Applied Mathematics (SIAM), Philadelphia, PA, 1990.

[CZ83a]   C. C. Conley and E. Zehnder. "The Birkhoff-Lewis fixed point theorem and a conjecture of V. I. Arnold". *Inventiones Mathematicae* 73.1 (1983), pp. 33–49.

[CZ83b]   C. Conley and E. Zehnder. "An index theory for periodic solutions of a Hamiltonian system". In: *Geometric dynamics (Rio de Janeiro, 1981)*. Vol. 1007. Lecture Notes in Math. Springer, Berlin, 1983, pp. 132–145.

[CZ84]   C. Conley and E. Zehnder. "Morse-type index theory for flows and periodic solutions for Hamiltonian Equations". *Communications on pure and applied mathematics* 37.2 (1984), pp. 207–253.

[Dan84]   E. Dancer. "Degenerate Critical Points, Homotopy Indices and Morse Inequalities". *Journal fur die Reine und Angewandte Mathematik* 1984.350 (1984), pp. 1–22.

[Din83]   W. Y. Ding. "A generalization of the Poincaré-Birkhoff theorem". *Proceedings of the American Mathematical Society* 88.2 (1983), pp. 341–346.

[DKV09]   S. Derivière, T. Kaczynski, and P.-O. Vallerand-Beaudry. "On the decomposition and local degree of multiple saddles". *Annales des Sciences Mathématiques du Québec* 33.1 (2009), pp. 45–62.

[DR02]   F. Dalbono and C. Rebelo. "Poincaré-Birkhoff fixed point theorem and periodic solutions of asymptotically linear planar Hamiltonian systems". *Università e Politecnico di Torino. Seminario Matematico. Rendiconti* 60.4 (2002), pp. 233–263.

[Dum14]   H. S. Dumas. *The KAM story.* A friendly introduction to the content, history, and significance of classical Kolmogorov-Arnold-Moser theory. World Scientific Publishing Co. Pte. Ltd., Hackensack, NJ, 2014.

[Eke83]   I. Ekeland. "A perturbation theory near convex Hamiltonian systems". *Journal of Differential Equations* 50.3 (1983), pp. 407–440.

[Fel92]   P. L. Felmer. "Periodic solutions of spatially periodic Hamiltonian systems". *Journal of Differential Equations* 98.1 (1992), pp. 143–168.

[FF05]   C. Fabry and A. Fonda. "Unbounded motions of perturbed isochronous hamiltonian systems at resonance". *Advanced Nonlinear Studies* 5.3 (2005), pp. 351–373.

[FG15]   A. Fonda and P. Gidoni. "A permanence theorem for local dynamical systems". *Nonlinear Analysis. Theory, Methods and Applications* 121 (2015), pp. 73–81.

[FG16a]   A. Fonda and P. Gidoni. "An avoiding cones condition for the Poincaré-Birkhoff Theorem," *submitted, preprint available at* `http : / / www . dmi . units . it / pubblicazioni / Quaderni_ Matematici / 647_ 2016 . pdf` (2016).

[FG16b]   A. Fonda and P. Gidoni. "Generalizing the Poincaré–Miranda theorem: the avoiding cones condition". *Annali di Matematica Pura ed Applicata. Series IV* 195.4 (2016), pp. 1347–1371.

[FGG16]   A. Fonda, M. Garrione, and P. Gidoni. "Periodic perturbations of Hamiltonian systems". *Advances in Nonlinear Analysis* to appear (2016).

[FM06]   A. Fonda and J. Mawhin. "Planar differential systems at reso-
           nance". *Advances in Differential Equations* 11.10 (2006), pp. 1111–
           1133.

[Fou+94]   G. Fournier et al. "Limit relative category and critical point
           theory". In: *Dynamics Reported.* Springer, 1994, pp. 1–24.

[Fra88]   J. Franks. "Generalizations of the Poincaré-Birkhoff theorem".
           Annals of Mathematics. Second Series 128.1 (1988), pp. 139–151.

[FS14]   A. Fonda and A. Sfecci. "Multiple periodic solutions of Hamilto-
           nian systems confined in a box". *submitted* (2014).

[FSZ12]   A. Fonda, M. Sabatini, and F. Zanolin. "Periodic solutions of
           perturbed Hamiltonian systems in the plane by the use of the
           Poincaré-Birkhoff theorem". *Topological Methods in Nonlinear
           Analysis* 40.1 (2012), pp. 29–52.

[FU13]   A. Fonda and A. J. Ureña. "On the higher dimensional Poincaré –
           Birkhoff theorem for Hamiltonian flows. 1. The indefinite twist."
           preprint available online. 2013.

[FU14]   A. Fonda and A. J. Ureña. "On the higher dimensional Poincaré–
           Birkhoff theorem for Hamiltonian flows. 2. The avoiding rays
           condition" (2014).

[FU16a]   A. Fonda and A. J. Ureña. "A higher dimensional Poincaré–
           Birkhoff theorem for Hamiltonian flows". *Annales de l'Institut
           Henri Poincare (C) Non Linear Analysis* (to appear 2016).

[FU16b]   A. Fonda and A. J. Ureña. "A higher-dimensional Poincaré-
           Birkhoff theorem without monotone twist". *Comptes Rendus
           Mathématique. Académie des Sciences. Paris* 354.5 (2016), pp. 475–
           479.

[FZ97]   A. Fonda and F. Zanolin. "Periodic oscillations of forced pendu-
           lums with very small length". *Proceedings of the Royal Society of
           Edinburgh. Section A. Mathematics* 127.1 (1997), pp. 67–76.

[GGJ10]   A. Garijo, A. Gasull, and X. Jarque. "A note on the period
           function for certain planar vector fields". *Journal of Difference
           Equations and Applications* 16 (2010), pp. 631–645.

[GH96]   M. Giaquinta and S. Hildebrandt. *Calculus of variations. II.* The
           Hamiltonian formalism. Springer-Verlag, Berlin, 1996.

[Gui97]   L. Guillou. "A simple proof of P. Carter's theorem". *Proceedings
           of the American Mathematical Society* 125.5 (1997), pp. 1555–
           1559.

[Had81]   G. Haddad. "Topological properties of the sets of solutions for
           functional differential inclusions". *Nonlinear Analysis* 5.12 (1981),
           pp. 1349–1366.

[Her83] M.-R. Herman. *Sur les courbes invariantes par les difféomorphismes de l'anneau. Vol. 1.* Vol. 103. Astérisque. Société Mathématique de France, Paris, 1983.

[HZ94] H. Hofer and E. Zehnder. *Symplectic invariants and Hamiltonian dynamics.* Birkhäuser Verlag, Basel, 1994.

[IJ05] A. Idzik and K. Junosza-Szaniawski. "Combinatorial lemmas for polyhedrons". *Discussiones Mathematicae. Graph Theory* 25.1-2 (2005), pp. 95–102.

[Jac76] H. Jacobowitz. "Periodic solutions of $x'' + f(x,t) = 0$ via the Poincaré-Birkhoff theorem". *Journal of Differential Equations* 20.1 (1976).

[Kra68] M. A. Krasnosel'skii. *The operator of translation along the trajectories of differential equations.* Translations of Mathematical Monographs, Vol. 19. Translated from the Russian by Scripta Technica. American Mathematical Society, Providence, R.I., 1968.

[Kry05] W. Kryszewski. "On the existence of equilibria and fixed points of maps under constraints". In: *Handbook of topological fixed point theory.* Springer, Dordrecht, 2005, pp. 783–866.

[LeC11] P. LeCalvez. "About Poincaré-Birkhoff theorem". *Publicaciones Matemáticas del Uruguay* 13 (2011), pp. 61–98.

[Liu89] J. Q. Liu. "A generalized saddle point theorem". *Journal of Differential Equations* 82.2 (1989), pp. 372–385.

[LL92] E. A. Lacomba and J. Llibre. "Integrals, invariant manifolds, and degeneracy for central force problems in $\mathbf{R}^n$". *Journal of Mathematical Physics* 33.6 (1992), pp. 2138–2147.

[Lon02] Y. Long. *Index theory for symplectic for symplectic paths with applications.* Vol. 207. Springer, 2002.

[LW10] P. LeCalvez and J. Wang. "Some remarks on the Poincaré-Birkhoff theorem". *Proceedings of the American Mathematical Society* 138.2 (2010), pp. 703–715.

[Maw13] J. Mawhin. "Variations on some finite-dimensional fixed-point theorems". *Ukrainian Mathematical Journal* 65.2 (2013), pp. 294–301.

[MM74] L. Markus and K. R. Meyer. *Generic Hamiltonian dynamical systems are neither integrable nor ergodic.* Memoirs of the American Mathematical Society, No. 144. American Mathematical Society, Providence, R.I., 1974.

[Mos86] J. Moser. "Recent developments in the theory of Hamiltonian systems". *SIAM Review. A Publication of the Society for Industrial and Applied Mathematics* 28.4 (1986), pp. 459–485.

[MP85]   R. S. MacKay and I. C. Percival. "Converse KAM: theory and practice". *Communications in Mathematical Physics* 98.4 (1985), pp. 469–512.

[MRZ02]   A. Margheri, C. Rebelo, and F. Zanolin. "Maslov index, Poincaré-Birkhoff theorem and periodic solutions of asymptotically linear planar Hamiltonian systems". *Journal of Differential Equations* 183.2 (2002), pp. 342–367.

[MU07]   R. Martins and A. J. Ureña. "The star-shaped condition on Ding's version of the Poincaré-Birkhoff theorem". *Bulletin of the London Mathematical Society* 39.5 (2007), pp. 803–810.

[MZ05]   J. Moser and E. J. Zehnder. *Notes on dynamical systems.* New York University, Courant Institute of Mathematical Sciences, New York; American Mathematical Society, Providence, RI, 2005.

[New01]   P. K. Newton. *The N-vortex problem.* Springer-Verlag, New York, 2001.

[Poi92]   H. J. Poincaré. *Les Méthodes nouvelle de la méchanique céleste.* Paris: Gauthier-Villars et fils, 1892.

[PZ01]   M. A. Pinsky and A. A. Zevin. "Monotonicity criteria for an energy-period function in planar Hamiltonian systems". *Nonlinearity* 14 (2001), pp. 1425–1432.

[Rab86]   P. H. Rabinowitz. *Minimax methods in critical point theory with applications to differential equations.* Published for the Conference Board of the Mathematical Sciences, Washington, DC; by the American Mathematical Society, Providence, RI, 1986.

[Reb97]   C. Rebelo. "A note on the Poincaré-Birkhoff fixed point theorem and periodic solutions of planar systems". *Nonlinear Analysis. Theory, Methods and Applications* 29.3 (1997), pp. 291–311.

[Rob70]   R. C. Robinson. "Generic properties of conservative systems". *American Journal of Mathematics* 92 (1970), pp. 562–603.

[RW98]   R. T. Rockafellar and R. J.-B. Wets. *Variational analysis.* Springer-Verlag, Berlin, 1998.

[Ryb87]   K. P. Rybakowski. *The homotopy index and partial differential equations.* Universitext. Springer-Verlag, Berlin, 1987.

[Sal04]   D. A. Salamon. "The Kolmogorov-Arnold-Moser theorem". *Mathematical Physics Electronic Journal* 10 (2004). Paper 3.

[Sel73]   G. R. Sell. "Differential equations without uniqueness and classical topological dynamics". *Journal of Differential Equations* 14 (1973), pp. 42–56.

[Sie54]   C. L. Siegel. "Über die Existenz einer Normalform analytischer Hamiltonscher Differentialgleichungen in der Nähe einer Gleichgewichtslösung". *Mathematische Annalen* 128 (1954), pp. 144–170.

[Srz85]   R. Srzednicki. "On rest points of dynamical systems". *Polska Akademia Nauk. Fundamenta Mathematicae* 126.1 (1985), pp. 69–81.

[Szu90]   A. Szulkin. "A relative category and applications to critical point theory for strongly indefinite functionals". *Nonlinear Analysis. Theory, Methods and Applications* 15.8 (1990), pp. 725–739.

[Szu92]   A. Szulkin. "Cohomology and Morse theory for strongly indefinite functionals". *Mathematische Zeitschrift* 209.3 (1992), pp. 375–418.

[Tre89]   D. V. Treshchëv. "A mechanism for the destruction of resonance tori in Hamiltonian systems". *Matematicheskiĭ Sbornik* 180.10 (1989), pp. 1325–1346, 1439.

[Wil87]   M. Willem. "Perturbations of nondegenerate periodic orbits of Hamiltonian systems". In: *Periodic solutions of Hamiltonian systems and related topics (Il Ciocco, 1986)*. Vol. 209. NATO Adv. Sci. Inst. Ser. C Math. Phys. Sci. Reidel, Dordrecht, 1987, pp. 261–265.

Bibliography of Part II

[AD11]   V. Agostiniani and A. DeSimone. "Γ-convergence of energies for nematic elastomers in the small strain limit". *Continuum Mechanics and Thermodynamics* 23.3 (2011), pp. 257–274.

[AD12]   V. Agostiniani and A. DeSimone. "Ogden-type energies for nematic elastomers". *International Journal of Non-Linear Mechanics* 47.2 (2012), pp. 402–412.

[AD14]   M. Arroyo and A. DeSimone. "Shape control of active surfaces inspired by the movement of euglenids". *Journal of the Mechanics and Physics of Solids* 62.1 (2014), pp. 99–112.

[ADL08]   F. Alouges, A. DeSimone, and A. Lefebvre. "Optimal strokes for low reynolds number swimmers: An example". *Journal of Nonlinear Science* 18.3 (2008), pp. 277–302.

[AKN06b]   V. I. Arnold, V. V. Kozlov, and A. I. Neishtadt. *Mathematical aspects of classical and celestial mechanics*. Third. Vol. 3. Encyclopaedia of Mathematical Sciences. [Dynamical systems. III], Translated from the Russian original by E. Khukhro. Springer-Verlag, Berlin, 2006.

[Ale03]   R. M. Alexander. *Principles of animal locomotion*. Princeton University Press, 2003.

[Ale16]   R. Alessi. "Energetic formulation for rate-independent processes: remarks on discontinuous evolutions with a simple example". *Acta Mechanica* (2016), pp. 1–25.

[Alo+13a]   F. Alouges et al. "Optimally swimming stokesian robots". *Discrete and Continuous Dynamical Systems - Series B* 18.5 (2013), pp. 1189–1215.

[Alo+13b]   F. Alouges et al. "Self-propulsion of slender micro-swimmers by curvature control: N-link swimmers". *International Journal of Non-Linear Mechanics* 56 (2013), pp. 132–141.

[Arr+12a]   M. Arroyo et al. "Reverse engineering the euglenoid movement". *Proceedings of the National Academy of Sciences* 109.44 (2012), pp. 17874–17879.

[Arr+12b]   M. Arroyo et al. "Reverse engineering the euglenoid movement". *Proceedings of the National Academy of Sciences of the United States of America* 109.44 (2012), pp. 17874–17879.

[AS08]   F. Al-Bender and J. Swevers. "Characterization of friction force dynamics". *IEEE Control Systems* 28.6 (2008), pp. 64–81.

[BTW93]   P. Bladon, E. Terentjev, and M. Warner. "Transitions and instabilities in liquid crystal elastomers". *Physical Review E* 47.6 (1993), R3838–R3840.

[Can+95]   C. Canudas De Wit et al. "A new model for control of systems with friction". *IEEE Transactions on automatic control* 40.3 (1995), pp. 419–425.

[Car+11]   L. Cardamone et al. "Cytoskeletal actin networks in motile cells are critically self-organized systems synchronized by mechanical interactions". *Proceedings of the National Academy of Sciences of the United States of America* 108.34 (2011), pp. 13978–13983.

[CBH05]   B. Chan, N. Balmforth, and A. Hosoi. "Building a better snail: Lubrication and adhesive locomotion". *Physics of Fluids* 17.11 (2005), pp. 1–10.

[CCD15]   M. Chaudhury, A. Chakrabarti, and S. Daniel. "Generation of Motion of Drops with Interfacial Contact". *Langmuir* 31.34 (2015), pp. 9266–9281.

[CD11]   P. Cesana and A. DeSimone. "Quasiconvex envelopes of energies for nematic elastomers in the small strain regime and applications". *Journal of the Mechanics and Physics of Solids* 59.4 (2011), pp. 787–803.

[CD15]   G. Cicconofri and A. DeSimone. "Motility of a model bristle-bot: A theoretical analysis". *International Journal of Non-Linear Mechanics* 76 (2015), pp. 233–239.

[CDD02a]   S. Conti, A. DeSimone, and G. Dolzmann. "Semisoft elasticity and director reorientation in stretched sheets of nematic elastomers". *Physical Review E - Statistical, Nonlinear, and Soft Matter Physics* 66.6 (2002), pp. 061710/1–061710/8.

[CDD02b]   S. Conti, A. DeSimone, and G. Dolzmann. "Soft elastic response of stretched sheets of nematic elastomers: A numerical study". *Journal of the Mechanics and Physics of Solids* 50.7 (2002), pp. 1431–1451.

[DB11]   B. Drinčić and D. S. Bernstein. "A sudden-release bristle model that exhibits hysteresis and stick-slip friction". In: *Proceedings of the 2011 American Control Conference*. IEEE. 2011, pp. 2456–2461.

[DD00]   A. DeSimone and G. Dolzmann. "Material instabilities in nematic elastomers". *Physica D: Nonlinear Phenomena* 136.1 (2000), pp. 175–191.

[DD02]   A. DeSimone and G. Dolzmann. "Macroscopic response of nematic elastomers via relaxation of a class of SO(3)-invariant energies". *Archive for Rational Mechanics and Analysis* 161.3 (2002), pp. 181–204.

[Den80]   M. Denny. "The role of gastropod pedal mucus in locomotion". *Nature* 285.5761 (1980), pp. 160–161.

[DeS+13]   A. DeSimone et al. "Crawlers in viscous environments: Linear vs non-linear rheology". *International Journal of Non-Linear Mechanics* 56 (2013), pp. 142–147.

[DeS99]   A. DeSimone. "Energetics of fine domain structures". *Ferroelectrics* 222.1 (1999), pp. 275–284.

[DGN15]   A. DeSimone, P. Gidoni, and G. Noselli. "Liquid crystal elastomer strips as soft crawlers". *Journal of the Mechanics and Physics of Solids* 84 (2015), pp. 254–272.

[Dre+05]   R. Dreyfus et al. "Microscopic artificial swimmers". *Nature* 437.7060 (2005), pp. 862–865.

[DT09]   A. DeSimone and L. Teresi. "Elastic energies for nematic elastomers". *European Physical Journal E* 29.2 (2009), pp. 191–204.

[DT12]   A. DeSimone and A. Tatone. "Crawling motility through the analysis of model locomotors: Two case studies". *European Physical Journal E* 35.9 (2012).

[FT04]   D. Fletcher and J. Theriot. "An introduction to cell motility for the physical scientist." *Physical biology* 1.1 (2004), T1–10.

[GD16a]   P. Gidoni and A. DeSimone. "On the genesis of directional friction through bristle-like mediating elements". *arXiv preprint arXiv:1602.05611* (2016).

[GD16b]   P. Gidoni and A. DeSimone. "Stasis domains and slip surfaces in the locomotion of a bio-inspired two-segment crawler". *Meccanica* (2016), to appear.

[GF09]   A. Ghost and P. Fischer. "Controlled propulsion of artificial magnetic nanostructured propellers". *Nano Letters* 9.6 (2009), pp. 2243–2245.

[GND14]   P. Gidoni, G. Noselli, and A. DeSimone. "Crawling on directional surfaces". *International Journal of Non-Linear Mechanics* 61 (2014), pp. 65–73.

[HF91]   D. A. Haessig and B. Friedland. "On the modeling and simulation of friction". *Journal of Dynamic Systems, Measurement, and Control* 113.3 (1991), pp. 354–362.

[HSD12]   M. Hancock, K. Sekeroglu, and M. Demirel. "Bioinspired directional surfaces for adhesion, wetting, and transport". *Advanced Functional Materials* 22.11 (2012), pp. 2223–2234.

[KLT13]   S. Kim, C. Laschi, and B. Trimmer. "Soft robotics: A bioinspired evolution in robotics". *Trends in Biotechnology* 31.5 (2013), pp. 287–294.

[KS04]   M. Kwak and H. Shindo. "Frictional force microscopic detection of frictional asymmetry and anisotropy at $(10\bar{1}4)$ surface of calcite". *Physical Chemistry Chemical Physics* 6.1 (2004), pp. 129–133.

[Lai+10]   J. Lai et al. "The mechanics of the adhesive locomotion of terrestrial gastropods". *Journal of Experimental Biology* 213.22 (2010), pp. 3920–3933.

[Lil+98]   M. Liley et al. "Friction anisotropy and asymmetry of a compliant monolayer induced by a small molecular tilt". *Science* 280.5361 (1998), pp. 273–275.

[Man+14]   T. Manwell et al. "Elastic mesh braided worm robot for locomotive endoscopy". In: *2014 36th Annual International Conference of the IEEE Engineering in Medicine and Biology Society*. IEEE. 2014, pp. 848–851.

[Mar+13]   M. Marchetti et al. "Hydrodynamics of soft active matter". *Reviews of Modern Physics* 85.3 (2013), pp. 1143–1189.

[MD15]   A. Montino and A. DeSimone. "Three-sphere low-Reynolds-number swimmer with a passive elastic arm". *The European Physical Journal E* 38.5 (2015), pp. 1–10.

[MDC04]   L. Mahadevan, S. Daniel, and M. Chaudhury. "Biomimetic ratcheting motion of a soft, slender, sessile gel". *Proceedings of the National Academy of Sciences of the United States of America* 101.1 (2004), pp. 23–26.

[Men+06] A. Menciassi et al. "Development of a biomimetic miniature robotic crawler". *Autonomous Robots* 21.2 (2006), pp. 155–163.

[Mie05]   A. Mielke. "Evolution of rate-independent systems". In: *Evolutionary equations. Vol. II*. Handb. Differ. Equ. Elsevier/North-Holland, Amsterdam, 2005, pp. 461–559.

[Mie12]   A. Mielke. "Emergence of rate-independent dissipation from viscous systems with wiggly energies". *Continuum Mechanics and Thermodynamics* 24.4-6 (2012), pp. 591–606.

[Mie15]   A. Mielke. "Variational approaches and methods for dissipative material models with multiple scales". In: *Analysis and computation of microstructure in finite plasticity*. Vol. 78. Lect. Notes Appl. Comput. Mech. Springer, Cham, 2015, pp. 125–155.

[MR15]   A. Mielke and T. Roubıček. *Rate-independent systems*. Theory and application. Springer, New York, 2015.

[MT04]   A. Mielke and F. Theil. "On rate-independent hysteresis models". *NoDEA. Nonlinear Differential Equations and Applications* 11.2 (2004), pp. 151–189.

[MT12]   A. Mielke and L. Truskinovsky. "From discrete visco-elasticity to continuum rate-independent plasticity: rigorous results". *Archive for Rational Mechanics and Analysis* 203.2 (2012), pp. 577–619.

[ND14]   G. Noselli and A. DeSimone. "A robotic crawler exploiting directional frictional interactions: Experiments, numerics and derivation of a reduced model". *Proceedings of the Royal Society A: Mathematical, Physical and Engineering Sciences* 470.2171 (2014).

[NTD14]   G. Noselli, A. Tatone, and A. DeSimone. "Discrete one-dimensional crawlers on viscous substrates: Achievable net displacements and their energy cost". *Mechanics Research Communications* 58 (2014), pp. 73–81.

[PG14]   V. L. Popov and J. Gray. "Prandtl-Tomlinson Model: A Simple Model Which Made History". In: *The History of Theoretical, Material and Computational Mechanics-Mathematics Meets Mechanics and Engineering*. Springer, 2014, pp. 153–168.

[Pop10]   V. Popov. *Contact mechanics and friction: physical principles and applications.* Springer Science & Business Media, 2010.

[PT05]   G. Puglisi and L. Truskinovsky. "Thermodynamics of rate-independent plasticity". *Journal of the Mechanics and Physics of Solids* 53.3 (2005), pp. 655–679.

[Pur77]   E. Purcel. "Life at low Reynolds number". *American Journal of Physics* 45.1 (1977), pp. 3–11.

[Qui99]   K. Quillin. "Kinematic scaling of locomotion by hydrostatic animals: Ontogeny of peristaltic crawling by the earthworm Lumbricus terrestris". *Journal of Experimental Biology* 202.6 (1999), pp. 661–674.

[RW98]   R. T. Rockafellar and R. J.-B. Wets. *Variational analysis.* Springer-Verlag, Berlin, 1998.

[Tan+12]   Y. Tanaka et al. "Mechanics of peristaltic locomotion and role of anchoring". *Journal of the Royal Society Interface* 9.67 (2012), pp. 222–233.

[Vik+15]   V. Vikas et al. "Design and locomotion control of soft robot using friction manipulation and motor-tendon actuation". *arXiv preprint arXiv:1509.06693* (2015).

[VTT15]   V. Vikas, P. Templeton, and B. Trimmer. "Design and control of a soft, shape-changing, crawling robot". *arXiv preprint arXiv:1509.07569* (2015).

[VWT96]   G. Verwey, M. Warner, and E. Terentjev. "Elastic instability and stripe domains in liquid crystalline elastomers". *Journal de Physique II* 6.9 (1996), pp. 1273–1290.

[WT03]   M. Warner and E. M. Terentjev. *Liquid crystal elastomers.* Vol. 120. OUP Oxford, 2003.

[Zha+09]   L. Zhang et al. "Artificial bacterial flagella: Fabrication and magnetic control". *Applied Physics Letters* 94.6 (2009).

[ZZ07]   K. Zimmermann and I. Zeidis. "Worm-like locomotion as a problem of nonlinear dynamics". *Journal of Theoretical and Applied Mechanics* 45 (2007), pp. 179–187.